

Repurposing Alzheimer’s disease medications in a drug combination for the study of the crosstalk between cell apoptosis and autophagy in the modulation of cell death in chronic myeloid leukaemia

Rosemary Isioma Ofili (PhD student)

Supervisors: Dr Sandra Appiah (DoS) and Dr Pontsho Moela

May 2022
Middlesex University
Faculty of Science and Technology
Department of Natural Sciences



Table of contents

Table of contents.....	1
List of figures.....	5
List of tables.....	6
List of appendices.....	6
Acknowledgements.....	8
Abstract.....	9
Chapter 1.....	10
1. Literature review.....	11
1.1 Introduction.....	11
1.2 Chronic myeloid leukaemia.....	12
1.2.1 Epidemiology of chronic myeloid leukaemia.....	12
1.2.2 Pathophysiology of chronic myeloid leukaemia.....	12
1.2.3 Phases and clinical features of chronic myeloid leukaemia.....	15
1.2.4 Current treatment for chronic myeloid leukaemia with tyrosine kinase inhibitors.....	16
1.2.5 Chemotherapeutic treatment of chronic myeloid leukaemia with Doxorubicin.....	17
1.3 Alzheimer’s disease.....	19
1.3.1 Epidemiology of Alzheimer’s disease.....	19
1.3.2 Classification and clinical features of Alzheimer’s disease.....	19
1.3.3 Pathology of Alzheimer’s disease.....	20
1.3.3.1 Amyloid beta pathology in AD.....	20
1.3.3.2 Tau pathology in AD.....	21
1.3.4 Current drug management for AD.....	23
1.4 AD drug repurposing in combination with anti-cancer drugs in CML treatment.....	26
1.5 Cell death and regulatory pathways.....	28
1.5.1 Apoptosis (programmed cell death I).....	28
1.5.2 Autophagy signalling pathway (programmed cell death II).....	28
1.6 Protein modulation of the apoptotic and autophagy pathways in CML and AD.....	32
1.7 Summary of the choice of methodology.....	35
1.7.1 Rationale for an <i>in vitro</i> study.....	35
1.7.2 Selection of cell lines for the study.....	35
1.7.2.1 Selection of cell lines for CML model.....	35

1.7.2.2 Selection of cell lines for an AD-aspect model	37
1.7.3 Drug selection for the study.....	40
1.7.4 Summary of the rationale for the study	44
1.8 Aims and Objectives	45
1.8.1 Aim of the study	45
1.8.2 Objectives of the PhD study	45
1.8.3. Novelty of the research.....	45
1.9 Outline of the thesis.....	45
Chapter 2.....	47
2. Method	48
2.1 Cell Culture and maintenance	48
2.2 Trypan blue exclusion assay	48
2.3 Cell viability measurement using CyQUANT® Direct assay	49
2.4 Flow cytometry cell death assessment using double staining of AlexaFluor® 488 Annexin V/PI	49
2.5 Gel electrophoresis and Western immunoblotting.....	50
2.5.1 Protein extraction and quantification.....	50
2.5.2 SDS-PAGE electrophoresis, immunoblotting and visualisation	51
2.6 Statistical analysis	52
Chapter 3.....	54
3. Evaluation of the effects of selected leukaemic and Alzheimer’s disease drugs on the apoptotic and autophagy pathways using cell models for AD and CML	55
3.1 Introduction	55
3.2 Aims and Objectives	56
3.2.1 Aim of the study	56
3.2.2 Objectives of the study	56
3.3 Results.....	57
3.3.1 Method development	57
3.3.1.1 Growth pattern of K-562 and HEK293T cell lines incubated under normal growth conditions.....	57
3.3.1.2 The effect of the vehicle (dimethyl sulfoxide) on K-562 and HEK293T cell lines.....	58
3.3.2 Dox inhibited the cell viability of non-cancerous HEK293T more potently than Memantine and Donepezil.....	59

3.3.3 Memantine and Donepezil did not promote apoptotic death in HEK293T and K-562 cells, in contrast to the effect of Dox.....	61
3.3.4 K-562 and HEK293T cells expressed contrasting amounts of proteins at basal level.	63
3.3.5 Imatinib promoted the expression of pro-apoptotic proteins in K-562 cells.....	65
3.3.6 Dox modulated both the apoptotic and autophagy proteins in HEK293T and K-562 cells.....	67
3.3.6.1 Chloroquine-induced autophagy inhibition upregulated Bcl-2 and downregulated Cytochrome c in Dox-treated K-562 cells.....	69
3.3.7 Donepezil inhibited autophagy activities in HEK293T cells.....	72
3.3.7.1 The levels of pro-apoptotic and anti-apoptotic regulators determine the fate of cells.....	75
3.3.8 Memantine upregulated anti-apoptotic proteins in HEK293T cells but not in K-562 cells.....	76
3.3.9 Summarised data of the drug-treated cells.....	83
3.4 Discussion.....	85
3.4.1 Basal protein expressions involved in cell apoptosis and autophagy.....	85
3.4.2 Modulation of the apoptotic and autophagy pathways by cancer drugs.....	89
3.4.2.1 The modulation of the apoptotic and autophagy pathways by Imatinib.....	89
3.4.2.2 The modulation of the apoptotic and autophagy pathways by Dox.....	91
3.4.2.3 Imatinib and Dox promote apoptosis in K-562 cells but Dox alone is able to modulate the alternative autophagy cell death pathway.....	95
3.4.2.4 Dox induced death in K-562 cells via the autophagy pathway.....	97
3.4.3 The modulation of the apoptotic and autophagy pathways by AD drugs.....	100
3.4.3.1 The modulation of the apoptotic and autophagy pathways by Donepezil.....	100
3.4.3.2 The modulation of the apoptotic and autophagy pathways by Memantine.....	101
Chapter 4.....	105
4. Investigating the effects of a combination drug on the modulation of the apoptotic and autophagic pathways to attenuate death in the non-cancer cells without inhibiting the death of CML cells.....	106
4.1 Introduction.....	106
4.2 Aims and Objectives.....	107
4.2.1 Aim of the study.....	107
4.2.2 Objectives of the study.....	107
4.3 Results.....	108

Dox/Memantine drug combination sustained Dox-killing effect by downregulating anti-apoptotic proteins in K-562 cells but not in HEK293T cells	108
4.4 Discussion	112
Dox/Memantine drug combination modulates both the apoptotic and autophagy pathways in K-562 and HEK293T cells.....	112
Chapter 5.....	116
5. Summary, conclusion and future works.....	117
5.1 Summary	117
5.1.1 Basal expressions.....	117
5.1.2 Molecular effects of anti-leukaemic drugs in K-562 and HEK293T cells.....	118
5.1.3 Molecular effects of AD drugs in K-562 and HEK293T cells.....	118
5.1.4 Molecular effects of anti-leukaemic and AD drug-combination in K-562 and HEK293T cells	119
5.1.5 Limitations of the study.....	120
5.2 Future studies	122
5.2.1 Investigating the Dox-induced autophagy pathway upstream of Beclin-1.....	122
5.2.2 Verifying the cell death effect of Memantine in K-562 CML cells	123
5.2.3 Investigating the effects of Dox/Memantine on BCR-ABL activities in K-562 cells	123
5.2.4 Investigation of an autophagy-related LC3 isoform in K-562 CML cells	124
5.2.5 Investigating the effects of Dox/Memantine in an <i>in vitro</i> model AD overexpressing amyloid beta	124
5.2.6 Evaluating the effects of Dox/Memantine on the cell death pathway in K-562 and HEK293T cells	125
5.3 Conclusion.....	126
5.3.1 What is already known?	126
5.3.2 Key findings and concluding comments	126
References.....	128
Appendices.....	201

List of figures

Figure 1.1 Schematic diagram showing the formation of BCR-ABL kinase from ABL and BCR genes	14
Figure 1.2 Amyloid beta mediated effects in the pathogenesis of Alzheimer’s disease.....	21
Figure 1.3 Tau protein dysfunction due to hyperphosphorylation.....	22
Figure 1.4 The chemical structure of the five symptomatic drugs used in the management of AD	23
Figure 1.5 Schematic representation of the intrinsic apoptotic pathway and autophagy pathway	31
Figure 3.1 Growth curve of K-562 and HEK293T cell lines under normal growth conditions ...	57
Figure 3.2 Effect of the vehicle (DMSO) on the cell viability of incubated K-562 and HEK293T cell lines	58
Figure 3.3 The effect of Donepezil and Memantine on HEK293T cell growth compared to Dox	60
Figure 3.4 Basal protein levels expressed in HEK293T and K-562 cell lines.....	64
Figure 3.5 Effects of Imatinib on the levels of proteins involved in apoptosis and autophagy in HEK293T and K-562 cell lines after 48 h treatment	66
Figure 3.6 Effects of Dox on the levels of proteins involved in apoptosis and autophagy in HEK293T and K-562 cell lines after 48 h treatment	68
Figure 3.7 Effects of Dox-CQ co-incubation compared to Dox or CQ sole treatments on the levels of proteins involved in apoptosis and autophagy in K-562 cell lines after 48 h treatment	71
Figure 3.8 Effects of Donepezil on the levels of proteins involved in apoptosis and autophagy in HEK293T and K-562 cells lines after 48 h treatment.....	74
Figure 3.9 Effects of Donepezil on apoptotic-related protein ratios in HEK293T cells.....	75
Figure 3.10 Effects of Memantine on the levels of proteins involved in apoptosis and autophagy in HEK293T and K-562 cells lines after 48 h treatment	82
Figure 4.1 Effects of Dox/Memantine combination treatments on the levels of proteins involved in apoptosis and autophagy in HEK293T and K-562 cell lines after 48 h treatment	111

List of tables

Table 1.1 Features of some commonly used cell lines in CML studies	36
Table 1.2 Features of some commonly used cell lines in AD studies	38
Table 1.3 <i>In vitro</i> effects of Imatinib in cancer and non-cancer cells.....	41
Table 1.4 Molecular effects of Dox in some experimental studies.....	42
Table 3.1 Cell death effects of anti-cancer and AD drugs in HEK293T and K-562 cells.....	62
Table 3.2 Effects of Imatinib and Dox in HEK293T and K-562 cells	83
Table 3.3 Effects of Donepezil and Memantine at lowest concentration tested in HEK293T and K-562 cells	84

List of appendices

Appendix I: Statistical analyses for the viability of K-562 and HEK293T cells using CyQUANT® Direct assay	201
Appendix II: Drug effects comparison amongst Dox, Memantine and Donepezil (1, 5 and 10 μ M) on the cell viability of HEK293T cells using CyQUANT® Direct assay	204
Appendix III: Comparison of the cell viability effects between Memantine and Donepezil (1, 5 and 10 μ M) at 24 and 48 h treatments using CyQUANT® Direct assay	207
Appendix IV: Statistical analyses for the cell death effect of Dox, Imatinib, Donepezil and Memantine on K-562 and HEK293T cells using flow cytometer	208
Appendix V. Flow cytometry analyses of the cell population of viable and non-viable K-562 and HEK293T cells exhibiting different cell death types following 48 h drug treatments	210
Appendix VI: Statistical analyses for the measurement of the basal levels of protein in HEK293T vs K-562 cells using Western blot	211
Appendix VII: Statistical analyses for the protein expression level in single drug-treated HEK293T vs K-562 cells using Western blot.....	212
Appendix VIII: Statistical analyses comparing protein expression levels in Dox 1 μ M, CQ10 μ M and Dox 1 + CQ 10 (μ M) drug-treated K-562 cells as detected through Western blot analyses	219
Appendix IX: Statistical analyses for the measurement of the Bax:Bcl-2 and Bax:Bcl-xL ratios in Donepezil treated HEK293T cells using Western blot.....	220
Appendix X: Statistical analyses for the protein expression levels in Dox/ Memantine combination-treated HEK293T and K-562 cells using Western blot	221
Appendix XI: Representative photos of some of the gels acquired from the Western blot analyses carried out	224

Appendix XII: Summarised description of the intended experimental procedures for the proposed plasmid construction 267

Appendix XIII: Plasmid construct overexpressing amyloid beta (Virtual construct)..... 269

Appendix XIV: Effects of cancer drugs in cancer and non-cancer cells 270

Acknowledgements

I would first like to acknowledge God Almighty for his favour throughout my PhD study. Special thanks to Dr Sandra Appiah for being such a wonderful Director of Studies and for providing me with the much-needed support and mentorship throughout this academic journey. I also appreciate the effort of the rest of my supervisory team and other members of staff who assisted me along the way: Dr Pontsho Moela, Dr Helen Roberts and Dr Celia Bell. I am thankful for the invaluable feedback provided throughout my research, which motivated me to keep striving for success.

I would especially like to acknowledge and honour the memory of my late parents, Engr. and Mrs. F.U Ofili, thank you for your love and advice. Although, you are no longer here, your numerous academic achievements and successful career paths continue to inspire me each day. May your souls continue to rest in the bosom of God. Amen.

In a special way I thank my wonderful siblings, Mrs. Irene Makanjuola (nee Ofili) and Mr. Felix Ofili for their continuous love, prayer and support. My wonderful family, the Okonjis', my ever-cheerful niece and nephew, Tamie and Tobie and my caring in-law, Mr. O. Makanjuola, you are all highly appreciated. Thank you for all the prayers and support, may God continually bless you all.

To all my wonderful colleagues who assisted me along the way, Dr Cynthia Osemeke, Katherine Nuttall, Noor Hasan and most especially, Dr Milan Vu. I am grateful for all the assistance rendered both in and outside the lab. Your expertise immensely contributed to my academic journey. Thank you all.

Many thanks to my Middlesex University co-workers and senior colleagues, on whose modules I taught thereby acquiring and expanding my scientific knowledge in vast areas while improving my confidence. I am very glad to have had the opportunity to work with the team. Some outstanding help was also provided by other researchers and friends both in and outside Middlesex University. My sincere apologies for not mentioning everyone by name. However, their opinions, guidance and support are acknowledged. Thank you all.

My success story would not have been complete without the special man in my life, Mr. Mathew I. Omeike, my darling friend, husband and my number one support system. You kept pushing, supporting and believing in me, even when I thought I could not go any further. You never gave up on helping me achieve my dreams. May God bless and grant all your innermost prayers. Thank you very much, my love.

Thank you everyone for supporting me in every possible way and being a part of my success story. I love you all and may God bless us all. Amen.

Abstract

The world population is ageing and with this shift is a concurrent rise in comorbidities such as Alzheimer's disease (AD) and cancer. Interestingly, an increasing number of studies have reported certain AD drugs to possess anti-cancer properties. This raises the possibility of repurposing these AD drugs for the treatment of cancers such as chronic myeloid leukaemia (CML). This requires the understanding of the possible interconnection between CML and AD at the molecular level. The overall aim of this research was to study the crosstalk between cell apoptosis and autophagy in the modulation of cell death and to determine if AD medications, singly and in combination with a CML drug, have the potential to be repurposed for the treatment of CML.

HEK293T (cell model of AD) and K-562 (cell model of CML) cells were individually treated with the test drugs for 24 and 48 h, depending on the assay. Cell viability was assessed by overlaying the treated cells with CyQUANT® Direct assay dye for 40 min before fluorescence signal detection at a wavelength of 485/520 nm excitation/emission. Cell death assay was also conducted using BD FACSCalibur flow cytometer to detect fluorescent emission at 530 nm (FL1), 575 nm (FL3) and excitation wavelength of 488 nm, in Annexin V/PI-stained treated cells. To examine the autophagic and apoptotic effects modulated by the drug treatments, Western blot analyses were carried out and the proteins of interest were quantified using Image Studio software on the Odyssey® Fc LI-COR Imaging System.

The results demonstrated that the chemotherapy drug, Doxorubicin, caused death in both HEK293T and K-562 cells by modulating the apoptotic pathway. In 48 h Doxorubicin (1 μ M)-treated K-562 cells, the autophagic proteins, Beclin-1 ($p < 0.05$) and LC3 ($p < 0.001$), were also upregulated. With the addition of Chloroquine (10 μ M), a known autophagy inhibitor, these autophagic activities were verified as being involved in the induction of cell death in the CML cells. When Imatinib (1 μ M), a known tyrosine kinase inhibitor, was used in the treatment of CML K562 cells, it was shown to also induce apoptotic cell death effect but without the involvement of the Beclin-1-induced autophagy pathway. Therapeutically relevant but low concentrations (1, 5 and 10 μ M) of Memantine and Donepezil (AD drugs) were shown to be non-toxic in this study, as they induced no measurable cell death in both cell lines tested, with Memantine (1 μ M) increasing the viability of HEK293T (the AD cell model) by 41% ($p < 0.05$). Following the results of the preliminary study, further investigations were carried out employing the combination of Doxorubicin (1 μ M) and Memantine (1 μ M) to determine if the Doxorubicin-killing effect in the CML cells can be enhanced while mitigating its adverse effects in HEK293T non-cancer cells. For the first time, we report herein the apoptotic and autophagic effects of Doxorubicin and Memantine as a combination drug in K-562 and HEK293T cells. The presence of Memantine in the combination induced an increase in the levels of anti-apoptotic Bcl-2 proteins in the non-cancerous HEK293T cells ($p = 0.001$), but not in K-562 cells. Also, the autophagy-mediated cell death pathway initially induced by Doxorubicin in K-562 cells was maintained in the Doxorubicin/Memantine (1 μ M)-treated CML cells.

The findings from this study indicated that the AD drug, Memantine, could modulate the apoptotic pathway to reduce the Doxorubicin-induced death effect in the non-cancerous HEK293T cells without suppressing its killing effect in the K-562 CML cells. Further studies (*in vitro* and *in vivo*) are warranted to help develop this therapeutic strategy that offers non-cancer cell protection while simultaneously providing therapeutic benefits against the cancer cell population in AD and CML comorbidity.

Chapter 1

Literature review

1. Literature review

1.1 Introduction

There is a global increase in life expectancy and with longevity comes the increased prevalence of individuals suffering from multiple conditions, ultimately leading to health and economic implications (Barnett *et al.*, 2012; DESA, 2019; Wenkstetten-Holub *et al.*, 2021). The existence of comorbidity occurs for varying reasons, including scenarios like, when the two diseases have a common underlying initiator or share a common risk factor, when the presence of one disorder abruptly increases the risk of having the second and by random chance (when the occurrence of both diseases are common within a population) (Valderas *et al.*, 2009). Cancer and neurodegeneration are two major human health threats which may exist in comorbidity. These two conditions have been shown to share a common molecular pathology as well as active cell cycling (Behrens *et al.*, 2009; Liu and Ander, 2012). However, since the major characteristics of AD involves degeneration and the main feature of cancer is cell proliferation, it is still believed that people suffering from cancer are less likely to get neurodegenerative disorders such as AD, while those with AD are less likely to get cancer (Freedman *et al.*, 2016; Bowles *et al.*, 2017). Nevertheless, bearing in mind that age is a big risk factor for both conditions, there is a possibility of co-morbidity with increasing age (American Cancer Society, 2021; NHS, 2021; Mendizabal *et al.*, 2016; SEER, 2019). Furthermore, cancer patients undergoing chemotherapy are at risk of neurological side effects of losing healthy cells, including nerve cells of the brain, along with the targeted cancer cells (Cheung *et al.*, 2018).

In cancers, such as chronic myeloid leukaemia (CML), there is an unregulated growth and accumulation of myeloid leukaemia cells in the bone marrow and blood (Wang *et al.*, 2014). Current treatment therapies are unable to eradicate all neoplastic cells involved in this disease, particularly in the central nervous system (CNS) (Branford *et al.*, 2002; Wolff *et al.*, 2003; Cortes and lang, 2021). AD drugs (Memantine and Donepezil) on the other hand are not only known for their protective effects (Chen *et al.*, 1998; Miki *et al.*, 2006; Noh *et al.*, 2009; Kafi *et al.*, 2014; Inagaki *et al.*, 2019) but have also been shown to be toxic against cancer cells (Abdul and Hoosein, 2005; Ki *et al.*, 2010; Kamal *et al.*, 2015; Seifabadi *et al.*, 2017; Yoon *et al.*, 2017; Albayrak *et al.*, 2018). With the possibility of an existence of a complex association between these two conditions, repurposing AD drugs to target CML may help improve the understanding of the common

mechanism(s) between CML and AD and aid in the development of a combination therapeutic strategy that can tackle both CML and AD through multiple pathways.

1.2 Chronic myeloid leukaemia

1.2.1 Epidemiology of chronic myeloid leukaemia

Leukaemia is the 15th most common cancer and the 11th leading cause of cancer mortality in the world (Sung *et al.*, 2021). CML accounts for approximately 15% of the recently diagnosed leukaemia cases in adults with an incidence of 1-2 cases per 100,000 adults (Jabbour and Kantarjian, 2020). In the United Kingdom, between 2016 and 2018, about 226 cases of CML deaths were reported per year, which is equivalent to over 4 individuals per week (Cancer Research UK, 2021). Due to the exiguity of acquiring reliable data from poor underdeveloped countries, the global prevalence of CML is not known but an extrapolation from existing data suggests a yearly occurrence of more than 100,000 patients worldwide. Thus, representing a significant global health burden (Tadwalkar, 2017; Lin *et al.*, 2020).

1.2.2 Pathophysiology of chronic myeloid leukaemia

CML is a myeloproliferative neoplastic disease involving unregulated growth and accumulation of myeloid leukaemia cells in the bone marrow and blood (Wang *et al.*, 2014). The occurrence of a truncated chromosome 22 known as the Philadelphia chromosome, is the hallmark of the disorder. This abnormal chromosome results from a balanced genetic translocation (t(9;22)(q34;q11.2)) formed from a fusion of the Abelson (ABL) gene, from chromosome 9q34.1 and the breakpoint cluster region (BCR) gene, on chromosome 22q11.2 (Jabbour and Kantarjian, 2020) (Figure 1.1). The exact breakpoint where the translocated genes are fused varies, resulting in the formation of three principal transcripts, following alternative splicing (Chasseriau *et al.*, 2004; Score *et al.*, 2010; Amin and Ahmed, 2021). These three recombination transcripts can evolve from the fusion of ABL between exons 1b and 2 with BCR at intron 13/14 (M-BCR (major breakpoint)), intron 1 (m-BCR (minor breakpoint)) or exon 19 (μ -BCR (μ breakpoint) regions to form p210, p190 or p230 transcripts, respectively (Fainstein *et al.*, 1987; Saglio *et al.*, 1990; Pane *et al.*, 1996). Regardless of the transcript formed, the aberrantly fused gene encodes a proto-oncogene region of BCR-ABL which persistently enhances tyrosine kinase activities. Thus,

resulting in a dysregulated proliferation of the hematopoietic stem cells, differentiation inhibition and cell death resistance. Unlike the non-constitutively active, receptor tyrosine kinases which get turned on only when an appropriate signalling molecule binds to its receptor, BCR-ABL is able to remain active, turning on multiple signalling pathways in a kinase-dependent manner. Thus, overriding the tightly regulated homeostatic circuit within cells. Within the BCR and ABL structures, there are various functionally distinct domains present which have been demonstrated to exhibit multiple functions in intracellular signalling (Narayanan *et al.*, 2013; Dölker *et al.*, 2014; Gao *et al.*, 2017; Peng *et al.*, 2021) (Figure 1.1). Moreover, the continuously increased activities observed in BCR-ABL may result from the interference of the BCR region with one of such active sites present in the normal ABL gene (Hantschel *et al.*, 2003). Some of the functionally active domains present in the 160 kDa BCR protein structure include a coiled-coil oligomerisation domain, tyrosine 177 domain, serine/threonine kinase activity domain, Rho guanine-nucleotide-exchange factor (RhoGEF) domain, pleckstrin homology domain and a Rac GTPase activating protein (Rac-GAP) domain (Chu *et al.*, 2007; Sahay *et al.*, 2008; Demehri *et al.*, 2010; Narayanan *et al.*, 2013; NCBI Gene, 2021; Peng *et al.*, 2021). On the other hand, ABL 145 kDa gene, consisting of 11 exons, contains an N-cap with a signal sequence for myristoylation, Src homology 3 and 2 (SH3 and SH2) domains and a catalytic site, within which lies a phosphorylation site, important for the regulation of enzymatic activities (Franz *et al.*, 1989; Mayer and Baltimore, 1994; Pluk *et al.*, 2002; Smith *et al.*, 2003; Dölker *et al.*, 2014; NCBI Gene, 2021). The N-cap as well as the SH3 domain act as important negative regulators of the tyrosine kinase. The N-cap binds the hydrophobic pocket in the C-terminal lobe of the catalytic domain and induces a conformational change that allows the SH3 domain to bind the linker, a segment which connects SH2 to the kinase catalytic domain, thereby maintaining the kinases' inactive state (Mayer and Baltimore, 1994; Pluk *et al.*, 2002; Hantschel *et al.*, 2003). However, in the pathophysiology of CML, during translocation, when the N-terminal of ABL is fused to the BCR sequence, the N-cap which blocks the catalytic site of the kinase in order to regulate its activities, is lost. Therefore, the kinase remains permanently on, promoting an unregulated constitutively active cellular pathway in the disease (Franz *et al.*, 1989; Hantschel, 2012).

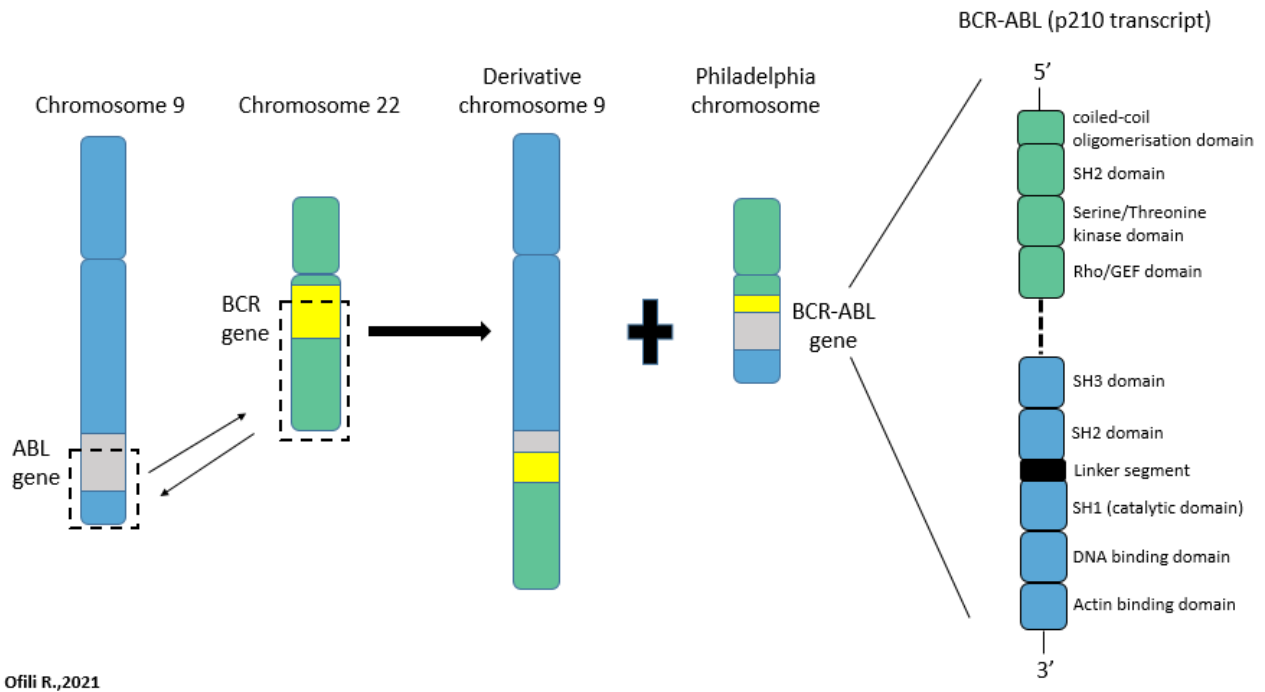


Figure 1.1 Schematic diagram showing the formation of BCR-ABL kinase from ABL and BCR genes

In CML, the exchange between the breakpoints of BCR and ABL genes generates two chromosomes: Derivative chromosome 9 and the hallmark of CML, the Philadelphia chromosome. Following translocation, the Philadelphia chromosome carries the aberrant BCR-ABL fusion gene. Different BCR-ABL transcripts encoding proteins with different molecular weights may be generated, depending on the exact position of the breakpoints. However, in CML, p210 (shown above), is the most commonly detected transcript. Some of the functionally distinct domains that can be observed in p210 BCR-ABL are also shown in the figure above, including the catalytic domain. This kinase catalytic domain is bound by a small myristoylation N-cap sequence in the normal ABL gene, to keep the kinase in an autoinhibited state. However, during the fusion of ABL to the BCR sequence, the N-cap is lost. The internal control mechanisms become disrupted, resulting in enhanced tyrosine kinase activities as seen in CML.

Besides CML, the expression and activities of BCR-ABL can be observed in acute lymphoblastic leukaemia (ALL) (Verrma *et al.*, 2014; Rafiei *et al.*, 2015), acute myeloid leukaemia (AML) (Zhang *et al.*, 2015) as well as in cases of mixed-phenotype acute leukaemia (MPAL) (Matutes *et al.*, 2011; Choi *et al.*, 2014). Studies have also shown that the BCR-ABL p210 transcript is the most commonly detected in CML and occasionally occurs in AML and ALL. The p190 transcript is commonly detected in B-cell ALL, occasionally in AML but rarely observed in CML (Hermans *et al.*, 1987; Fainstein *et al.*, 1987; Li *et al.*, 1999; Kang *et al.*, 2016). However, regardless of the transcript distribution, the BCR-ABL oncogene remains most prominent in CML with its expression pattern worsening as the disease progresses through the various phases.

1.2.3 Phases and clinical features of chronic myeloid leukaemia

CML is diagnosed and categorised into phases mainly based on the number of immature white blood cells (blasts) detected in the blood or bone marrow (American Cancer Society, 2018). Some patients experience symptoms relating to anaemia and splenomegaly such as fatigue, anorexia, left upper quadrant fullness, pain and weight loss. However, about 40% of CML cases are asymptomatic and diagnosed accidentally during routine tests (Sawyers, 1999; Ebert and Hagspiel, 2012; Ahmad *et al.*, 2021). Typically, CML progresses through three phases: the chronic phase, accelerated phase and the blast crisis phase. At the relatively benign chronic phase, patients are found to have less than 10% blasts in their blood and bone marrow samples. Within 3-5 years, this chronic phase may progress to an accelerated phase and finally to the rapidly fatal, blast crisis phase (Kantarjian *et al.*, 1988; Faderl *et al.*, 1999). There are no universally accepted criteria for the signs of the accelerated phase but according to the World Health Organisation (WHO), some of the indicators of this phase include an increase in the percentage of blasts (10-19%), presence of $\geq 20\%$ of basophils in the peripheral blood, persistent thrombocytopenia ($<100 \times 10^9/L$) and thrombocytosis ($>1000 \times 10^9/L$), persistent splenomegaly (unresponsive to therapy) and multiple chromosomal changes in the Philadelphia chromosome-positive cells that occurs during therapy (Baccarani *et al.*, 2013; Arber *et al.*, 2016). CML in the accelerated phase is less responsive to treatment compared to the chronic phase. At the treatment-refractory blast crisis phase, $\geq 20\%$ of blasts are present in the blood and bone marrow, extramedullary blast proliferation occurs and large blasts clusters can be seen in bone marrow biopsies (Kantarjian *et al.*, 1988; Baccarani *et al.*, 2013; Arber *et al.*, 2016). The phenotype of the blast crisis phase can be myeloid, lymphoid or both (Khalidi *et al.*, 1998; Sumimoto *et al.*, 2010; Liu *et al.*, 2020). At this rapidly fatal stage, the blasts resemble acute leukaemia cells morphologically but are highly resistant to chemotherapy, leading to death within 12 months (Vallejos *et al.*, 1974; Cortes and Kantarjian, 2003; Jain *et al.*, 2017). The pathological transformation from one phase to another involves various complex molecular processes, an increase in the expression levels of BCR-ABL and the development of drug-resistant cells leading to relapse after an initial response (Elmaagacli *et al.*, 2000; Marum *et al.*, 2016; Jain *et al.*, 2017). Thus, making CML treatment more challenging, especially in the advanced blast crisis phase.

1.2.4 Current treatment for chronic myeloid leukaemia with tyrosine kinase inhibitors

CML was initially managed with various treatment options such as busulfan, hydroxyurea, interferon-alfa and cytarabine (Negrin and Schiffer, 2016; American Cancer Society, 2022). However, the drugs were palliative, unstable and limited by their non-specificity, toxicities and harmful side effects (Hehlmann *et al.*, 1988; Bhagwatwar *et al.* 1996; Cortes *et al.*, 1996; Thiele *et al.*, 2000; Stone, 2004; Begna *et al.*, 2016). Over time, the clinical outcome of patients with CML improved with the development of tyrosine kinase inhibitors (TKIs), compounds that inhibit BCR-ABL activities. Presently, Imatinib is the gold standard, frontline therapy for CML (Johnson *et al.*, 2003; Medeiros *et al.*, 2018). Imatinib inhibits the growth of leukaemic cells by competitively binding to BCR-ABL tyrosine kinase, thereby preventing the normal binding of ATP and the subsequent removal and transfer of phosphate groups from ATP to tyrosine residues on various substrates (Capdeville *et al.*, 2002; Druker, 2008). Imatinib specific mode of action helps to reduce tyrosine kinase activities and prevent the excess proliferation of CML cells. However, little is known about the long term effect of this drug, with suggestions that Imatinib is unable to completely destroy all neoplastic stem cells, especially in the CNS, thereby leading to the development of resistance in patients as the BCR-ABL subclones increases and mutates (Gorre *et al.*, 2001; Branford *et al.*, 2002; Takayama *et al.*, 2002; Wolff *et al.*, 2003; Druker *et al.*, 2006; Hochhaus *et al.*, 2020). This led to the introduction of patients to other TKIs including, the second-generation (Dasatinib, Nilotinib, Bosutinib) and third-generation (Ponatinib) TKIs (Cortes *et al.*, 2013). This represented progress and additional options for CML treatment. In fact, the widespread use of TKIs has reduced the number of CML patients who progress to the blast crisis phase, thereby increasing the life expectancy of these patients to almost equal the life expectancy of the general population (Sasaki *et al.*, 2015). However, these drugs are still not without side effects nor have their introduction been translated into improved long-term survival or permanent remission (Cortes *et al.*, 2012; Delphine *et al.*, 2012; Larson *et al.*, 2014; Jain *et al.*, 2017; FDA, 2018). Most importantly, despite the use of these TKIs, a significant minority of patients still transform to the fatal blast crisis phase, wherein, even the gold standard CML treatment, Imatinib, has been observed to have no significant outcome on a long-term basis (Palandri *et al.*, 2008; Druker *et al.*, 2006; Cortes *et al.*, 2012; Cortes *et al.*, 2013; Hochhaus *et al.*, 2020). Furthermore, varying mutations occur in the BCR-ABL kinases which interfere with the ability of TKIs to bind, thus

contributing to the development of treatment resistance in CML (Gorre *et al.*, 2001; Branford *et al.*, 2002; Shah *et al.*, 2002; Von Bubnoff *et al.*, 2006). Also, the exact molecular mechanism involved in the evolution of CML cells and the process by which leukaemic cells are able to reactivate their BCR-ABL signal transduction with the aid of the non-eradicated leukaemic stem cells, following a previous inhibition to TKIs, remains a major problem in CML treatment therapy. Therefore, patients undergoing TKI treatments and living a nearly normal life have to be monitored regularly for BCR-ABL burden or evidence of genetic mutation that may lead to sudden resistance in treatment and disease progression (Baccarani *et al.*, 2013). Bearing in mind that the acquisition of additional genetic defects coupled with the multistep phenomenon is known to be involved in the development of resistance, a feature accompanied or shortly followed by progression of CML from chronic to blast crisis phase (Sacha *et al.*, 2003; Soverini *et al.*, 2005), the pursuit for alternative mechanisms and treatment strategies, such as intensive chemotherapy is necessary. Such treatment strategies may help circumvent the resistance in CML, especially at the blast crisis phase.

1.2.5 Chemotherapeutic treatment of chronic myeloid leukaemia with Doxorubicin

Despite the fact that majority of CML patients have increased life expectancy from treatment with TKIs, a significant number of patients still progress to the blast crisis phase and become even more resistant to these TKI treatments. This may be a result of genetic changes which occur in the leukaemic cells as the disease progresses. In the advanced blast crisis phase of CML, about 25% of the cells exhibit morphological features similar to lymphoblastic leukaemia cells, while a higher proportion is almost indistinguishably similar to AML cells (Derderian *et al.*, 1993; Cortes *et al.*, 2016). Thus, for more effective targeting of CML at this phase, treatment regimen usually includes the use of other conventional anti-cancer drugs, such as Doxorubicin (hereafter referred to as Dox), with or without TKIs, to inhibit leukaemic cells via different signalling pathways (Vallejos *et al.*, 1974; Synowiec *et al.*, 2015; Li *et al.*, 2018; Li *et al.*, 2019). Dox is categorised as one of the most potent chemotherapeutic drugs employed in the treatment of cancers with poor prognosis (Nylén *et al.*, 1989; Kamthan *et al.*, 1990; Verschoor *et al.*, 2020). It is a class I anthracycline that is non-selective in its actions. Dox interacts with the DNA of the cell, intercalating with the base pairs (Meriwether and Bachur, 1972; Momparler *et al.*, 1976). This prevents the activities of the DNA-

associated enzymes such as the topoisomerase enzymes. Topoisomerases are ubiquitous enzymes which are essential in the viability of all living organisms. They play a vital role in various DNA processes including replication, transcription and chromatin organisation (Watt and Hickson, 1994). DNA topoisomerase I and II are involved in the relaxation of supercoiled DNA. Anthracyclines such as Dox, which intercalates with the cell's DNA are known as topoisomerase II inhibitors. The inhibitory activity of topoisomerase II enzymes or other molecular targets make them capable of inhibiting critical steps involved in the catalytic processes of the cells, including transcription and DNA replication, thus producing a range of cytotoxic effects and inducing cell death (Laroche-Clary *et al.*, 2000; Lebrecht *et al.*, 2004). Dox can be used in conjunction with other alternative cancer treatments, such as allogeneic stem cell transplant. The combination of allogeneic stem cell transplant with higher doses of the chemotherapy drugs aid in increasing the patients' chance of remission. However, the treatment involves a risk of morbidity and mortality (Gratwohl, 2016). Therefore, the combination is recommended for CML patients in the blast crisis phase with no optimal treatment response and limited treatment alternatives. Dox, even as a singular drug has been documented as being effective at the molecular level of cancer (Leung and Wang, 1999; Luo *et al.*, 2000; Vu *et al.*, 2020). However, due to its lack of selectivity on cancer cells and its detrimental cytotoxic effects to various organs, including the heart (Wang *et al.*, 2004; Ueno *et al.*, 2006; Xu *et al.*, 2012; Li *et al.*, 2016) and kidney (Lebrecht *et al.*, 2004; Lahoti *et al.*, 2012), the drug's use is limited. It is noteworthy that 50% of Dox molecules are eliminated from the body in an unchanged state (Camaggi *et al.*, 1988). This gives the drug ample opportunity to interact with essential organs in the body including the kidney which is the main organ of excretion (Bárdi *et al.*, 2007). Thus, promoting Dox-induced organ toxicity. Nonetheless, such an effective drug, with an alternative mechanism of action may be considered for the TKI-resistant patient population but should be combined with another compound with the ability to reduce the Dox-accompanied toxic effects in the non-cancer cells, especially in cases where co-morbidity with other ailments, like Alzheimer's disease (AD), exists.

1.3 Alzheimer's disease

1.3.1 Epidemiology of Alzheimer's disease

Currently, more than 55 million individuals have been reported as being affected by dementia worldwide, with an occurrence of almost 10 million new cases every year (WHO, 2021). AD is the most common form of dementia contributing 50% to 75% of reported dementia cases in the United Kingdom (Alzheimer's Society, 2021). In 2019, the UK Alzheimer's Society commissioned a report from the Care Policy and Evaluation Centre (CPEC) at the London School of Economics and Political Science. The report estimated that about 850,000 individuals living in the UK, had dementia, with a projected increase of 1.6 million people in 2040 (Wittenberg *et al.*, 2020). Also, the mortality rate of AD and other dementias in the United Kingdom has overtaken ischaemic heart diseases, cerebrovascular diseases, chronic lower respiratory diseases and lung cancer, four diseases previously conceded as the major causes of death in the United Kingdom (ARUK, 2021).

1.3.2 Classification and clinical features of Alzheimer's disease

AD is an irreversible neurodegenerative disease characterised by the progressive loss of neurons which are essential for cognitive and memory functions (Alzheimer's Society, 2021). Based on the individual's age at onset, this condition can be grouped into early- and late-onset AD. Early-onset AD is uncommon and occurs in individuals less than 65 years of age, with about 13% being familial Alzheimer's disease (FAD) (Campion *et al.*, 1999; McMurtray *et al.*, 2006; Mendez, 2019). FAD occurs as a result of inherited genetic mutation in Amyloid Precursor Protein (APP), presenilin1 (PSEN1) and presenilin2 (PSEN2); subunits of gamma secretase, thereby causing an increase in the production ratio of amyloid beta 42:40 (Sherrington *et al.*, 1996; Tanzi and Bertram, 2005; Bird, 2012). Late-onset AD is more common and age has been implicated as its major risk factor, with a rising prevalence of the disease between the ages of 65 and 85 years (Sloane *et al.*, 2002; Bekris *et al.*, 2010; Prince *et al.*, 2014). The timely detection and accurate diagnosis of AD provides a better chance for the management of the disease. However, there is no simple, reliable test to diagnose the disease and a definitive diagnosis can only be possible post-mortem (NHS, 2021; NIA, 2021). Regardless of the varying forms or age at which AD is clinically diagnosed, the common histological findings include neuron degeneration, plaques and tangles (Tomlinson *et al.*, 1970; Brookmeyer *et al.* 2018).

1.3.3 Pathology of Alzheimer's disease

AD is a neurodegenerative condition whose neuropathological features include aggregates of amyloid beta ($A\beta$) forming highly insoluble and proteolysis-resistant fibrils called plaques, misfolded hyperphosphorylated tau proteins forming neurofibrillary tangles and accumulation of cytosolic lipids, leading to neuronal and synaptic loss (Murphy and LeVine, 2010; Perl, 2010; King *et al.*, 2020).

1.3.3.1 Amyloid beta pathology in AD

$A\beta$ is a self-aggregating 36 to 43 amino acid peptide (about 28 extracellular amino acids and 12 to 15 residues of hydrophobic transmembrane domain) generated from the proteolytic cleavage of APP in the acidic compartments of the endosomes, by β and γ -secretase during amyloidogenesis (Haass and Selkoe, 1993; Lahiri *et al.*, 1994; Robert, 2004; Murphy and LeVine, 2010; Chen *et al.*, 2017). APP is a type I transmembrane protein synthesised in the endoplasmic reticulum (O'Brien and Wong, 2011, Muresan and Muresan, 2015) and found in high abundance in the CNS (Zheng and Koo, 2011; Ramaker *et al.*, 2016). It undergoes alternative splicing and generates APP mRNA encoding proteins of 695 (the most abundant isoform found in neurons), 751 and 770 amino acids. APP is cleaved into fragments by enzymes (α , β and γ -secretases) in order to become more functional. In the amyloidogenic pathway, when β -secretase (BACE1) cleaves APP, soluble APP β (sAPP β) is released leaving a membrane-bound fragment referred to as C-terminal fragment beta (CTF β ; C99) (Figure 1.2). CTF β is cleaved almost immediately by γ -secretase releasing $A\beta$ and APP Intracellular Domain (AICD) (Thinakaran and Koo, 2008). The cleavage by γ -secretase is somewhat imprecise, causing the production of many isoforms of $A\beta$, with the most common forms being the $A\beta_{40}$ (~80-90%) and $A\beta_{42}$ (~5-10%) (Mori *et al.*, 1992; Haass *et al.*, 1993; Murphy and LeVine, 2010; Sun *et al.*, 2015). $A\beta_{42}$, is more hydrophobic and commonly found in plaques deposited on the walls of the blood vessels of the brain due to its high tendency to aggregate (Selkoe, 2001). However, the plaques do not cause an immediate interference with the functioning of the vessels until their involvement becomes severe, leading to vascular rupture, haemorrhaging, inflammatory processes and other complications (Kuchibhotla *et al.*, 2008; Meyer-Luehmann *et al.*, 2008; Perl, 2010) (Figure 1.2).

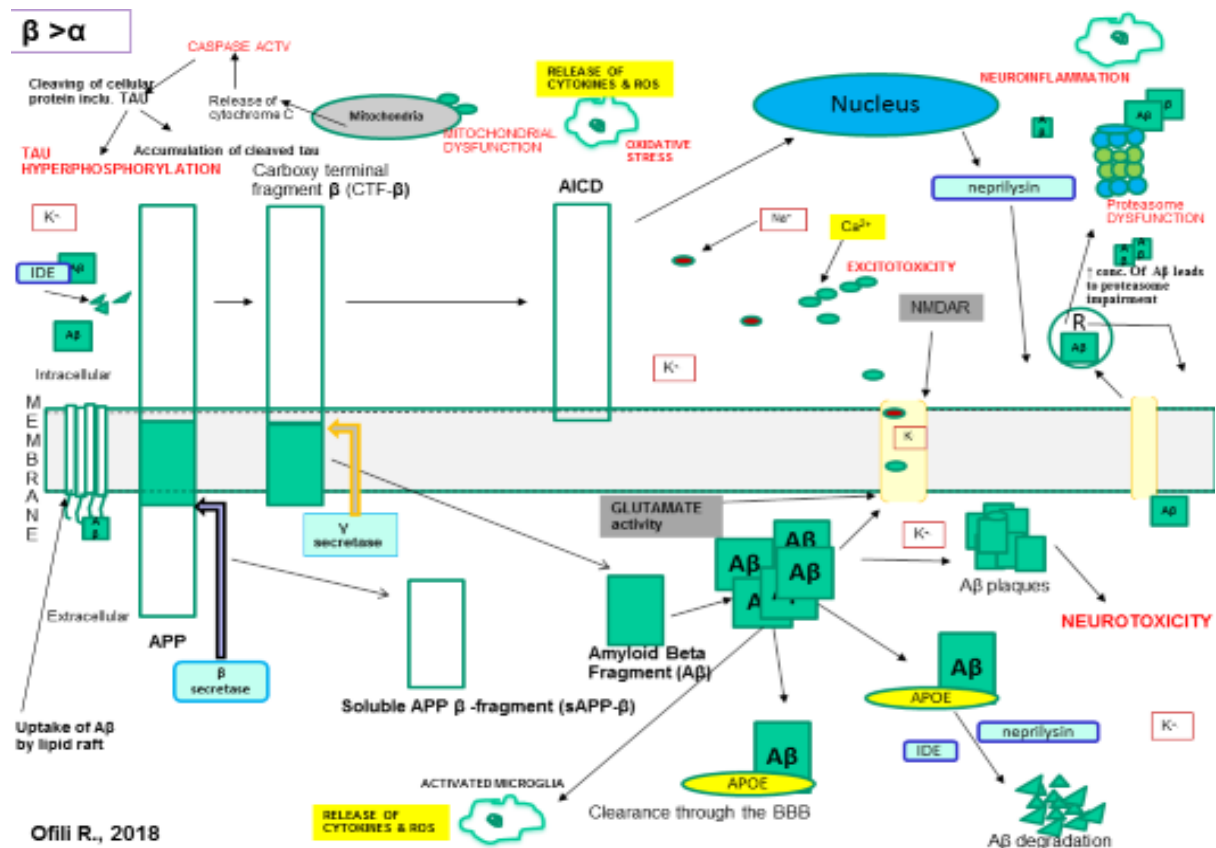


Figure 1.2 Amyloid beta mediated effects in the pathogenesis of Alzheimer's disease

Overexpression of β-secretase leads to the cleavage of APP by β and γ-secretase resulting in the formation of Aβ monomers and eventually plaques. Plaques obstruct neuron signalling. Its sticky nature allows it to aggregate and adhere to the blood vessels causing vascular rupture, haemorrhaging and accumulation of blood in the brain. Aβ also binds to glutamate receptors leading to an endocytic process of receptor-bound Aβ and improper functioning of the proteasome. The binding of Aβ to the NMDA receptor causes the permeabilisation of the membrane allowing an increased influx of calcium ions into the cell cytoplasm. The ions migrate into the matrix of the mitochondria, leading to its permeability, reduced activity, release of Cytochrome c and caspases activation.

1.3.3.2 Tau pathology in AD

Tau is a major microtubule-associated protein usually located in the axon of neurons. It acts as a support structure for growing axons, binding to the tubulin of microtubules thereby ensuring stability and facilitating intracellular transport (Weingarten *et al.*, 1975; Griffin, 2006; Mietelska-Porowska *et al.*, 2014). Tau is a phosphoprotein with about 80 serine/threonine and five tyrosine potential phosphorylation sites, whose involvement in the development of AD and other tauopathies is yet to be fully validated (Buée *et al.*, 2000; Blennow, 2004; Wang *et al.*, 2013). In

individuals with AD, tau is abnormally hyperphosphorylated causing conformational changes and aggregation into paired helical filaments mixed with straight filaments forming neurofibrillary tangles (NFTs) (Grundke-Iqbal *et al.*, 1986; Wang and Mandelkow, 2016) (Figure 1.3). The sequence of events leading to the formation of NFTs causes the microtubule to fall apart as tau detaches. This compromises the integrity of the cytoskeleton, disrupts the intracellular transport system of the neuronal functioning and initiates a disease cascade leading to symptoms associated with AD (Evans *et al.*, 2000; Iqbal *et al.*, 2000).

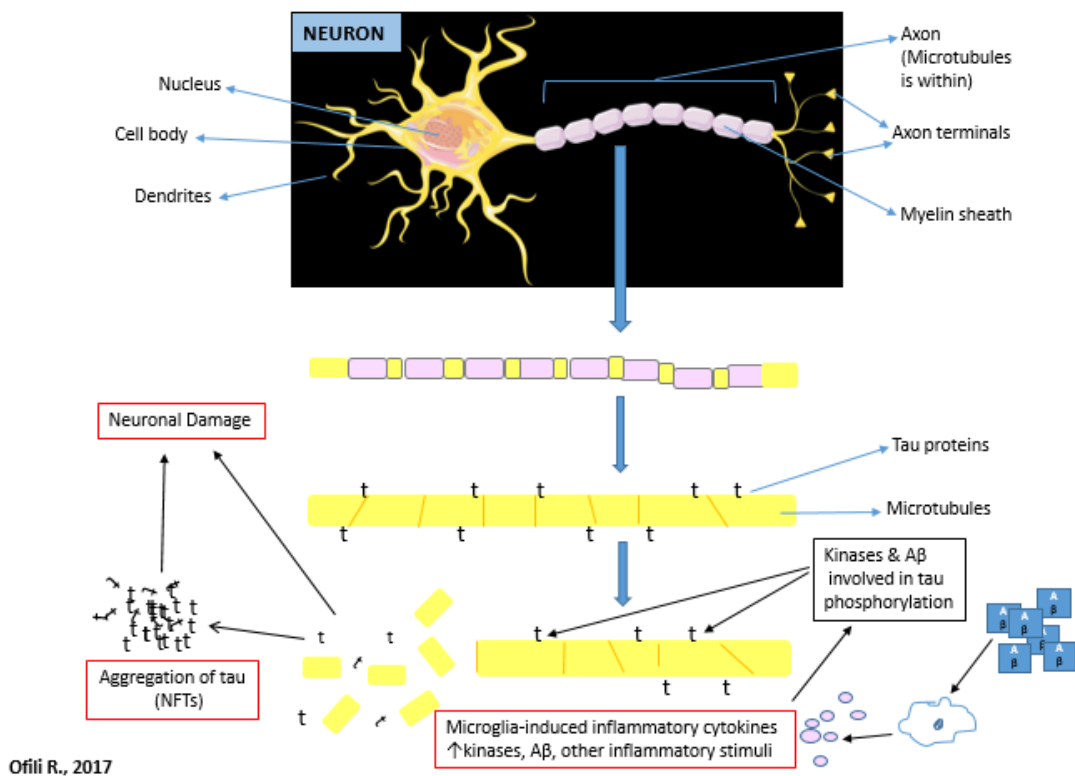
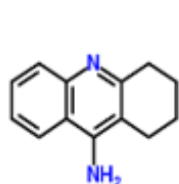


Figure 1.3 Tau protein dysfunction due to hyperphosphorylation

Under normal physiological conditions, tau is a microtubule-associated protein. However, due to its multiple phosphorylation sites, tau could be abnormally phosphorylated by the activities of various protein kinases. This causes tau to detach from the microtubules, misfold and form both soluble and insoluble filaments which aggregates to form NFTs. Tau pathology is suggested as a downstream phenomenon involving various stimulatory activities, including A β . The interference of A β with various biological pathways causes the phosphorylation of proteins such as tau. This leads to inflammation and stimulation of microglial cells to produce cytokines, thereby resulting in the upregulation of kinases involved in tau phosphorylation and increased tauopathy.

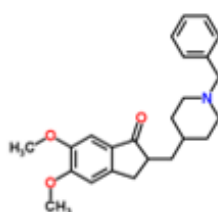
1.3.4 Current drug management for AD

A limited number of drugs have been approved for the management of AD. They include the acetylcholinesterase (AChE) inhibitors: Tacrine (NYT, 1993; Crismon, 1994; NICE, 2011), Donepezil (ALZFORUM, 1996, NICE, 2011), Rivastigmine (ALZFORUM, 1996; NICE, 2011; Yiannopoulou and Papageorgiou, 2013), Galantamine (NICE, 2011; Kim and Park, 2017); the N-methyl-D-aspartate (NMDA) receptor antagonists: Memantine (Annicchiarico *et al.*, 2007; NICE, 2011) and a recently approved amyloid plaque targeted drug, Aducanumab (marketed as Aduhelm) (FDA, 2021).



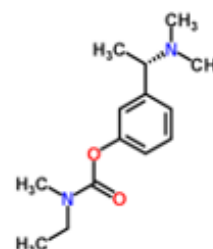
Cholinesterase inhibitor

Tacrine (Cognex/
Tetrahydroaminoacridine) is a synthetic drug with about 17% oral bioavailability, approved in 1993 but has presently been discontinued due to its liver toxicity effect.



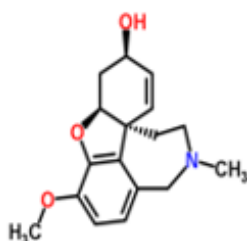
Cholinesterase inhibitor

Donepezil (Aricept) is a synthetic drug approved in 1996 for the treatment of mild to moderate AD. It has a longer half-life and higher oral bioavailability (100%).



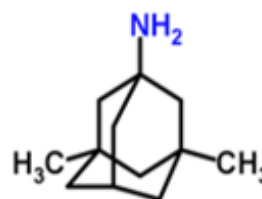
Cholinesterase inhibitor

Rivastigmine (Exelon) is a semi-synthetic drug used for the symptomatic treatment of mild to moderately severe AD. It was approved in 2000 and has a mean oral bioavailability of 71.7%. The product is available as patches.



Cholinesterase inhibitor

Galantamine (Reminyl, Razadyne, Razadyne ER) is a naturally originated drug which was approved in 2001. It has an average oral bioavailability of about 88.5%.



N-methyl-D-aspartate (NMDA) receptor antagonist

Memantine (Namenda) is a synthetic drug which was approved in 2004 for the treatment of moderate to severe AD. It has a bioavailability of approximately 100% and is beneficial in decreasing glutamate excitotoxicity.

Ofili R., 2017

Figure 1.4 The chemical structure of the five symptomatic drugs used in the management of AD

The first five approved AD drugs are symptomatic treatments and their limitation in usage includes, short half-lives, generally poor tolerability and excessive side effects, such as headache, anorexia, nausea, diarrhoea, diaphoresis, asthenia, urinary incontinence, severe hepatotoxicity and sleep disorder (Egger *et al.*, 1991; Rubio *et al.*, 2007; Tinklenberg *et al.*, 2007; Schneider, 2009; Ma *et al.*, 2014). The use of Tacrine has been discontinued in some countries such as the U.S, due to its hepatotoxic effect (Satpute *et al.*, 2015). The other four AD symptomatic drugs, which are less toxic and better tolerated are still used in the palliative management of the disease. However, these medications are not curative and lose their efficacy as the disease progresses.

Just recently, after almost two decades of continuous research, an immunotherapeutic drug known as Aducanumab (Aduhelm) was newly added to the list of approved AD drugs (FDA, 2021). The drug is a human anti-A β monoclonal antibody originally derived from healthy aged, cognitively normal donors whose immune systems were observed to have successfully resisted AD (ALZFORUM, 2021). Unlike the previously approved AD drugs (Tacrine, Donepezil, Rivastigmine, Galantamine and Memantine) which targeted the symptoms of the disease, Aducanumab targets the underlying pathophysiological process of AD by reducing the amount of aggregated amyloid beta plaques present in the brain (Bussiere *et al.*, 2013; Sevigny *et al.*, 2016). The anti-A β drug is also able to cross the blood-brain barrier and can still be detected weeks after dosage. Thus, suggesting a long-term retention (Sevigny *et al.*, 2016). The drug has also been observed to preferentially bind parenchymal amyloids over the vascular ones (Bussiere *et al.*, 2013; Sevigny *et al.*, 2016). However, similar to most treatments, the use of Aducanumab has been observed to present side effects. In a previously conducted clinical trial, drug dosage of ≤ 30 mg/kg was observed to be generally well tolerated with no severe side effects (Ferrero *et al.*, 2016). However, patients who received dosages of 60 mg/kg were reported to show side effects. One such unwanted drug reaction was amyloid-related imaging abnormalities (ARIA) (Ferrero *et al.*, 2016). ARIA has been described as the most common side effect of Aducanumab usage, even at a lower dosage of 10 mg/kg (Sevigny *et al.*, 2016). This drug-related effect is presented as swelling in some areas of the brain and can be detected using Magnetic resonance imaging (MRI) scans. Some other Aducanumab drug side effects include headache, dizziness, diarrhea, urinary and upper respiratory tract infection (Ferrero *et al.*, 2016; Sevigny *et al.*, 2016). Although these side effects are said to resolve over time, some scientists are of the opinion that more research needs to be done to determine if the benefit of the drug outweighs its side effects. In addition, some experts believe

that the use of the drug does not translate into a meaningful difference in the patients' health (Alexander *et al.*, 2021; The Guardian, 2021). Despite these conflicting opinions, evidence has suggested that the aggregation of amyloids forming plaques is neurotoxic and contributes to neuronal function abnormalities (Kuchibhotla *et al.*, 2008; Meyer-Luehmann *et al.*, 2008). Thus, the clearance of these proteins can aid in the modification of AD progression. Therefore, with the ability of Aducanumab to target the hallmark of AD (amyloid plaques), its potentials seem to be very promising and provides a meaningful therapeutic advantage over the already existing AD drugs. However, due to limited information available as at the time of this present study as well as imminent post-approval investigations to verify the benefits of this drug, this research focused on the already well-known approved AD drugs (Donepezil, Rivastigmine, Galantamine and Memantine) and selections were made based on the scientific evidence available.

In the management of AD, various criteria need to be considered in selecting the best regimen for each individual. During the pathogenesis of the disease, there is an upregulated amount of acetylcholinesterase (AChE) catalysing the breakdown of the available acetylcholine (ACh) (Zhou *et al.*, 2015). This causes a compromise of the cholinergic pathway in the brain, resulting in AD symptoms (Herholz, 2008; Zhou *et al.*, 2015; Biswas *et al.*, 2016). The cholinesterase inhibitors (Donepezil, Rivastigmine, Galantamine) help to improve these symptoms by enhancing the communication between neurons. These drugs increase the concentration and duration of ACh, an essential neurotransmitter which is reduced as AD progresses (Colovic *et al.*, 2013). Amongst the three AChE currently being used in the management of AD, Donepezil is suggestive to be the most advantageous. Firstly, the drug has an oral bioavailability of 100% compared to Rivastigmine and Galantamine which have a bioavailability of 71.7% and 88.5%, respectively. Secondly, Donepezil has a longer duration of action (70 to 80 h) in comparison to most of the other cholinesterase inhibitors (0.3 to 12 h). Thus, allowing for a convenient once-a-day dosing (Ohnishi *et al.*, 1993; Nordberg and Svensson, 1998). Furthermore, in a comparative study by Hansen *et al.* (2008), Donepezil and Rivastigmine were reported to be more efficacious than Galantamine. Moreover, based on a major drug selection criteria, side effects experienced by the individual, Donepezil has been observed to give the least adverse effect, with Rivastigmine showing the highest out of the three AChE. Above all, Donepezil has also been observed to activate both initiator and activation caspases 8, 9 and 3 in acute promyelocytic leukaemia cells and increased the cleavage of PARP-1, thereby resulting in the death of the cancer cells (Ki *et al.*, 2010). Another

mechanism of AD treatment involves the use of a receptor antagonist called Memantine. The drug acts as a reversible NMDA receptor blocker thereby preventing excitotoxicity through the regulation of calcium influx and glutamate activity in the brain (Parsons *et al.*, 1999). Besides the use of Memantine in the management of AD, the drug has been reported to be cytotoxic against breast cancer cells (Seifabadi *et al.*, 2017). With the ability of these AD drugs (Donepezil and Memantine) to target a number of pathways in various diseased conditions, a possibility of an unknown beneficial effect on blood cancer, such as CML, may also exist.

1.4 AD drug repurposing in combination with anti-cancer drugs in CML treatment

In a bid to find potentially better therapeutic strategies, several drugs have been used in targeting diseases they were not originally developed for (Ki *et al.*, 2010; Fantini *et al.*, 2014; Andresen and Gjertsen, 2017; Oral *et al.*, 2017; Seifabadi *et al.*, 2017; Albayrak *et al.*, 2018). Some of the drugs used in the treatment of cancer have been shown to have effects in AD treatment (Hayes *et al.*, 2013; Brunden *et al.*, 2010; Kitaoka *et al.*, 2013; Fantini *et al.*, 2014). This could be due to the biological theory that cancer and AD may share common mechanistic links where an alteration in certain proteins lead to either carcinogenesis or neurodegeneration. During AD neurodegeneration, there is an upregulated amount of AChE enzymes which breaks down the amount of acetylcholine released into the synaptic cleft, thereby decreasing the stimulating signals (Zhou *et al.*, 2015). Previously, this cholinergic system was believed to be specific to acetylcholine-producing nerve cells only. However, emerging evidence indicates that acetylcholine is produced and released in both neuronal and some non-neuronal neoplastic cells (Song *et al.*, 2003; Schlereth *et al.*, 2006; Cheng *et al.*, 2008). Besides neurotransmission, acetylcholine is now recognised as being involved in other functional roles such as proliferation (Song *et al.*, 2003; Cheng *et al.*, 2008; Dobrovinskaya *et al.*, 2016), apoptosis (De Sarno *et al.*, 2003; Kakinuma *et al.*, 2005) and cellular migration (Tang *et al.*, 2012; Yang *et al.*, 2015; Kato *et al.*, 2021). These roles are fundamental processes observed, not only in neurons, but also in non-neuronal cells as well as in tumourigenic cells. Thus, suggesting the involvement of the cholinergic pathway in the pathogenesis of malignancies. The cholinergic pathway is one of the major targets in AD management involving the use of cholinesterase inhibitors. The drugs work by inhibiting AChE, thereby increasing the level of

acetylcholine available in the synapses to help alleviate patient symptoms (Colovic *et al.*, 2013). Since cancer cells also exhibit a cholinergic system, the use of cholinesterase inhibitors may be an effective target against CML cells, acting differently, compared to the protective effects the drugs give in the cholinergic pathway of neurons.

Another AD therapeutic strategy involves the use of NMDA receptor antagonist which targets the NMDA receptors in order to prevent cell excitotoxicity due to glutamate activities. These glutamate activities seem to be selectively detrimental to non-cancer cells compared to malignant cells, as cancer cells have been reported to take in very low concentrations of glutamate but release amounts that are sufficient to induce cell toxicity to surrounding cells (Ye and Sontheimer, 1999; Seidlitz *et al.*, 2009). This high amount of glutamate released into the extracellular space could result in over-stimulation of other NMDA-receptor-expressing cells. Hence, the presence of growing cancer cells, such as brain tumour cells, could actively induce cell death in other healthy cells surrounding them via excitotoxicity. The inhibitory actions of NMDA receptor antagonists, Memantine could aid in attenuating healthy cells from cancer cell-induced toxicity. Therefore, the repurposing of AD drugs in the treatment of cancers, such as CML, may prove to be a useful approach since these AD drugs are also able to cross the blood-brain barrier, thereby targeting cancer cells which may have migrated to the brain and spinal cord, an unfortunate complication sometimes associated with CML (Wolff *et al.*, 2003; Radhika *et al.*, 2011; Chiba *et al.*, 2018). Furthermore, in previous studies, AD drugs, such as Memantine and Donepezil, have been used to target various molecular pathways involved in cancers such as leukaemia (Ki *et al.*, 2010; Kamal *et al.*, 2015), prostate (Albayrak *et al.*, 2018) and breast cancer (Seifabadi *et al.*, 2017). At certain doses, these AD drugs are seen to be cytotoxic in cancer. In addition, bearing in mind that the major limitation of anti-cancer drugs is its toxicity in non-cancer cells, the repurposing of AD drug in CML and its use as a combinatory treatment with an anti-cancer drug may help alleviate the toxicity observed in normal healthy cells, since AD drugs are known to be cytoprotective. However, the mechanism(s) by which these drugs may affect two common regulatory pathways (autophagy and apoptosis) in both CML and AD, through the differential modulation of common regulatory proteins, under the same experimental condition, is yet to be elucidated. Understanding the mechanistic difference cancer and AD drugs (as single and combination treatment) have in non-cancer versus cancer cells will be useful in informing our decision in choosing drugs that selectively mitigate toxicity in non-cancer cells without affecting its anti-cancer actions.

1.5 Cell death and regulatory pathways

1.5.1 Apoptosis (programmed cell death I)

Apoptosis is a form of programmed cell death that occurs via a regulated sequence of events. The process is characterised by morphological and biochemical hallmarks, including cell shrinkage, nuclear DNA fragmentation and membrane blebbing, eventually leading to the elimination of cells without the release of harmful substances (Hengartner, 2000; Nikolettou *et al.*, 2013). Apoptosis involves the activation of caspases, a family of cysteine proteases, which can be initiated through the extrinsic or intrinsic pathway (Loreto *et al.*, 2014). The extrinsic pathway of apoptosis is activated when death ligands attach to the death receptors on the plasma membrane of the cells. The stimulation of these death receptors (Tumour necrosis factor (TNF), TNF-related apoptosis-inducing ligands (TRAIL) and Fas receptor) result in the activation of the initiator caspase-8, which can propagate the apoptosis signals by direct cleavage of downstream effector caspases, such as caspase-3, thereby leading to cell death (Loreto *et al.*, 2014). The intrinsic pathway is controlled by the Bcl-2 family of proteins and is initiated by the release of the Cytochrome c, from the inner space of the mitochondria due to various apoptotic stimuli (Caltabiano *et al.*, 2013) (Figure 1.5). The release of Cytochrome c into the cytosol leads to the formation of the cytochrome c/Apaf-1/caspase-9-containing apoptosome complex and the eventual activation of the executioner caspase-3 leading to cell death (Hu *et al.*, 1999; Qin *et al.*, 1999; Jan, 2019) (Figure 1.5). The Bcl-2 family of proteins has been suggested to be key regulators involved in this process (Kuwana *et al.*, 2002). The family consists of pro-apoptotic and anti-apoptotic members. The expression levels and interaction amongst these proteins play an essential role in the cellular regulation of apoptosis. Hence, anti-apoptotic Bcl-2 or Bcl-xL is able to inhibit apoptosis by binding to pro-apoptotic proteins (such as Bax and Bak) and interfering with their actions (Oltval *et al.*, 1993; Loreto *et al.*, 2014). Besides the apoptotic pathway, Bcl-2 proteins also interact with Beclin-1, a protein involved in autophagy (programmed cell death II) (Liang *et al.*, 1998; Li *et al.*, 2020).

1.5.2 Autophagy signalling pathway (programmed cell death II)

Autophagy is a cellular process that plays a dual role by enhancing survival or promoting cell death (Nikolettou *et al.*, 2013; Mizushima, 2018). During stressful conditions, aged cellular materials are degraded to generate amino acids and fatty acids which can be used for protein

synthesis and ATP generation in the cell (Zare-shahabadi *et al.*, 2015). However, prolonged autophagy can lead to non-apoptotic cell death through excessive self-digestion or activation of apoptosis (Shimizu *et al.*, 2004; Linder and Kögel, 2019). Autophagy is characterised by a chain of physiological events induced by stimuli such as oxidative stress (Lin and Kuang, 2014; Chang *et al.*, 2022), excitotoxicity (Shacka *et al.*, 2007; Davis *et al.*, 2021) and nutrient unavailability (Kawamata *et al.*, 2017). The process may occur in three forms: chaperone-mediated autophagy (CMA), microautophagy and macroautophagy. CMA is a selective degradation process that involves the targeting and lysosomal translocation of soluble intracellular proteins with an amino acid sequence related to KFERQ (Q-glutamine flanked by basic-acid-bulky basic/bulky) (Kirchner *et al.*, 2019; Robert *et al.*, 2019). The process involves the activity of the chaperone complex proteins comprising of heat shock cognate 70 (hsc70), hsc70 interacting protein (hip), heat shock protein 40 (hsp40), heat shock protein 90 (hsp90), bcl-2 association anthagogene 1 (Bag-1) and the lysosomal proteins including Lysosome Associated Membrane Protein(s) (LAMP) and cathepsins. Activation of the CMA causes the cytosolic chaperone complex via hsc70 to selectively bind to the recognised motif of a soluble protein and translocate it via the LAMP2A receptor in an unfolded state, with the aid of a lysosomal hsc70 (lys-hsc70), into the lysosomal lumen, where protein degradation occurs (Gorantla and Chinnathambi, 2021; Ikami *et al.*, 2022). Microautophagy is a non-selective process which complements the other two forms of lysosomal degradation. The process involves the direct engulfment of cytoplasmic cargoes by lysosomal invagination and autophagic tube formation. Macroautophagy, commonly referred to as autophagy, is a degradative process involving the formation of autophagosomes which fuses with lysosomes to degrade their contents. The process consists of five steps: initiation, nucleation, elongation, maturation and fusion (Figure 1.5). The initiation phase begins in the ER with the action of a protein complex involving Unc-51 Like autophagy activating Kinase1 (ULK1), which is upregulated during energy deficiency via the 5'-adenosine monophosphate-activated protein kinase (AMPK) pathway (Laker *et al.*, 2017). AMPK pathway is a highly conserved cellular energy sensor found in almost all eukaryotic cells (Vara-Ciruelos *et al.*, 2019). The kinase is activated when there is biological stress or a cellular deplete of ATP/AMP or ATP/ADP ratio. This causes the binding of AMP or ADP to the binding pocket of AMPK, resulting in a conformational change of the kinase and the induction of numerous downstream molecules, either directly or indirectly (Davies *et al.*, 1995; Oakhill *et al.*, 2010; Vara-Ciruelos *et al.*, 2019). The activation of

AMPK may have dual functionality. The kinase could inhibit the mammalian target of rapamycin complex 1 (mTOR1) activities and other energy-consuming pathways to decrease ATP consumption (Inoki *et al.*, 2003; Leprivier *et al.*, 2013; Vara-Ciruelos *et al.*, 2019). On the other hand, AMPK could promote cell survival by maintaining the levels of intracellular NADPH (Jeon *et al.*, 2012) and through the activation of autophagy via ULK1 (Egan *et al.*, 2011; Vara-Ciruelos *et al.*, 2019). As autophagy progresses through the initiation phase, ULK1 phosphorylates another protein, Beclin-1, which together with its complexes (Vps15, Vps34 and Atg14) form a core component of Phosphatidylinositol-4,5-bisphosphate 3-kinase (PI3K) class III kinase complex (McKnight and Yue, 2013; Menon and Dhamija, 2018) (Figure 1.5). Increasing concentration of PIP3 causes the rapid recruitment of WIPI (WD-repeat protein Interacting with Phosphoinositide) proteins which accumulate at the ER forming a cradle-like structure called the phagophore. This leads to the recruitment of Atg complex for microtubule-associated protein 1 light chain 3 (LC3) lipidation which helps to target selected substrates and proteins to the developing phagophore in order to form a mature autophagosome (Strong *et al.*, 2021; Verma *et al.*, 2021). The autophagosome then fuses with the lysosome via SNARE proteins and Rab7, forming an autolysosome. This results in the degradation of the membrane of the autophagosome with its content through proteolytic enzymes and acidification (Zare-shahabadi *et al.*, 2015; Verma *et al.*, 2021). These proteolytic enzymes are beneficial in cellular recycling, however, an elevated amount of enzymes, such as cathepsins, could result in cell death (Talukdar *et al.*, 2016).

As previously mentioned, the AMPK pathway is regulated by AMP/ATP ratio. Therefore, in the presence of high amount of nutrients and energy, mTOR, a downstream effect of the PI3K pathway occurring via the phosphorylation and inactivation of Tuberous Sclerosis Complex 2 (TSC2) by AKT, is activated. ULK1 activity which is negatively regulated by activated mammalian target of rapamycin complex 1 (mTORC1) is turned off, leading to the downregulation of Beclin-1, an essential autophagy initiator, which could also be inhibited by anti-apoptotic Bcl-2 (a protein involved in apoptosis) (Marquez and Xu, 2012; Menon and Dhamija, 2018), thereby turning off the catabolic pathway of autophagy.

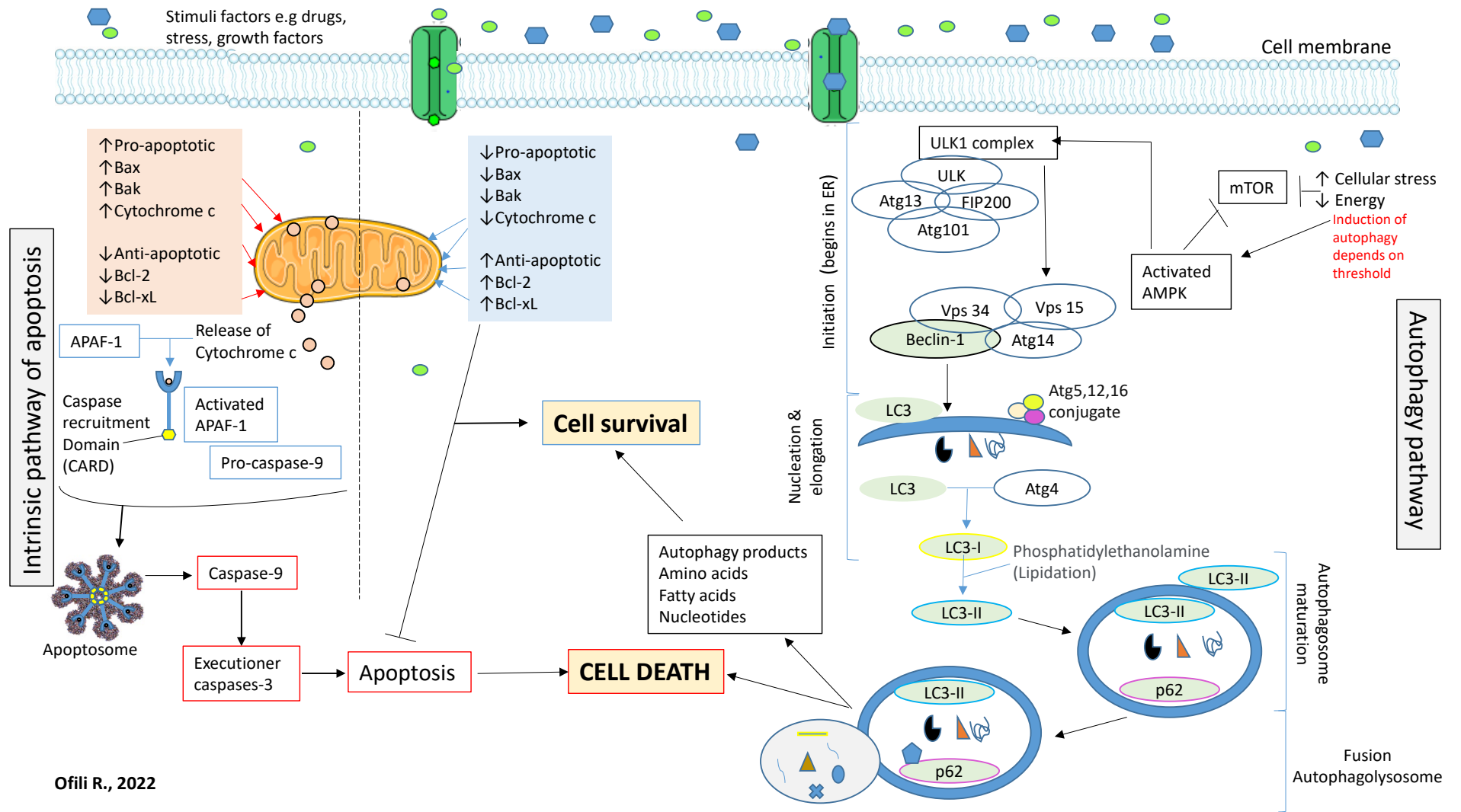


Figure 1.5 Schematic representation of the intrinsic apoptotic pathway and autophagy pathway

1.6 Protein modulation of the apoptotic and autophagy pathways in CML and AD

AD and CML are two conditions where common biological malfunctioning results in opposite effects, leading to an inverse correlation of death in AD and cell survival in CML. In AD, there is progressive death of neuronal cells, while in CML, the cancer cells have the ability to continuously divide by bypassing the cell death pathways. Cancer cells are known to be more resistant to death stimuli compared to non-cancerous cells. This may be due to the presence of different gene expressions in the varying cell types as well as the complex regulation of cell apoptosis and autophagy modulated by multiple proteins. Cancer cells are able to alter the processes that could detect irregularities in their functions, thereby, preventing the proper signals for cell death activation. Therefore, an understanding of the mechanistic differences protein-modulating cancer and AD drugs have in non-cancer versus cancer cells will be useful in finding drugs that will selectively mitigate toxicity in healthy cells without affecting its anti-cancerous actions.

Drug targeting in diseases such as CML and AD has been possible through the modulation of various intracellular processes, including, autophagy and apoptosis. The promotion and inhibition of these processes contribute to the difference between death and survival in cells. The processes of autophagy and apoptosis may be regulated by the same proteins (such as Bcl-2 and p62) and respond to similar signals (such as growth factors and calcium) (Marquez and Xu, 2012; Song *et al.*, 2018; Menon and Dhamija, 2018; Sukumaran *et al.*, 2021). Proteins such as the Bcl-2 family are able to induce death or survival by acting on each other or by influencing other molecules, including the autophagy-related proteins. The balance between the expression levels of anti-apoptotic and pro-apoptotic proteins is crucial to the regulation of both the apoptotic and the non-apoptotic cell death pathways.

In previous studies, anti-apoptotic proteins such as Bcl-2 have been detected, not only in malignant cells, but also in some non-cancerous tissues which demonstrate high cellular turnovers, like the intestine, skin, neuronal cells and bone marrow (Hockenbery *et al.*, 1991; Kønig *et al.*, 2019). The overexpression of Bcl-2 proteins has been implicated in the promotion of cell survival and poor prognosis in cancer (Benito *et al.*, 1995 Ozretic *et al.*, 2018; Song *et al.*, 2019). Although, K-562 CML cells have been reported to be relatively more resistant to apoptosis-inducing stimuli compared to other leukaemic cells such as HL-60 (Diomedea *et al.*, 1990; Benito *et al.*, 1995; Yin

et al., 2011), NB4 (Zhang *et al.*, 2005; Yin *et al.*, 2011), U937 and KCL22 (Yin *et al.*, 2011), the cell line expresses little to no detectable level of Bcl-2 proteins (Benito *et al.*, 1995; Yin *et al.*, 2011; Cerella *et al.*, 2017; Vu *et al.*, 2020). The relatively higher survival advantage of K-562 cells has instead been linked to the increased expression of Bcl-xL, a protein which like Bcl-2, functions as an apoptotic death repressor (Zhang *et al.*, 2005; Yin *et al.*, 2011). The Bcl-2 family of proteins are able to downregulate apoptosis by inhibiting the permeabilisation of the outer membrane of the mitochondria and the release of Cytochrome c through the formation of partnerships with the pro-apoptotic proteins based on their Bcl-2 homology 3 (BH3) domains (Kale *et al.*, 2018). For instance, Bcl-2 is able to form a bond with its heterodimer partner, Bax, while Bcl-xL may bond to its heterodimer partner, Bak (Chen *et al.*, 2005; Kale *et al.*, 2018).

Another functional property of the Bcl-2 family of proteins includes their involvement in autophagy. The anti-apoptotic Bcl-2 proteins, which downregulate apoptosis by antagonising the activities of the pro-apoptotic proteins, can also downregulate autophagy through its involvement with Beclin-1. Thus, emphasising the possible interconnection existing between the apoptotic and autophagy pathways. At the inception of autophagy, Beclin-1, together with its complexes (Vps15, Vps34 and Atg14) form a core component of the phosphatidylinositol-4,5-bisphosphate 3-kinase (PI3K) class III kinase complex (McKnight and Yue, 2013; Menon and Dhamija, 2018), thus, making the protein an essential autophagy initiator. Beclin-1 is able to interact with anti-apoptotic Bcl-2 family members including Bcl-2 and Bcl-xL, via its BH3 domain (amino acids 114–123) (Shimizu *et al.*, 2004; Pattingre *et al.*, 2005; Xu and Qin, 2019). When pro-apoptotic Bax or Bak levels are reduced compared to the levels of anti-apoptotic Bcl-2 or Bcl-xL, the dominant anti-apoptotic proteins could interact with Beclin-1, thereby preventing the association of Beclin-1 with the class III PI3K complex and resulting in the inhibition of the autophagy pathway. The inhibitory effect of the protein interaction occurs in the endoplasmic reticulum, but not in the mitochondria (Pattingre *et al.*, 2005; Maiuri *et al.*, 2007; Marquez and Xu, 2012). Inhibition of the initiation stage of autophagy results in the modulation of LC3 autophagosomal proteins and upregulation of p62 proteins (Bjørkøy *et al.*, 2005; Komatsu *et al.*, 2007; Runwal *et al.*, 2019). Several studies have reported Beclin-1 as being involved in both the autophagic and apoptotic pathways (Furuya *et al.*, 2005; Daniel *et al.*, 2006; Huang *et al.*, 2014). However, Beclin-1 overexpression is unable to inhibit the anti-apoptotic action of Bcl-2 or Bcl-xL (Ciechomska *et al.*, 2009). This unidirectional action may be possible as a result of the weak binding of Beclin-1 to the anti-

apoptotic proteins, thereby allowing an ample amount of Bcl-2 or Bcl-xL to be available for anti-apoptotic functioning (Maiuri *et al.*, 2007). The interaction between Beclin-1 and Bcl-2 or Bcl-xL proteins may be disrupted through phosphorylation or ubiquitination of Beclin-1. It can also be due to mutation of the BH3 domain of Beclin-1 or the BH3 receptor domains of the anti-apoptotic proteins. Alternatively, the disruption could occur due to a displacement of the weak interaction, allowing other BH3 only proteins to competitively bind to Bcl-2/ Bcl-xL (Maiuri *et al.*, 2007), thus releasing Beclin-1 to be available for autophagic activities.

Autophagy may serve as an adaptive survival mechanism to protect cells during stressful conditions or it could result in a self-destructive process. In malignancies, the role of autophagy remains debatable and maybe cancer subtype-specific. A number of studies have described the ability of autophagy to function as a tumour suppressant pathway (Laane *et al.*, 2009; Goussetis *et al.*, 2012; Tong *et al.*, 2013; Neri *et al.*, 2014; Ristic *et al.*, 2014), while others have documented it as a cancer survival pathway (Degenhardt *et al.*, 2006; Samaddar *et al.*, 2008; Wang *et al.*, 2014; Cheong *et al.*, 2016). Also, in non-cancer cells, several studies have presented conflicting reports about the involvement of autophagy in these cells. There have been contradicting reports of cell death due to upregulated autophagy (Matsui *et al.*, 2007; Song *et al.*, 2015; Pabón *et al.*, 2018) and cell survival (Hamacher-Brady *et al.*, 2006; McKnight *et al.*, 2014; Yazdankhah *et al.*, 2014). It is important to note that non-cancer cells are probably never defective of apoptosis and only induce the autophagic cell death pathway when there is no alternative pathway for them to die (Yonekawa and Thorburn, 2013).

The interactions of apoptotic and autophagic modulating proteins may result in the death or survival of cells. However, the exact mechanism by which their interactions differ in CML and AD models is yet to be elucidated. Thus, the exploration of the protein expression profiles, before and after drug treatments, is necessary to give an insight into the differential roles played by these proteins under normal physiological conditions in CML and AD models and to aid in better understanding the sensitivity of the cells towards cancer and AD drug treatments.

1.7 Summary of the choice of methodology

1.7.1 Rationale for an *in vitro* study

Clinical trials play a pivotal role in providing the evidential basis for modern therapies (Bondemark and Ruf, 2015; NIHR, 2019). The methodology involves the comparison of drug efficacy in patients suspected or diagnosed with a condition versus those confirmed not to have or are not showing any perceptible signs of the disease. However, it must be preceded by *in vivo* (animal studies) and *in vitro* work to help reduce cost while identifying the relevant biomarkers at the early stages of the conditions (Polli, 2008). In most disease conditions such as AD, there is no perfect disease model, however, it is essential that an appropriate preclinical model is selected to efficiently translate the findings from *in vitro* to human studies. The adoption of experimental models is highly dependent on the specific aspect to be investigated (Drummond and Wisniewski, 2017). Thus, in order to study specific pathways at the molecular levels in AD, *in vitro* studies are preferable. In oncology, the selection of the most effective therapy remains a major challenge and is dependent on continuous trials (Artemov *et al.*, 2015). Hence, *in vitro* studies are necessary to allow for a specie-specific, less complicated and more detailed analysis of the mechanism of drugs before progressing to animal and human studies. Moreover, the use of cancer cells distinctly similar to the parent histology from which they were obtained, allows for a more detailed study of the mechanisms involved and the direct comparison of experimental results (Greshock *et al.*, 2007). Undisputedly, clinical trials remain the gold standard for the evaluation of drug efficacy in humans, however, as mentioned above, they must be preceded by *in vivo* (animal studies) and *in vitro* work. *In vitro* studies may not fully simulate *in vivo* conditions but they form the bedrock for studying diseases at a molecular level in order to understand their molecular mechanisms. At Middlesex University, *in vivo* studies are currently not permitted for biomedical research. Hence, in this study, an *in vitro* model was employed for the investigation of the drug modulation of the pathways involved in CML and AD.

1.7.2 Selection of cell lines for the study

1.7.2.1 Selection of cell lines for CML model

Since the advent of TKIs, CML has had a better prognosis compared to the other forms of leukaemia. However, some patients still develop resistance to TKIs and advance to the deadly blast

crisis phase (Gorre *et al.*, 2001; Druker *et al.*, 2006; Prakash *et al.*, 2021). This resistant cancer prototype exhibits genes which are centrally involved in neoplastic changes and cellular differentiation. One important gene is BCR/ABL, which occurs as a result of the translocation balance of the Abelson gene (ABL1) from chromosome 9q34 with the breakpoint cluster region (BCR) gene on chromosome 22q11.2 (Jabbour and Kantarjian, 2018). The BCR-ABL protein generated is a constitutively active tyrosine kinase that influences a number of major signalling pathways. The use of established tumour cell lines which have the distinct phenotypic and karyotypic characters of CML have been extremely useful models in the molecular investigation of the disease (Table 1.1). One of such cell lines is K-562, which is derived from the pleural effusion of a 53-year old female CML patient in the myeloid blast phase (Lozzio and Lozzio 1975). Considering the great variability amongst CML cell lines, K-562 which has been well described in literatures and shows no difference in its transcript expression compared to CML patients (Drexler, 1994; Peng *et al.*, 2007; Sales *et al.*, 2019), was employed in this study.

Table 1.1 Features of some commonly used cell lines in CML studies

K-562 cells
<ul style="list-style-type: none"> ➤ K-562 is a CML cell derived from the pleural effusion of a 53-year old female patient in the terminal blast phase ➤ The cell line is the first CML-derived continuous cell line ➤ Erythroid lineage ➤ Ph+, -, BCR/ABL+: myeloid, erythroid (Lozzio and Lozzio 1975; Klein <i>et al.</i>, 1976; Drexler, 1994; Clarke and Holyoake, 2017)
KU812 cells
<ul style="list-style-type: none"> ➤ CML in myeloid blast phase ➤ Derived from the peripheral blood of a 38-year-old male patient in blast phase of CML (Clarke and Holyoake, 2017)
Bv-173
<ul style="list-style-type: none"> ➤ Bv-173 is a B-cell precursor leukaemia cell ➤ Derived from the peripheral blood of a 45-year-old man with CML in blast crisis ➤ Ph+ (Drexler, 1994; Clarke and Holyoake, 2017)
NALM-1
<ul style="list-style-type: none"> ➤ NALM-1 is a B-cell precursor lymphoid cell derived from the peripheral blood of a 3-year-old girl with CML in lymphoid blast phase ➤ Ph+ (Minowada <i>et al.</i>, 1977; Drexler, 1994; Clarke and Holyoake, 2017)
KCL-22
<ul style="list-style-type: none"> ➤ KCL-22 is Ph+ cells derived from the pleural effusion of a 32-year-old woman with CML in myeloid blast phase (Kubonishi and Miyoshi, 1983; Clarke and Holyoake, 2017)

KYO-1
<ul style="list-style-type: none"> ➤ CML in myeloid blast phase ➤ Derived from the peripheral blood of a 22-year-old man with CML in blast phase ➤ Ph+ ➤ Undifferentiated myeloid cell line (Ohkubo <i>et al.</i>, 1985; Clarke and Holyoake, 2017)
MOLM-1
<ul style="list-style-type: none"> ➤ CML in blast phase ➤ Derived from the bone marrow of a 41-year-old man with CML in blast phase ➤ Megakaryocytic lineage (Drexler, 1994; Clarke and Holyoake, 2017)
MOLM-6
<ul style="list-style-type: none"> ➤ CML in blast phase ➤ Derived from the peripheral blood of a 44-year-old man with CML in blast phase (Clarke and Holyoake, 2017)

1.7.2.2 Selection of cell lines for an AD-aspect model

Primary neuronal cells are suitable for neurological studies as they are more biologically relevant and resemble *in vivo* neurons (Gresch and Altrogge, 2012). However, mature neurons do not undergo cell division and therefore are challenging to culture *in vitro* to obtain sufficient cell numbers for experiments (Gordon *et al.*, 2013). This poses a challenge to reproducibly measure and interpret pharmacological data based on the primary neuronal cells. In addition, primary cell lines are also more difficult to transfect (Gordon *et al.*, 2013). Cell transfection will be necessary for further studies when developing an *in vitro* AD model expressing specific proteins. Several AD-related *in vitro* studies have successfully used immortalised cancer cells including SH-SY5Y (human neuroblastoma) (Feng *et al.*, 2009; Shi *et al.*, 2011; Liu *et al.*, 2011), IMR-32 (human neuroblastoma) (Lahiri *et al.*, 1994; Sarkar *et al.*, 2017), PC12 (rat pheochromocytoma) (Park *et al.*, 2008; Chen *et al.*, 2018) and MC65 (sub-clone of human neuroblastoma SK-N-MC) (Lin *et al.*, 2009). Non-cancerous cell lines have also been utilised in AD-related *in vitro* studies including CRL-2467 murine microglial cells (Zhao *et al.*, 2013) and HEK293 (human embryonic kidney) cells (Peters *et al.*, 2009; Zhu *et al.*, 2011; Rocchi *et al.*, 2017). The use of non-human mammalian cell lines overexpressing AD disease-related proteins was initially considered as models for the study, however, to limit the evolutionary gap between such models and humans, they were ruled out from utilisation in the present study. Table 1.2 provides a summary of some of the commonly used cell lines which were considered as AD models for this research.

Table 1.2 Features of some commonly used cell lines in AD studies

SH-SY5Y (human neuroblastoma)
<ul style="list-style-type: none"> ➤ SH-SY5Y includes both adherent and suspended cells as it was sub-cloned from SK-N-SH cell line, which has been reported to contain dual morphological phenotypes, similar to neuroblasts and epithelial cells (Ross <i>et al.</i>, 1983) ➤ Retinoic acid can be employed in the differentiation of SH-SY5Y cells resulting in characteristics similar to neurons while inhibiting epithelial growth. It aids the stimulation of a homogenous neuronal cell population, thereby allowing the cells in the culture to be at the same phase of the cell cycle. However, this forced differentiation manipulation could lead to inconsistent results even after the same differentiation treatment, maybe due to slight variation in passage number (Kovalevich and Langford, 2013).
HEK293 (Human Embryonic Kidney 293)
<ul style="list-style-type: none"> ➤ HEK293 is a human-derived fast-growing cell suitable for expression studies as the cell line possesses the biochemical ability to carry out most of the post-translational modifications to robustly express the protein of the artificially inserted nucleic acids (Thomas and Smart, 2005) ➤ The cell line is originated from a similar biological process as neurons and have similar regulatory mechanisms (protein folding, trafficking, translation, transcription) (Graham <i>et al.</i>, 1977) ➤ HEK293 shows characteristics of an immature neuron, expressing neurofilament subunits and neuron-specific proteins (Shaw <i>et al.</i>, 2002) ➤ HEK293T is a variant of HEK293 which contains the SV40 T-antigen and also neurological properties (Shaw <i>et al.</i>, 2002).
N-Tera-2/ NT2 (human embryonal carcinoma neuronal)
<ul style="list-style-type: none"> ➤ NT2 cells is a human-derived cell line isolated from a male patient with embryonal carcinoma ➤ The cell line can be induced into a neuronal culture with retinoic acid and other inhibitors of mitosis ➤ Retinoic acid can be used in the differentiation of NT2 cells to generate cells comprising of neuronal phenotype (Coyle <i>et al.</i>, 2011).
IMR-32 (human neuroblastoma)
<ul style="list-style-type: none"> ➤ IMR-32 is a human-derived cell line which may be differentiated via a multistep process to produce a complex feature associated with the cell line (Rao and Kisaalita, 2002) ➤ IMR-32 cells have been shown to form intracellular fibrillary material that reacts with anti-Paired helical Filament (PHF) specific antibodies, under certain culture conditions. Thus, is employed in APP and PHF (Hughes <i>et al.</i>, 1994; Neill <i>et al.</i>, 1994)
PC12 (rat pheochromocytoma of the adrenal medulla)
<ul style="list-style-type: none"> ➤ PC12 has a neural origin and is extensively used for neuronal studies involving neurosecretion, differentiation and neurite outgrowth (Westerink and Ewing, 2008) ➤ The cell line can be differentiated into neuronal-like cells by treating them with nerve growth factor (NGF) in the absence of serum (Gordon <i>et al.</i>, 2013)
HT-22 (mouse hippocampal neuronal)
<ul style="list-style-type: none"> ➤ HT-22 is a mouse neuronal cell line sub-cloned from HT-4 cells (Morimoto and Koshland, 1990) ➤ The cell line is usually employed in neuronal study involving glutamate-induced due to its sensitivity to glutamate (Pfeiffer <i>et al.</i>, 2014; Sato <i>et al.</i>, 2016)

No cell line optimally mimics AD. However, based on the characteristics of HEK293 (Table 1.2), the cellular aspect and pathways of interest in this study, the HEK293 variant, HEK293T cells, were employed as an *in vitro* model for this AD-related study. HEK293 was originally derived from the kidney cells of a human embryo and transformed by exposure to sheared adenovirus type 5 (Ad5) DNA in a laboratory in the Netherlands, in 1973 (Graham *et al.*, 1977). The cell line has been considered a kidney embryonic epithelial cell (Ashokkumar *et al.*, 2006; Cusick *et al.*, 2010), as well as fibroblasts (Cooper *et al.*, 1998; Yung *et al.*, 2012). Several studies have mentioned the cell as a non-neuronal cell line since they do not express the heterotetrameric amino acid receptors (NMDA) which functions as a membrane calcium channel and are essential for the activities of the excitatory neurotransmitter in the CNS (Grant *et al.*, 1997; Collett and Collingridge, 2004). However, there are contradictory reports that HEK293 cells are derived from a neuronal lineage as they exhibit some neuronal traits such as the expression of over 60 neuron-specific genes such as neurofilament proteins, neuroreceptors and other ion channel subunits (Berjukow *et al.*, 1996; Gunthorpe *et al.*, 2001; Shaw *et al.*, 2002; Thomas and Smart, 2005). It is thought that the adenovirus employed for cell transformation specifically targets neuronal lineage cells, turning on genes which could otherwise remain quiescent, even after the differentiation of the cells. Several variants of HEK293 cells have been developed. However, in this study, HEK293T, a variant that is able to amplify vectors containing the SV40 origin of replication, thus increasing protein expression levels during transfection (Lin *et al.*, 2014), was employed. HEK293T, was selected for this study for various reasons including, its human origin and neuronal lineage. Unlike some other human-derived cell lines used in AD studies, which had to undergo forced differentiation in order to express characteristics similar to neurons, HEK293T needed no such manipulation. Also, to rule out the issue of changes in karyotype, selection and tumorigenicity, HEK293T cells were utilised at low passage numbers of less than 10. Since very high passage numbers have been observed to be associated with tumorigenicity in the original HEK293 cell line (Shen *et al.*, 2008). Furthermore, due to the presence of SV40 origin of replication in its biochemical machinery, HEK293T is able and allows a robust expression of any protein of interest from artificially inserted nucleic acids (Thomas and Smart, 2005). This feature would be necessary for the transfection studies envisaged to follow this present one, wherein the expression of gene(s) of interest, related to AD, will be targeted and investigated.

1.7.3 Drug selection for the study

In order to investigate the common pathways involved in CML and AD, already known drugs used in the treatment of these conditions were utilized.

Imatinib is the gold standard, frontline therapy for CML (Johnson *et al.*, 2003; Medeiros *et al.*, 2018). Its specific mode of action helps reduce tyrosine kinase activity and prevents excess proliferation of cells in CML. Prior to drug selection, literature search was done to acquire more knowledge regarding the effects of Imatinib in the considered pathways as well as other molecular pathways (Table 1.3). Also, the cell types used as well as drug concentrations, were considered. Based on the importance of Imatinib in CML treatment and scientific findings, the drug was included in this study. However, due to drug intolerance or resistance, not all patients respond to Imatinib treatment and as such, the drug has been reported to fail or have a suboptimal response in some patients (Gorre *et al.*, 2001; Branford *et al.*, 2002; Stagno *et al.*, 2007; Baccarani *et al.*, 2013; Prakash *et al.*, 2021). Therefore, an alternative treatment strategy also needed to be considered.

In this study, K-562 cells were employed as cell models for the blast phase of CML. A phase where treatment is very worrisome due to mutations and increased drug resistance. In the blast crisis phase of CML, the cells are observed to act like ALL cells (Derderian *et al.*, 1993; Cortes *et al.*, 2016; Houshmand *et al.*, 2019). Acute lymphoblastic leukaemia cells have been shown to be more sensitive to chemotherapeutic drugs such as Vincristine, Dox and Dexamethasone (Kantarjian *et al.*, 2000). Dox is an anti-cancer agent with a different mode of cytotoxic action. The drug is a broad-spectrum antibiotic used in the treatment of cancers due to its potent killing effect (Gamen *et al.*, 2000; Pilco-Ferreto and Calaf, 2016). It is one of the most effective anti-cancer drugs reported to effectively reduce cell viability of cancer cells by inducing apoptosis, as a single drug or in combination (Sadeghi-Aliabadi *et al.*, 2010; Pilco-Ferreto and Calaf, 2016). Dox is one of the most useful anti-cancer agents and still represents the cornerstone in the therapy of many carcinoma types. For these reasons, further literature reviews were carried out on the molecular effects of Dox, considering the cell lines and drug concentrations used (Table 1.4) and Dox was also included in the study.

Table 1.3 *In vitro* effects of Imatinib in cancer and non-cancer cells

Experimental models	Drug(s) used (Conc.)	Incubation time	Molecular effects	References
*Chronic myeloid leukaemia K-562 cells	Imatinib (1 μ M)	48 h	<ul style="list-style-type: none"> ↑ apoptotic cell death ↑ LC3B-II (+ bafilomycin) ↑ senescence ↓ in p21 ↑ in p27 	Drullion <i>et al.</i> , 2012
*Human gastric cancer cell lines: AGS, MKN45, and SNU638 *Mouse Embryonic Fibroblasts (MEF)	Imatinib (30, 50, 100 μ M)	48 h	<ul style="list-style-type: none"> ↓ cell viability in all three gastric cancer cell lines ↓ cell proliferation in a time- and dose-dependent manner ↑ cell cycle arrest at the G2/M phase ↑ apoptosis in AGS and SNU638 cells ↑ ROS in AGS cells in a time-dependent manner 	Kim <i>et al.</i> , 2019
*BCR/ABL+ (K-562, BV173, KCL22, KU812, MC3, LAMA84) cell lines *BCR/ABL – (KG1, SU-DHL-1, U937, Daudi, NB4, NB4.306) cell lines *Non-neoplastic (PHA blasts, LAK, fibroblasts, LCL, renal epithelial cells, endothelial cells, CD34(+)) and fresh human leukemic cells	CGP57148B (Imatinib 0.1, 0.3, 1, 3, 10 μ M and 1,2,4,16 μ M)	1 h – 4 days	<ul style="list-style-type: none"> ↓ proliferation in all BCR/ABL+ cell lines ↑ apoptosis ↓ tyrosine phosphorylation in K-562 and LAMA84 cells 	Gambacorti-Passerini <i>et al.</i> , 1997
*Mouse neuroblastoma (N2a), muscle (C2C12), hypothalamic (GT1) cell lines *Murine neuronal septum (SN56 cells), fibroblast (NIH3T3) *Monkey kidney (COS-7, Vero) cell lines *Chinese hamster ovary cells CHO *Human lung carcinoma cell line (A549), peripheral blood mononuclear, semi-permanent foreskin fibroblasts	Imatinib (0.25 - 20 μ M)	24 h	<ul style="list-style-type: none"> ↑ in size and amount of lysosomes ↑ LC3-II ↑ autophagosomes in N2a, COS-7, A549, GTI, SN56 	Ertmer <i>et al.</i> , 2007
*Human leukaemia cell lines: K-562 and TK6 cells	Imatinib (0.01 - 10 μ M) Dox (0.001 - 1 μ M) Fucoxanthin (0.1 - 10 μ M)	24, 48, 72 h	<ul style="list-style-type: none"> ↑ cytotoxicity in TK6 cells ↓ proliferation in K-562 cells ↓ cell viability (both cell lines) ↓ proliferation (both cell lines) ↑ cytotoxicity in K-562 cells ↓ cell proliferation (both cell lines) ↓ Bcl-2 and caspase-3 	Almeida <i>et al.</i> , 2018

Where, ↑ = Activation, upregulation, induced

↓ = Deactivation, downregulation, inhibited

Table 1.4 Molecular effects of Dox in some experimental studies

Experimental models	Drug(s) used (Conc.)	Incubation time	Molecular effects	References
*Hela tumour cells	Dox (0.1, 1 and 2 μ M)	72 h	↓ cell survival	Sadeghi-Aliabadi <i>et al.</i> , 2010
	Simvastatin (0.25, 0.5, 1, 2, 5 and 10 μ M)		↑ cell viability (0.25 μ M) ↓ cell survival (2, 5 and 10 μ M)	
*Breast cancer cells MCF-10F, MCF-7, MDA-MB-231	Dox (1, 2, 4 and 8 μ M)	24 and 48 h	↓ cell viability ↑ apoptosis ↑ oxidative stress	Pilco-Ferreto and Calaf, 2016
*Male rats (Sprague Dawley; 500-520g)	Dox (12 mg/kg) (i.p administration)	Sacrificed 7 days later	↑ kidney damage ↑ oxidative stress ↑ apoptosis and necrosis	Lahoti <i>et al.</i> , 2012
*MCF-7 breast cancer cells	Adriamycin (1-5 μ M)	0 - 48 h	↑ apoptotic cell death	Leung and Wang, 1999
*Human hepatoblastoma cell line: HepG2	Taxol (50 nM) + Dox (5 μ M)	0 - 72 h	Inability of Bcl-2 protein alone to protect cells from drug-induced apoptosis	Luo <i>et al.</i> , 2000
*Acute myeloid leukaemia (MOLM-13, OCI-AML2) cells *U-937 histiocytic lymphoma monocytic cells *Chronic myeloid leukaemia K-562 cells	Dox (0.5, 1, 5 μ M)	48 h	↓ viability of MOLM-13 cells Selective toxicity against MOLM-13 vs U-937 cells ↓ proliferation in MOLM-13 cells ↑ apoptotic and necrotic death in U-937 cells ↓ Beclin-1 protein expression in MOLM-13 cells Bcl-2 (15-20 kDa isoform) was found to be selectively expressed in MOLM-13 cells only	Vu <i>et al.</i> , 2020

Where, ↑ = Activation, upregulation, induced

↓ = Deactivation, downregulation, inhibited

In the management of AD, a limited number of drugs have been approved. They include the acetylcholinesterase (AChE) inhibitors: Tacrine (NYT, 1993; NICE, 2011), Donepezil (ALZFORUM, 1996, NICE, 2011), Rivastigmine (ALZFORUM, 1996; NICE, 2011; Yiannopoulou and Papageorgiou, 2013), Galantamine (NICE, 2011; Kim and Park, 2017); the N-methyl-D-aspartate (NMDA) receptor antagonists, Memantine (Annicchiarico *et al.*, 2007; NICE, 2011) and the newly approved immunotherapeutic drug, Aducanumab. Tacrine was excluded from drug the selection because it is known for its cytotoxicity and has been banned in most countries (Satpute *et al.*, 2015). Also, for the lack of substantial evidence at the time of this research, Aducanumab was exempted from the study. Amongst the AChE, Donepezil was selected for various reasons. Firstly, the drug has an oral bioavailability of 100% compared to Rivastigmine and Galantamine which had a bioavailability of 71.7% and 88.5%, respectively. Donepezil also has a longer duration of action (70 to 80 h) in comparison to most of the other cholinesterase inhibitors (0.3 to 12 h). The drug has also been reported to show the least adverse effect, with Rivastigmine showing the highest out of the three AChE (Hansen *et al.* 2008). Donepezil has been observed as being involved in the apoptosis of acute promyelocytic leukaemia cells (Ki *et al.*, 2010). Memantine, the only approved NMDA antagonist which has been reported to promote cell survival by exerting anti-autophagic and anti-apoptotic effects, was also recruited for the study (Song *et al.*, 2015; Chen *et al.*, 2017). In cancers, such as prostate (Albayrak *et al.*, 2018) and breast (Seifabadi *et al.*, 2017) cancers, Memantine has been shown to induce apoptosis. Based on the multiple modes of action of these AD drugs, an AChE, Donepezil and NMDA antagonist, Memantine were selected for this study. Moreover, based on the author's literature findings, both drugs seemed to be the most documented in cancer research amongst all the approved AD drugs.

With extremely limited data available on the potential cancer-killing effect of neuroprotective drugs, it would be interesting to investigate the effects of Donepezil and Memantine in CML. Thus, both drugs were employed in this study along with approved frontline CML drug, Imatinib and the very potent chemotherapy drug, Dox.

1.7.4 Summary of the rationale for the study

Target-specific CML drugs are unable to eradicate all sub-clones of neoplastic stem cells in CML, particularly in the CNS. Therefore, it is necessary to investigate other non-target-specific cancer drugs, such as Dox, as well as drugs known to penetrate the CNS (Donepezil and Memantine), as alternative strategies for CML treatment. Currently, there are limited data comparing drugs for AD and CML. Therefore, studies involving the effect of these drugs as single treatments and in combination, in cell models of these diseases are warranted. Apoptosis and autophagy are two complex regulatory pathways common in AD and CML. Thus, investigating the modulation of these pathways by CML and AD drugs may help elucidate the possible interconnection between these two conditions and provide strategies to tackle them.

1.8 Aims and Objectives

1.8.1 Aim of the study

To study the crosstalk between cell apoptosis and autophagy in the modulation of cell death and to determine if AD medications, singly and in drug combination with a CML drug, has the potential to be repurposed for the treatment of CML.

1.8.2 Objectives of the PhD study

The objectives for achieving the aims were:

- To evaluate the effects of selected cancer (Imatinib and Doxorubicin) and AD (Memantine and Donepezil) drugs on apoptotic and autophagy pathways, using cell models of CML and AD.
- To investigate the effects of combination drug, Doxorubicin and Memantine, on the modulation of the apoptotic and autophagic pathways to attenuate death in the non-cancer cells without inhibiting the death of the CML cells.

1.8.3. Novelty of the research

AD drugs, such as Memantine, have been reported to have anti-cancerous effects via the NMDA channels. However, their role in the apoptotic and autophagic pathway of CML is limited. Herein, the molecular effects of selected AD and anti-cancer drugs were studied in a cell model of CML compared to non-cancerous HEK293T cells, under the same experimental conditions. Furthermore, as an innovative therapy approach, Memantine was combined with an anti-cancer drug, Doxorubicin, to complement its chemotherapeutic effect in CML while decreasing toxicity in non-cancer cells.

1.9 Outline of the thesis

Background literature, rationale, aims and objectives of this study have been provided in this chapter. Chapter 2 outlines the experimental procedures used to achieve the objectives of this PhD work. Chapter 3 reports the basal levels of apoptotic and autophagic proteins in cell models of CML (K-562) compared to AD (HEK293T). It also describes the effects of anti-cancer (Imatinib

and Dox) and AD (Donepezil and Memantine) drugs, as single-drug treatments in the cells. For further studies, a combination drug (Dox/Memantine) was selected based on the results acquired in chapter 3. Chapter 4 reveals the potentials of Dox/Memantine drug combination in K-562 and HEK293T cells. Chapter 5 summarises the key findings, overall discussion and conclusion of the study.

Chapter 2

Method

2. Method

2.1 Cell Culture and maintenance

Human embryonic kidney cells, HEK293T, from American Type Culture Collection (ATCC) was cultured in Dulbecco's Modified Eagle's Medium (DMEM) (Thermo Fischer Scientific, UK), while K-562 chronic myelogenous leukaemia cells (purchased from ATCC) were cultured in Gibco RPMI 1640 medium (purchased from Thermo Fischer Scientific, UK) as recommended by ATCC. The individual media were supplemented with 10% foetal bovine serum, 1% L-glutamine and 1% penicillin/streptomycin (sourced from Thermo Fischer Scientific, UK). The cells were maintained at 37°C in a 5% CO₂ humidified incubator. Cell passaging was performed at least twice a week or when the cells were about 80% confluent. All experiments carried out utilised cells at passage number 3 to 6. Trypan blue dye exclusion test was carried out using HyClone™ Trypan blue dye to determine the number of viable cells and cell viability of 97% and above was the accepted standard for proceeding with any experimental assay.

2.2 Trypan blue exclusion assay

Growing cells were assessed periodically and percentage cell viability was determined using the trypan blue exclusion assay. The method is based on the principle that live cells possess intact membranes which excludes dyes while dead cells have a compromised cell membrane that is penetrable by dyes. To determine the percentage viability of the cells (K-562 and HEK293T), an aliquot of the cell suspensions containing a convenient-to-count number of cells was centrifuged and re-suspended in 5 mL of media. A volume of the re-suspended cell suspension was then mixed with trypan blue dye in a 1:2 dilution and incubated for 2 min at room temperature. Afterwards, a drop of the cell-dye mixture was then applied on a clean haemocytometer and viewed under a light microscope. The number of viable (unstained) and dead (stained) cells were counted to determine the total number of cells. While the percentage of viable cells was calculated thus:

$$\text{Viable cells (\%)} = \frac{\text{Total number of viable cells per aliquot}}{\text{Total number of cells per aliquot}} \times 100$$

The assay was also utilised to determine the doubling time of the cells. The exponential phase was then determined and experiments were carried out using cells in this phase.

2.3 Cell viability measurement using CyQUANT® Direct assay

Human embryonic kidney cells (1×10^5 cells/mL) were individually treated with Memantine, Donepezil and Dox at final concentrations of 1, 5 and 10 μM for 24 and 48 h in 96 well plates. Cells treated with dimethyl sulfoxide (DMSO) (final conc. 0.05%) (vehicle) served as a control for the experiment. Actively dividing cells in their exponential phase were used for this experiment and the treatments were performed in triplicates. After the incubation periods, 48 μL of CyQUANT® Direct nucleic acid stain, a live cell-permeable reagent, and 240 μL of the background suppressor I masking dye both from the CyQUANT® Direct Cell Proliferation Assay kit (Invitrogen, UK) were combined with 11.7 mL of PBS, to make a total reagent-mix of 12 mL, which was sufficient for each microplate. CyQuant® Direct assay was the preferred option for assessing cell viability as it measures the DNA content of the cells, which is a tightly regulated indicator that directly correlates to cell number. The assay employs a combination of dyes. The masking dye blocks the staining of dead cells or cells with compromised cell membranes resulting in only healthy live cells being stained by the CyQuant® Direct nucleic acid intercalation dye. Following the preparation of the detection reagent-mix, 100 μL was added to the cell treatments in each well. The microplates were then incubated at 37°C for 40 minutes in the dark and fluorescence signals (excitation 485 nm, emission 520 nm) were detected using a microplate reader. Cell viability was quantified based on the number of stained live cells, which was linearly dependent on the fluorescence intensity given off by these cells.

2.4 Flow cytometry cell death assessment using double staining of AlexaFluor® 488 Annexin V/PI

HEK293T cells (1×10^6 cells/mL) were treated with Dox (final concentration of 1 μM , 5 μM), Imatinib (final concentrations of 1 μM), Memantine (final concentration of 1 μM , 5 μM , 10 μM) and Donepezil (final concentration of 1 μM , 5 μM , 10 μM). The same density of K-562 CML cells were also treated with Dox (final concentration of 1 μM), Imatinib (final concentrations of 1 μM) and Memantine (final concentration of 1 μM , 5 μM , 10 μM). Following a 48 h incubation period, the cells were harvested by centrifugation (5,000 rpm for 5 min), washed twice in cold PBS and re-suspended in 1X Annexin-binding buffer. The cell suspension was then stained with Alexa Fluor® 488 Annexin V (5 μL), propidium iodide (PI; 1 μL of 100 $\mu\text{g/mL}$) and incubated in the

dark at room temperature for 15 minutes. Prior to analysis using BD FACSCalibur flow cytometer, the cells were further diluted in 400 – 500 μ L of annexin-binding buffer.

Annexin V conjugated to the Alexa Fluor® 488 dye and Propidium iodide (PI) was used in combination to label and differentiate the cell population based on their membrane integrity and permeability. Healthy cells possess an intact plasma membrane composed of lipids which are distributed on the inner and outer surface of the membrane. One of such lipids located in the inner leaflet of the cell membrane is called phosphatidylserine (PS). In the early stages of apoptosis, the membrane of the cell is altered causing PS to be translocated from the inner to the outer part of the plasma membrane. Annexin V, is a calcium dependent phospholipid-binding protein with high affinity for PS. The protein (conjugated to a fluorescence dye) binds to the exposed PS on the cell surface causing the cells to show green fluorescence. During necrosis, the integrity of the plasma membrane decreases and the cells becomes permeable to PI, which causes cells to show red fluorescence. Hence, dead cells show both red and green fluorescence. Viable cells maintain an intact membrane and show little to no fluorescence. This dual staining technique allows for discrimination between viable, apoptotic and necrotic cells during the analysis on BD FACSCalibur flow cytometer. Flow cytometry is a valuable tool for the measurement of the properties of a population of cells. The technique is based on the principle of light scattering and emission of fluorescence as laser beam hits the cells. Detectors within the system are able to measure fluorescence in tagged cells, forward and side scatter which corresponds to the size and complexity of the cells, respectively.

BD CellQuest Pro Software was used for general data acquisition and analysis. The total event was set at 10,000. The fluorescence emission was measured at 530 nm (FL1) and 575 nm (FL3), using wavelength 488 nm excitation and the viable cell population which had a low fluorescence were distinguished from the non-viable cells based on the differential staining.

2.5 Gel electrophoresis and Western immunoblotting

2.5.1 Protein extraction and quantification

To probe for the expression of apoptotic and autophagy regulating proteins, as well as amyloid beta 40 and 42 proteins, gel electrophoresis and Western blot analyses were carried out. HEK293T and K-562 cells were individually treated with Dox (1 μ M), Imatinib (1 μ M), Donepezil (1, 5, 10 μ M) and Memantine (1, 5, 10, 20, 30, 50 μ M). K-562 cells were also treated with a combination

of Dox (1 μM) and chloroquine (1 μM). In a follow-up investigation, HEK293T as well as K-562 cells were treated with a combination of Dox (1 μM) and Memantine (1 μM). Following a 48 h incubation period, the drug-treated cells were harvested, washed with cold PBS buffer and lysed for total protein extraction. Cell lysing was carried out using Pierce™ RIPA Buffer (Thermo Scientific, UK) containing undiluted Halt Protease Inhibitor Cocktail (HPIC, Thermo Scientific, UK) to prevent proteolytic degradation during cell lysis and protein extraction. HEK293T adherent cells were scraped off the walls of the treatment flask. Cells were sonicated and centrifuged at 14,000 rpm for 10 min at (4°C). The total volume of supernatant containing the protein extracts were collected and the total protein concentration was determined using Bio-Rad Bradford protein assay reagent. Absorbance acquisition was determined with the aid of the FLUOstar Omega (BGM Labtech) plate reader at 595 nm wavelength. A standard curve was constructed based on the absorbance measurements of a set of protein standards whose concentrations (100 - 1500 $\mu\text{g}/\text{mL}$) span the range that can be quantified by the Bradford assay. Afterward, regression lines and equations were then generated and used to calculate the concentrations of the HEK293T and K-562 protein samples.

2.5.2 SDS-PAGE electrophoresis, immunoblotting and visualisation

Following protein quantification, protein samples (30 μg each) were separated using SDS-PAGE (sodium dodecyl sulfate polyacrylamide gel electrophoresis) technique, in Bio-Rad Mini-PROTEAN® TGX™ precast polyacrylamide gels. SDS is an anionic detergent that disrupts the tertiary structure of proteins, giving the molecules a negative charge. When the proteins have the same charge, their electrophoretic mobility is inversely proportional to the molecular size of the proteins, under a given electric field. Therefore, larger proteins receive more friction and migrate slower through the gel. For amyloid beta, separation was carried out using 18% acrylamide/ bisacrylamide tris-tricine gels due to the small size of the protein. Gel electrophoresis was carried out for 1h at a constant voltage of 100 V and then transferred onto a 0.2 μM Trans-Blot Turbo nitrocellulose membrane (Bio-Rad, UK). Due to the interaction of the proteins with SDS during gel electrophoresis, the negatively charged proteins can successfully migrate onto the anode-facing nitrocellulose membrane, under electric current. The membrane blots were blocked in 5% BSA or 5% non-fat milk (depending on the protein of interest to be probed) prepared in PBS containing 0.01% Tween-20 (PBS-T) for 1 h at room temperature.

Blocking steps were necessary to prevent background noise due to non-specific binding of antibodies. Subsequently, corresponding blots were incubated overnight, on a rocker at 4°C with the following primary antibodies (specific to the target protein) diluted in either 5% w/v BSA or non-fat milk, 1X PBS-T: anti-Bcl-2 (1:1000; cat#ab32124, Abcam), anti-Bcl-xL (1:1000; cat#ab32370, Abcam), anti-Bax (1:1000; cat#ab32503, Abcam), anti-Bak (1:1000; cat#ab32371, Abcam), anti-Cytochrome c (1:5000; cat#ab133504, Abcam), anti-Becclin-1 (1:2000; cat#ab207612, Abcam), anti-p62 (1:1000; cat#ab91526, Abcam), anti-LC3B (1:3000; cat#ab51520, Abcam), anti-beta Amyloid 1-42 (1:1000; cat#ab12267, Abcam) or anti-beta Amyloid 1-40 (1:1000; cat#ab20068, Abcam) and mouse monoclonal antibodies against the loading control, β -actin (1:3000 dilution; Bio-Rad, UK). After the overnight incubations, the membrane blots were washed with PBS-T prior to a 1 h incubation at room temperature with Goat Anti-Rabbit/ Anti-Mouse IgG (H+L)-HRP conjugated secondary antibody (Bio-Rad, UK). Secondary antibodies were selected based on their ability to recognise the host species used for producing each primary antibody. It was also ensured that the host animals for the primary and secondary antibodies differ in order to increase binding specificity. Antibody complexes were visualised using Thermo Scientific Pierce ECL Western Blotting Substrate. This chemiluminescent assay depends on the reaction between the HRP conjugated on the secondary antibodies and the luminol substrate, thereby emitting light which can be captured and measured to quantify the analyte in the sample. The protein band intensities were quantified using Image Studio Software on the Odyssey® Fc LI-COR Imaging System. Protein expressions were normalised to the loading control, β -actin. This was achieved by dividing the quantified expression of each protein by the corresponding β -actin detected in that same lane. The ratio obtained is more reliable than using the absolute expression values in comparing protein expression from one lane to another. This normalisation method helps to minimise or rule out the issue of variation which may arise from unequal sample loading across gel lanes and/or uneven transfer of proteins from gel to membrane.

2.6 Statistical analysis

Each procedure was performed in at least three independent experiments and data were expressed as mean \pm standard error of the mean (S.E.M.). Statistical analyses were performed using Minitab 18® software. Normality and equal variance tests were conducted to determine if the data were

parametric. Parametric data were then analysed using one-way ANOVA for group analyses with the application of Tukey test. Statistical significance was accepted when p-value was found to be less than or equal to 0.05. All relevant outputs of the statistical analyses performed are in the Appendices (I – X).

Chapter 3

Evaluation of the effects of selected leukaemic and Alzheimer's disease drugs on the apoptotic and autophagy pathways using cell models for AD and CML

3. Evaluation of the effects of selected leukaemic and Alzheimer's disease drugs on the apoptotic and autophagy pathways using cell models for AD and CML

3.1 Introduction

CML is a stem cell disease in which the presence of BCR-ABL oncoprotein causes an unregulated growth and accumulation of myeloid leukaemia cells in the bone marrow and blood (Wang *et al.*, 2014). Unlike non-cancer cells, these genetically altered cells are able to devise multiple ways to circumvent cell death (Wuilleme-Toumi *et al.*, 2005; Agrawal *et al.*, 2008; Sakuma *et al.*, 2013; Zhao *et al.*, 2014). One such mechanism is the modulation of proteins involved in the apoptotic pathway, perhaps through the increased and decreased expressions of anti-apoptotic (such as Bcl-2 and Bcl-xL) and pro-apoptotic (such as Bax, Bak and Cytochrome C) proteins, respectively. The de-stabilisation of these proteins inhibits dimerisation of the pro-apoptotic proteins in the mitochondrial outer membrane through the counteraction of the anti-apoptotic proteins, thereby suppressing apoptotic death in leukaemic cells. Apoptotic proteins may also interact with autophagy-related proteins (including Beclin-1, LC3-I, LC3-II and p62). Thus, dysregulation of apoptosis may be involved in the poor regulation of autophagy, contributing to poor treatment outcomes.

Presently, Imatinib is the gold standard, frontline therapy for CML treatment (Johnson *et al.*, 2003; Medeiros *et al.*, 2018). The drug is action-specific and inhibits the growth of CML cells by competitively binding to BCR-ABL oncoprotein (Capdeville *et al.*, 2002; Druker, 2008; Moschovi and Kelaidi, 2021). However, during the deadly blast crisis phase of CML, where the cells resemble AML cells, the prognosis is dismal. Hence, a more aggressive therapy, such as Dox, is often included (Bassan *et al.*, 1987; American Cancer Society, 2022). Dox is known for its effectiveness against several cancers, including haematological (Panaretakis *et al.*, 2002; Li *et al.*, 2019), stomach (Florou *et al.*, 2013) and breast (Pilco-Ferreto and Calaf, 2016) cancers, due to its ability to interact with a cell's DNA structure. This results in the inhibition of the action of DNA-associated enzymes, leading to cell death (Meriwether and Bachur, 1972; Momparler *et al.*, 1976). However, due to the non-selective killing action of Dox (Wang *et al.*, 2004; Li *et al.*, 2016; Fraczkowska *et al.*, 2018), there is a need to study ways of reducing its toxicity in non-cancerous

cells. Interestingly, a number of studies have reported Donepezil (Ki *et al.*, 2010) and Memantine (Kamal *et al.*, 2015; Seifabadi *et al.*, 2017; Yoon *et al.*, 2017; Albayrak *et al.*, 2018) as possessing anti-cancer properties. This raises the possibility of repurposing AD drugs for the treatment of cancers such as CML. However, little is known about the mode of action that AD drugs exert to give the cytotoxic effect in cancer cells, with almost no report on their effects in CML. Therefore, in this chapter, two intricately connected pathways (apoptosis and autophagy) which may respond to the same key regulatory proteins were investigated to evaluate how therapeutically relevant doses of established anti-cancer and AD drugs may possibly modulate these pathways in *in vitro* models of CML and AD.

3.2 Aims and Objectives

3.2.1 Aim of the study

To investigate the molecular effects of leukaemic and AD drugs in the modulation of the apoptotic and autophagic pathways in cell models of CML (K-562 cells) and AD (HEK293T cells).

3.2.2 Objectives of the study

- To determine if AD drugs (Donepezil and Memantine) exert an inhibitory effect on the viability of non-cancerous HEK293T cells compared to Dox
- To determine the cell death effects induced in leukaemic- and AD- drug-treated K-562 and HEK293T cells
- To compare the basal levels of apoptotic and autophagy proteins in K-562 and HEK293T cells
- To evaluate how leukaemic and AD drugs, as individual drug treatments, are able to modulate the apoptotic and autophagic pathways in the investigated cell lines
- To select potential compounds for a combinational drug study

3.3 Results

3.3.1 Method development

3.3.1.1 Growth pattern of K-562 and HEK293T cell lines incubated under normal growth conditions

Under normal growth conditions, the pattern of growth for K-562 CML cells and non-cancerous HEK293T cells were periodically assessed to ensure that the growth condition was optimal for the cells to be investigated. A representative of a trypan blue dye exclusion assay carried out is shown in Figure 3.1. The growth of the cells was observed to increase slowly during the lag phase as a result of the initial adaptation of the cells to the growth environment. The lag phase was then followed by the exponential (log) growth phase. The doubling time for both cell lines was approximately 24 h. All experiments were carried out with cells showing growth within the exponential phase. Cell viability was required to be 97% or above before proceeding with any experimental assay.

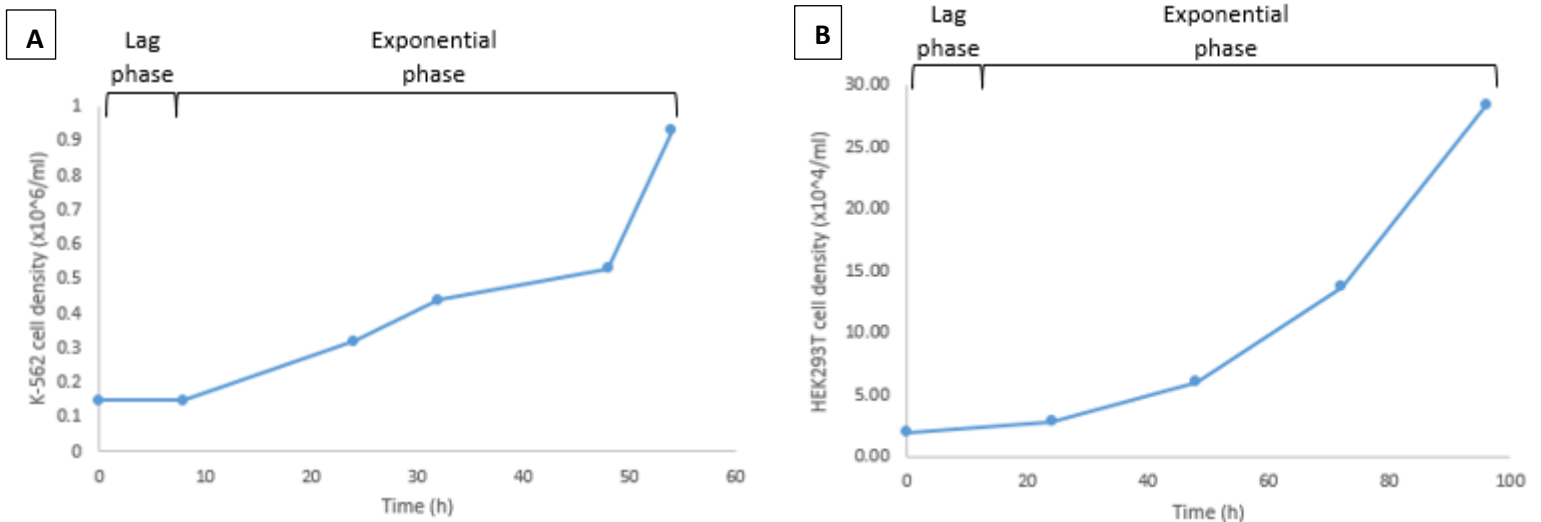


Figure 3.1 Growth curve of K-562 and HEK293T cell lines under normal growth conditions

Trypan blue assay was used to assess the growth pattern of viable (A) K-562 cells within a 54 h incubation period (B) HEK293T cells within a 96 h incubation period. The doubling time for both cell lines was approximately 24 h.

3.3.1.2 The effect of the vehicle (dimethyl sulfoxide) on K-562 and HEK293T cell lines

To determine if the solvent had an effect on the cell viability of K-562 and HEK293T, the cells were incubated in DMSO (final conc. 0.05%) and the effect was compared to cells separately co-incubated in culture media (RPMI or DMEM) for 24, 48 and 72 h. Cell viability test was then conducted using CyQUANT® Direct assay. An initial decrease in K-562 and HEK293T cells incubated in media for 24 h compared to the 0 h (control cells), was observed (both $p < 0.01$). However, the cell viability of K-562 cells was later (at 72 h) observed to increase significantly compared to the control cells ($p < 0.05$). No statistically significant difference was observed between cells treated with 0.05% DMSO (vehicle control) compared to untreated cells in media ($p > 0.05$) (Figure 3.2). As the test drugs required organic solvent for dissolution, for further experiments DMSO (final conc. 0.05%) was used for the drug preparations and as vehicle control.

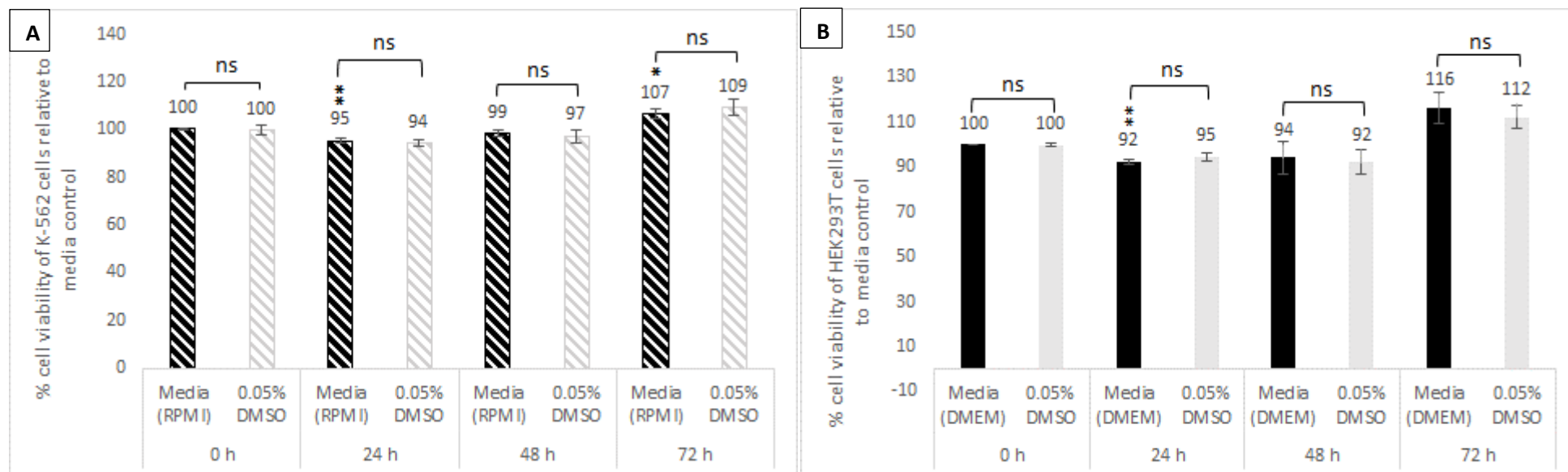


Figure 3.2 Effect of the vehicle (DMSO) on the cell viability of incubated K-562 and HEK293T cell lines

CyQUANT® Direct assay was employed to measure the cell viability of (A) K-562 and (B) HEK293T cells after 24, 48 and 72 h incubation in DMSO (final conc. 0.05%) compared to media control. Experiments were repeated three times and data are expressed as mean \pm SE of percentage control. Basic statistical analysis was performed using 2-sample t-test and significant difference are shown as: * when $p \leq 0.05$, significant; ** when $p \leq 0.01$, highly significant. No statistical difference, indicated as 'ns', was seen between the cells incubated in 0.05% DMSO versus cells in media control.

3.3.2 Dox inhibited the cell viability of non-cancerous HEK293T more potently than Memantine and Donepezil

In order to determine if the established AD drugs, Memantine and Donepezil, had an effect on the growth of non-cancerous HEK293T cells at therapeutically relevant concentrations, cell viability was assessed using CyQUANT® Direct assay. HEK293T cells were treated separately with 0.05% DMSO (the vehicle control), 1, 5 and 10 μM of Dox, Memantine and Donepezil. Dox, an anthracycline antibiotic known to be toxic to both non-cancerous and cancerous cells served both as a test compound and a positive control drug in the experiment (Figure 3.3).

Dox inhibited the cell viability in a dose- and time-dependent manner with a very high statistical significance ($p < 0.001$, at all three concentrations) compared to the vehicle control (Figure 3.3). At 48 h, the drug reduced cell viability by 64%, 88% and 93% in 1, 5 and 10 μM Dox-treated HEK293T cells, respectively (Figure 3.3).

When treated with Memantine, HEK293T cells showed no statistically significant difference from the untreated control cells ($p > 0.05$), except for the 24 h Memantine 1 μM -treated cells, which increased viability by 41% ($p < 0.05$). Contrary to this, the lowest tested concentration of Donepezil (1 μM) significantly inhibited cell viability by 49% ($p < 0.01$) and 43% ($p = 0.001$) at 24 and 48 h, respectively, compared to the vehicle control. However, a higher concentration of Donepezil (10 μM) induced a slight but statistically significant increase in the viability of HEK293T cells at 48 h ($p < 0.05$) (Figure 3.3). Noteworthy is that time (24 and 48 h) did not affect the activities of Memantine or Donepezil (at 1, 5 and 10 μM) (Appendix IIB). However, the activity of Memantine (1 μM) was observed to be significantly different from the inhibitory action observed in the Donepezil (1 μM)-treated HEK293T cells at both the 24 and 48 h time point tested ($p < 0.05$) (Appendix IIIB).

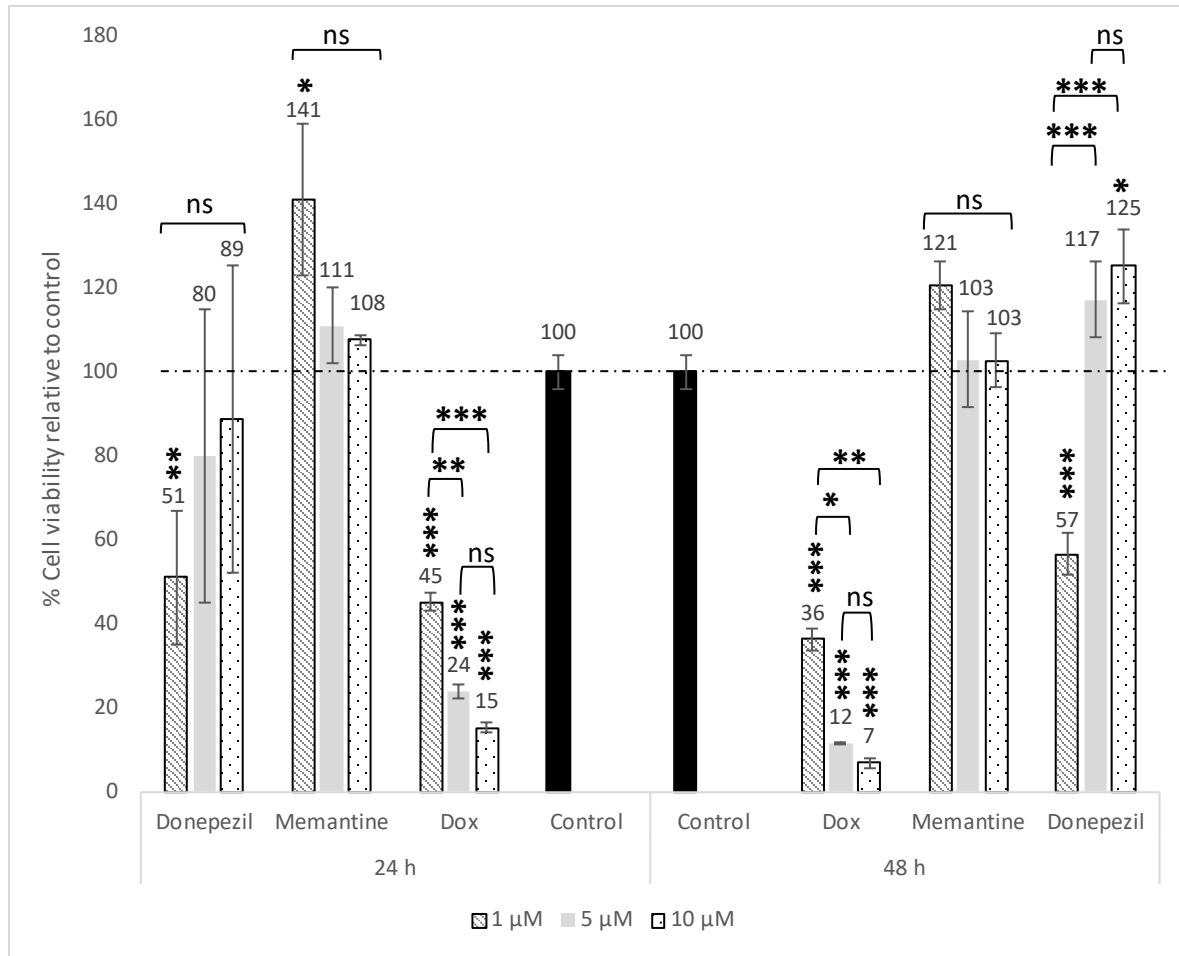


Figure 3.3 The effect of Donepezil and Memantine on HEK293T cell growth compared to Dox

The cell viability of HEK293T cells treated with Dox, Memantine and Donepezil (1, 5 and 10 μM) was assessed using CyQUANT® Direct assay. Dox inhibited HEK293T cell viability in a dose- and time-dependent. At the lowest concentration tested (1 μM), Memantine increased the cells viability. On the other hand, Donepezil (1 μM) inhibited HEK293T cell viability by 49% and 43% at the 24 and 48 h, respectively. But at the highest dose of tested (10 μM), Donepezil caused an increased cell viability at 48 h.

Experiments were repeated at least three times and the data are expressed as mean ± SE. Statistical analysis was performed using one-way ANOVA, Tukey post-hoc test for grouping and pairwise comparison. Basic statistics were performed using 2-sample t-test to compare HEK293T cells treated with 0.05% DMSO versus media. Statistical differences were accepted as: $p > 0.05$, no significance (ns); *, $p \leq 0.05$, significant; **, $p \leq 0.01$, highly significant; ***, $p \leq 0.001$, very highly significant.

3.3.3 Memantine and Donepezil did not promote apoptotic death in HEK293T and K-562 cells, in contrast to the effect of Dox

Unusually, Donepezil at a low concentration of 1 μM showed more cytotoxic effect to HEK293T cells than at higher concentrations (5 and 10 μM) (Figure 3.3). In order to verify the validity of these results, cell death analyses using Annexin V/PI assay were carried out on Donepezil-treated HEK293T cells. For comparison, the effects of Memantine on HEK293T and K-562 cells were also assessed. All cell treatments were compared to the vehicle cells, which acted as the negative control. Dox (5 μM) and Imatinib (1 μM) were employed as positive controls for HEK293T and K-562 cells, respectively.

Minimal cell death (< 5%) was observed in all Memantine and Donepezil drug-treated HEK293T and K-562 cells (Table 3.1). However, when the Memantine treatments were compared in both cell lines, Memantine 1, 5 and 10 μM were shown to kill 9.6%, 11.6% and 10% more K-562 cells than HEK293T cells, respectively. This effect was found to be significant in Memantine 10 and 1 μM treated cells ($p < 0.05$).

At 48 h, Dox 1 and 5 μM killed 37% and 57% of HEK293T cells, respectively, which was significant compared to the untreated HEK293T negative control cells ($p < 0.01$) (Table 3.1). Dox (1 μM) also decreased the cell viability in K-562 cells by 26% compared to the control cells ($p < 0.05$). However, 11% more HEK293T cells were observed to be killed compared to the cancerous K-562 cells ($p < 0.05$) (Table 3.1). When K-562 cells were incubated in Imatinib (1 μM), the drug caused a reduction in the viability of the CML cells by 23% at 48 h, compared to the control cells ($p < 0.05$). Even though Dox (1 μM) reduced K562 cell viability by 3% more than observed in Imatinib (1 μM)-treated cells, the difference was not statistically significant ($p > 0.05$) (Table 3.1).

Table 3.1 Cell death effects of anti-cancer and AD drugs in HEK293T and K-562 cells

Treatments	HEK293T		K-562	
	Viable cells	Non-viable cells	Viable cells	Non-viable cells
Control cells	97.6 ± 0.10	2.4 ± 0.10	88.0 ± 1.22	12.0 ± 1.22
Dox 5 µM	43.0 ± 1.50***	57.0 ± 1.50	NT	NT
Dox 1 µM	63.1 ± 2.36**	36.9 ± 2.36	74.1 ± 0.84*	25.9 ± 0.84
Donepezil 10 µM	98.6 ± 0.28	1.5 ± 0.28	NT	NT
Donepezil 5 µM	98.0 ± 0.07	2.0 ± 0.07	NT	NT
Donepezil 1 µM	96.5 ± 0.76	3.5 ± 0.76	NT	NT
Memantine 10 µM	98.9 ± 0.16	1.1 ± 0.16	88.9 ± 0.19	11.1 ± 0.19
Memantine 5 µM	98.7 ± 0.10	1.3 ± 0.10	87.1 ± 3.11	12.9 ± 3.11
Memantine 1 µM	99.3 ± 0.53	0.7 ± 0.53	89.7 ± 0.79	10.3 ± 0.79
Imatinib 1 µM	NT	NT	77.1 ± 1.97*	22.9 ± 1.97

The results are presented as the mean cell population (%) ± standard error. n=2. Statistical difference was accepted as *, p ≤ 0.05, significant; **, p ≤ 0.01, highly significant; ***, p ≤ 0.001, very highly significant. compared to untreated cells. NT = not tested

3.3.4 K-562 and HEK293T cells expressed contrasting amounts of proteins at basal level

Before studying the modulation of proteins in drug-treated cells, the expression levels of some proteins involved in apoptosis (Bcl-2, Bcl-xL, Cytochrome c, Bak and Bax) and autophagy (Beclin-1, p62, LC3) were investigated in HEK293T and K-562 cells under basal (untreated) cell growth conditions.

K-562 cells showed lower basal expressions of the pro-apoptotic proteins (Cytochrome c, Bak and Bax) (all $p \leq 0.001$) and a higher level of anti-apoptotic Bcl-xL ($p = 0.01$) compared to HEK293T cells (Figure 3.4A & C). The levels of Bcl-xL in K-562 cells were observed to be 3.8 times higher than the amount detected in HEK293T cells (Figure 3.4C). However, the expression of anti-apoptotic Bcl-2 in the leukaemia K-562 cells was below the detection level (Figure 3.4C).

Beclin-1 was highly expressed in both cell lines, with HEK293T showing a 2.9-fold higher expression compared to K-562 cells ($p < 0.01$, Figure 3.4C). The level of the autophagosome formation proteins (LC3-II/ LC3-I) was 2.6-fold higher in HEK293T than in the CML cells ($p < 0.05$, Figure 3.4C). Also, there was an 8.6-fold less expression of p62 proteins in HEK293T compared to K-562 cells which were very highly significant ($p < 0.001$) (Figure 3.4C).

In order to assess the basal level of amyloid beta proteins expressed in the HEK293T cells, amyloid beta 40 and 42 proteins were probed. However, the proteins were observed to be below the limit of detection (Figure 3.4B).

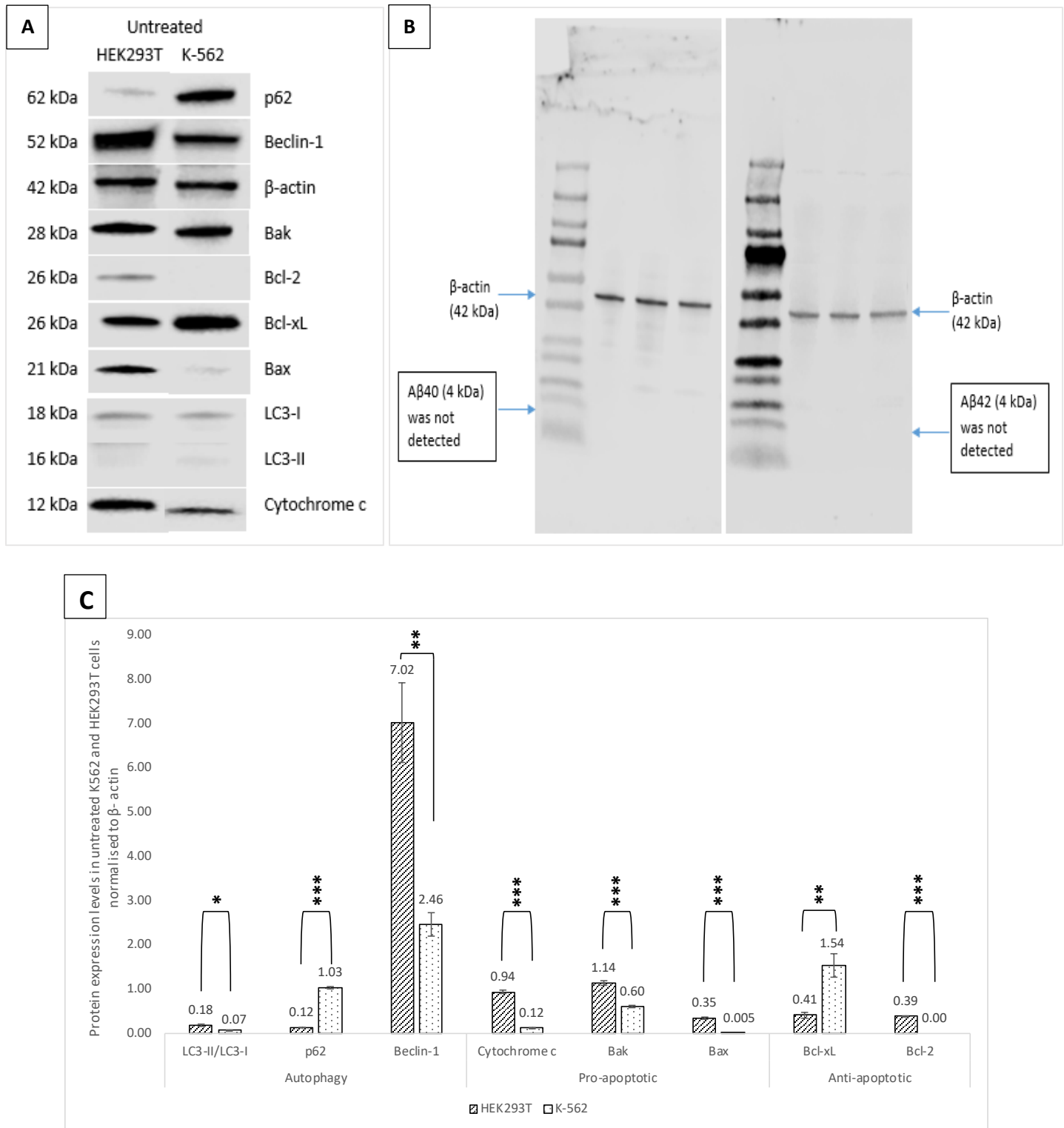


Figure 3.4 Basal protein levels expressed in HEK293T and K-562 cell lines

(A) Representative blot image showing the protein expression levels in 48 h incubated HEK293T and K-562 cells

(B) Representative blot image for Aβ40 and Aβ42 probing in HEK293T cells. Aβ protein was below the limit of detection

(C) Bar chart showing the detected apoptotic and autophagy protein levels, normalised to β-actin

Protein expressions were determined using Western blot analyses. Unstressed K-562 cells showed greater survival ability compared to HEK293T cells by downregulating the expression of pro-apoptotic proteins.

Experiments were repeated three times and data are expressed as mean ± SE. Basic statistical analysis was performed using 2-sample t-test and significant differences were shown as: * when $p \leq 0.05$, significant; ** when $p \leq 0.01$, highly significant; and ***, $p \leq 0.001$, very highly significant.

3.3.5 Imatinib promoted the expression of pro-apoptotic proteins in K-562 cells

To determine the effect of the first-line treatment for CML, K-562 cells were treated with Imatinib (1 μ M) and compared to the non-cancerous HEK293T cells.

In HEK293T cells, Imatinib increased the expression of pro-apoptotic Bak ($p = 0.001$) as well as anti-apoptotic Bcl-2 ($p < 0.001$) and Bcl-xL ($p = 0.01$) proteins (Figure 3.5B & C). A 5-fold increase of Bax proteins was also observed in these cells but was not statistically significantly different from the untreated HEK293T cells (Figure 3.5B). In addition, Imatinib had no effect on the expression of Cytochrome c in the HEK293T cells ($p > 0.05$) (Figure 3.5B).

For the autophagic markers, a decrease in the levels of Beclin-1 was observed, however, the 1.2-fold decrease was not statistically different compared to the levels of Beclin-1 expressed in untreated HEK293T cells ($p > 0.05$) (Figure 3.5D). LC3 protein levels were also unaffected by Imatinib treatment but the sequestosome1-multifunctional adaptor protein, p62/SQSTM1, was increased 8.2-fold ($p < 0.001$) (Figure 3.5D).

When the apoptotic markers were assessed in Imatinib-treated K-562 cells, the CML cells showed an increase in Bak ($p < 0.05$) and Cytochrome c ($p = 0.001$) expressions with a concomitant decrease in the level of anti-apoptotic Bcl-xL ($p < 0.01$) (Figure 3.5B & C). However, the 1.3-fold Bak increase observed in the Imatinib-treated K-562 cells ($p < 0.05$, compared to untreated K-562 cells) was much lower compared to the 10.2-fold change increase observed in Imatinib-treated HEK293T cells ($p = 0.001$, compared to untreated HEK293T cells; $p = 0.001$, comparison between the cells) (Figure 3.5B). Also, the very low levels (near to the detection limit) of Bax and the non-detectable levels of Bcl-2 which were observed in untreated K-562 cells were not significantly altered by Imatinib treatment (Figure 3.5B & C).

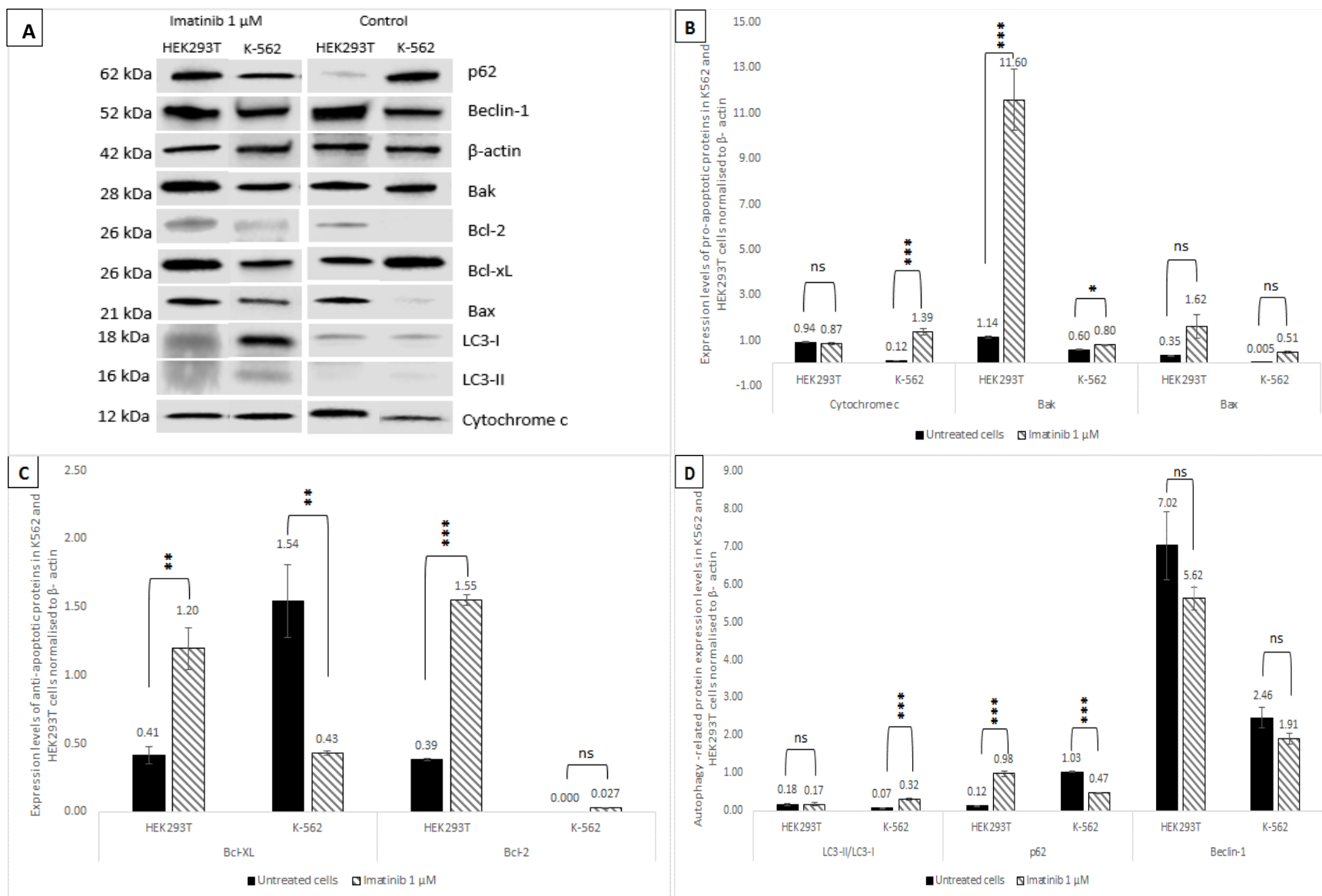


Figure 3.5 Effects of Imatinib on the levels of proteins involved in apoptosis and autophagy in HEK293T and K-562 cell lines after 48 h treatment

(A) Representative Western blot image

(B) Pro-apoptotic proteins: Cytochrome c, Bak and Bax (C) Anti-apoptotic proteins: Bcl-xL and Bcl-2 (D) Autophagy-related proteins: LC3, p62 and Beclin-1

Imatinib modulated the apoptotic pathway. In K-562 cells it caused an increase in the levels of Bak and Cytochrome c, while decreasing the levels of Bcl-XL proteins. But in HEK293T cells, the drug increased the levels of Bcl-XL as well as Bcl-2 anti-apoptotic proteins.

Data were normalised to β-actin expression levels. Experiments were repeated thrice and data are expressed as mean ± SE. Basic statistical analysis was performed using 2-sample t-test and significant differences were shown as: $p > 0.05$, no significance (ns); * when $p \leq 0.05$, significant; ** when $p \leq 0.01$, highly significant and ***, $p \leq 0.001$, very highly significant.

3.3.6 Dox modulated both the apoptotic and autophagy proteins in HEK293T and K-562 cells

The effects of Dox (1 μ M) on different proteins involved in the apoptotic and autophagic pathways were evaluated.

In both cell lines (HEK293T and K-562) tested, Dox had no significant effect on the levels of anti-apoptotic Bcl-2 proteins expressed, compared to their individual controls ($p > 0.05$, for both cell lines). However, the drug caused an 8.6 and 6-fold decrease in the levels of Bcl-xL in K-562 and HEK293T cells, respectively, when compared to their untreated control cells ($p < 0.01$, for both cell lines) (Figure 3.6C).

When the pro-apoptotic proteins were evaluated, Dox-treated HEK293T cells showed a 3.5-fold reduction, 1.1 and 1.4-fold increase in the expressions of Bax ($p < 0.01$), Bak ($p < 0.05$) and Cytochrome c proteins, respectively, compared to the untreated HEK293T control cells (Figure 3.6B).

In the Dox-treated K-562 cells, there was a significant decrease of 1.9-fold in the levels of pro-apoptotic Bak proteins compared to the untreated K-562 cells ($p < 0.001$) (Figure 3.6B). Also, the initially observed low levels of Bax proteins (0.005, normalised to β -actin) were observed to further decrease below the level of detection. However, these decreased levels were not significant when compared to the low levels of Bax in the untreated K-562 cells ($p > 0.05$) (Figure 3.6B). Despite the reduced levels observed in both pro-apoptotic Bak and Bax proteins, a statistically significant high amount of 8.8-fold increase of Cytochrome c protein was detected, compared to the untreated K-562 control cells ($p = 0.001$) (Figure 3.6B).

When autophagy proteins were assessed, Dox-treated K-562 cells showed a 1.4-fold increase in the levels of Beclin-1 protein compared to the untreated K-562 cells ($p < 0.05$). Also, in comparison to the untreated K-562 control cells, Dox-treated K-562 cells showed a very highly significant increase of LC3-II to LC3-I ratio ($p < 0.001$) with an extremely low level of p62 proteins, which was below the limit of detection ($p = 0.001$) (Figure 3.6D). In contrast to K-562 cells, in Dox-treated HEK293T cells, an accumulation of p62 proteins occurred ($p < 0.001$), as the level of Beclin-1 declined 2-fold compared to the control ($p = 0.001$) (Figure 3.6D).

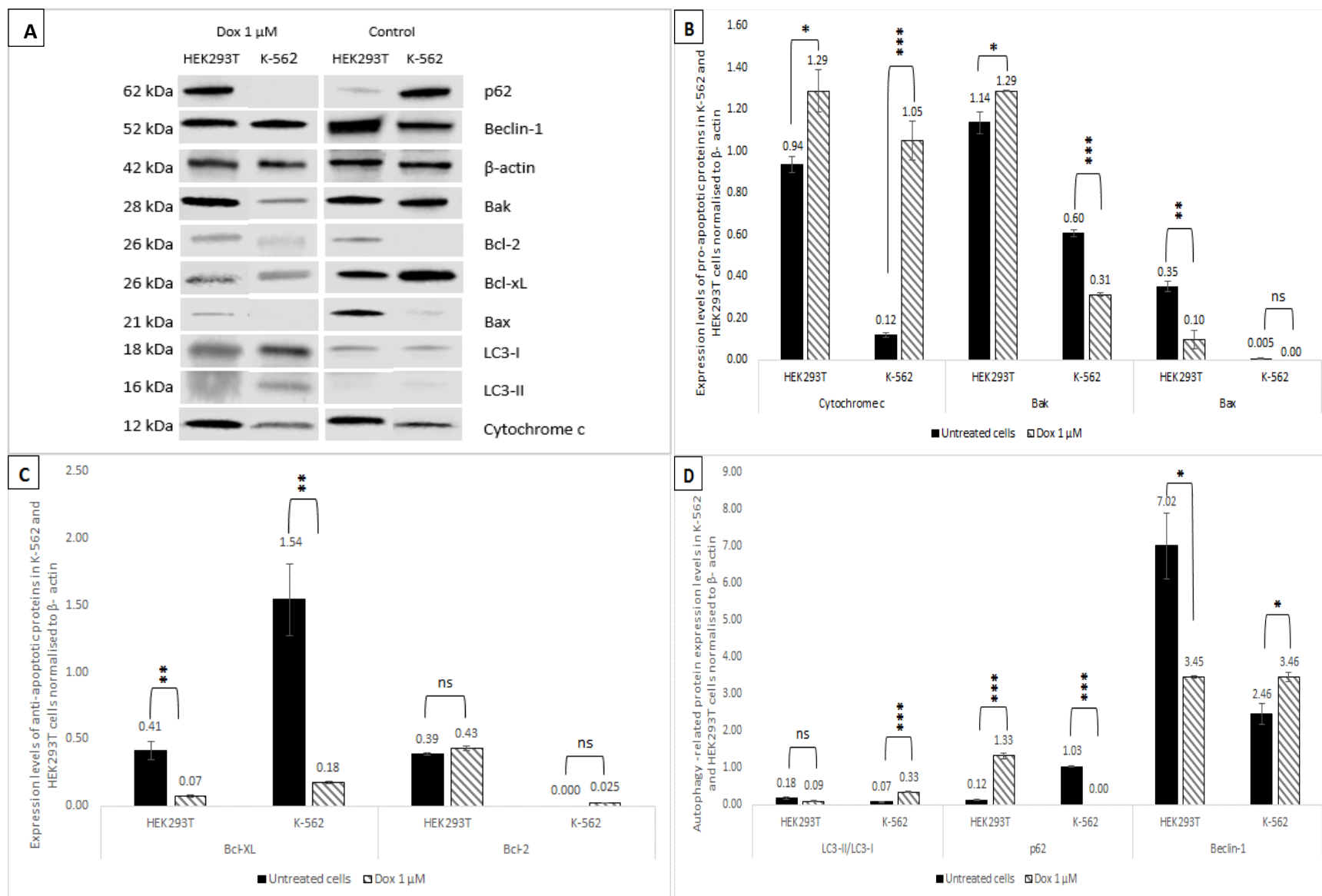


Figure 3.6 Effects of Dox on the levels of proteins involved in apoptosis and autophagy in HEK293T and K-562 cell lines after 48 h treatment

(A) Representative Western blot image

(B) Pro-apoptotic proteins: Cytochrome c, Bak and Bax (C) Anti-apoptotic proteins: Bcl-xL and Bcl-2 (D) Autophagy-related proteins: LC3, p62 and Beclin-1

Dox modulated the apoptotic and autophagy pathways. The drug downregulated the levels of Bcl-XL and upregulated Cytochrome c in both K-562 and HEK293T cell lines. In the autophagy pathway, Dox induced an increase in the autophagic activities in K-562 cells but reduced it in HEK293T cells.

Data were normalised to β-actin expression levels. Experiments were repeated thrice and data are expressed as mean ± SE. Basic statistical analysis was performed using 2-sample t-test and significant differences were shown as: p > 0.05, no significance (ns); * when p ≤ 0.05, significant; ** when p ≤ 0.01, highly significant and ***, p ≤ 0.001, very highly significant.

3.3.6.1 Chloroquine-induced autophagy inhibition upregulated Bcl-2 and downregulated Cytochrome c in Dox-treated K-562 cells

In order to verify if the autophagy activities absent in HEK293T but observed in Dox (1 μ M)-treated K-562 cells acted as a cytoprotective mechanism or contributed to its cytotoxic death effects, chloroquine diphosphate (CQ) was employed to cause a blockage in the observed autophagy flux in K-562 cells.

The incubation of K-562 cells with Dox (1 μ M) alone showed autophagic activities with the involvement of upregulated Beclin-1 proteins (Figure 3.6D). When the CML cells were treated with CQ (10 μ M), there was still no significant effect on the expression levels of Beclin-1 compared to the levels observed in untreated and Dox 1 + CQ 10 (μ M) combination-treated cells, respectively (both $p > 0.05$) (Figure 3.7B).

When the final stage of autophagy was probed through the investigation of p62 (an adaptor protein which itself is degraded during autophagy), the levels of the proteins remained unchanged in the CQ-treated cells compared to the untreated K-562 control cells ($p > 0.05$) (Figure 3.7B). However, these unchanged p62 protein levels were very significantly higher when compared to K-562 cells treated with Dox alone, where an undetectable level was initially observed ($p < 0.001$) (Figure 3.7B).

An examination of the Dox-CQ combination-treated K-562 cells showed a 1.7-fold decrease in p62 levels compared to the untreated control cells ($p < 0.001$) (Figure 3.7B). The combination-treated cells also showed an increase in p62 proteins when compared to Dox and a decrease when compared to CQ, both with very high statistically significant differences ($p < 0.001$) (Figure 3.7B).

Furthermore, the effect of the CQ-induced autophagy inhibition was examined in the apoptotic pathway. The treatment of K-562 cells with CQ showed an increase in the expression levels of anti-apoptotic Bcl-2 proteins compared to the untreated control and Dox 1 μ M treated K-562 cells (both $p < 0.001$) (Figure 3.7C). When the Dox-CQ combination-treated cells were examined, the cells showed a level of Bcl-2 which was very significantly higher than the untreated control cells ($p < 0.001$) and 7.7-fold higher compared to the levels observed in the K-562 cells treated with Dox 1 μ M alone ($p < 0.001$) (Figure 3.7C). However, these Bcl-2 levels in the Dox-CQ-treated K-562 cells remained 1.4-fold lower than the levels observed in K-562 cells treated with CQ alone ($p < 0.05$) (Figure 3.7C).

For pro-apoptotic protein, Cytochrome c, CQ-treated K-562 cells resulted in a non-significant increase of the protein compared to the untreated control cells ($p > 0.05$) (Figure 3.7C). However, these increased Cytochrome c levels were observed to be 3.3-fold lower than the amount expressed in Dox-treated K-562 cells ($p = 0.001$) (Figure 3.7C). When the Dox-CQ combination-treated cells were assessed, a 1.9-fold non-significant increase in Cytochrome c was measured ($p > 0.05$, compared to the untreated control cells). These levels were also observed to be lower (5-fold) than the amounts expressed in the Dox-treated K-562 cells ($p < 0.001$) (Figure 3.7C).

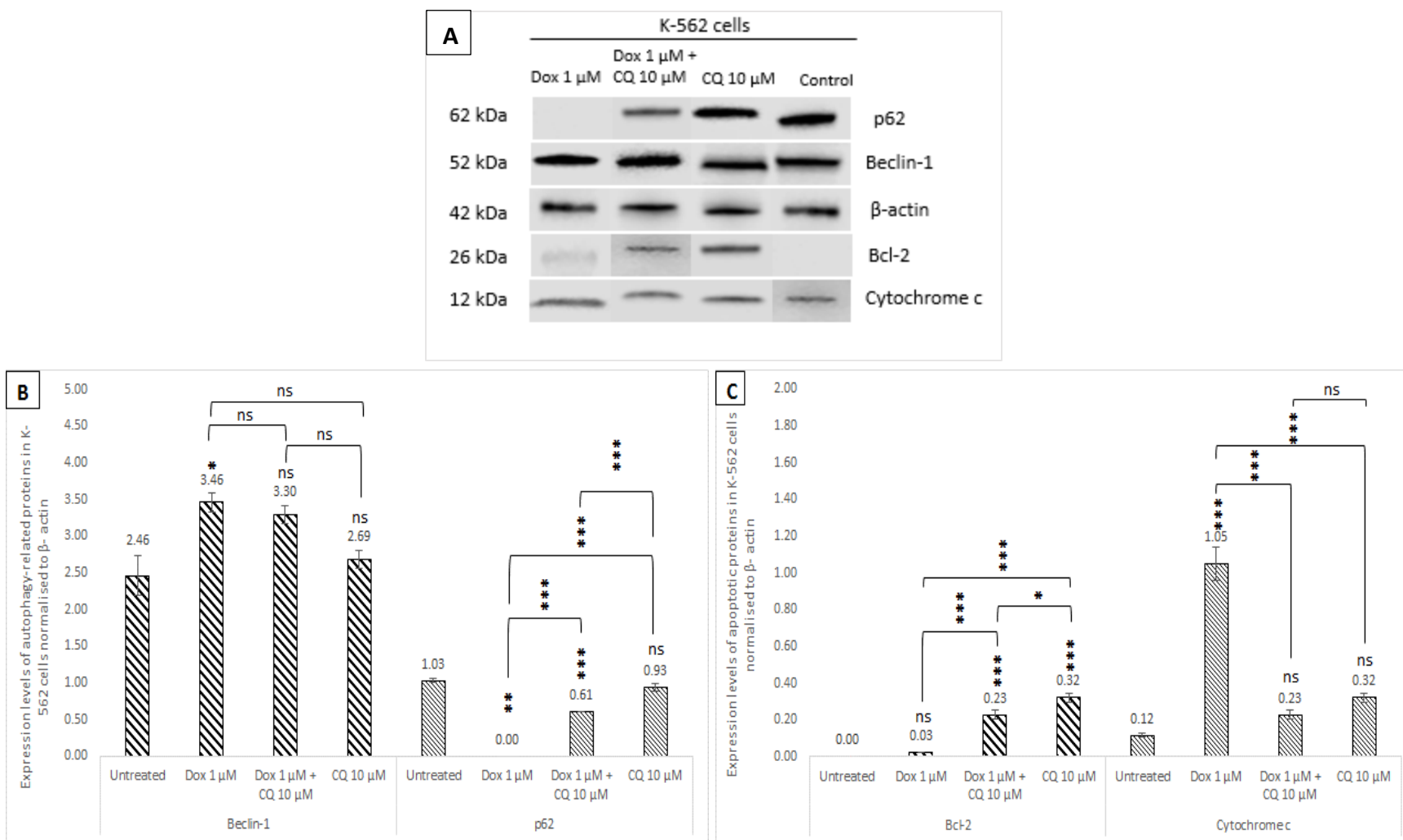


Figure 3.7 Effects of Dox-CQ co-incubation compared to Dox or CQ sole treatments on the levels of proteins involved in apoptosis and autophagy in K-562 cell lines after 48 h treatment

(A) Representative Western blot image

(B) Autophagy-related proteins: Beclin-1 and p62

(C) Anti-apoptotic Bcl-2 and pro-apoptotic Cytochrome c

Cells were treated with Dox (1 μ M) + CQ (10 μ M), Dox (1 μ M) or CQ (10 μ M) and protein expressions were determined using Western blot. The CQ-treated K-562 cells indicated autophagy blockage through the increase of p62 levels. The levels of anti-apoptotic Bcl-2 was also elevated in these autophagy-inhibited K-562 cells.

Data were normalised to β -actin expression levels. Experiments were repeated at least twice and data are expressed as mean \pm SE. Statistical analysis was performed using one-way ANOVA, Tukey test and the statistical differences amongst treatments and/or controls were accepted as: $p > 0.05$, no significance (ns); * when $p \leq 0.05$, significant; ** when $p \leq 0.01$, highly significant and ***, $p \leq 0.001$, very highly significant.

3.3.7 Donepezil inhibited autophagy activities in HEK293T cells

The effects of Donepezil (1, 5 and 10 μM) on different proteins involved in the apoptotic and autophagic pathways of HEK293T and K-562 cells were evaluated.

An upregulation of Bak proteins by 8, 4.9 and 6.7-fold was observed in HEK293T cells treated with 1, 5 and 10 μM of Donepezil, respectively (Figure 3.8B). In addition, Cytochrome c levels were also increased except in the 5 μM Donepezil-treated cells, where a 1.3-fold decrease was observed but this was statistically non-significant compared to the untreated control cells ($p > 0.05$) (Figure 3.8B). The levels of Bax proteins were also increased in the HEK293T Donepezil-treated cells, however, the increase was not significant compared to the control ($p > 0.05$) (Figure 3.8B).

When anti-apoptotic proteins were examined, Bcl-2 was observed to be upregulated at all concentrations of Donepezil tested ($p < 0.01$) (Figure 3.8C). The levels of Bcl-xL were also increased in Donepezil-treated HEK293T cells. However, the 3.5 and 3.9-fold increases observed in Donepezil 5 μM and 10 μM treated cells, respectively, were not significant when compared to the untreated HEK293T control cells ($p > 0.05$) (Figure 3.8C). At the lowest concentration, Donepezil 1 μM , which was initially observed to reduce HEK293T cell viability (Figure 3.3), showed a significant increase of 4.9-fold in the expression level of Bcl-xL proteins ($p < 0.05$) (Figure 3.8C).

In K-562 cells, Cytochrome c levels were increased by 4.8, 8.5 and 8.3-fold in 1, 5 and 10 μM Donepezil-treated cells, respectively ($p < 0.01$) (Figure 3.8B). The levels of Bax proteins were also increased in K-562 cells. However, the 6-fold increase observed at the lowest concentration of Donepezil tested, 1 μM , was not statistically significant compared to the untreated K-562 cells ($p > 0.05$) (Figure 3.8B). The levels of Bak showed a non-significant increase of 1.2, 1.3 and 1.3-fold in Donepezil 1, 5 and 10 μM -treated K-562 cells, respectively (Figure 3.8B).

The assessment of the anti-apoptotic proteins in K-562 cells showed that the levels of Bcl-xL in all concentrations of Donepezil tested were not statistically different from the untreated K-562 control cells ($p > 0.05$) (Figure 3.8C). Also, the expression of Bcl-2, which was initially observed to be below the limit of detection, was increased in all the Donepezil-treated K-562 cells. However, this increase was not significantly different when compared to the control ($p > 0.05$) (Figure 3.8C).

In the autophagy pathway, all Donepezil treatments showed a highly significant decrease in the levels of Beclin-1 in HEK293T ($p \leq 0.001$, at all three concentrations) with upregulation of p62 proteins ($p < 0.01$, at all three concentrations) (Figure 3.8D). The levels of LC3-II/LC3-I in the Donepezil 1 and 5 μM -treated HEK293T cells were increased by 3 and 2.3-fold, respectively ($p < 0.01$) (Figure 3.8D).

In K-562 cells, Beclin-1 levels were also highly significantly decreased in all Donepezil treatments compared to the untreated K-562 control cells ($p < 0.01$, at all three concentrations). The levels of p62 showed no statistically significant change compared to the control ($p > 0.05$), except at the highest concentration of Donepezil (10 μM), where a 1.4-fold reduction was observed ($p < 0.05$) (Figure 3.8D). An increase of 4.3, 1.6 and 1.1-fold in LC3-II/LC3-I levels was observed in Donepezil 1, 5 and 10 μM -treated K-562 cells, respectively. However, the increase was non-significant when compared to the untreated K-562 cells (Figure 3.8D).

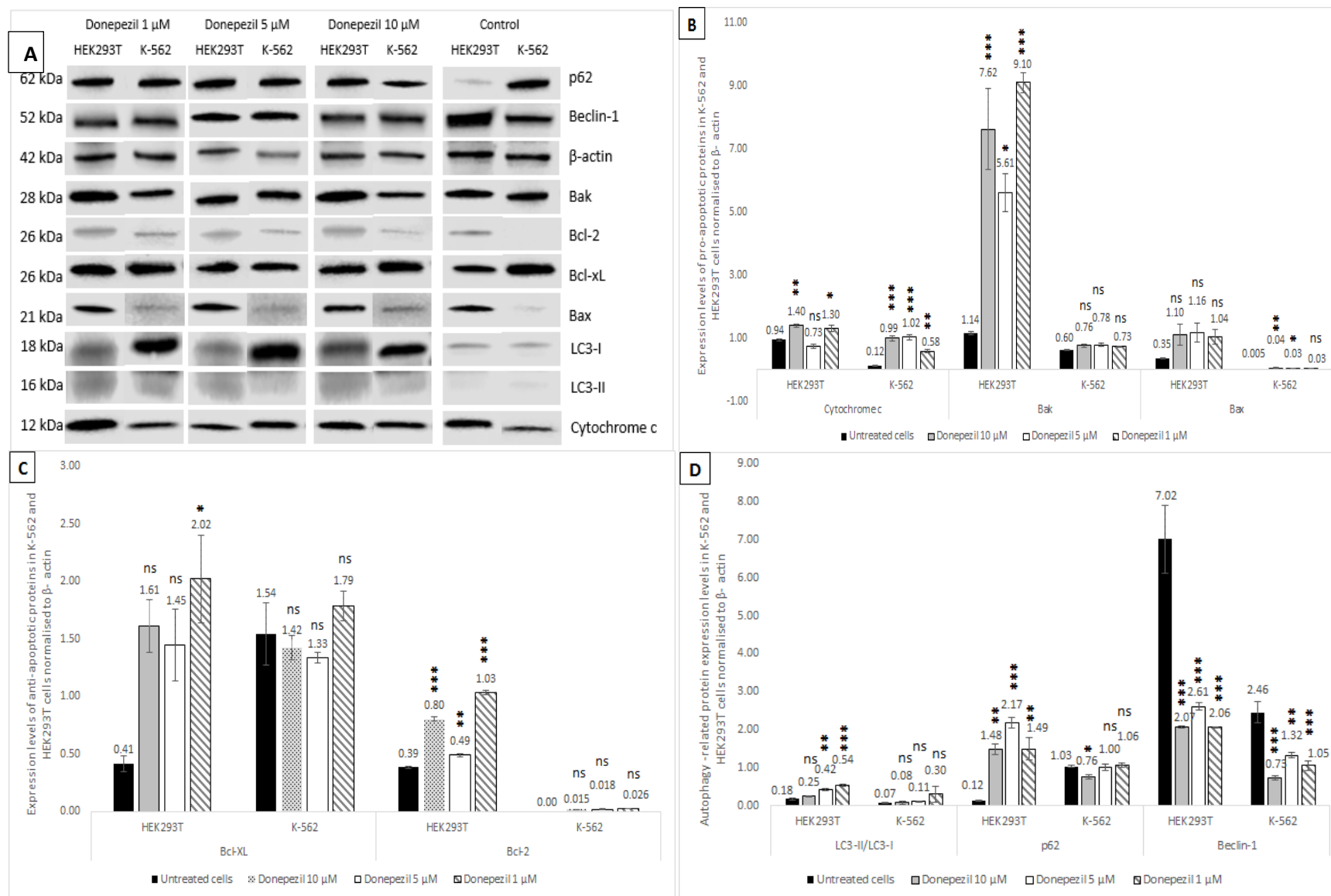


Figure 3.8 Effects of Donepezil on the levels of proteins involved in apoptosis and autophagy in HEK293T and K-562 cells lines after 48 h treatment

(A) Representative Western blot image

(B) Pro-apoptotic proteins: Cytochrome c, Bak and Bax (C) Anti-apoptotic proteins: Bcl-xL and Bcl-2 (D) Autophagy-related proteins: LC3, p62 and Beclin-1

Cells were treated with Donepezil (1, 5, 10 μM) and protein expressions were determined using Western blot. In K-562 cells, at 5 and 10 μM Donepezil induced an increase in Bax levels. Cytochrome c was also upregulated in the K-562 cells at all concentrations tested. In the autophagy pathway, Donepezil was observed to reduce autophagy activities in HEK293T cells by reducing Beclin-1 levels and increasing the expression of p62.

Data were normalised to β-actin expression levels. Experiments were repeated thrice and data are expressed as mean ± SE. Basic statistical analysis was performed using 2-sample t-test and significant differences were shown as: p > 0.05, no significance (ns); * when p ≤ 0.05, significant; ** when p ≤ 0.01, highly significant and ***, p ≤ 0.001, very highly significant.

3.3.7.1 The levels of pro-apoptotic and anti-apoptotic regulators determine the fate of cells

In order to verify if HEK293T Donepezil 1 and 10 μM -treated cells, which showed an increase in both pro-apoptotic (including Cytochrome c) and anti-apoptotic proteins (Figure 3.8B & C), were more susceptible to apoptotic cell death rather than survival, the Bax:Bcl2 and Bax:Bcl-xL ratios were examined.

The ratio of Bax:Bcl2 was increased by 10%, 161% and 50% in Donepezil 1, 5 and 10 μM -treated HEK293T cells, respectively (Figure 3.9). However, Bax:Bcl-xL ratio was observed to decrease by 37% and 16% in Donepezil 1 and 10 μM -treated HEK293T cells, respectively (Figure 3.9). However, both alterations of Bax:Bcl2 and Bax:Bcl-xL ratios were non-significant compared to the untreated HEK293T control cells ($p > 0.05$). The levels of Bax:Bcl-xL in Donepezil 5 μM -treated HEK293T cells remained unaltered (Figure 3.9).

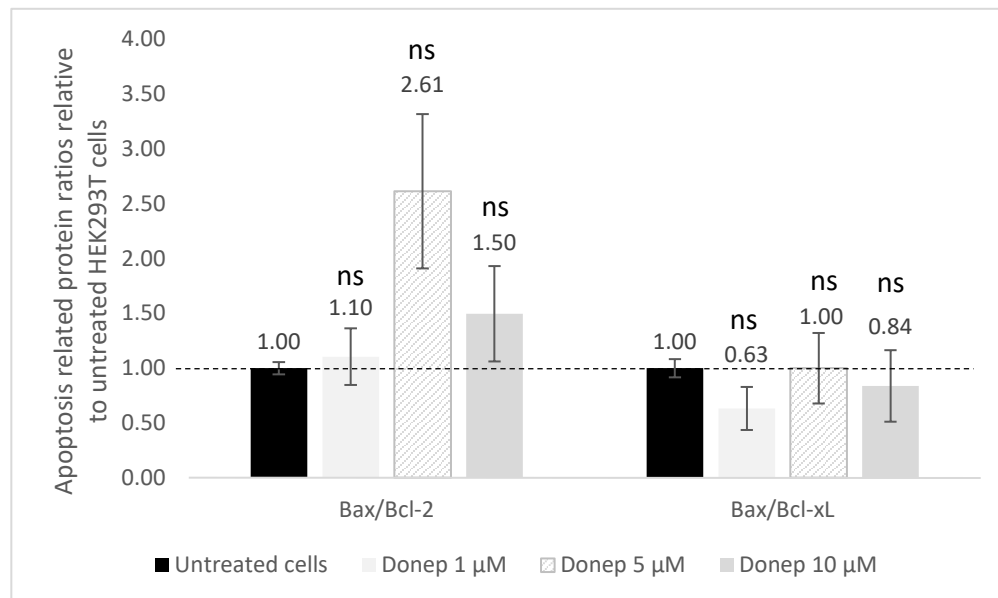


Figure 3.9 Effects of Donepezil on apoptotic-related protein ratios in HEK293T cells

Cells were treated with Donepezil (1, 5, 10 μM) and protein expressions were determined using Western blot. Donepezil-treated HEK293T cells (48 h) showed no modification to Bax:Bcl-2 nor Bax:Bcl-xL ratios. Protein expression levels were normalised to β -actin and expressed as mean \pm SE ($n=3$). Basic statistical analysis was performed using 2-sample t-test and no statistical difference, indicated as 'ns', was seen between the untreated HEK293T control cells versus the Donepezil-treated cells.

3.3.8 Memantine upregulated anti-apoptotic proteins in HEK293T cells but not in K-562 cells

Following the ability of the NMDA receptor antagonist, Memantine, to promote cell viability in HEK293T cells (Figure 3.3), the drug was investigated to determine its effects in the apoptotic and autophagy protein expression levels in both non-cancerous HEK293T and K-562 CML cells.

In the autophagy pathway, a highly significant decrease of 2.1, 1.7 and 1.7-fold in Beclin-1 levels were observed in HEK293T cells incubated in Memantine 1, 5 and 10 μM , respectively ($p < 0.01$, for all three concentrations), compared to the untreated cells. The levels of p62 proteins in these Memantine-treated cells were also observed to be significantly upregulated, compared to the untreated HEK293T control cells ($p < 0.01$, at all three concentrations) (Figure 3.10D). When LC3-II to LC3-I ratio were measured, the levels of the autophagosome formation marker in Memantine (5 and 10 μM)-treated HEK293T cells were observed to be non-significantly altered, except in HEK293T cells treated with the lowest tested concentration of Memantine, 1 μM , which showed a highly significant 2.2-fold increase ($p < 0.01$) (Figure 3.10D).

In K-562 cells, Beclin-1 showed a very highly significant 2.5, 2.1 and 2-fold decrease in Memantine 1, 5 and 10 μM treatments, respectively, compared to the untreated K-562 control cells ($p < 0.001$, at all three concentrations) (Figure 3.10D). The levels of p62 and LC3-II/LC3-I proteins were increased at the same Memantine concentrations. However, the 1.5-fold increase of p62 observed in Memantine 5 μM -treated K-562 cells as well as the increased levels of LC3 in Memantine 1, 5 and 10 μM -treated cells, were not significantly different from the untreated control cells ($p > 0.05$) (Figure 3.10D).

To determine if higher doses of Memantine would have a different effect on the protein levels expressed compared to the investigated lower concentrations (1, 5 and 10 μM), 20, 30 and 50 μM of Memantine were included in the experimental study.

In HEK293T cells, Beclin-1 levels were observed to remain low showing a decrease of 2.7, 2.8 and 2.5-fold in Memantine 20, 30 and 50 μM -treated cells compared to the untreated HEK293T control cells ($p < 0.001$, at all three concentrations) (Figure 3.10D). The expression levels of p62 in these higher-concentration Memantine-treated cells were lowered to the level of the control.

LC3-II/LC3-I was reduced below the control levels and was non-significant when compared to the untreated cells ($p > 0.05$) (Figure 3.10D).

When the pro-apoptotic proteins were investigated, the high concentrations (20, 30 and 50 μM) of Memantine exerted a 3.6, 2.1 and 2.4-fold reduction in the levels of Cytochrome c in HEK293T cells, respectively ($p < 0.01$, at all three concentrations). But at the lower tested concentrations, the high levels of Cytochrome c remained similar to the control, except at 5 μM where a significant increase of 1.4-fold was observed ($p < 0.01$) (Figure 3.10B). In Bax proteins, an increase of 5.3, 1.7 and 4.2-fold was observed in HEK293T cells treated with Memantine 1, 5 and 10 μM , respectively. However, the Bax levels decreased, even below the control and showed a 3.5, 2.5 and 1.9-fold reduction when the cells were treated with the higher concentrations of 20, 30 and 50 μM of Memantine, respectively, compared to the untreated cells. None of the changes in the Bax levels were significant when compared to the untreated HEK293T control cells ($p > 0.05$) (Figure 3.10B). Furthermore, pro-apoptotic Bak levels were also observed to increase in HEK293T cells treated with low doses of Memantine. At 5 μM , a significant increase of 4.7-fold was observed ($p < 0.05$), while Memantine 1 and 10 μM treatments induced a very highly significant increase of 9.5 and 11.8-fold of Bak proteins, respectively ($p < 0.001$) (Figure 3.10B). At higher concentrations of Memantine, Bak levels were much lower but still showed a 3.3, 1.6 and 1.8-fold increase compared to untreated cells. However, the Bak increased levels observed at these higher concentrations were not significant compared to the control ($p > 0.05$) (Figure 3.10B).

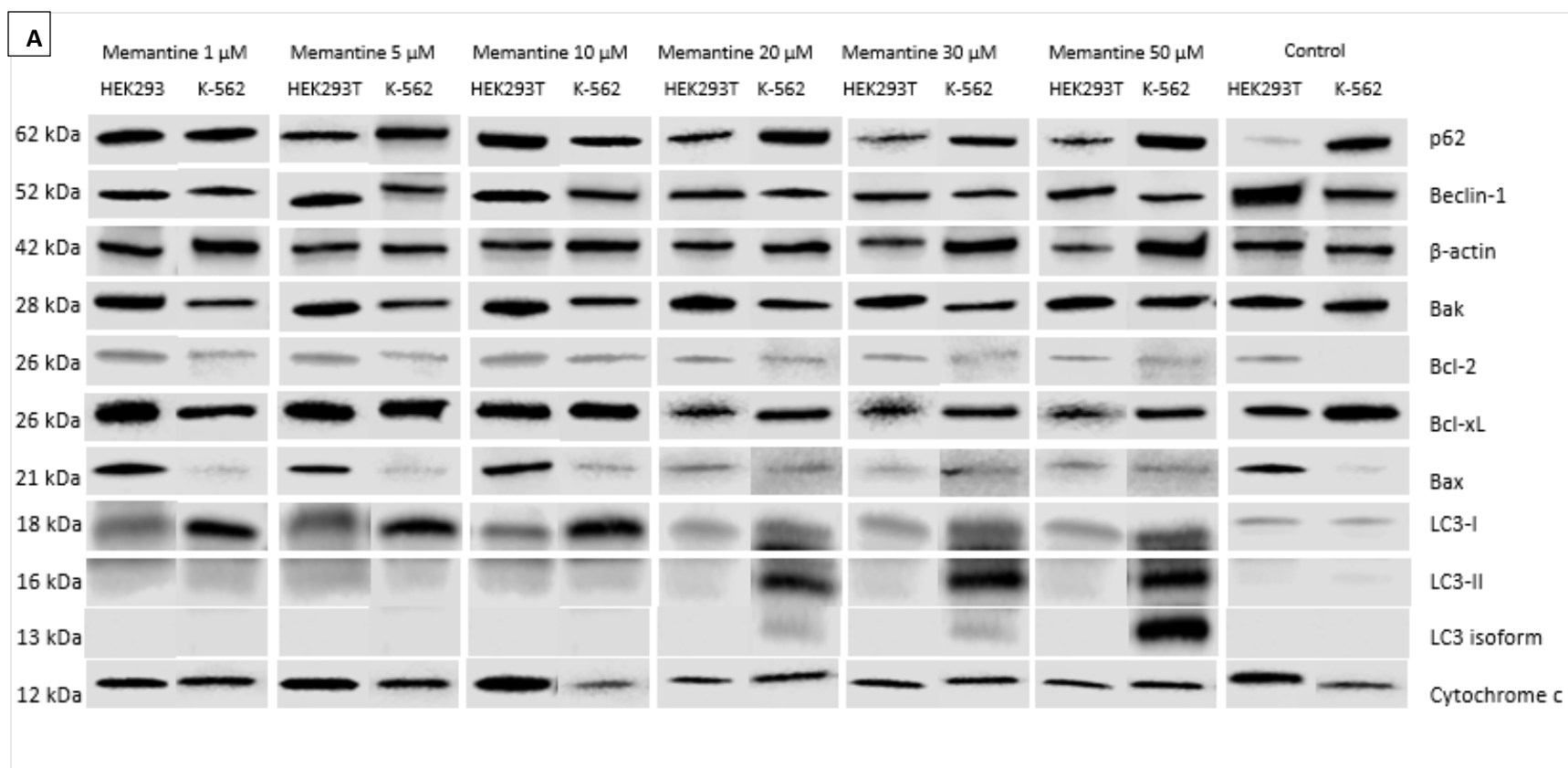
In HEK293T cells, anti-apoptotic Bcl-2 proteins showed a 4, 1.9 and 1.6-fold increase in 1, 5 and 10 μM Memantine low-dose treated cells, respectively ($p < 0.01$, at all three concentrations). At higher concentrations of 20, 30 and 50 μM , Bcl-2 levels were reduced to similar levels as the untreated HEK293T cells, showing no statistical difference compared to the control ($p > 0.05$) (Figure 3.10C). In Memantine 20, 30 and 50 μM -treated HEK293T cells, another anti-apoptotic protein, Bcl-xL, showed a 2.4, 2.6 and 3.7-fold reduction below the control. However, the decrease was statistically non-significantly different compared to the untreated HEK293T cells ($p > 0.05$) (Figure 3.10C).

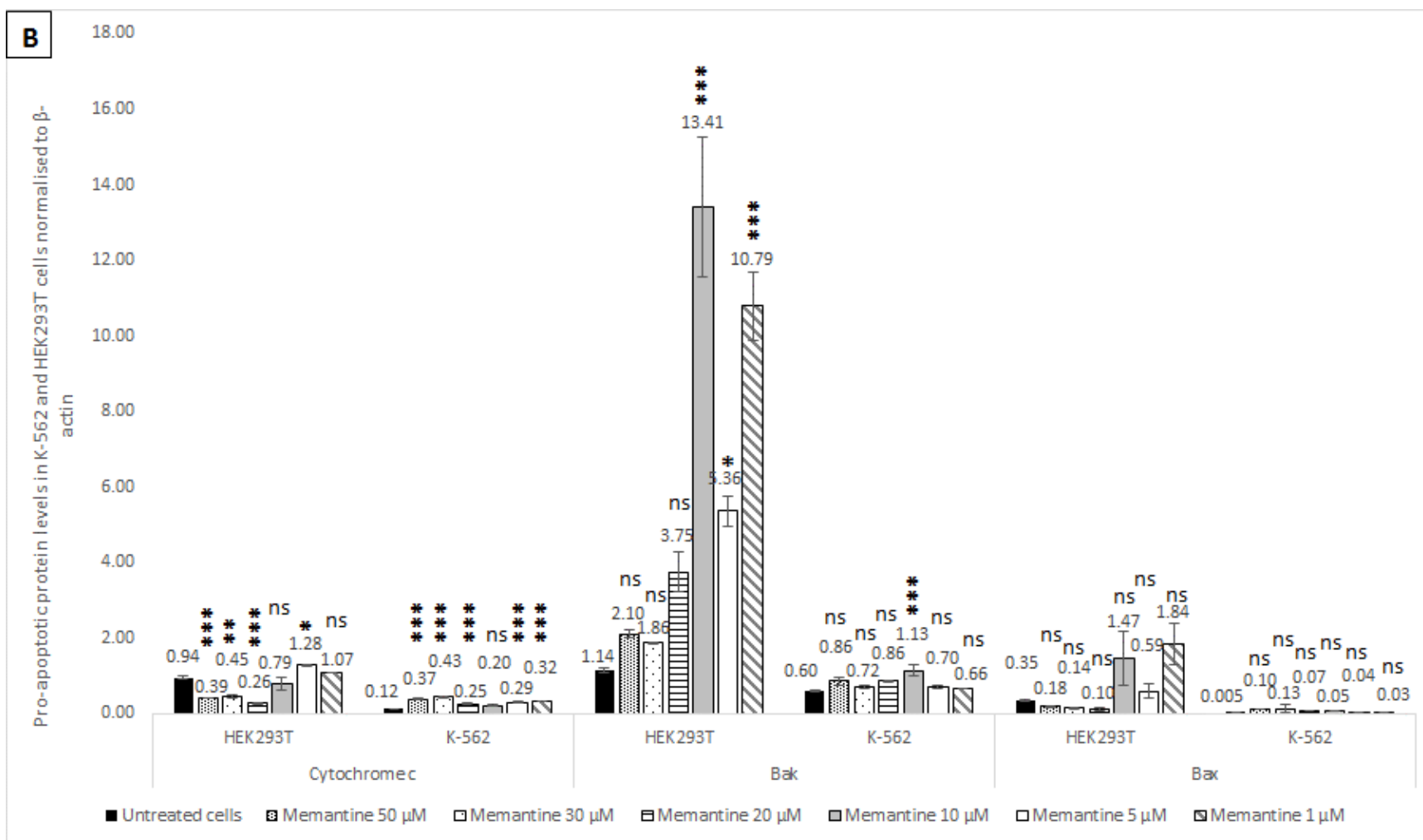
In K-562, high-dose Memantine treatments caused the LC3-II to LC3-I ratio which was initially similar to the control levels at lower Memantine concentrations (1, 5 and 10 μM), to be upregulated, especially at the highest tested concentration of 50 μM Memantine, where a 26.7-fold

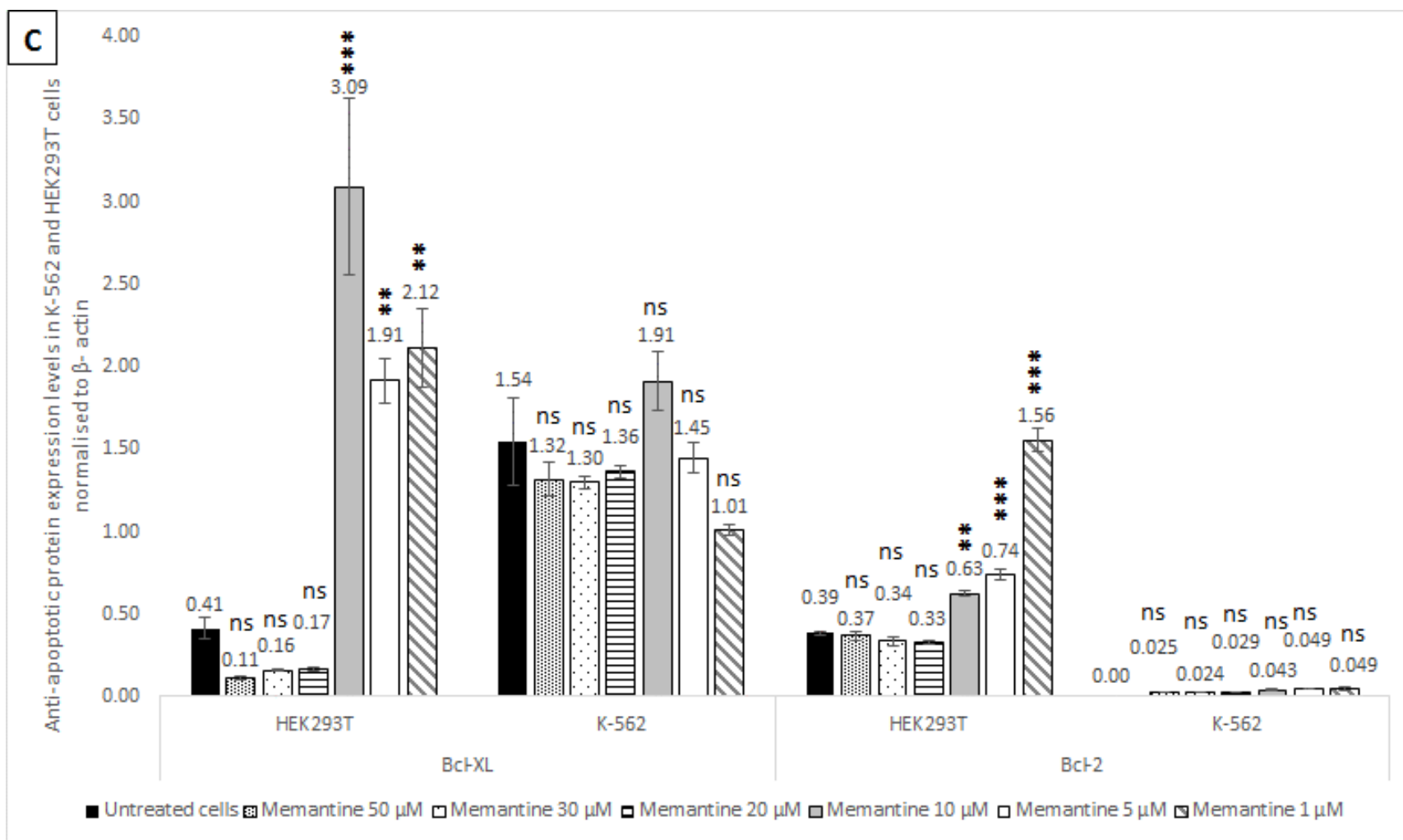
increase occurred ($p < 0.001$), with a simultaneous 3.5-fold increase in p62 protein level ($p < 0.001$) (Figure 3.10D). In addition, an LC3 isoform (~13kDa), which was not detected in any of the low-dose Memantine-treated cells, was observed only in the K-562 cells treated with Memantine 20, 30 and 50 μM (Figure 3.10A).

In the assessment of the pro-apoptotic proteins, all Memantine-treated K-562 cells were observed to show an increment in Bax protein levels from 6 to 26-fold. However, the increase observed was not statistically significant when compared to the untreated control cells ($p > 0.05$) (Figure 3.10B). In both low and high-doses of Memantine-treated K-562 cells, Bak also showed a non-significant increase in its expression levels compared to the untreated K-562 cells ($p > 0.05$), except at 10 μM Memantine treatment, where a very highly significant increase of 1.9-fold was observed (Figure 3.10B) ($p = 0.001$). Noteworthy, the apoptosis triggering protein, Cytochrome c, was observed to be very highly upregulated in all Memantine-treated K-562 cells ($p \leq 0.001$) except at the 10 μM concentration, where the 1.7-fold protein increase showed no significant difference when compared to the control cells ($p = 0.056$) (Figure 3.10B).

For the anti-apoptotic proteins, in all Memantine-treated K-562 cells, Bcl-2 proteins, which were below detection level in untreated K-562 cells, showed a non-significant increase compared to the control ($p > 0.05$) (Figure 3.10C). On the other hand, the levels of Bcl-xL were reduced in K-562 cells, except at 10 μM , where a 1.2-fold increase was observed (Figure 3.10C). However, similar to the Bcl-2, all expression changes observed in Bcl-xL levels were also not significant when compared to the untreated K-562 control cells (Figure 3.10C). Although, it is noteworthy to point out that the amount of Bcl-2 proteins expressed in the Memantine-treated K-562 cells was relatively low compared to the high level of Bcl-xL proteins that were expressed in the cells (Figure 3.10C).







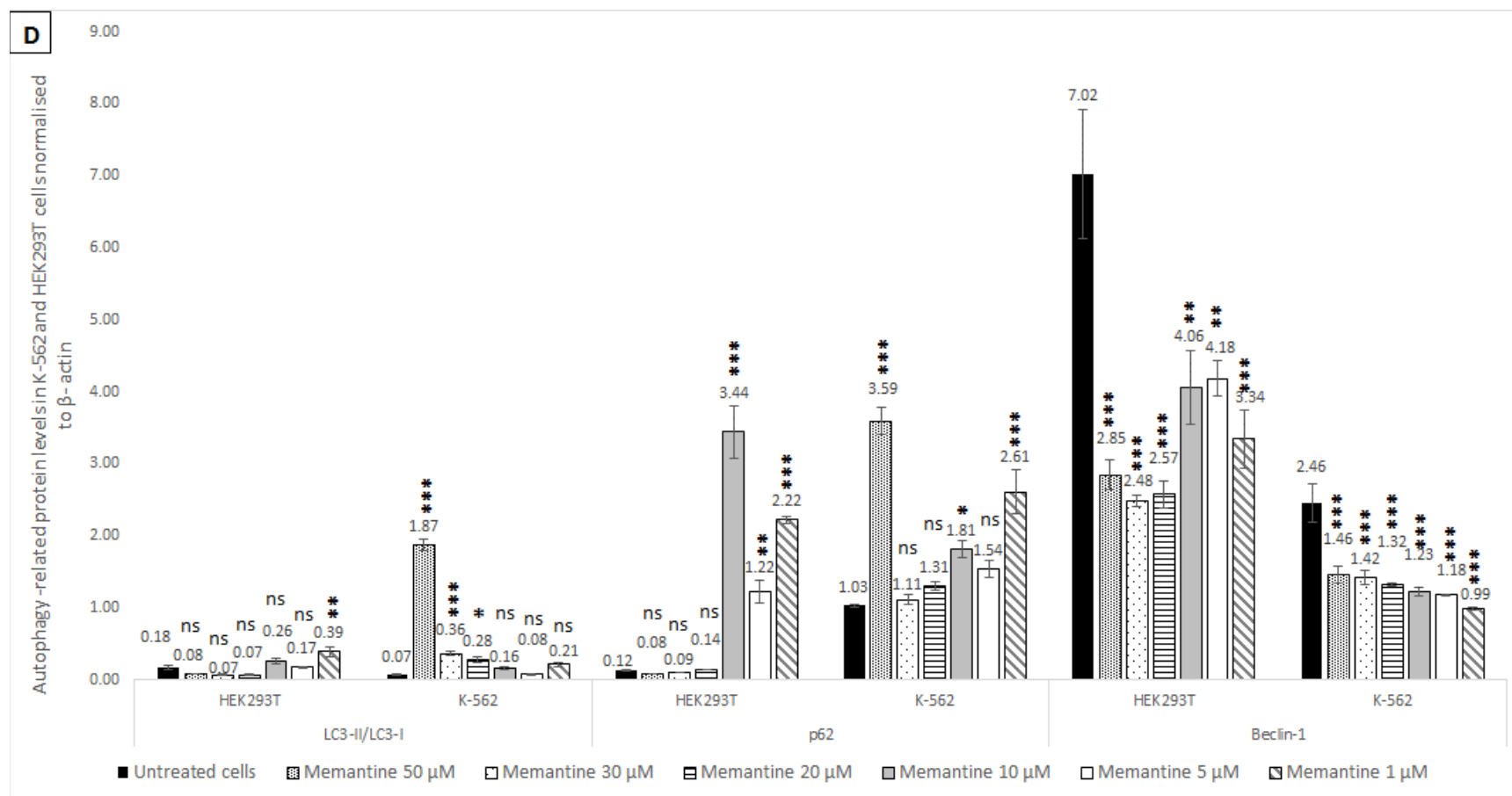


Figure 3.10 Effects of Memantine on the levels of proteins involved in apoptosis and autophagy in HEK293T and K-562 cells lines after 48 h treatment

(A) Representative Western blot image

(B) Pro-apoptotic proteins: Cytochrome c, Bak and Bax

(C) Anti-apoptotic proteins: Bcl-xL and Bcl-2

(D) Autophagy-related proteins: LC3, p62 and Beclin-1

Cells were treated with Memantine high-dose (50, 30 and 20 μM) and low-dose (10, 5 and 1 μM) and protein expressions were determined using Western blot.

At the lowest concentrations tested (5 and 1 μM), Memantine increased the expression of Cytochrome c in K-562 cells. Low-dose Memantine (10, 5 and 1 μM) upregulated anti-apoptotic proteins (Bcl-2 and Bcl-XL) in HEK293T cells. Memantine (10, 5 and 1 μM) was observed to reduce autophagy activities in HEK293T cells by reducing Beclin-1 levels and increasing the expression of p62.

Data were normalised to β-actin expression levels. Experiments were repeated thrice and data are expressed as mean ± SE. Basic statistical analysis was performed using 2-sample t-test (compare treatments vs control). Significant differences were shown as: p > 0.05, no significance (ns); * when p ≤ 0.05, significant; ** when p ≤ 0.01, highly significant and ***, p ≤ 0.001, very highly significant.

3.3.9 Summarised data of the drug-treated cells

Table 3.2 Effects of Imatinib and Dox in HEK293T and K-562 cells

Proteins	Imatinib (1 μ M)		Dox (1 μ M)		Summary of the statistically significant results
	HEK293T	K-562	HEK293T	K-562	
	Proteins levels normalised to β -actin Fold change \uparrow or \downarrow compared to control				
Anti-apoptotic proteins					
Bcl-2	1.55 4.0 \uparrow p<0.001	0.027 \uparrow ns	0.43 1.1 \uparrow ns	0.025 \uparrow ns	Imatinib increased Bcl-2 in HEK293T cells Imatinib increased the levels of Bcl-xL in HEK293T cells whilst Dox reduced the expression of the anti-apoptotic protein
Bcl-xL	1.20 2.9 \uparrow p=0.01	0.43 3.6 \downarrow p<0.01	0.07 5.9 \downarrow p<0.01	0.18 8.6 \downarrow p<0.01	Both Imatinib and Dox caused a decrease in the levels of Bcl-xL in K-562 cells. However, Dox gave a 2-fold decreased effect
Pro-apoptotic proteins					
Bax	1.62 4.6 \uparrow ns	0.51 102 \uparrow ns	0.10 3.5 \downarrow p<0.01	Not detected \downarrow ns	Dox increased the levels of pro-apoptotic Bak and Cytochrome c in HEK293T cells but decreased the levels of Bax
Bak	11.60 10.2 \uparrow p=0.001	0.80 1.3 \uparrow p<0.05	1.29 1.1 \uparrow p<0.05	0.31 1.9 \downarrow p<0.001	In K-562 cells, Dox also caused an increase in Cytochrome c but with a decrease in Bak Imatinib promoted Bak expression in HEK293T cells
Cytochrome c	0.87 1.1 \downarrow ns	1.39 11.6 \uparrow p=0.001	1.29 1.4 \uparrow p<0.05	1.05 8.8 \uparrow p=0.001	In K-562 cells, Imatinib increased the levels of Bak and Cytochrome c
Autophagic proteins					
Beclin-1	5.62 1.2 \downarrow ns	1.91 1.3 \downarrow ns	3.45 2.0 \downarrow p<0.05	3.45 1.4 \uparrow p<0.05	In K-562 cells, Dox induced an increase in the levels of Beclin-1 but reduced it in HEK293T cells
LC3-II/ LC3-I	0.17 1.1 \downarrow ns	0.32 4.6 \uparrow p=0.001	0.09 2.0 \downarrow ns	0.33 4.7 \uparrow p<0.001	Both Dox and Imatinib-treated K-562 cells showed an increase in LC3-II/LC3-I and decrease in p62
p62	0.98 8.2 \uparrow p<0.001	0.47 2.2 \downarrow p<0.001	1.33 11.1 \uparrow p<0.001	Not detected \downarrow p=0.001	Conversely, in HEK293T cells, both Dox and Imatinib increased the levels of p62

Table 3.3 Effects of Donepezil and Memantine at lowest concentration tested in HEK293T and K-562 cells

Proteins	Donepezil (1 μ M)		Memantine (1 μ M)		Summary of the statistically significant results
	HEK293T	K-562	HEK293T	K-562	
	Proteins levels normalised to β -actin Fold change \uparrow or \downarrow compared to control				
Anti-apoptotic proteins					
Bcl-2	1.03 2.6 \uparrow p<0.001	0.026 \uparrow ns	1.56 4.0 \uparrow p<0.001	0.049 \uparrow ns	Donepezil and Memantine increased the levels of both Bcl-2 and Bcl-xL in HEK293T cells, but not in K-562 cells
Bcl-xL	2.02 4.9 \uparrow p<0.05	1.79 1.2 \uparrow ns	2.12 5.2 \uparrow p<0.01	1.01 1.5 \downarrow ns	
Pro-apoptotic proteins					
Bax	1.04 3.0 \uparrow ns	0.03 6.0 \uparrow ns	1.84 5.3 \uparrow ns	0.03 6.0 \uparrow ns	Donepezil and Memantine increased the levels of Bak in HEK293T cells
Bak	9.10 8.0 \uparrow p<0.001	0.73 1.2 \uparrow ns	10.79 9.5 \uparrow p<0.001	0.66 1.1 \uparrow ns	Donepezil promoted Cytochrome c expressions in HEK293T and K-562 cells. Memantine increased the expression of Cytochrome c only in K-562 cells
Cytochrome c	1.30 1.4 \uparrow p<0.05	0.58 4.8 \uparrow p<0.01	1.07 1.1 \uparrow ns	0.32 2.7 \uparrow p<0.001	
Autophagic proteins					
Beclin-1	2.06 3.4 \downarrow p<0.001	1.05 2.3 \downarrow p=0.001	3.34 2.1 \downarrow p=0.001	0.99 2.9 \downarrow p<0.001	Memantine decreased the levels of Beclin-1 in both cell lines with a simultaneous increase in p62 levels
LC3-II/ LC3-I	0.54 3.0 \uparrow p<0.001	0.30 4.3 \uparrow ns	0.39 2.7 \uparrow p<0.01	0.21 3.0 \uparrow ns	Donepezil decreased the levels of Beclin-1 in both cell lines. In addition, p62 levels were increased the Donepezil-treated HEK293T cells
p62	1.49 12.4 \uparrow p<0.01	1.06 1.0 \uparrow ns	2.22 18.5 \uparrow p<0.001	2.61 2.5 \uparrow p<0.001	In HEK293T cells, Donepezil and Memantine induced an increase in the levels of LC3-II/LC3-I in HEK293T cells

3.4 Discussion

3.4.1 Basal protein expressions involved in cell apoptosis and autophagy

The protein profile of cancer cells, unlike non-cancer cells, constitutes factors that allow the cells to grow uncontrollably with a higher level of survival developed via various mechanisms. One such mechanism involves the deregulation of apoptotic proteins (Hinz *et al.*, 2000; Trauzold *et al.*, 2003). Apoptotic proteins are a group of regulatory proteins, some of which are constituted, in the Bcl-2 family of proteins. The Bcl-2 family of proteins is comprised of the pro-apoptotic (including Bax and Bak) and anti-apoptotic (including Bcl-2 and Bcl-xL) proteins. These groups of proteins interact amongst themselves and may also interact with the autophagy-related proteins (Beclin-1, LC3-I, LC3-II and p62).

In the Bcl-2 family, protein interactions are possible due to the possession of Bcl-2 Homology (BH) domain(s) (Banjara *et al.*, 2020). There are four BH domains namely BH1, BH2, BH3 and BH4. The Bcl-2 family of proteins can be characterised based on the specific domain(s) they possess. These BH domains are critical to the proper functioning of the proteins, including their ability to interact with family members and other regulatory proteins (Pistritto *et al.*, 2016). Protein-protein interaction is an important partnership which dictates whether or not death will occur in a cell. In the apoptotic pathway, the anti-apoptotic Bcl-2 proteins, which possess all four BH domains, are able to inhibit the permeabilisation of the outer membrane of the mitochondria and the subsequent release of Cytochrome c through the formation of partnerships with the multi-BH domain pro-apoptotic proteins (Bax and Bak), through their BH3 domain (Ku *et al.*, 2011; Kale *et al.*, 2018). In response to various death stimuli, these interactions may be inhibited by the BH3-only proteins, such as Bim and Puma. These BH3-only pro-apoptotic proteins can induce death in a Bax/Bak-dependent manner or by binding to the anti-apoptotic proteins. Thus, activating the multi-BH domain pro-apoptotic proteins to cause cell death via the permeabilisation of the mitochondrial outer membrane. The BH3 domains are not restricted to apoptosis regulation alone. They are also important in the autophagy pathway, where under certain circumstances, the actions of Beclin-1, an important autophagy initiator, also referred to as BH3-only protein, can be halted (Xu and Qin, 2019). With the aid of a BH3 receptor domain, anti-apoptotic Bcl-2 and/or Bcl-xL proteins are able to interact with Beclin-1 via its BH3 domain, thereby downregulating its autophagic functions (Maiuri *et al.*, 2007; Oberstein *et al.*, 2007; Xu and Qin, 2019). Although, various models have described the interaction of the Bcl-2 family of proteins, differently, the BH3 domain has consistently been suggested as being critical for the interactive functioning amongst the

proteins and as such is contained by all Bcl-2 family members (Lomonosova and Chinnadurai, 2008; Pistritto *et al.*, 2016). Furthermore, in drug development, the targeting of the BH3 domains, which are necessary for protein interaction, have also proven useful in the emergence of anti-cancer therapies with the development of BH3-mimetics (Zhang *et al.*, 2007; Townsend *et al.*, 2021).

Aside from the presence of BH regions, protein interaction also depends on binding affinity as well as relative protein concentration (Shamas-Din *et al.*, 2013). The availability and distribution of proteins in a particular action site is important and could occur as a result of transportation, post-modification, in response to a defined stimulus (Yang and Qian, 2017). This could be termed as protein localisation. This designated protein-recruitment strategy helps to regulate protein functions by allowing the physical segregation of proteins and simultaneous execution of their various biochemical processes within the same cell. Many proteins function on a localisation-dependent basis or may need to perform a particular function in multiple compartments (Zaretsky and Wreschner, 2008). The Bcl-2 family of proteins are distributed in diverse parts of the cells, probably due to their varying affinities for different intracellular membranes and/or binding partners. Based on their localisation, studies are able to suggest diverse roles of these proteins in various organelles. For instance, a vast amount of Bcl-2 family members is located in the mitochondria and can be referred to as regulators of the mitochondrial outer membrane integrity (Karbowski *et al.*, 2006; Berman *et al.*, 2009). However, these proteins have also been reported to localise to the endoplasmic reticulum, where the pro-apoptotic and the anti-apoptotic proteins exert opposing effects on calcium (White *et al.*, 2005). Furthermore, anti-apoptotic Bcl-2 proteins localised in the endoplasmic reticulum, but not in the mitochondria, have been suggested to negatively regulate Beclin 1-dependent autophagy by disrupting the interaction between the autophagy initiator protein and VPS34 (Pattingre *et al.*, 2005). All of these emphasises the diverse roles Bcl-2 family of proteins may play based on their localisation. The varying localisation of proteins helps to prevent spontaneous actions thereby tightly regulating activities within the cell. Protein localisation as well as the binding interactions of Bcl-2 family proteins is predominantly dictated by the relative abundance of each protein expressed, due to cell signalling (Kale *et al.*, 2018). Therefore, for the purpose of this study, cellular protein expression was focused on.

In molecular pathways where pro-apoptotic, anti-apoptotic and autophagy proteins are involved their expression levels are associated with the progression of various diseases and participate in the determination of cells fate. This emphasises the importance of investigating

the cells' protein expression levels. Also, in an effort to eliminate cancer cells while preserving the non-cancerous ones, understanding the characteristics of cells through knowledge of their basal expressions is necessary. In this study, the levels of apoptotic and autophagic proteins expressed in K-562 and HEK293T under normal physiological conditions, were assessed.

Cancer cells have been reported to express anti-apoptotic proteins as a form of protection. In previous studies involving apoptotic induction in K-562 (Zhang *et al.*, 2005) and in functional studies where murine FL5.12 cells were transfected to express a high amount of Bcl-xL (Boise *et al.*, 1993; Minn *et al.*, 1995), the overexpression of anti-apoptotic proteins was observed to promote the cells resistant to a variety of apoptotic stimuli. In addition, Bcl-xL has also been demonstrated as being necessary for the survival and advancement of CML disease progression phenotype (Harb *et al.*, 2013). In this study, overexpression of Bcl-xL, shown to be 3.8 times higher in the leukaemic (K-562) cells compared to the non-cancerous (HEK293T) cells, occurred ($p < 0.01$) (Figure 3.4C). However, unexpectedly but in agreement with a previous report by Benito *et al.* (1995), in this present study, K-562 did not express a detectable level of Bcl-2 proteins (Figure 3.4A & C). The increased expression of another repressor of apoptotic cell death, Bcl-xL, over Bcl-2 in K-562 cells emphasises an indication of the higher contribution of Bcl-xL in the CML cells' viability and its possible involvement in the cells insensitivity towards anti-cancer drugs, perhaps, via the autophagy pathway. The K-562 CML cells also expressed a lower level of pro-apoptotic proteins (especially Bax) compared to HEK293T cells (Figure 3.4C). This upregulation of anti-apoptotic proteins and downregulation of the pro-apoptotic proteins emphasises a survival mechanism of leukaemic cells. The expression levels of these apoptosis regulating proteins play a pivotal role in the decision of the cell's fate, together with autophagy proteins (Tanner *et al.*, 2011; Rubinstein and Kimchi, 2012; Delou *et al.*, 2016).

The degradative process of autophagy helps in generating energy in the cells. The release of Beclin-1 (a master autophagy mediator) from anti-apoptotic Bcl-2/ Bcl-xL proteins allows the autophagy regulating protein to bind to VPS34, VPS15 and ATG14 proteins. This formed Beclin-1 complex is activated by ULK1, thus initiating the process of autophagy (Russell *et al.*, 2013) (Figure 1.5). Another autophagy-related protein is LC3, which acts as an ubiquitin-like protein. The active form of this protein, LC3-II, is generated by the conjugation of cytosolic LC3-I to phosphatidylethanolamine. This active form is expressed on the autophagosomal membranes (Figure 1.5). Hence, it closely correlates with the number or level of autophagosomes accumulated and as such, it can be detected as an autophagosome biomarker

(Mizushima *et al.*, 2010). Therefore, an increase in the expression level of LC3-I itself, does not necessarily translate to an increase in the number of autophagosomes, rather, the amount of LC3-II or the ratio between LC3-II and LC3-I is considered a better correlation for the number of autophagosomes (Kabeya *et al.*, 2000). Furthermore, the expression level of LC3 does not spontaneously guarantee autophagic degradation, as LC3 structures have been identified in autophagy-deficient cells where it forms an association with p62 proteins (Runwal *et al.*, 2019). p62 is an autophagy receptor protein that possesses an LC3 interacting region (Pankiv *et al.*, 2007). However, both proteins are not completely inversely correlated. p62 protein can be described as a multifunctional protein as it contains several binding motifs including an ubiquitin-binding domain, which facilitates its ability to selectively bind cargoes to be engulfed during autophagy. Thus, making p62 an autophagy substrate itself and decreasing its amount during a functional autophagy flux (Bjørkøy *et al.*, 2005; Komatsu *et al.*, 2007; Pankiv *et al.*, 2007; Han *et al.*, 2017). High expression of p62 is not necessarily associated with malfunction or decline in autophagy, as the protein has been observed to be involved in multiple pathways (Jin *et al.*, 2009; Jain *et al.*, 2010). Therefore, bearing in mind that these three proteins (Beclin-1, LC3 and p62) are major participants in autophagy and with the acknowledgment that the measurement of autophagy flux is challenging due to its dynamic multiple-stage processes, herein, the expression levels of these central autophagy-flux related proteins (Beclin-1, LC3 and p62) were investigated in unstressed K-562 and HEK293T cells. The distinct role of autophagy in cancer is yet to be completely understood. On one hand, the overexpression of Beclin-1 and LC3 in colorectal cancer have been linked to the declined overall survival of patients (Baginska *et al.*, 2013; Myung *et al.*, 2013; Schmitz *et al.*, 2016). With high LC3 expressions, being reported to be associated with aggressive disease and poor outcomes in cancer (Lazova *et al.*, 2012; Wu *et al.*, 2014). Furthermore, the inhibition of Beclin-1 mediated autophagy has been reported as being beneficial in CML treatment (Yu *et al.*, 2012; Yu *et al.* 2020). Increased autophagy inhibition which was characterised by elevated levels of p62 was observed to cause sensitisation to lysis in drug-resistant CML cells (Han *et al.*, 2017). On the other hand, studies demonstrated that the overexpression of Beclin-1 was favourable, as it inhibited cell growth and proliferation in CML cells (Huang *et al.*, 2019) and breast cancer (Won *et al.*, 2010), while its inactivation promoted tumorigenesis *in vivo* (Qu *et al.*, 2003). Herein, the current study showed a lower basal expression of Beclin-1 in K-562 CML cells compared to the non-cancerous HEK293T (Figure 3.4A & C). HEK293T cells expressed 2.9 times more of Beclin-1 ($p < 0.01$) with a lower p62 level ($p < 0.001$) compared to the cancer cells (Figure 3.4C). In addition, the membrane-bound LC3 ratio was low in both

cells, with HEK giving a slightly higher expression of 2.6-fold ($p < 0.05$) (Figure 3.4C). These results demonstrate that under normal conditions, the leukaemic cells modulate the apoptotic pathway for their maintenance and that the autophagy pathway may be induced as an alternative path for adaptation or survival. However, it is pertinent to remember that besides apoptotic cell death, under some stressful circumstances, the induction of autophagy may also promote autophagic cell death.

3.4.2 Modulation of the apoptotic and autophagy pathways by cancer drugs

3.4.2.1 The modulation of the apoptotic and autophagy pathways by Imatinib

Imatinib is a commercially available drug approved for the treatment of CML. In CML, during the formation of the dysregulated BCR-ABL protein, the activities of varying regulatory domains present in the BCR and ABL genes are affected, including the SH3 domain which is a negative regulator of the tyrosine kinase of the ABL gene (Pendergast *et al.*, 1991; Gross *et al.*, 1999; Smith *et al.*, 2003). The disruption of these domains causes the BCR-ABL kinase to remain permanently on and in turn mediate an array of intracellular effects leading to cellular transformation and CML progression. Thus, making the aberrant fusion protein, BCR-ABL, an important target for the treatment of CML. Imatinib is a 2-phenylaminopyrimidine TKI that selectively targets this constitutively active BCR-ABL kinase responsible for the activation of numerous signalling pathways that results in uncontrollable cell growth and disrupted genomic stability in CML. The inhibitory effect of Imatinib on BCR-ABL phosphorylation causes a blockage in CML cells proliferation and induces apoptosis (Gambacorti-Passerini *et al.*, 1997). The drug has also been reported to activate apoptosis in gastric cancer (Kim *et al.*, 2019) and other leukaemic cells (Gambacorti-Passerini *et al.*, 1997).

In CML, where the enhanced BCR-ABL expression correlates with the disease phase, Imatinib has been observed to have significant activities in the chronic and the accelerated phases (Druker *et al.*, 2001; Kantarjian *et al.*, 2002; Talpaz *et al.*, 2002; Jabbour *et al.*, 2006). However, a lesser effect has been reported in the advanced blast crisis phase (Druker *et al.*, 2001; Sawyer *et al.*, 2002; Palandri *et al.*, 2008; Ghahramanyan *et al.*, 2019). In addition, despite the clinical results achieved by the use of Imatinib, the emergence of resistance and its ineffectiveness in leukaemic stem cells remain a major challenge (Gorre *et al.*, 2001; Branford *et al.*, 2002). These leukaemic stem cells do not depend on BCR-ABL activity for their survival and as such, they

are able to resist the conventional therapy of Imatinib, leading to a repopulation of the malignancy via various pathways (Chomel *et al.*, 2011; Chu *et al.*, 2011; Corbin *et al.*, 2011).

In a previous study by Ertmer *et al.* (2007), Imatinib was reported to induce autophagy in both cancer and non-cancerous mammalian cells probably by inhibiting the ABL gene. Further research reported that Imatinib-induced autophagy acted as a survival mechanism in CML cells. Thus, its suppression potentiates the sensitivity of CML cells to Imatinib (Carew *et al.*, 2007; Bellodi *et al.*, 2009). These findings suggested an important role played by autophagy in leukaemogenesis. However, in this study, Imatinib (1 μM) was unable to modulate the autophagy pathway in both K-562 CML cells as well as in HEK293T cells (Figure 3.5D). In the non-cancerous HEK293T cells, Imatinib 1 μM induced survival by increasing the expression of anti-apoptotic Bcl-2 ($p < 0.001$) and Bcl-xL ($p = 0.01$) proteins in the treated cells compared to the untreated control cells (Figure 3.5C). However, evident from the unchanged levels of Beclin-1 and an 8.2-fold increase in p62 proteins, autophagy was not stimulated in the Imatinib (1 μM)-treated HEK293T cells (Figure 3.5D). On the other hand, Imatinib 1 μM promoted cell death in K-562 via the apoptotic pathway. The drug inhibited the death repressor, Bcl-xL and stimulated the expression of the pro-apoptotic proteins (Bak and Cytochrome c) in the CML cells (Figure 3.5). This was similar to the report by Lee *et al.* (2013) where an increase in apoptotic activities was observed following the treatment of K-562 cells with 0.2 μM of Imatinib; a dose much lower than the concentration employed herein. Also, when cell death analysis was carried out, Imatinib 1 μM caused 23% of K-562 cells to die (Table 3.1) with 19% of the cells dying via the apoptotic pathway (Appendix V). Furthermore, similar to HEK293T cells, Imatinib did not stimulate a Beclin-1-induced autophagy in K-562 cancer cells (Figure 3.5D). This was contrary to a previous report by Ertmer *et al.* (2007), where the inhibition of BCR-ABL by Imatinib was suggested to have induced autophagy, independent of tissue type or cell immortalisation status. However, it is imperative to mention that the researchers did not include models of CML in that particular study. In a more recent CML investigation, where models of the blast crisis phase were included, Imatinib (0.01 – 10 μM) was shown to have no cytotoxic effect against the K-562 cells (Almeida *et al.*, 2018). This spiked a speculation that the presence of autophagy in drug modulated CML cells may be as a result of activities against the BCR-ABL kinase which may lead to disease regression or probably cell death. However, in the advanced blast crisis phase, such as was investigated herein, Imatinib (1 μM) may have been unable to effectively target the BCR-ABL molecules to bring about an increased death effect, especially in the non-apoptotic pathway. This

emphasises the challenges encountered in the management of CML, especially in the blast crisis phase, where only an extremely low percentage of patients have been observed to achieve complete cytogenetic remission (Sawyers *et al.*, 2002). In this phase, the leukaemic cells have evolved and gained more resistance against TKIs including Imatinib, probably due to genetic instability and alterations including amplification and increased mutations of the BCR-ABL gene. Moreover, Imatinib has been reported as being unable to eliminate the non-oncogenic addicted, quiescent stem cells in CML (Corbin *et al.*, 2011), thereby resulting in unforeseen activities, relapse or short term remission of patients in the blast crisis phase (Gorre *et al.*, 2001; Branford *et al.*, 2002; Palandri *et al.*, 2008; Prakash *et al.*, 2021).

In this present study, despite the non-stimulation of Beclin-1 in the Imatinib treated CML cells, surprisingly, an unexplainable increase in the levels of autophagosomes evident from the increased LC3-II/LC3-I ratio ($p = 0.001$) as well as a 2.2-fold decrease in p62 levels ($p < 0.001$) was observed (Figure 3.5D). Besides TKIs such as Imatinib, some ABL-independent agents have also been proven to be effective in the treatment and probable survival of CML patients, particularly the anthracycline drug, Dox (Bacigalupo *et al.*, 1997; Van Rhee *et al.*, 1997; Trialists, 1997; Quintás-Cardama *et al.*, 2007; Allan *et al.*, 2011; Synowiec *et al.*, 2015; Almeida *et al.*, 2018).

3.4.2.2 The modulation of the apoptotic and autophagy pathways by Dox

Dox is a broad-spectrum anti-cancer drug and one of the most effective agents reported to reduce cell viability in cancer cells by inducing apoptosis, as a singular drug or as a combination therapy (Jakubowska *et al.*, 2007; Maurel *et al.*, 2010; Sadeghi-Aliabadi *et al.*, 2010; Pilco-Ferreto and Calaf, 2016; Almeida *et al.*, 2018). Previous studies have reported Dox as demonstrating multiple effects on various cancer cells, ranging from growth inhibition in gastric carcinoma cells (Florou *et al.*, 2013), to apoptosis in myeloma, lymphoma and leukaemic cells (Panaretakis *et al.*, 2002; Li *et al.*, 2019). However, the use of the drug is limited due to its toxicity in non-cancer cells (Wang *et al.*, 2004; Li *et al.*, 2016; Fraczkowska *et al.*, 2018). In an effort to better understand the molecular mechanisms of Dox in both CML and AD, experiments were conducted to investigate the effect of the drug on the apoptotic and autophagic pathways in CML K-562 and non-cancerous HEK293T cells.

As anticipated, the cytotoxic drug reduced the viability of HEK293T cells in a dose- and time-dependent manner (Figure 3.3), with Dox (1 and 5 μM) inducing significant death in the non-

cancerous cells (Table 3.1). For the first time, the effects of a therapeutic relevant dose of Dox in CML versus AD *in vitro* models were compared. Dox (1 μ M) induced 11% more cell death in HEK293T compared to K-562 CML cells ($p < 0.05$) (Table 3.1). This pattern is suggestive of Dox's capability of inducing escalated apoptotic death in non-cancer cells, possibly due to diminished levels of cytoprotective proteins, compared to the leukaemic cells.

When protein expressions were probed, it was observed that the DNA damaging drug, Dox, induced some apoptotic effects in both HEK293T and K-562 cells (Figure 3.6). In HEK293T cells, Dox (1 μ M) induced a significant decrease in the expression of anti-apoptotic Bcl-xL ($p < 0.01$), with an increase in the levels of pro-apoptotic Bak ($p < 0.05$) and Cytochrome c ($p < 0.05$), compared to the untreated HEK293T cells. An unexplainable decrease in the levels of Bax ($p < 0.01$) was also observed (Figure 3.6). These findings were similar to reports by Lahoti *et al.* (2012), where upregulation of some pro-apoptotic proteins was reported, leading to the release of caspases. A few studies have specifically documented the cytotoxicity of Dox in HEK293 cells (Mehdizadeh *et al.*, 2020; Benyettou *et al.*, 2017), however, more attention has been drawn to other cell types, such as cardiomyocytes. Herein, the apoptotic effects observed in HEK293T cells emphasise the toxic ability of Dox in non-cancer cells, even at a therapeutic dose of 1 μ M. The data also reveals a suggestive pattern of Dox (1 μ M) exposing HEK293T cells to death via the intrinsic pathway of apoptosis. This is evident by the reduction in the expression of Bcl-xL, leading to the unavailability of the anti-apoptotic proteins to interact with the increasing levels of the death promoter, Bak (which augments the formation of mitochondrial pores), thus resulting in a consistent increase in the release of Cytochrome c into the cytosol (Figure 3.6).

In cancer cells, Dox is known to exert a range of effects, ultimately leading to death (Yu *et al.*, 1996; Lahoti *et al.*, 2012). In this study, the leukaemic K-562 cells treated with Dox (1 μ M) showed some form of toxicity as reflected in the decreased levels of Bcl-xL, a protein whose expression had previously been reported to act as a major form of protection in CML cells (Shimizu *et al.*, 2004; Zhang *et al.*, 2005; Yin *et al.*, 2011), with a concomitant increase in Cytochrome c levels (Figure 3.6). This increased expression of Cytochrome c illustrated activities of the intrinsic apoptotic pathway. However, the observed downregulation of Bak and the non-participation of Bax proteins suggested the cells' inability to activate a robust death cascade (Figure 3.6). This was previously indicated in the apoptotic cell death evaluation, where only 9.9% of the K-562 cells were observed to have died via the apoptotic pathway (Appendix V). This observed minimal death effect could be as a result of the ability of the cancer cells to exert mechanisms in order to resist or minimise Dox toxicity in the cells. One

of such mechanism of action in K-562 cells may be brought about by the de-regulated activities of BCR-ABL kinase, which include the continuous stimulation of STAT5, a signalling pathway involved in cell viability, growth and accelerated DNA repair mechanisms within cells (Sillaber *et al.*, 2000; Slupianek *et al.*, 2001). Through the enhancement of DNA repair, such resistant activities may lead to suppression of apoptosis as previously demonstrated in BCR-ABL positive cells, even after the release of Cytochrome c (Deming *et al.*, 2004). Herein, the apoptotic cell death effect of the Dox-treated K-562 cells could be likened to the observations from previous studies, where the leukaemic cells were shown to exhibit some form of resistance to Dox treatment, reflected by their marginal cell death number of less than 40% (Blagosklonny *et al.*, 2001; Srdic-Rajic *et al.*, 2016).

It is worth mentioning that Dox which has previously been reported as not affecting Bcl-2 (p26-Bcl-2- α) isoform protein levels in either MOLM-13 or U-937 cancer cells (Vu *et al.*, 2020), was also observed herein, to have no statistically significant effect on the levels of the Bcl-2 proteins in both K-562 and HEK293T cells, compared to their individual controls ($p > 0.05$) (Figure 3.6C). However, as previously mentioned, in both cell lines tested, the drug caused a significant reduction in the levels of another anti-apoptotic protein, Bcl-xL, compared to their untreated controls ($p < 0.01$) (Figure 3.6C). Furthermore, when cell death was assessed using flow cytometry, the drug demonstrated a level of selectivity in its cytotoxicity against non-cancerous HEK293T compared to K-562 cells ($p < 0.05$) (Table 3.1), with 6.1% more K-562 cells observed to have died via the non-apoptotic pathway (Appendix V). This spiked the speculations that another route(s) may have been activated causing the cancer cells death via a non-apoptotic pathway. A critical look at the involvement of the pro-apoptotic proteins in the K-562 cells emphasized this by showing a decline in the levels of Bak and a non-participation of the Bax proteins. Pro-apoptotic Bax has previously been reported to inhibit autophagy by enhancing caspase-mediated cleavage of Beclin-1 and reducing the levels of autophagosome formation (Luo and Rubinsztein, 2010). However, in this study, Bax was not involved in the observed Dox-induced apoptotic effect in K-562 cells (Figure 3.6). Hence, the autophagy pathway was investigated.

The activities of autophagy in cells may serve dual roles. In cancer cells, several mechanisms have been devised to inhibit cell death, one of which is autophagy (Sakuma *et al.*, 2013; Zhao *et al.*, 2014). The initial activation of autophagy activities has been observed to act as an adaptive response to survive stressful drug treatment in cancer cells (Abedin *et al.*, 2007; Ding *et al.*, 2007; Zhao *et al.*, 2014). However, continuity in the autophagy activation may promote

apoptosis or lead to non-apoptotic cell death (Liu *et al.*, 2016). In Dox-treated cancer cells, varying effects have also been reported to occur via the autophagy pathway. These autophagy-modulating capacities of the chemotherapeutic drug (Dox) have been reported in multiple myeloma cells (Pan *et al.*, 2011), liver cancer cells (Qian and Yang, 2009) and breast cancer cells (Cosan *et al.*, 2010; Amani *et al.*, 2020). In breast cancer cells, Dox at 0.05 - 0.5 μM concentrations, was reported to induce autophagy which acted as a cell survival mechanism, but at $>1 \mu\text{M}$, death was induced via apoptosis (Cosan *et al.*, 2010). In contrast, in a more recent breast cancer study, Dox, at an even higher concentration of 26 μM , was observed to induce a cytoprotective autophagic mechanism (Amani *et al.*, 2020). In CML, Dox-induced autophagy functionalities have also been documented, however, in comparison to other forms of cancer, very little is still known. In a previous study by Wang *et al.* (2017), the induction of autophagy was observed to be involved in the increased drug-resistant abilities when CML cells were treated with 0.75 μM of Dox. This was contradictory to a more recent study where an increased anti-tumour effect was observed when autophagy was induced in Dox (0.5 μM) treated K-562 cells, through the use of Rapamycin (Li *et al.*, 2019). From these reports, it is critical to note that Dox-induced effects may vary depending on the exact concentration administered. To the best of the author's knowledge, there is yet to be a report on the effect of Dox on the autophagic pathways of CML cells at a therapeutic relevant dose of exactly 1 μM .

In non-cancer cells, several studies have also presented conflicting reports about the involvement of autophagy in Dox-induced toxicity of the same cells. The observation of cell death in cardiomyocytes, due to upregulated Beclin-1, has previously been reported (Lu *et al.*, 2009; Xu *et al.*, 2012) with evidence of cardiomyocytes survival in contrasting studies (Sishi *et al.*, 2013; Johnson *et al.*, 2017; Yi *et al.*, 2017). Furthermore, a more recent study demonstrated that the downregulation of autophagy in Dox-treated heart cells induced apoptosis (Gu *et al.*, 2018). Based on these previous studies, there is compelling evidence that the effect of autophagy in Dox-treated cells may lead to either death or survival, depending on the concentration of Dox and the cell models employed. However, nothing is known about the effect of autophagy-related proteins in Dox (1 μM)-treated K-562 cells (CML model) compared to non-cancerous HEK293T (AD model), under the same experimental conditions.

Herein, the results from the investigations of the autophagy pathway employing Dox at a therapeutic relevant dose of 1 μM , revealed an induction of Beclin-1 regulated autophagy in K-562 cells but not in the non-cancerous HEK293T cells. A thorough assessment of the pathway showed a negative correlation in the levels of Beclin-1 in both Dox-treated cell lines;

with a downregulation in HEK293T cells ($p < 0.05$) but upregulation in K-562 cells ($p < 0.05$) (Figure 3.6D). In addition, LC3-II/LC3-I, an effective biomarker for monitoring autophagosome formation, was upregulated ($p < 0.001$) in Dox-treated K-562 cells, with a decreased expression of p62 proteins to a non-detectable level ($p = 0.001$), compared to the control (Figure 3.6D). In contrast, Dox-treated HEK293T cells showed a non-significant decrease in the levels of LC3-II/LC3-I ($p > 0.05$) with an increased level of p62 proteins ($p < 0.001$) (Figure 3.6D), compared to the control HEK293T cells. The protein expression profiles indicated that the autophagy activities in Dox (1 μM) treated K-562 cells, which was initially lower under basal conditions, were distinctly enhanced compared to HEK293T cells. These observations are similar to the effect seen in the study by Myung *et al.* (2013), where cancer cells were reported to increase the expression of autophagy markers relative to the normal epithelial cells. Due to the complexity of the association amongst the physiological processes, elucidating the exact role of autophagy in drug-induced conditions remains challenging. However, in this study, it was observed that HEK293T cells which showed downregulation in autophagy markers (Figure 3.6D), resulted in an 11% higher Dox-induced cell death compared to K-562 cells ($p < 0.05$) (Table 3.1). This may be because the non-cancerous cells possess less potency to resist stressors, thus having a lower survival threshold compared to the leukaemic cells. In addition, the induced autophagy activities in K-562 cells may have improved the cancer cells' survival chances or even contributed to its death.

Altogether, the observed results suggest an important role played by autophagy in the cancerous cells indicated by the upsurge of autophagic activities in the Dox-treated K-562 cells compared to its activities at basal levels (Figure 3.6). Unlike Imatinib (1 μM) which had no significant effect on Beclin-1 to induce autophagy, a pathway previously demonstrated to be modulated as a result of Imatinib activities against the dysregulated BCR-ABL kinase (Ertmer *et al.* 2007), Dox (1 μM) which is known to affect multiple pathways was able to modulate both the autophagy as well as the apoptotic pathways.

3.4.2.3 Imatinib and Dox promote apoptosis in K-562 cells but Dox alone is able to modulate the alternative autophagy cell death pathway

Imatinib and Dox have both been used in the treatment of cancer. However, in the advanced blast crisis phase of CML where various pathways are turned on, the use of a chemotherapeutic

drug with multiple modes of action is suggested to be more beneficial in promoting the death of the CML cells. Dox has been demonstrated as being more effective than Imatinib in increasing cytotoxicity and decreasing CML cells proliferation (Almeida *et al.*, 2018). In contrast to Imatinib which initiates its inhibitory effect by specifically targeting BCR-ABL, a path that is hindered when the kinases mutate, Dox acts differently and induces its anti-neoplastic effects through varying alternative pathways including, the non-selective intercalation of the cell's DNA thereby inhibiting the activities of topoisomerase II enzymes. This leads to the blockage of various downstream steps that are critical in the catalytic processes of the cells, including transcription and DNA replication, thus producing a range of cytotoxic effects and eventually leading to the death of cells (Laroche-Clary *et al.*, 2000; Lebrecht *et al.*, 2004). Despite the effectiveness of Dox, its non-selective action makes its induced toxicity in non-cancerous cells outweigh the enthusiasm of making use of the drug.

In the management of CML, one essential factor is the prevention of the cells from advancing to the blast crisis phase. However, for patients whose conditions have already evolved to the highly modified stage of blast crisis, the prognosis is dismal and requires more aggressive treatment of intensive chemotherapy. At this phase, the blast cells have been observed to resemble the immature cells seen in patients with other types of leukaemia, specifically acute lymphoblastic leukaemia (ALL) for about 25% of patients, acute myeloid leukaemia (AML) for about 50% of patients or undifferentiated immunophenotype in 25% of patients (Derderian *et al.*, 1993; Cortes *et al.*, 2016). With the emergence of these leukaemia-like blast cells and the presence of mutated BCR-ABL kinases which are insensitive to Imatinib treatment, a subpopulation of patients desperately needing alternative therapeutic strategies is generated. Therefore, at such a stage, Dox, which unlike Imatinib has effective cytotoxicity against leukaemic stem cells (Sonneveld *et al.*, 1981; Perry *et al.*, 2020) and is effective against ALL as well as AML (Bhutani *et al.*, 2002; Wunderlich *et al.*, 2013; Shi *et al.*, 2019; Vu *et al.*, 2020), is preferable over the standard Imatinib treatment.

The results of the protein expression profile when HEK293T and K-562 cells were incubated in Imatinib or Dox as single drug treatments are summarised in table 3.2. Both drugs were able to modulate the apoptotic pathway in K-562 CML cells, with Dox promoting the release of Cytochrome c despite the non-involvement and downregulation of Bax and Bak, respectively (Table 3.2). However, when cell death was analysed using Annexin V/PI, Imatinib showed a 9.1% increase in the number of K-562 cells that died via apoptosis, compared to Dox (Appendix V). The reduced apoptotic cell death number detected in the Dox-treated cells may

have been as a result of the effect of Dox on the PI-stained cells. PI is a fluorescent DNA intercalating dye that stains cells in the late apoptotic and necrotic stages. However, Dox is also an intercalating agent that inhibits DNA synthesis. Hence, the drug may alter the binding of PI to the DNA of the cells, thus inhibiting the nuclear fluorescence of the PI-stained cell population that can be detected during analysis (Krishan *et al.*, 1978). It is pertinent for such interference to be taken into account as this may have resulted in an underestimation of the total number of dead cells, particularly the PI-stained Dox-treated cell population in the late stage of apoptosis.

Furthermore, analysis of the autophagy-related proteins showed Dox, but not Imatinib, to have promoted the expression of Beclin-1 in the K-562 CML cells. The observed autophagy-modulating ability of Dox in addition to its apoptotic effects emphasised the ability of the drug to act through more than one pathway, unlike Imatinib which specifically acts on the BCR-ABL kinase and is unable to effectively combat leukaemic stem cells and BCR-ABL mutated cells. Thus, considering that autophagy is a double-edged sword with the ability to suppress or encourage the growth of tumour cells, the autophagy modulating effect of Dox in K-562 cells made this drug a more interesting candidate for further investigation. Furthermore, based on this apoptotic and autophagic effects observed in the Dox-treated K-562 cells and the interactions which exist amongst the apoptotic and autophagic proteins, it was hypothesised herein that the Dox-induced downregulation of Bcl-xL (a major anti-apoptotic protein in K-562 cells) may have been sufficient and involved in the upregulation of Beclin-1, thus promoting possible cytotoxicity or chemoresistance in the Dox-treated leukaemic cells, via the autophagy pathway. This emphasises the interaction between Bcl-xL and Beclin-1 and is similar to observations by Pattingre *et al.* (2005), who reported the involvement of anti-apoptotic Bcl-2 in the inhibition of autophagy, based on its interaction with Beclin-1. Thus, it was worth investigating further to confirm if the Dox-induced autophagy observed in this study acted as a cytoprotective mechanism or contributed to the cytotoxic death effects observed in the K-562 CML cells.

3.4.2.4 Dox induced death in K-562 cells via the autophagy pathway

Increasing evidence points to the importance of autophagy induction in cancer cells. However, the role of autophagy in these cells remains debatable as previous studies have documented the presence of autophagy as a survival mechanism (Degenhardt *et al.*, 2006; Samaddar *et al.*,

2008; Wang *et al.*, 2014; Cheong *et al.*, 2016), as well as a death pathway (Laane *et al.*, 2009; Goussetis *et al.*, 2012; Tong *et al.*, 2013; Neri *et al.*, 2014). Therefore, since autophagy induction does not strictly result in the death of cells it was important to determine its role in the Dox-treated K-562 cells. To better understand the dynamic nature of autophagy, it is necessary for the artificial blocking of the turnover of autophagy-related proteins to be done.

Herein, the blockage of autophagy was employed using CQ (10 μ M) in order to obtain further information regarding the autophagic activities initially observed in the Dox (1 μ M)-treated K-562 cells. To avoid complicating the interpretation of the CQ-autophagy inhibition, it is worth mentioning that although the drug is termed an autophagy inhibitor, it does not affect the initiation phase of autophagy but rather influences the final degradative phase of the process. CQ is able to block autophagic flux by inhibiting the fusion between the autophagosomes and lysosomes. This autophago-lysosomal blockage ability of CQ, even after the subsequent increase in autophagosome numbers, has previously been documented (Yoon *et al.*, 2010; Musiwaro *et al.*, 2013; Mauthe *et al.*, 2018). Based on such previous studies, the treatment of K-562 cells with a therapeutically relevant dose of 10 μ M of CQ was also considered to be sufficient to inhibit autophagy with almost no involvement in the activation of cell death (Shacka *et al.*, 2006; Yoon *et al.*, 2010; Hirata *et al.*, 2011; Maycotte *et al.*, 2012; Zhou *et al.*, 2019).

In this study, it was initially hypothesised that the CML cells may have modified some amino acids necessary for the complete activation of apoptosis, post the mitochondrial level, due to the reduced expression of Bak ($p < 0.001$) and non-involvement of Bax ($p > 0.05$) in the Dox (1 μ M)-treated K-562 cells compared to the untreated K-562 control cells (Figure 3.6B). However, a previous study in mouse embryonic fibroblast had shown that despite the non-involvement of pro-apoptotic Bak and Bax, cell death was still able to occur via the non-apoptotic pathway (Shimizu *et al.*, 2004). Hence, with the observed increased levels of a major autophagy regulator protein, Beclin-1, and the percentage of dead K-562 cells (26%) (Table 3.1), it was then speculated that the CML cells may have activated the autophagy pathway through the upregulation of Beclin-1 in an attempt to survive the stressful Dox-induced apoptosis. However, the continuous autophagy activities may have acted as a cell death scaffold, resulting in the non-apoptotic death of the K-562 cells at 48 h. Therefore, in order to confirm if the effect of the autophagic activities observed in K-562 Dox-treated cells, enhanced cell death or promoted survival, the cells were treated with an autophagy inhibitor, CQ (10 μ M).

The co-incubation of K-562 cells with Dox (1 μ M) and CQ (10 μ M) resulted in the inhibition of the Dox-induced autophagy, evident by the increased levels of p62, an autophagy degradative protein, in the co-treated cells, compared to the K-562 cells treated with Dox (1 μ M) alone ($p < 0.001$) (Figure 3.7). Also, as envisaged, since CQ does not affect the initiation stage of autophagy, the levels of Beclin-1 remained unchanged in the CQ (10 μ M)-treated K-562 cells compared to the untreated cells ($p > 0.05$) (Figure 3.7). Furthermore, there was an increase in the levels of Bcl-2 ($p < 0.001$) and a decrease in the levels of Cytochrome c ($p = 0.001$) in the CQ (10 μ M)-treated K-562 cells compared to the Dox (1 μ M)-treated cells (Figure 3.7). This demonstrated a level of survival in the autophagy inhibited K-562 CQ-treated cells. Thereby suggesting that the presence of autophagic activities in the Dox-treated K-562 acted as a tumour suppressor and promoted cell death at the 48 h timeline tested.

The anti-apoptotic effect observed in the CQ-treated cells was in contrast to a previous study where CQ-autophagy inhibition was observed to potentiate the cytotoxicity of Dox in liver cancer cells (Zhou *et al.*, 2019). However, based on the cell death analysis initially carried out (Table 3.1), the decreased levels of Bcl-xL ($p < 0.01$) (Figure 3.6C), increased expression of Cytochrome c ($p = 0.001$) (Figure 3.6B) and further acquired autophagy inhibition results on the Dox (1 μ M)-treated K-562 cells, wherein CQ-autophagy inhibition was shown to have promoted survival in the Dox-treated CML cells, it can be deduced that the activation of the autophagy pathway in the Dox (1 μ M)-treated CML cells eventually promoted K-562 cell death (Figure 3.7). Thus, reporting for the first time that Dox at a therapeutically relevant dose of 1 μ M is able to induce death in K-562 CML cells, not only through the apoptotic pathway but also through the non-apoptotic (autophagy) pathway via the modulation of their shared regulatory proteins.

Taken together, the data implied that autophagy may have compensated for the deficiency in apoptotic cell death thereby promoting an autophagy-mediated cell death. Thus, the result of this study identifies an importance of Dox (1 μ M) in CML cells which is in accordance with its anti-cancerous effects, thereby strengthening the reports about the function of Dox in cancer cells. Furthermore, bearing in mind that Dox at a therapeutically low dose of 1 μ M was also able to induce significant cell death in non-cancerous HEK293T cells via the apoptotic pathway (Table 3.1; Figure 3.6), it is of great importance that further studies be carried out to investigate how this Dox-induced killing effect may be prevented or minimised in the non-cancerous HEK293T cells without affecting the drug effectiveness in K-562 CML cells. Such research involving drug combination through the modulation of the apoptotic and/or autophagy pathway

may hereby prove useful, especially, in rare conditions where patients present co-morbidity involving CML and AD.

3.4.3 The modulation of the apoptotic and autophagy pathways by AD drugs

Approved AD drugs are known for their neuroprotective effects and possess two well-studied modes of action: inhibiting acetylcholinesterase and blocking the NMDA. However, the drugs have also been suggested to affect other pathways, including the apoptotic and autophagy pathways (Noh *et al.*, 2009; Ki *et al.*, 2010; Yoon *et al.*, 2017; Albayrak *et al.*, 2018).

3.4.3.1 The modulation of the apoptotic and autophagy pathways by Donepezil

Studies involving AD drugs have reported the ability of Donepezil, an acetylcholinesterase inhibitor, to attenuate non-cancer cells from death through prevention of GSK-3 activity and inhibition of the apoptotic pathway at clinically relevant concentrations of 0.1 - 10 μM (Noh *et al.*, 2009; Mortazavian *et al.*, 2013; Sharifipour *et al.*, 2014). The drug has also been shown to protect against Dox-induced cognitive impairment (Ongnok *et al.*, 2021). Donepezil has been observed to induce cytotoxic effects on solid tumours and leukaemic cells at extremely high concentrations ranging from 100 μM to above 200 μM (Ki *et al.*, 2010). The drug induced apoptosis by activating both initiator and activator caspases 8, 9 and 3 in acute promyelocytic leukaemia cells, thereby increasing the cleavage of PARP-1 and resulting in the death of cancer cells (Ki *et al.*, 2010).

In this present study, the effect of Donepezil was investigated in K-562 CML cells and HEK293T cells. At clinically relevant concentrations of 1 - 10 μM , Donepezil-treated K-562 CML cells were observed to upregulate Cytochrome c expression with an increase in Bax (Figure 3.8B). In HEK293T cells, Donepezil, at the lowest concentration tested, 1 μM , surprisingly caused a decrease in cell viability (Figure 3.3B) but was unable to stimulate the death of the cells via the apoptotic pathway (Table 3.1).

When the protein expression levels in Donepezil (1, 5, 10 μM)-treated HEK293T cells were probed, the cells were observed to show upregulation in both anti-apoptotic (Bcl-2) and pro-apoptotic proteins (Bak and Cytochrome c) (Figure 3.8). The increased expression of both the anti-apoptotic as well as pro-apoptotic proteins in the Donepezil-treated HEK293T cells was not expected. Although, the initially observed cell viability reduction in Donepezil-treated

HEK293T cells suggested a reduction in the cells' survival. Hence, the ratio of the pro-apoptotic to anti-apoptotic proteins was evaluated to determine the cell's fate (Figure 3.9). This method was considered since the ratio between pro-apoptotic and anti-apoptotic protein gives more information as to whether the cells are susceptible to apoptotic cell death rather than survival, compared to individual protein expressions (Oltval *et al.*, 1993; Sato *et al.*, 1994; Hengartner, 2000). However, no significant difference was observed in the levels of pro-apoptotic to anti-apoptotic protein ratios (Bax:Bcl2 and Bax:Bcl-xL) in the HEK293T Donepezil-treated cells compared to the untreated cells ($p > 0.05$) (Figure 3.9). This suggested that the increased levels of anti-apoptotic Bcl-2 proteins in HEK293T cells may have kept Bax in check but might not have been sufficient to restrain pro-apoptotic Bak, which may directly influence the release of Cytochrome c even without a commitment to apoptosis. Thus, leading to a high percentage (> 96%) of viable HEK293T Donepezil-treated cells observed in the cell death analysis (Table 3.1). Furthermore, Donepezil was observed to modulate the autophagy pathway. The drug decreased Beclin-1 expression in both cell lines investigated, with an increased expression of p62 in HEK293T cells (Figure 3.8D).

Although, Donepezil did not cause significant death in HEK293T cells (Table 3.1), the reduced viability effect of the drug on the non-cancerous HEK293T cells (Figure 3.3) cast a bit of doubt on the use of Donepezil as a combination drug. Thus, Memantine, which was seen to consistently increase HEK293T cells viability was considered as a better option for further investigation in the combinatory study.

3.4.3.2 The modulation of the apoptotic and autophagy pathways by Memantine

Another AD-approved drug with a different mode of action compared to Donepezil, is Memantine. The ability of this NMDA antagonist drug to promote cell survival in non-cancer cells by exerting anti-autophagic and anti-apoptotic effects has been reported (Song *et al.*, 2015; Chen *et al.*, 2017). In prostate cancer, Memantine has also been shown to induce apoptosis (Albayrak *et al.*, 2018). Low-dose Memantine is neuroprotective (Chen *et al.*, 1998; Kafi *et al.*, 2014; Song *et al.*, 2015), however, care needs to be taken as a conducted study concluded that Memantine gave off adverse effects at doses lower than is required to provide a therapeutic benefit (Creeley *et al.* 2006). Also, the concentration of Memantine in the serum of AD patients receiving oral doses of 10 – 20 mg/day has been reported to be about 1 μM (Parsons *et al.*, 2008). Thus, in this study, clinically relevant concentrations of 1, 5 and 10 μM

Memantine were investigated. All three concentrations were observed to be non-toxic and promoted viability in non-cancerous HEK293T cells (Table 3.1; Figure 3.3).

Memantine (1, 5 and 10 μM) was observed to significantly increase anti-apoptotic Bcl-2 ($p < 0.01$, at all three concentrations) and Bcl-xL ($p < 0.01$, at all three concentrations) in HEK293T cells but not in K-562 cells (Figure 3.10C). In fact, the initially high Bcl-xL basal expression in K-562 cells, which measured 3.8-fold compared to HEK293T cells ($p = 0.01$), was surpassed in the Memantine-treated HEK293T cells. The levels of the anti-apoptotic Bcl-xL protein increased by 2.1 ($p = 0.01$) and 1.3-fold ($p < 0.05$) in the Memantine-treated HEK293T cells, compared to the levels in K-562 cells having the same Memantine concentrations of 1 and 5 μM , respectively (Figure 3.10C). Furthermore, in K-562 cells, Memantine upregulated the expression of Cytochrome c and was observed to kill about 10% more CML cells than HEK293T cells (Table 3.1; Figure 3.10B). The cell death effect of Memantine in K-562 cells was similar to their untreated cells but when compared to Memantine-treated HEK293T cells, a significant difference was observed, especially, in Memantine 1 μM ($p = 0.01$) and Memantine 10 μM ($p = 0.001$)-treated cells (Table 3.1). These observations demonstrated a possible selectivity of Memantine in killing CML cells.

When autophagy-related proteins were investigated, the drug was observed to induce similar effects in HEK293T and K-562 cells. Both cell lines gave a decreased Beclin-1 expression and in Memantine 1, 5 and 10 μM -treated cells, upregulated p62 proteins were observed (Figure 3.10D).

Under the same experimental conditions, the effect of Memantine at higher concentrations of 20, 30 and 50 μM in both cell lines was also investigated. High doses of Memantine have previously been reported to be efficacious, safe, and well-tolerated in AD patients (Grossberg *et al.*, 2013). In this study, Memantine (20, 30 and 50 μM) reduced the expression of Cytochrome c in HEK293T but not in K-562 cells (Figure 3.10B). In the CML cells, Cytochrome c levels were upregulated independent of Bax nor Bak expression (Figure 3.10B). These obtained results further emphasised the selectivity of Memantine against CML cells, even at higher concentrations. Downstream effects may need to be assessed in further studies to conclude if the release of Cytochrome c in K-562 cells triggered apoptosis. The observed cytotoxic effects of Memantine in cancer cells, at higher doses, have previously been documented (Seifabadi *et al.*, 2017; Albayrak *et al.*, 2018). However, very little data is available about its effect in CML. In a study by Abdul and Hoosein (2005), growth inhibition

and cell death were observed in Memantine-treated colon, breast and prostate cancer cell lines with an IC_{50} ranging from 23 to 92 μ M. In a similar study, Kamal *et al.* (2015) treated leukaemia cells with Memantine (5 –100 μ M) and reported that the drug reduced cell numbers by inhibiting proliferation. Furthermore, in a more recent study, Memantine was employed at a very high concentration of up to 600 μ M and was observed to inhibit proliferation and induce cell death by autophagy in glioma cells (Yoon *et al.*, 2017).

On assessment of the autophagy-related proteins, high concentration of Memantine (20, 30 and 50 μ M) was observed to inhibit Beclin-1 expression and increase the levels of LC3-II/LC3-I ratio in K-562 cells. The levels of p62 proteins were also upregulated in the CML cells, particularly, at the highest Memantine concentration tested (50 μ M) (Figure 3.10D). The high-dose Memantine may have acted as a chemotherapy agent in K-562, by inducing the release of Cytochrome c while inhibiting autophagy, a mechanism which may promote cell survival or induce death of the cells. The increase in both LC3-II/LC3-I ratio and p62 may have been an indication of impairment in the autophagic flux, as the high concentrations of Memantine (20, 30 and 50 μ M) were observed to cause a disruption of LC3 processing in K-562 cells producing an LC3 isoform yet to be reported (Figure 3.10A). This may be a pre-lipidated LC3 or maybe, an intermediate cleavage (pro-LC3B) that occurred as a result of Atg4 impairment. However, the bands seemed to have a smaller molecular weight compared to pro-LC3B which was previously described by Agrotis *et al.* (2019), hence, needs to be investigated further. The uppermost LC3 band visualised was ~18 kDa (LC3-I), the middle band was about 16 kDa, corresponding to LC3-II and the lowest band with the greatest mobility was visualised at ~13kDa (Figure 3.10A). Although, both the high and low-dose Memantine-treated K-562 cells showed a downregulation of Beclin-1, only the K-562 cells treated with high-dose Memantine expressed these LC3 ~13kDa isoforms as well as an increased level of LC3-II/ LC3-I ratio (Figure 3.10D). In addition, the intensity of the detected LC3 (~13kDa) isoform in the K-562 Memantine-treated cells was observed to be greatest at the highest Memantine concentration tested (50 μ M) with an accumulation of p62 at this concentration (Figure 3.10D). In contrast, HEK293T cells treated with both low and high concentrations of Memantine, did not show this ~13kDa LC3 isoform (Figure 3.10A).

Besides the detection of the LC3 (~13kDa) isoform in the higher concentrations of Memantine-treated K-562 cells, the results of the investigations on both the low and high concentrations of Memantine revealed similar inhibition of Beclin-induced autophagy as well as modulated apoptotic activities in both HEK293T and K-562 cell lines (Figure 3.10). However, a closer

look at the lowest concentration of Memantine tested (1 μM) suggested the drug's ability to promote survival in HEK293T cells but not in K-562 cells. This was evident from the increased levels of Bcl-2 and Bcl-xL proteins observed in the HEK293T cells (Figure 3.10C). Contrary to this, the levels of the anti-apoptotic Bcl-2 and Bcl-xL proteins remained unaltered in the HEK293T cells treated with higher concentrations of Memantine, compared to the control (Figure 3.10C). Thus, suggesting Memantine, at a clinically relevant concentration of 1 μM , as an optimal dosage to further investigate in the combinatory study.

The results obtained from the activities of the AD drugs in K-562 and HEK293T cells showed Donepezil and Memantine as exhibiting similar effects on the expressions of autophagy and apoptotic proteins. When cell viability was compared for each treatment in the non-cancerous HEK293T cells, the 24 h activities for Memantine or Donepezil (at 1, 5 and 10 μM) were not different from their drug activities at 48 h ($p > 0.05$, in both treatments). However, a comparison between the two treatments showed the activity of Memantine (1 μM) to be statistically significantly different from the inhibitory action observed in Donepezil (1 μM) for both 24 ($p < 0.05$) and 48 h ($p = 0.001$) HEK293T drug-treated cells (Figure 3.3). Thus, Memantine (1 μM) was selected as a more suitable option to include in the drug combinatory investigation.

Chapter 4

Investigating the effects of a combination drug on the modulation of the apoptotic and autophagic pathways to attenuate death in the non-cancer cells without inhibiting the death of CML cells

4. Investigating the effects of a combination drug on the modulation of the apoptotic and autophagic pathways to attenuate death in the non-cancer cells without inhibiting the death of CML cells

4.1 Introduction

The standard frontline treatment for CML utilises the action-specific Imatinib (Johnson *et al.*, 2003). However, pathological transformation and complex molecular mutations leading to increased BCR-ABL expressions in leukaemic cells, thus rendering the cells insensitive to BCR-ABL-inactivation by targeted drugs, continues in a subpopulation of patients. With the inclusion of a non-specific potent chemotherapeutic drug, Dox, in the treatment of CML, the outcome is improved (Bassan *et al.*, 1987; Palamà *et al.*, 2015; Almeida *et al.*, 2018; American Cancer Society, 2022). However, since these drugs are unable to cross the blood-brain barrier in amounts sufficient to reach a pharmacologic drug concentration, eradication of all sub-clones of neoplastic stem cells, particularly in the CNS, remains a challenge (Ohnishi *et al.*, 1995; Takayama *et al.*, 2002; Wolff *et al.*, 2003; Sardi *et al.*, 2014). Thus, leading to the rise in the number of CML relapses after an initial response (Elmaagacli *et al.*, 2000; Bornhauser *et al.*, 2004; Leis *et al.*, 2004; Matsuda *et al.*, 2005; Marum *et al.*, 2016; Jain *et al.* 2017). Furthermore, due to the non-selective cytotoxicity of Dox in cells, a need for a drug combination which can help alleviate this Dox-induced toxicity in non-cancerous cells, is warranted.

Drugs used in the management of AD, a condition that shares the same active cell cycling and inversely mirrors the effects observed in cancer (Behrens *et al.*, 2009; Liu and Ander, 2012), are known for their neuroprotective effects and better delivery system across the blood-brain barrier. Interestingly, these AD medications, such as Donepezil and Memantine, have also been shown to be cytotoxic in cancer by targeting various molecular pathways including the apoptotic and autophagy pathways (Ki *et al.*, 2010; Seifabadi *et al.*, 2017; Yoon *et al.*, 2017; Albayrak *et al.*, 2018).

Therefore, it was envisaged that the combination of an anti-cancer drug, which possesses multi-targeted effects against molecules involved in malignant transformation, with an AD drug, may help combat CML. However, it was of prime importance that the effect(s) of selected leukaemic and AD drugs were investigated as singular treatments in AD compared to CML cells, as very limited reports are available for such studies. Hence, a preliminary study was

done (Chapter 3) to investigate the effects of Imatinib, Dox, Donepezil and Memantine as single drug treatments in cell models of CML (K-562 cells) and AD (HEK293T). Based on the acquired results from the single-drug study, Dox and Memantine were selected for the combination study. In this chapter, the potential benefits of combining well-studied drugs, Dox and Memantine, which have effective chemotherapeutic and blood-brain barrier penetrating potentials were explored in the apoptotic and autophagic pathways of CML and AD.

4.2 Aims and Objectives

4.2.1 Aim of the study

To investigate the molecular effects of combination drug (Doxorubicin and Memantine) in the modulation of the apoptotic and autophagic pathways to attenuate death in the non-cancerous HEK293T cells without inhibiting the Dox-induced death of the CML cells.

4.2.2 Objectives of the study

- To determine if the combination of anti-cancer (Dox) and AD (Memantine) drugs exert an effect on the apoptotic and autophagic proteins expressed in cell models of CML (K-562 cells) and AD (HEK293T cells)
- To evaluate if a combination of Dox and Memantine would have an effect on the cell death induced by Dox in HEK293T cells
- To investigate if co-incubation of K-562 cells in Dox-Memantine treatment will sustain the Dox-induced cell death effect in the CML cells

4.3 Results

Dox/Memantine drug combination sustained Dox-killing effect by downregulating anti-apoptotic proteins in K-562 cells but not in HEK293T cells

Following the experimental results acquired from the single drug-treated cells (Section 3.3), Dox, a drug with a different mode of action compared to Imatinib, as well as Memantine, the preferred option for conferring cytoprotection in HEK293T cells, compared to Donepezil, were selected for further investigation. Dox and Memantine were explored as a combination therapy in CML and AD, using K-562 and HEK293T as cell models of the disease. Herein, the expression of apoptosis and the autophagy-related proteins were assessed in Dox/Memantine combination-treated HEK293T and K-562 cells. The levels were compared to the protein expressions in sole treatments of Dox and Memantine.

In HEK293T cells, Dox/Memantine (1 μ M) combination caused a statistically significant 2.2-fold decrease in Bax ($p < 0.05$) and a non-significant 1.1-fold decrease in Cytochrome c ($p > 0.05$) compared to the untreated HEK293T control cells (Figure 4.1B). The decreased Cytochrome c levels in the combination-treated cells were observed to be statistically significantly lower compared to the levels expressed in the Dox-treated HEK293T cells ($p < 0.05$) but non-significant compared to the levels seen in Memantine (1 μ M)-treated HEK293T cells ($p > 0.05$) (Figure 4.1B). However, when the levels of pro-apoptotic Bax in the Dox/Memantine HEK293T cells were compared with the Memantine-treated HEK293T cells, a highly significant decrease of 11.5-fold was observed ($p < 0.01$) (Figure 4.1B). The levels of Bak in HEK293T cells, which was initially increased in the Dox and Memantine sole treatments, were still observed to be upregulated in the Dox/Memantine combination-treated cells compared to the untreated HEK293T cells ($p < 0.05$) (Figure 4.1B). When compared to Dox-treated HEK293T cells, the levels of Bak in the combination-treated cells were observed to be 3-fold higher ($p < 0.05$) (Figure 4.1B). However, compared to the expression of Bak in the Memantine single-treated HEK293T cells, the protein levels in the combination treatment were much lower (2.9-fold) ($p < 0.01$) (Figure 4.1B).

When anti-apoptotic proteins were examined, Bcl-xL and Bcl-2 showed a 5.7 ($p < 0.01$) and 2.1-fold ($p = 0.001$) increase, respectively, in the Dox/Memantine-treated HEK293T cells compared to Dox-treated cells. However, the increase in the protein levels was not as high as the levels observed in Memantine-treated HEK293T cells (Figure 4.1C). In comparison to

Memantine-treated HEK293T cells, the levels of Bcl-xL expressed in the combination treatment were decreased 5.3-fold ($p < 0.01$) back to a similar level as observed in the untreated HEK293T control cells (Figure 4.1C). Similarly, Bcl-2 proteins were also decreased 1.7-fold ($p < 0.01$) but were still statistically significantly higher than the untreated cells ($p = 0.001$) (Figure 4.1C).

In K-562 cells, an undetectable level of Bax ($p > 0.05$) and a significant 1.9-fold decrease in Bak proteins ($p < 0.01$) were observed in Dox/Memantine (1 μ M)-treated K-562 cells compared to untreated K-562 cells (Figure 4.1B). The decreased levels of Bak were not statistically significantly different from the levels observed in the Dox (1 μ M)-treated K-562 cells ($p > 0.05$). However, in comparison to Memantine (1 μ M)-treated cells, the protein levels were 2.1-fold significantly less expressed in the combination treatment ($p < 0.01$) (Figure 4.1B). The undetectable level of Bax in Dox/Memantine combination-treated K-562 cells was not statistically different from the levels observed in K-562 cells treated with Dox or Memantine alone ($p > 0.05$) (Figure 4.1B). An upregulation of Cytochrome c was also observed in the Dox/Memantine-treated K-562 cells compared to the untreated cells ($p < 0.001$) (Figure 4.1B). The levels were not significantly different from the levels observed in Dox-treated cells ($p > 0.05$), however, the increase of 2.6-fold in Dox/Memantine-treated cells was very highly statistically significant when compared to the single treatment of Memantine ($p < 0.001$) (Figure 4.1B).

In the assessment of the anti-apoptotic proteins, Bcl-2, which were initially observed to be below the limits of detection in untreated K-562 cells, showed a difference of 0.005 increase (normalised to β -actin) in Dox/Memantine-treated cells (Figure 4.1C). However, these expressed Bcl-2 levels were not significant compared to the untreated cells ($p > 0.05$). When the levels of Bcl-2 in Dox/Memantine-treated K-562 cells were compared to sole treatments of Dox and Memantine, a statistically significant decrease of 5 ($p < 0.001$) and 9.8-fold ($p < 0.01$), respectively, were observed (Figure 4.1C). Dox/Memantine (1 μ M) treatment also induced a 2.4-fold decrease in the levels of Bcl-xL expressed in K-562 cells compared to the untreated K-562 cells ($p < 0.05$) (Figure 4.1C). These decreased levels were observed to be 3.5-fold higher than the levels observed in Dox ($p < 0.05$), yet lower, compared to the levels observed in Memantine-treated K-562 cells ($p < 0.05$) (Figure 4.1C).

When the autophagy proteins were examined, Beclin-1 levels which were initially decreased in Dox (1 μ M) and Memantine (1 μ M) single-treated HEK293T cells, remained at a low level

of 1.8-fold decrease compared to untreated HEK293T cells ($p < 0.05$) (Figure 4.1D). However, a slight increase of 1.1-fold was observed in the combination-treated cells compared to both Dox and Memantine single-treated HEK293T cells (both $p < 0.05$) (Figure 4.1D). When LC3-II/LC3-I autophagosome-related proteins were probed, the levels of the protein remained unaltered in the Dox/Memantine combination-treated HEK293T cells compared to the untreated cells ($p > 0.05$) (Figure 4.1D). However, when compared to the single-treated cells, the Dox/Memantine-treated cells showed a 2-fold increase and 2.2-fold decrease in the levels of LC3-II/LC3-I compared to Dox ($p < 0.05$) and Memantine ($p < 0.05$)-treated cells, respectively (Figure 4.1D). Similar to the increased p62 levels observed in single-treated Dox (1 μM) and Memantine (1 μM) HEK293T cells, the levels of p62 proteins remained increased in the Dox/Memantine combination-treated cells compared to untreated HEK293T control cells ($p = 0.001$) (Figure 4.1D). The observed p62 levels in Dox/Memantine 1 μM treated cells were observed to be 1.2-fold non-significantly higher than Dox-treated HEK293T cells ($p > 0.05$) and 1.3-fold significantly lower than Memantine-treated HEK293T cells ($p = 0.049$) (Figure 4.1D).

In K-562 cells, Beclin-1 levels were increased in the combination-treated cells compared to their untreated control cells ($p < 0.05$) (Figure 4.1D). These increased levels were not statistically different compared to the levels observed in the Dox-treated K-562 cells ($p > 0.05$). However, they were observed to be 3.4-fold higher than the levels detected in Memantine (1 μM)-treated K-562 cells ($p < 0.001$) (Figure 4.1D). Also, upregulation of LC3-II/LC3-I ($p < 0.001$) and downregulation of p62 ($p = 0.001$) proteins were observed in the Dox/Memantine combination-treated cells, compared to the untreated K-562 cells (Figure 4.1D). The increase of LC3-II/LC3-I was not significantly higher than the expression levels observed in Memantine (1 μM)-treated K-562 cells ($p > 0.05$) but was observed to be 1.3-fold statistically significantly lower than expressed in Dox-treated cells ($p < 0.05$) (Figure 4.1D). Furthermore, on assessment of the membrane blots, the LC3 (~13kDa) isoform previously observed in high-dose Memantine-treated K-562 cells (Figure 3.10A), were also observed in Dox/Memantine combination-treated K-562 cells (Figure 4.1A). In addition, a statistically significant increase in p62 expression levels was observed in the Dox/Memantine-treated K-562 cells ($p < 0.05$) compared to Dox-treated cells, where an undetectable level was initially observed (Figure 4.1D). However, these increased levels of p62 proteins expressed in the Dox/Memantine combination-treated K-562 cells were 3-fold lower compared to levels observed in Memantine 1 μM -treated K-562 cells ($p < 0.01$) (Figure 4.1D).

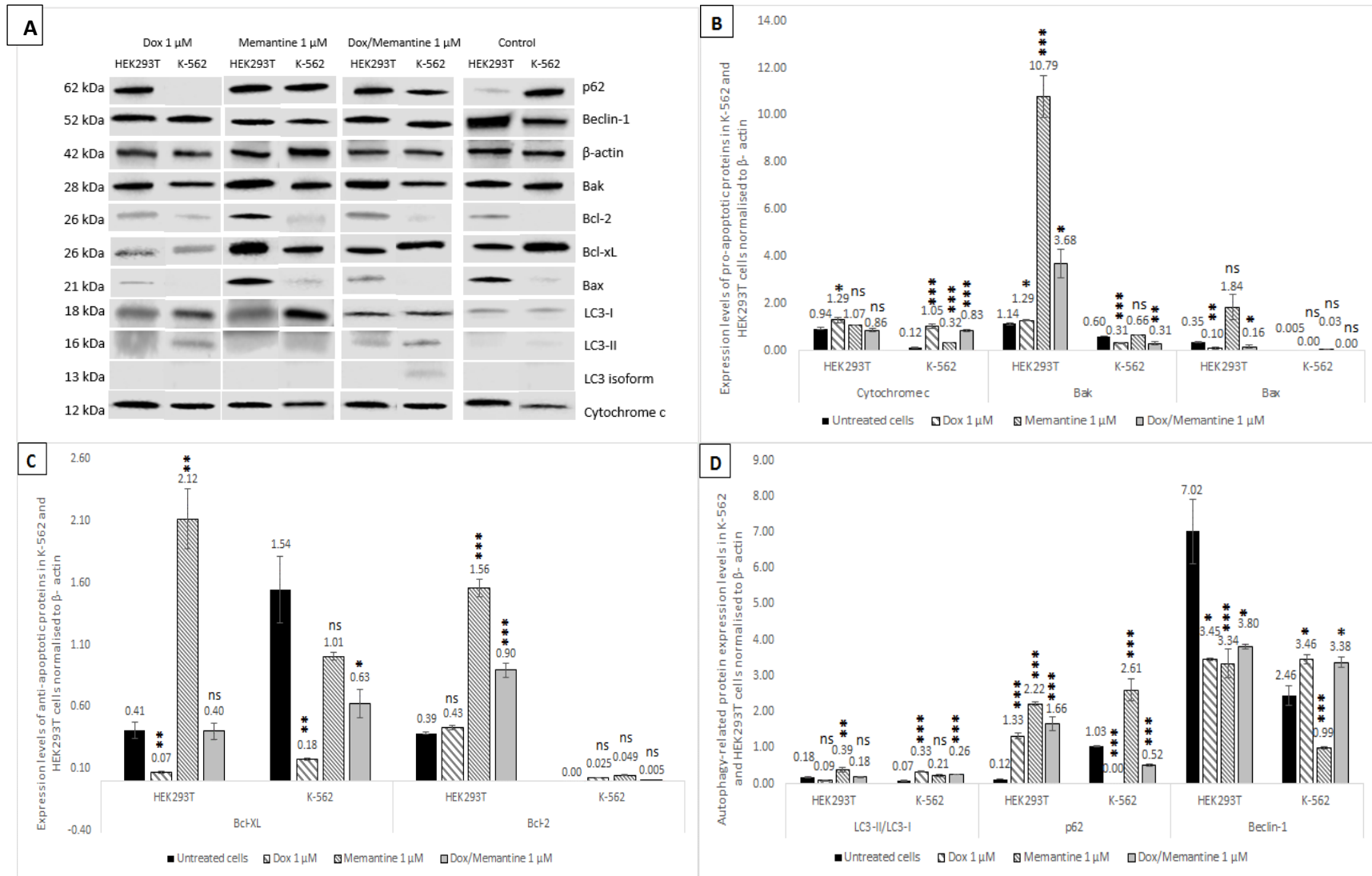


Figure 4.1 Effects of Dox/Memantine combination treatments on the levels of proteins involved in apoptosis and autophagy in HEK293T and K-562 cell lines after 48 h treatment

(A) Representative Western blot image

(B) Pro-apoptotic proteins: Cytochrome c, Bak and Bax (C) Anti-apoptotic proteins: Bcl-xL and Bcl-2 (D) Autophagy-related proteins: LC3, p62 and Beclin-1

Dox/Memantine (1 μM) caused a decrease and increase of Bcl-xL and Cytochrome c proteins in K-562 cells, respectively. In HEK293T, the levels of Bcl-2 were increased. In the autophagy pathway, Dox/Memantine combination is observed to increase autophagy activities in K-562 cells by increasing Beclin-1 and LC3-II/LC3-I levels while decreasing the expression of p62.

Data were normalised to β-actin expression levels. Experiments were repeated thrice and data are expressed as mean ± SE. Basic statistical analysis was performed using 2-sample t-test and significant differences were shown as: p > 0.05, no significance (ns); * when p ≤ 0.05, significant; ** when p ≤ 0.01, highly significant and ***, p ≤ 0.001, very highly significant.

4.4 Discussion

Dox/Memantine drug combination modulates both the apoptotic and autophagy pathways in K-562 and HEK293T cells

The inability of non-specific chemotherapeutic drugs to differentiate cancer from non-cancer cells, the failure of TKIs to improve the overall survival of CML patients, especially those in the blast crisis phase, as well as the situations where an individual suffers the double blow of both AD and CML, prompted this investigation. The approach taken in this chapter was to combine and explore if two drugs initially observed (Chapter 3) to have independent effects in the investigated cell lines (K-562 and HEK293T) would modulate the apoptotic and autophagic pathways differently in order to give a better therapeutic result compared to their effects as singular drug treatments. Herein, Dox, a broad-spectrum antibiotic was combined with Memantine, an NMDA antagonist drug, to promote death in CML cells while mitigating adverse effects in HEK293T non-cancer cells. This strategy was conceived since the repurposing of drugs had become a cornerstone therapy in combating various ailments.

Dox is known to induce increasing cytotoxicity with an increase in drug concentration (Müller *et al.*, 1997; Pilco-Ferreto and Calaf, 2016; Zhao and Zhang, 2017). However, even at a low therapeutic dosage of 1 μ M, the results of this present study showed that Dox also induces cytotoxicity in non-cancerous HEK293T cells. Various studies have sort strategies that could reduce this Dox-induced toxicity in normal cells of cancer patients, especially cardiotoxicity (Swain *et al.*, 1997; O'Brien *et al.*, 2004; Cardinale *et al.*, 2006). Herein, the author reports a drug combination strategy that limits Dox-associated toxicity in HEK293T, a kidney cell with neurological lineage, without affecting the molecular anti-cancer effects of the drug in CML cells. Dox possesses a non-selective ability to combat rapidly dividing cells and achieves its killing effects via various mechanisms, including the targeting of the intracellular apoptotic pathway (Laroche-Clary *et al.*, 2000; Childs *et al.*, 2002; Lebrecht *et al.*, 2004). On the other hand, Memantine is known for its protective features (Chen *et al.*, 1998; Jantas *et al.*, 2008; Kafi *et al.*, 2014) and has also been reported as being cytotoxic in cancer cells by targeting various molecular pathways including the apoptotic and autophagy pathways (Abdul and Hoosein, 2005; Seifabadi *et al.*, 2017; Albayrak *et al.*, 2018). The repurposing strategy of these two drugs was considered since both Dox and Memantine, as single treatments, were observed, herein, to act differently in HEK293T but similarly in their cytotoxic effect against K-562 cells. Also, a limited number of studies involving the protective effects of Memantine, have reported the drugs' ability to prevent Dox-induced cell damage in non-cancer cells (Jantas *et al.*, 2008;

Jantas and Lason, 2009), with almost none, to the best of the author's knowledge, exploring both drugs as a combination therapy in CML and AD. Therefore, it was hypothesised that the amalgamation of both drugs would bring about similar effects when used in models of CML and AD. In CML, disease progression involves the activation of a combination of signalling pathways which may not be effectively targeted with an action-specific drug. Also, as the disease progresses, the cancer cells migrate to various regions of the body, including the brain and the spinal cord (Evans *et al.*, 1970; Radhika *et al.*, 2011; Chiba *et al.*, 2018). Although rare, leukaemic cells are able to infiltrate the CNS and up to date, there is yet to be an established treatment regime for CML patients suffering from such complications. Dox is effective against these cells, however, the drug is unable to cross the blood-brain barrier (Ohnishi *et al.*, 1995; Sardi *et al.*, 2014). Thus, the targeting of CML cells with Dox and Memantine combination to enhance the killing effect in K-562 cells while inhibiting adverse effects in non-cancer HEK293T cells, seemed interesting to investigate.

The results obtained in this drug combination study, showed the combined drugs at a concentration of 1 μM to promote the increase of Cytochrome c expression in K-562 cells but not in HEK293T cells (Figure 4.1B). The levels of anti-apoptotic Bcl-xL, which was initially expressed in the CML cells at a very high level under normal physiological conditions, were reduced 2.4-fold in the Dox/Memantine-treated K-562 cells (Figure 4.1C). In addition, the initially observed apoptotic effect of Dox as a single drug in K-562 CML cells, through the upregulation of Cytochrome C, was not disrupted by Memantine in the drug-combined treated cells (Figure 4.1B). Instead, the combination treatment resulted in the reversal of the apoptotic effects Dox had on HEK293T cells (Figure 4.1). Thus, demonstrating the ability of these combined drugs to promote cell death and survival in cancer and non-cancer cells, respectively.

The presence of Memantine in the combination drug was observed to limit the initially observed Dox-induced toxicity in HEK293T cells. Memantine may have achieved this by accelerating the reparation of the damaged biomolecules in the cells. Thus, leading to the increased expression of anti-apoptotic Bcl-2, a protein that had previously been reported (Vu *et al.*, 2020) and confirmed herein, not to be modulated by Dox. The Bcl-2 protein levels in Dox/Memantine-treated HEK293T cells were increased by 2.1-fold compared to the low levels observed in the Dox (1 μM)-treated HEK293T cells ($p = 0.001$), where a significant percentage of 34.1% of the non-cancer cells were initially observed to die by apoptosis. These results were similar to reports by Ju *et al.* (2009) where Memantine was described to have blocked apoptosis

in the retina of glaucomatous 9-month-old mice through the upregulation and downregulation of Bcl-2 and Bax mRNA expression, respectively.

The observed anti-leukaemic activities of Memantine, herein, evident by the sustained increase of Cytochrome c in K-562 cells, may also be due to the action the drug shows by inhibiting NMDA receptors, a structure previously reported to be present in megakaryoblastic leukaemic cells, such as K-562 cells (Kamal *et al.*, 2015). Although, it is yet to be established if the presence of these receptors contributes to the megakaryocytic malignancies. However, the receptors have been described to act as a channel for calcium to enter the cells and support the survival of leukaemic cells (Kamal *et al.*, 2015). Herein, NMDA receptor antagonist, Memantine, in combination with Dox was able to inhibit survival in the CML cells. The observed effect of the NMDA receptor antagonist aligns with the effects reported by Kamal *et al.* (2015), where Memantine (5–100 μM) was observed to reduce cell numbers in K-562 by suppressing proliferation.

In a study by Song *et al.*, 2015, Memantine was observed to downregulate the levels of autophagy-related proteins (LC3-II/LC3-I ratio and ATG5), which was initially induced using Rapamycin, in SH-SY5Y cell model of AD. Similarly, in this present study, when Memantine (1 μM) was employed as a single drug treatment in HEK293T cells, downregulation of Beclin-1 and increased expression of p62 proteins levels were observed (Figure 4.1D). Thus, suggesting an inhibition of autophagy. Dox acted in a similar way to Memantine by inhibiting autophagy, however, the chemotherapeutic drug was observed to stimulate death in the HEK293T cells via the apoptotic pathway (Table 3.1). Further investigation with Dox and Memantine combination did not alter the inhibited autophagic process in the HEK293T cells (Figure 4.1D). The combination therapy caused Beclin-1 to be slightly increased above the levels observed in the single drug treatments ($p < 0.05$, compared to Dox and Memantine individually), however, remained lower than the untreated HEK293T control cells ($p < 0.05$). The level of p62 proteins also remained higher compared to the untreated cells ($p = 0.001$) (Figure 4.1D). When the individual treatment of cells with Dox (1 μM) and Memantine (1 μM) was assessed in the autophagy pathway of K-562 cells, both drugs acted differently. Dox promoted autophagy while Memantine caused a downregulation of Beclin-1 ($p < 0.001$) with an increase in p62 levels ($p < 0.001$) compared to the untreated K-562 cells (Figure 4.1D). Dox/Memantine drug combination modulated the autophagy pathway, causing a significant increase in Beclin-1 compared to K-562 untreated cells ($p < 0.05$). These increased levels of Beclin-1 were observed to be at a similar level as it was initially observed in Dox-treated K-

562 cells but with a slightly increased level of p62, compared to the Dox-treated CML cells ($p = 0.05$) (Figure 4.1D). As previously mentioned, cancer cells are able to devise mechanisms by which they inhibit cell death, such mechanisms include the activation of autophagy (Mathew *et al.*, 2007; Sakuma *et al.*, 2013; Zhao *et al.*, 2014). However, continuous autophagy activities may result in non-apoptotic death or even serve as a scaffold for other efficient autophagy-mediated cell deaths (Laane *et al.*, 2009; Tong *et al.*, 2013; Ristic *et al.*, 2014). In this present study, the promotion of autophagic activities in Dox (1 μM)-treated K-562 cells led to the death of over 25% of the CML cells. Although, this was 11% lower compared to the dead cells observed in the non-cancer Dox (1 μM)-treated HEK293T cells ($p < 0.05$) (Table 3.1).

The findings of this present study show the ability of Dox/Memantine drug combination to sustain the activated autophagy-mediated cell death effect initially observed in Dox-treated K-562 cells. In addition, the potential of the combination drug to encourage cell death through the downregulation of Bcl-xL and upregulation of pro-apoptotic Cytochrome c in K-562 CML cells, but not in HEK293T non-cancerous cells, is highlighted. Thus, suggesting a strategy of non-cancer cell protection while simultaneously providing therapeutic benefits against the CML cell population.

Chapter 5

Summary, conclusion and future works

5. Summary, conclusion and future works

5.1 Summary

There is an increase in the number of individuals living with age-related diseases such as CML and AD (Holliday, 1996; Jaul and Barron, 2017; WHO, 2022). Drug resistance and the inability to achieve total eradication of these diseases, remain a major challenge. Moreover, the inability of anti-cancer drugs to distinguish between healthy and unhealthy cells poses a greater risk to patients undergoing cancer treatment, during which, complaints of cognitive dysfunction are common.

In this study, in order to explore the modulation of two connected pathways (apoptosis and autophagy), cells (K-562 and HEK293T) were treated with approved cancer drugs, Imatinib (Section 3.3.5) and Dox (Section 3.3.6) and AD drugs, Donepezil (Section 3.3.7) and Memantine (Section 3.3.8). Increasing understanding of the molecular bases of diseases has demonstrated that the abnormal expression and activities of proteins involved in signalling pathways contribute to the development of diseased conditions and as such, this was investigated.

5.1.1 Basal expressions

In order for cancer cells to meet their growth and survival requirements, they usually have altered metabolic pathways in comparison to non-cancer cells. Under normal growth conditions, the unstressed cell lines (K-562 and HEK293T) expressed contrasting levels of proteins. The increase of autophagy proteins, Beclin-1 ($p < 0.01$) and LC3-II/LC3-I ($p < 0.05$), with the concomitant decrease in p62 ($p < 0.001$) proteins in HEK293T cells compared to K-562 cells, indicated more autophagy flux in the non-cancerous cells (Figure 3.4C). However, it was not clear if at these basal levels the autophagy modulation conferred protection or cytotoxicity in the cells. In the apoptotic pathway, K-562 cells expressed lower levels of pro-apoptotic proteins (Bak, Bax and Cytochrome c) and an increased amount of anti-apoptotic Bcl-xL. This was 3.8 times higher compared to the levels expressed in non-cancerous HEK293T cells ($p < 0.01$) (Figure 3.4C). This signified a major difference in the apoptotic pathway of the CML versus the non-cancer cells. The CML cells used the tactics of expressing anti-apoptotic proteins while downregulating the pro-apoptotic ones as a survival mechanism under normal growth conditions. The approach taken in this work helped to characterise how

the protein file in K-562 CML cells differs from HEK293T non-cancer cells, prior to drug treatments.

5.1.2 Molecular effects of anti-leukaemic drugs in K-562 and HEK293T cells

When the cells were separately incubated in the anti-cancer drug, both Imatinib and Dox modulated the intrinsic apoptotic pathway of the CML cells, causing a decrease in the levels of Bcl-xL in the K-562 cells (Figure 3.5C & 3.6C). However, Dox showed a double-fold decrease (8.6-fold) in the anti-apoptotic protein compared to Imatinib (3.6-fold). Also, Dox was able to enhance autophagy activities in K-562 cells by increasing the levels of Beclin-1 and causing the levels of p62 to reduce to a non-detectable level (Figure 3.6D). At present, the relationship between autophagy and cell death remains unclear. However, cancer cells are known to deregulate different molecular pathways. Therefore, therapies with multiple activities are considered better, even in CML treatment. Hence, in order to explore the Dox-induced effect of autophagy in the CML cells, the autophagy activities were blocked using CQ. It was then discovered that autophagy contributed to the inhibition of the survival of K-562 CML cells. The addition of CQ resulted in increased levels of Bcl-2 and a decrease in Cytochrome c proteins in K-562 cells (Figure 3.7). Despite the favourable anti-cancerous activities displayed by Dox in K-562 cells, the drug also showed cytotoxicity in the non-cancerous HEK293T cells. Despite the wide use of Dox in cancer treatment, the non-selective toxicity of the drug towards non-cancer cells remains a problem. Therefore, an approach that can utilise the anti-leukaemic activities of Dox in CML cells while abating the cell death effects in HEK293T cells, was desired.

5.1.3 Molecular effects of AD drugs in K-562 and HEK293T cells

Neuroprotective drugs such as Donepezil and Memantine, which help to prevent deleterious effects leading to cell death in AD, have been reported to enhance cell death in tumour cells (Rzeski *et al.*, 2001; Abdul and Hoosein, 2005) and as such, they may be effective in the treatment of cancers such as CML. In this study, the apoptotic and autophagic effects of Donepezil and Memantine were examined in K-562 CML cells and non-cancerous HEK293T cells.

Donepezil (1 μ M) upregulated Bcl-2 and Bcl-xL levels in HEK293T cells (Figure 3.8C). Surprisingly, the drug also inhibited cell viability (Figure 3.3), increased the levels of Bak and

Cytochrome c in the non-cancerous cells (Figure 3.8C). These results suggested the ability of Donepezil to modulate the proteins involved in the apoptotic pathway by increasing anti-apoptotic protein levels while inducing apoptosis in HEK293T cells via a mitochondria-mediated pathway. The ratio of the pro-apoptotic to anti-apoptotic proteins was calculated to determine the cell's fate. However, no statistically significant difference was observed between the pro-apoptotic to anti-apoptotic proteins activities (Figure 3.9). It would be interesting to explore the possibility of an interfering pathway in the HEK293T-Donepezil treated cells which may have led to the contradictory behaviours observed.

Memantine, another AD drug with a different mode of action to Donepezil was investigated. Memantine is a known NMDA channel blocker. The molecular effects of Memantine via the NMDA pathway in cancer cells, have been reported (Li and Hanahan, 2013; Yoon *et al.*, 2017; Albayrak *et al.*, 2018; Li *et al.*, 2018). However, more work needs to be done to determine its cancer-modulating abilities through other pathways. Thereby helping to broaden the knowledge about employing this NMDA antagonist drug in the treatment of other diseases like CML. Herein, similar to Donepezil, the effects of Memantine (1 μ M) were also probed. Memantine was observed to increase the cell viability of HEK293T cells (Figure 3.3). Anti-apoptotic Bcl-2 and Bcl-xL proteins were also enhanced in the cells (Figure 3.10C). Memantine also showed a selective inhibition against the CML cells by killing 9.6% more K-562 cells compared to the non-cancerous HEK293T cells ($p = 0.01$) (Table 3.1). When some distinct apoptotic proteins were investigated, the drug was observed to potentiate an increase in the expression of Cytochrome c in the CML cells (Figure 3.10B). These attributes made Memantine a more suitable candidate to explore in combination with Dox.

5.1.4 Molecular effects of anti-leukaemic and AD drug-combination in K-562 and HEK293T cells

The growth of tumour cells in locations distant from the primary site of the cancer, is a common occurrence. In leukaemia, cancer cells have been observed in the CNS (Wolff *et al.*, 2003). Although many chemotherapeutic drugs have been utilized in the treatment of leukaemia, the toxicity induced in surrounding healthy cells, the drug penetration ability as well as the rate in achieving complete remission, is far from satisfactory. In CML, treatment with chemotherapy, especially when the cancer cells have metastasised to the brain, results in serious toxicities associated with cognitive dysfunction (Ongnok *et al.*, 2021). Presently, there are no approved

pharmacological interventions for such conditions. Drug advances have encouraged various combinatory treatments to aid in combating CML more effectively. New compounds or repurposing of existing drugs with minimal adverse effects is desirable for a drug combinatory approach. In this study, we examined the susceptibility of CML and non-cancerous cells to death or survival when treated with Dox and Memantine drug combination. In an effort to attenuate HEK293T cells from the Dox-induced cytotoxicity, the cells were co-incubated with Dox and Memantine. The selected drug combination was anticipated to give an increased molecular therapeutic outcome in the CML cells with reduced side effects in the non-cancerous cells. The results obtained from this drug combination study showed the Dox/Memantine combination to promote survival in the non-cancerous HEK293T cells by upregulating Bcl-2 (Figure 4.1C), a protein that was initially observed not to be modulated by Dox (Figure 3.6C). In addition, the apoptotic effect of Dox as a single drug in K-562 CML cells, through the upregulation of Cytochrome C, was not disrupted by the presence of Memantine in the drug-combined treated CML cells ($p > 0.05$) (Figure 4.1B). Dox/Memantine drug combination gave an additive and antagonistic drug effect in K-562 and HEK293T cells, respectively. In K-562 cells, the combination of both drugs maintained the killing effect which was initially observed when cells were treated with Dox alone. But in the non-cancerous HEK293T cells, the presence of Memantine attenuated the cells from the Dox-induced death by increasing the levels of the anti-apoptotic Bcl-2, a protein observed not to be regulated by Dox. This suggests that combined Dox and Memantine treatment could be a therapeutic strategy to enhance cell death in CML. Also, bearing in mind that cognitive dysfunction is prevalent amongst patients receiving chemotherapy and there are presently no approved pharmacological interventions for such conditions, the use of Dox and Memantine may prove to be of therapeutic benefit to such patients.

5.1.5 Limitations of the study

There are several limitations to this study and as such, certain shortcomings must be highlighted.

Firstly, the research was performed on HEK293T as a non-cancerous AD model. Without the transfection of an AD-involved protein to mimic a path in AD *in vivo*, this model may be seen as an apparent limitation of the study. However, the future direction of this study involves the development and analysis of a HEK293T AD model expressing amyloid beta (a hallmark of

AD) and as such preliminary pre-transfection data was necessary for comparison post-transfection of the cells. Hence, this study can be seen as an introduction to the investigation of CML and AD co-morbidity.

Another limitation involved the use of only one inhibitory work. Experiments with inhibitors can provide a better understanding of various signalling pathways. Thus, in this study, chloroquine was employed to block autophagy. Chloroquine blocks the late stage of autophagy by raising the pH of lysosomes, thereby inhibiting the autophagosome-lysosome fusion. Other inhibitory works should have also been included. For example, K-562 CML cells were observed to express high levels of Bcl-xL. When the cells were treated with Dox, the anti-apoptotic proteins were observed to be decreased and death induced. The use of Bcl-xL inhibitors, such as WEHI-539, to block Bcl-xL expression would have been used to verify if the selective inhibition of the protein could have sensitised the CML cells to enhance Dox-induced cell death. Furthermore, it has been reported that when inhibitors are used at certain concentrations, they can cause non-specific toxic effects (Callus and Vaux, 2007). Therefore, a range of Chloroquine concentrations should have been tested before usage for the inhibitor work. However, based on results from previous studies which had documented the non-involvement of the drug to cell death activation at this concentration (Shacka *et al.*, 2006; Yoon *et al.*, 2010; Hirata *et al.*, 2011; Maycotte *et al.*, 2012; Zhou *et al.*, 2019), Chloroquine (10 μ M) was selected without further investigations.

Apoptosis and autophagy were determined using Western blot analyses to detect protein levels. To avoid bias and to verify both cell death and the autophagic compartments, some confocal work would have been included. However, the present study focused on the comparison of protein levels in apoptosis and autophagy. Thus, different proteins which played varying roles at intervals of each pathway were selected. Although, it would have been preferable to include both Western blot analysis and confocal work and then compare the two sets of results. However, taking the acquired data together, a comprehensive overview of apoptotic and autophagic activities in the cells was given. Also, the study was limited to the expression of proteins. Maybe some gene expression study might have added more value to the acquired data in this study. However, since the study focused on the mechanism of action, protein expression seemed sufficient, herein.

In the combination study, only one scientific technique was used to assess the effects of the combination drug in the cells. This was an obvious limitation of the study. The inclusion of a

second method would have aided in verifying the acquired results. Furthermore, the observation of an increased level of anti-apoptotic Bcl-2 in the Dox/Mem-treated HEK293T cells was interpreted as cell survival in the non-cancer cells. These increased levels were suggested to have inhibited the apoptotic effects initially observed in HEK293T cells treated with Dox alone. Although, an increase in the levels of anti-apoptotic Bcl-2 in cells enhances survival. However, all other signals must be considered before concluding that the upregulated Bcl-2 levels observed in the Dox/Mem-treated HEK293T cells inhibited the apoptotic effects initially observed in Dox-treated HEK293T. An extrapolation based on the increased Bcl-2 levels, alone, is not sufficient to be interpreted as apoptotic inhibition and as such must be highlighted as another limitation in this study. A cell viability experiment to determine if the combination treatment promoted survival in HEK293T cells, would have been helpful. Most importantly, the inclusion of a cell death assay to measure the apoptotic cells present in the Dox/Mem-treated HEK293T compared to the apoptotic cells present in Dox-treated HEK293T cells would have provided evidence to determine if apoptosis was inhibited in the combination-treated HEK293T cells or not.

Finally, this study involved the determination of the mechanism of action of selected drugs in CML and AD models. The inclusion of an *in vivo* study would provide added information on the effects of the drugs. However, this was beyond the scope of the current study.

5.2 Future studies

5.2.1 Investigating the Dox-induced autophagy pathway upstream of Beclin-1

The physiological process of autophagy, which is not limited to a single signalling pathway needs to be further investigated upstream of Beclin-1 expression to evaluate how specific molecules played roles that resulted in the Dox-induced autophagy-mediated cell death in CML cells but not in HEK293T cells. It would be interesting to know if the 5'-adenosine monophosphate-activated protein kinase (AMPK) pathway was involved in the downstream effects observed. AMPK has a dual function as it acts as a cellular energy sensor. The kinase could inhibit the mammalian target of rapamycin complex 1 (mTOR1) activities and other energy-consuming pathways to decrease ATP consumption (Inoki *et al.*, 2003; Leprivier *et al.*, 2013; Vara-Ciruelos *et al.*, 2019). On the other hand, AMPK could promote cell survival (Jeon *et al.*, 2012; Vara-Ciruelos *et al.*, 2019). Exploring these upstream processes will give more

information as to what pathways were turned on in the CML cells different from HEK293T cells.

5.2.2 Verifying the cell death effect of Memantine in K-562 CML cells

Emerging evidence report that cell commitment to death may be regulated even after the release of Cytochrome c (Deveraux *et al.*, 1998; Jäättelä *et al.*, 1998; Beere *et al.*, 2000). Since Memantine (1 μ M) was able to induce an increase in the levels of Cytochrome c independent of Bak and Bax in K-562 cells, it would be necessary to verify if these increased levels led to the activation of caspases and other downstream apoptotic cell death stimuli in the CML cells. Also, other pathways which may have been involved in the expression of Cytochrome c in the Memantine-treated CML cells need to be explored. This investigation will help to ascertain if Memantine aided in the Dox-killing of K-562 cells. Such a synergistic effect of the two drugs will aid in uncovering another therapeutic benefit of Memantine to induce apoptotic cell death of CML cells. Also, with further research involving the CNS, it will better elucidate the use of Dox/Memantine combination in destroying CML cells in areas like the CNS where Dox at pharmacologically relevant dosages may not be able to reach.

5.2.3 Investigating the effects of Dox/Memantine on BCR-ABL activities in K-562 cells

In CML, the abnormal BCR-ABL is known to be constitutively activated. Due to the importance of this fusion protein in CML, Western blot analysis and other relevant scientific techniques should be performed in K-562 cells to determine if the combination drug is capable of modulating the expression and activities of BCR-ABL oncoprotein in the CML cells compared to the Dox-treated cells as well as the untreated counterpart. Abnormal interactions between the BCR-ABL and other cytoplasmic molecules can lead to the disruption of various cellular processes including Ras (Puil *et al.*, 1994), Janus kinase/signal transducer and activator of transcription (JAK/STAT) (Ilaria and Van Etten, 1996; Chai *et al.*, 1997) and Phosphatidylinositol 3 kinase (Sattler *et al.* 1996) pathways. It would be interesting to explore if the drug combination is able to inhibit any of these pathways and encourage cell death. Results from such studies will provide additional opportunities to develop more effective therapeutic strategies against CML through the targeting of the molecular pathways and may also help to overcome resistance to tyrosine kinase inhibitors.

5.2.4 Investigation of an autophagy-related LC3 isoform in K-562 CML cells

The high-doses of Memantine (20, 30 and 50 μM) may have acted as a chemotherapy agent in K-562, by inducing the release of Cytochrome c while modulating autophagy. An LC3 isoform which maybe as a result of disruption in LC3 processing in K-562 cells was observed. This isoform was also seen in K-562 cells treated with Dox/Memantine combination drug. The reason for the formation of this isoform (yet to be reported) is unknown. The LC3 isoform was detected at $\sim 13\text{kDa}$, a much lower band weight than previously described LC3 proteins. A closer look into the mechanisms involved in LC3 processing, in the presence of Atg impairments, may shed light in regards to the detected LC3 isoform ($\sim 13\text{kDa}$).

5.2.5 Investigating the effects of Dox/Memantine in an *in vitro* model AD overexpressing amyloid beta

One major neuropathological feature involved in AD is the formation of amyloid plaques which aggregates over the years from smaller amyloid molecules. The targeting of amyloid oligomers prior to the formation of plaques may help to slow down or prevent the progression of AD. Increasing evidence suggests that apoptotic (Engidawork *et al.*, 2001; Su *et al.*, 2001; Rissman *et al.*, 2004) and autophagic (Nixon *et al.*, 2005; Nilsson *et al.*, 2013) mechanisms play a role in AD pathogenesis. Therefore, to study the pathogenic processes in AD, levels of apoptotic and autophagic proteins involved in mediating/ modulating cell death will be examined in an amyloid beta expressing model of the disease. Further investigations are underway to develop the *in vitro* AD model expressing amyloidosis. Information regarding the experimental procedure as well as the proposed virtual construct can be viewed in Appendix XII and XIII. The intrinsic pathway will be carefully examined as amyloid beta are known to bind and cause stress in the mitochondria, leading to the activation of apoptotic proteins and caspases which may be capable of cleaving other AD-related proteins such as tau (Su *et al.*, 2001; Rissman *et al.*, 2004). Upstream of this pathway, autophagy has been implicated in the secretion of amyloid beta into the extracellular space, thereby influencing plaque formation, a major hallmark of AD (Nilsson *et al.*, 2013). In this present study, Dox/Memantine combination drug has been observed to modulate both the apoptotic and autophagy pathways in CML and in a pre-transfected AD model. Thus, it will be interesting to investigate how the combination drug can modulate these pathways and probably reduce amyloids in an AD model expressing amyloidosis. In the proposed future work, the combination drug will be tested in the developed

AD model and some amyloid protein degradation studies will be carried out. Also, the alterations in the expression of apoptotic and autophagic proteins will be examined and the levels will be compared to the drug combination effect in CML. This will help to further verify the combination drug effects in CML-AD co-morbidity. Further experimental approaches will also be incorporated to elucidate the mechanism of Dox/Memantine in the investigated cell lines. The modulation of the proteins by the combination drug may suggest it as a pharmacological combination with promise in AD therapy, acting via the apoptotic and/or autophagic pathways.

5.2.6 Evaluating the effects of Dox/Memantine on the cell death pathway in K-562 and HEK293T cells

In the combination study, the levels of anti-apoptotic Bcl-xL, which was initially expressed in the CML cells at a very high level under normal physiological conditions, were observed to be downregulated with an increase in the levels of Cytochrome c. On the other hand, the levels of Bcl-2 protein were increased in Dox/Memantine-treated HEK293T cells. These results suggested the promotion of cell death and survival in the cancer and non-cancer cells, respectively. However, a downstream caspase detection as well as a functional cell death assay such as the Annexin V/PI staining prior to flow cytometry, will be needed to verify the response of the Dox/Memantine-treated cells to death.

5.3 Conclusion

5.3.1 What is already known?

Over time, the clinical outcome of patients with CML improved with the development of TKIs. However, during the blast crisis phase, where the cells resemble AML cells and migrate to secondary sites, such as the CNS, high relapse rates are common (Wolff *et al.*, 2003; Healey *et al.*, 2021). Hence, for a more effective treatment, non-targeted drugs such as Dox, is included (Bassan *et al.*, 1987; American Cancer Society, 2022). Dox is known for its effectiveness but due to its toxicity in non-cancer cells, its use is limited (Wang *et al.*, 2004; Li *et al.*, 2016; Fraczkowska *et al.*, 2018). Another condition that inversely mirrors the effects observed in cancer is AD (Behrens *et al.*, 2009; Liu and Ander, 2012). Approved AD drugs are known for their protective effects. However, at various concentrations, these drugs have also been suggested to affect other pathways, including GSK-3 activities (Noh *et al.*, 2009), apoptotic (Ki *et al.*, 2010; Albayrak *et al.*, 2018) and autophagy (Yoon *et al.*, 2017) pathways. Converse to non-cancer cells, in leukaemic cells, anti-apoptotic proteins (Bcl-2 and Bcl-xL) are known to be overexpressed while pro-apoptotic proteins (Bak, Bax and Cytochrome c) are under-expressed. Furthermore, Bcl-2 proteins are also known to interact with Beclin-1, a protein involved in autophagy (Liang *et al.*, 1998). Hence, a critical look at the expression of these proteins may elucidate how to better tackle CML and AD.

5.3.2 Key findings and concluding comments

In this study, under normal physiological conditions, K-562 CML cells showed a greater survival ability by expressing lower levels of pro-apoptotic proteins (Bak, Bax and Cytochrome c) compared to HEK293T cells. In addition, the CML cells did not express detectable levels of anti-apoptotic Bcl-2. Instead, it expressed four times more Bcl-xL proteins compared to the non-cancerous HEK293T cells.

Following drug treatments, Dox, not Imatinib, was observed to induce an autophagy-cell death mediated pathway in K-562 cells. Apoptosis is the canonical way for cells to die. However, in this study, a crosstalk between the apoptotic and autophagy pathways was observed. Dox-induced Beclin-1 increment, resulting in decreased and increased expressions of Bcl-xL and Cytochrome c in the CML cells, respectively. Hence, the halting of this path induced the progression of the blast phase CML cells. Also, Memantine, not Donepezil, demonstrated consistent protection on HEK293T cells. Together, both drugs (Dox and Memantine)

potentiated an effect against the survival of K-562 CML cells while attenuating HEK293T non-cancer cells from the Dox-mediated apoptotic cell death. Thus, for the first time, the molecular evidence of the ability of Memantine to attenuate HEK293T cells from the deleterious effects of Dox through the upregulation of anti-apoptotic Bcl-2 proteins without affecting its anti-cancerous effects as well as its induction of cellular autophagy in K562 cells, when both drugs were administered as combined therapy, is reported.

These findings suggest the use of Dox/Memantine (1 μ M) drug combination as a therapeutic strategy against CML resistant cells and in the treatment of conditions involving AD and CML co-morbidity. This drug strategy may also apply to other malignancies that are capable of infiltrating the CNS. However, there is still a lot of work to be done in order to transform these fundamental findings into a functional tool for the treatment of CML and AD *in vivo*. Additional studies will be necessary to confirm the drug action between the combined drugs. However, one major advantage of the selected drug combination is the fact that the use of the drugs individually has already been established in the diseases they were intended for. Hence, the safety, efficacy as well as toxicity profiles of Dox and Memantine in CML and AD, respectively, are well studied

Future studies should explore other *in vitro* effects of the combination drugs in CML and AD including other scientific techniques. With the aid of appropriate staining and microscopy techniques, the apoptotic and autophagy effects can be visualised. Also, the work should be investigated in other non-cancer and cancer cell lines, including brain cancer cells and most importantly primary cells. This will give more comparison of the effects of the drugs in different *in vitro* models of disease.

References

Abdul, M., & Hoosein, N. (2005). N-methyl-D-aspartate receptor in human prostate cancer. *The Journal of membrane biology*, 205(3), 125-128.

Abedin, M. J., Wang, D., McDonnell, M. A., Lehmann, U., & Kelekar, A. (2007). Autophagy delays apoptotic death in breast cancer cells following DNA damage. *Cell Death & Differentiation*, 14(3), 500-510.

Agrawal, S. G., Liu, F. T., Wiseman, C., Shirali, S., Liu, H., Lillington, D., ... & Jia, L. (2008). Increased proteasomal degradation of Bax is a common feature of poor prognosis chronic lymphocytic leukemia. *Blood, The Journal of the American Society of Hematology*, 111(5), 2790-2796.

Agrotis, A., Pengo, N., Burden, J. J., & Ketteler, R. (2019). Redundancy of human ATG4 protease isoforms in autophagy and LC3/GABARAP processing revealed in cells. *Autophagy*, 15(6), 976-997.

Ahmad, R., Ali, E., Okar, L., Elaiwy, O., Abdelrazek, M., Mulikandathil, Y., & Yassin, M. (2021). Acute appendicitis revealing a diagnosis of chronic myelogenous leukemia. *Clinical Case Reports*, 9(4), 1913-1916.

Albayrak, G., Konac, E., Dikmen, A. U., & Bilen, C. Y. (2018). Memantine induces apoptosis and inhibits cell cycle progression in LNCaP prostate cancer cells. *Human & experimental toxicology*, 37(9), 953-958.

Alexander, G., Emerson, S., & Kesselheim, A. (2021). Evaluation of Aducanumab for Alzheimer Disease: Scientific Evidence and Regulatory Review Involving Efficacy, Safety, and Futility. *JAMA*, 325(17), 1717-1718. doi: 10.1001/jama.2021.3854

Allan, E. K., Holyoake, T. L., Craig, A. R., & Jørgensen, H. G. (2011). Omacetaxine may have a role in chronic myeloid leukaemia eradication through downregulation of Mcl-1 and induction of apoptosis in stem/progenitor cells. *Leukemia*, 25(6), 985-994.

Almeida, T. P., Ferreira, J., Vettorazzi, A., Azqueta, A., Rocha, E., & Ramos, A. A. (2018). Cytotoxic activity of fucoxanthin, alone and in combination with the cancer drugs imatinib and doxorubicin, in CML cell lines. *Environmental toxicology and pharmacology*, 59, 24-33.

ALZFORUM (2021). Aduhelm. Retrieved 25 November 2021, from <https://www.alzforum.org/therapeutics/aduhelm>

ALZFORUM (1996). "Donepezil." ALZFORUM, 1996-2018, www.alzforum.org/therapeutics/donepezil

Alzheimer's Research UK (ARUK) (2021). Deaths due to dementia - Dementia Statistics Hub. Retrieved 25 November 2021, from <https://www.dementiastatistics.org/statistics/deaths-due-to-dementia/>

Alzheimer's Society (2021). Alzheimer's disease. Retrieved 25 November 2021, from <https://www.alzheimers.org.uk/about-dementia/types-dementia/alzheimers-disease>

Alzheimer's Society (2021). Facts for the media. Retrieved 25 November 2021, from <https://www.alzheimers.org.uk/about-us/news-and-media/facts-media>

Amani, N., Shokrzadeh, M., & Shaki, F. (2020). Clarithromycin effectively enhances doxorubicin-induced cytotoxicity and apoptosis in MCF7 cells through dysregulation of autophagy. *Advances in Medical Sciences*, 65(2), 235-243.

American Cancer Society (ACS) (2022). Chemotherapy for Chronic Myeloid Leukemia. Retrieved 10 April 2022, from <https://www.cancer.org/cancer/chronic-myeloid-leukemia/treating/chemotherapy.html>

American Cancer Society (ACS) (2021). Key Statistics for Chronic Myeloid Leukemia. Retrieved 31 October 2021, from <https://www.cancer.org/cancer/chronic-myeloid-leukemia/about/statistics.html>

American Cancer Society (ACS) (2018). Phases of Chronic Myeloid Leukemia. Retrieved 21 November 2021, from <https://www.cancer.org/cancer/chronic-myeloid-leukemia/detection-diagnosis-staging/staging.html>

American Cancer Society (ACS) (2022). Treating Chronic Myeloid Leukemia by Phase. Retrieved 11 February 2022, from <https://www.cancer.org/cancer/chronic-myeloid-leukemia/treating/treating-by-phase.html>

Amin, H., & Ahmed, S. (2021). Characteristics of BCR–ABL gene variants in patients of chronic myeloid leukemia. *Open Medicine*, 16(1), 904-912.

Andresen, V., & Gjertsen, B. T. (2017). Drug repurposing for the treatment of acute myeloid leukemia. *Frontiers in medicine*, 4, 211.

Annicchiarico, R., Federici, A., Pettenati, C., & Caltagirone, C. (2007). Rivastigmine in Alzheimer's disease: Cognitive function and quality of life. *Therapeutics and clinical risk management*, 3(6), 1113.

Arber, D. A., Orazi, A., Hasserjian, R., Thiele, J., Borowitz, M. J., Le Beau, M. M., ... & Vardiman, J. W. (2016). The 2016 revision to the World Health Organization classification of myeloid neoplasms and acute leukemia. *Blood*, 127(20), 2391-2405.

Artemov, A., Aliper, A., Korzinkin, M., Lezhnina, K., Jellen, L., Zhukov, N., ... & Buzdin, A. (2015). A method for predicting target drug efficiency in cancer based on the analysis of signaling pathway activation. *Oncotarget*, 6(30), 29347.

Ashokkumar, B., Vaziri, N. D., & Said, H. M. (2006). Thiamin uptake by the human-derived renal epithelial (HEK-293) cells: cellular and molecular mechanisms. *American Journal of Physiology-Renal Physiology*, 291(4), F796-F805.

Baccarani, M., Deininger, M. W., Rosti, G., Hochhaus, A., Soverini, S., Apperley, J. F., ... & Hjorth-Hansen, H. (2013). European LeukemiaNet recommendations for the management of chronic myeloid leukemia: 2013. *Blood, The Journal of the American Society of Hematology*, 122(6), 872-884.

Bacigalupo, A., Soracco, M., Vassallo, F., Abate, M., Van Lint, M. T., Gualandi, F., ... & Valbonesi, M. (1997). Donor lymphocyte infusions (DLI) in patients with chronic myeloid leukemia following allogeneic bone marrow transplantation. *Bone marrow transplantation*, 19(9), 927-932.

Baginska, J., Viry, E., Berchem, G., Poli, A., Noman, M. Z., van Moer, K., ... & Bleackley, R. C. (2013). Granzyme B degradation by autophagy decreases tumor cell susceptibility to natural killer-mediated lysis under hypoxia. *Proceedings of the National Academy of Sciences*, 110(43), 17450-17455.

Banjara, S., Suraweera, C. D., Hinds, M. G., & Kvansakul, M. (2020). The Bcl-2 family: ancient origins, conserved structures, and divergent mechanisms. *Biomolecules*, 10(1), 128.

Bárdi, E., Bobok, I., Oláh, A. V., Kappelmayer, J., & Kiss, C. (2007). Anthracycline antibiotics induce acute renal tubular toxicity in children with cancer. *Pathology & Oncology Research*, 13(3), 249-253.

Barnett, K., Mercer, S. W., Norbury, M., Watt, G., Wyke, S., & Guthrie, B. (2012). Epidemiology of multimorbidity and implications for health care, research, and medical education: a cross-sectional study. *The Lancet*, 380(9836), 37-43.

Bassan, R., Battista, R., Comotti, B., Minetti, B., Chisesi, T., Dini, E., & Barbui, T. (1987). Treatment of the lymphoid blast crisis of chronic myeloid leukemia. *European Journal of Cancer and Clinical Oncology*, 23(5), 513-515.

Beere, H. M., Wolf, B. B., Cain, K., Mosser, D. D., Mahboubi, A., Kuwana, T., ... & Green, D. R. (2000). Heat-shock protein 70 inhibits apoptosis by preventing recruitment of procaspase-9 to the Apaf-1 apoptosome. *Nature cell biology*, 2(8), 469-475.

Begna, K., Abdelatif, A., Schwager, S., Hanson, C., Pardani, A., & Tefferi, A. (2016). Busulfan for the treatment of myeloproliferative neoplasms: the Mayo Clinic experience. *Blood cancer journal*, 6(5), e427-e427.

Behrens, M. I., Lendon, C., & Roe, C. M. (2009). A common biological mechanism in cancer and Alzheimer's disease?. *Current Alzheimer Research*, 6(3), 196-204.

Bekris, L. M., Yu, C. E., Bird, T. D., & Tsuang, D. W. (2010). Genetics of Alzheimer disease. *Journal of geriatric psychiatry and neurology*, 23(4), 213-227.

Bellodi, C., Lidonnici, M. R., Hamilton, A., Helgason, G. V., Soliera, A. R., Ronchetti, M., ... & Calabretta, B. (2009). Targeting autophagy potentiates tyrosine kinase inhibitor-induced cell death in Philadelphia chromosome-positive cells, including primary CML stem cells. *The Journal of clinical investigation*, 119(5), 1109-1123.

Benito, A., Grillot, D., Nuñez, G., & Fernández-Luna, J. L. (1995). Regulation and function of Bcl-2 during differentiation-induced cell death in HL-60 promyelocytic cells. *The American journal of pathology*, 146(2), 481.

Benyettou, F., Fahs, H., Elkharrag, R., Bilbeisi, R. A., Asma, B., Rezgui, R., ... & Piano, F. (2017). Selective growth inhibition of cancer cells with doxorubicin-loaded CB [7]-modified iron-oxide nanoparticles. *RSC advances*, 7(38), 23827-23834.

Berjukow, S., Döring, F., Froschmayr, M., Grabner, M., Glossmann, H., & Hering, S. (1996). Endogenous calcium channels in human embryonic kidney (HEK293) cells. *British journal of pharmacology*, 118(3), 748-754.

Berman, S. B., Chen, Y. B., Qi, B., McCaffery, J. M., Rucker III, E. B., Goebbels, S., ... & Hardwick, J. M. (2009). Bcl-xL increases mitochondrial fission, fusion, and biomass in neurons. *Journal of Cell Biology*, 184(5), 707-719.

Bhagwatwar, H. P., Phadungpojna, S., Chow, D. S., & Andersson, B. S. (1996). Formulation and stability of busulfan for intravenous administration in high-dose chemotherapy. *Cancer chemotherapy and pharmacology*, 37(5), 401-408.

Bhutani, M., Kumar, L., Vora, A., Bhardwaj, N., Pathak, A. K., Singh, R., & Kochupillai, V. (2002). Randomized study comparing 4'-epi-doxorubicin (Epirubicin) versus doxorubicin as a part of induction treatment in adult acute lymphoblastic leukemia. *American journal of hematology*, 71(4), 241-247.

Bird, T. D. (2012). Early-onset familial Alzheimer disease. In: Adam MP, Ardinger HH, Pagon RA, Wallace SE, Bean LJH, Stephens K, Amemiya A, editors. SourceGeneReviews®. Seattle (WA): University of Washington, Seattle; 1993-2018. 1999 Sep 24 [updated 2012 Oct 18].

Biswas, J., Goswami, P., Gupta, S., Joshi, N., Nath, C., & Singh, S. (2016). Streptozotocin induced neurotoxicity involves Alzheimer's related pathological markers: a study on N2A cells. *Molecular neurobiology*, 53(5), 2794-2806.

Bjørkøy, G., Lamark, T., Brech, A., Outzen, H., Perander, M., Øvervatn, A., ... & Johansen, T. (2005). p62/SQSTM1 forms protein aggregates degraded by autophagy and has a protective effect on huntingtin-induced cell death. *The Journal of cell biology*, 171(4), 603-614.

Blagosklonny MV, Fojo T, Bhalla KN, et al. 2001. The Hsp90 inhibitor geldanamycin selectively sensitizes Bcr-Abl-expressing leukemia cells to cytotoxic chemotherapy. *Leukemia* 15: 1537–1543.

Blennow, K. (2004). Cerebrospinal fluid protein biomarkers for Alzheimer's disease. *NeuroRx*, 1(2), 213-225.

Boise, L. H., González-García, M., Postema, C. E., Ding, L., Lindsten, T., Turka, L. A., ... & Thompson, C. B. (1993). bcl-x, a bcl-2-related gene that functions as a dominant regulator of apoptotic cell death. *cell*, 74(4), 597-608.

Bondemark, L., & Ruf, S. (2015). Randomized controlled trial: the gold standard or an unobtainable fallacy?. *European Journal of Orthodontics*, 37(5), 457-461.

Bornhauser, M., Jenke, A., Freiberg-Richter, J., Radke, J., Schuler, U. S., Mohr, B., ... & Schleyer, E. (2004). CNS blast crisis of chronic myelogenous leukemia in a patient with a major cytogenetic response in bone marrow associated with low levels of imatinib mesylate and its N-desmethylated metabolite in cerebral spinal fluid. *Annals of Hematology*, 83(6), 401-402.

Bowles, E. J. A., Walker, R. L., Anderson, M. L., Dublin, S., Crane, P. K., & Larson, E. B. (2017). Risk of Alzheimer's disease or dementia following a cancer diagnosis. *PloS one*, 12(6).

Branford, S., Rudzki, Z., Walsh, S., Grigg, A., Arthur, C., Taylor, K., ... & Hughes, T. P. (2002). High frequency of point mutations clustered within the adenosine triphosphate-binding region of BCR/ABL in patients with chronic myeloid leukemia or Ph-positive acute lymphoblastic leukemia who develop imatinib (STI571) resistance. *Blood, The Journal of the American Society of Hematology*, 99(9), 3472-3475.

Brookmeyer, R., Abdalla, N., Kawas, C. H., & Corrada, M. M. (2018). Forecasting the prevalence of preclinical and clinical Alzheimer's disease in the United States. *Alzheimer's & dementia: the journal of the Alzheimer's Association*, 14(2), 121-129.

Brunden, K. R., Zhang, B., Carroll, J., Yao, Y., Potuzak, J. S., Hogan, A. M. L., ... & Smith, A. B. (2010). Epothilone D improves microtubule density, axonal integrity, and cognition in a transgenic mouse model of tauopathy. *Journal of Neuroscience*, 30(41), 13861-13866.

Buée, L., Bussiere, T., Buée-Scherrer, V., Delacourte, A., & Hof, P. R. (2000). Tau protein isoforms, phosphorylation and role in neurodegenerative disorders1. *Brain Research Reviews*, 33(1), 95-130.

Bussiere, T., Weinreb, P. H., Dunstan, R. W., Qian, F., Arast, M. F., & Li, M. (2013). Differential in vitro and in vivo binding profiles of BIIB037 and other anti-abeta clinical antibody candidates. *Neurodegener Dis*, 11(1).

Callus, B. A., & Vaux, D. L. (2007). Caspase inhibitors: viral, cellular and chemical. *Cell Death & Differentiation*, 14(1), 73-78.

Caltabiano, R., Leonardi, R., Musumeci, G., Bartoloni, G., Rusu, M. C., Almeida, L. E., & Loreto, C. (2013). Apoptosis in temporomandibular joint disc with internal derangement involves mitochondrial-dependent pathways. An in vivo study. *Acta Odontologica Scandinavica*, 71(3-4), 577-583.

Camaggi, C. M., Compari, R., Stocchi, E., Testoni, F., Angelelli, B., & Pannuti, F. (1988). Epirubicin and doxorubicin comparative metabolism and pharmacokinetics. *Cancer chemotherapy and pharmacology*, 21(3), 221-228.

Campion, D., Dumanchin, C., Hannequin, D., Dubois, B., Belliard, S., Puel, M., ... & Raux, G. (1999). Early-onset autosomal dominant Alzheimer disease: prevalence, genetic heterogeneity, and mutation spectrum. *The American Journal of Human Genetics*, 65(3), 664-670.

Cancer Research UK. (2021). Chronic myeloid leukaemia (CML) statistics. [online] Available at: <https://www.cancerresearchuk.org/health-professional/cancer-statistics/statistics-by-cancer-type/leukaemia-cml#heading-Zero> [Accessed 31 Oct. 2021].

Capdeville, R., Buchdunger, E., Zimmermann, J., & Matter, A. (2002). Glivec (STI571, imatinib), a rationally developed, targeted anticancer drug. *Nature reviews Drug discovery*, 1(7), 493-502.

Cardinale, D., Colombo, A., Sandri, M. T., Lamantia, G., Colombo, N., Civelli, M., ... & Cipolla, C. M. (2006). Prevention of high-dose chemotherapy–induced cardiotoxicity in high-risk patients by angiotensin-converting enzyme inhibition. *Circulation*, 114(23), 2474-2481.

Carew, J. S., Nawrocki, S. T., Kahue, C. N., Zhang, H., Yang, C., Chung, L., ... & Cleveland, J. L. (2007). Targeting autophagy augments the anticancer activity of the histone deacetylase inhibitor SAHA to overcome Bcr-Abl–mediated drug resistance. *Blood, The Journal of the American Society of Hematology*, 110(1), 313-322.

Cerella, C., Gaigneaux, A., Mazumder, A., Lee, J. Y., Saland, E., Radogna, F., ... & Kim, K. W. (2017). Bcl-2 protein family expression pattern determines synergistic pro-apoptotic effects of BH3 mimetics with hemisynthetic cardiac glycoside UNBS1450 in acute myeloid leukemia. *Leukemia*, 31(3), 755-759.

Chai, S. K., Nichols, G. L., & Rothman, P. (1997). Constitutive activation of JAKs and STATs in BCR-Abl-expressing cell lines and peripheral blood cells derived from leukemic patients. *The Journal of Immunology*, 159(10), 4720-4728.

Chang, K. C., Liu, P. F., Chang, C. H., Lin, Y. C., Chen, Y. J., & Shu, C. W. (2022). The interplay of autophagy and oxidative stress in the pathogenesis and therapy of retinal degenerative diseases. *Cell & Bioscience*, 12(1), 1-20.

Chasseriau, J., Rivet, J., Bilan, F., Chomel, J. C., Guilhot, F., Bourmeyster, N., & Kitzis, A. (2004). Characterization of the different BCR-ABL transcripts with a single multiplex RT-PCR. *The Journal of molecular diagnostics*, 6(4), 343-347.

Chen, B., Wang, G., Li, W., Liu, W., Lin, R., Tao, J., ... & Wang, Y. (2017). Memantine attenuates cell apoptosis by suppressing the calpain-caspase-3 pathway in an experimental model of ischemic stroke. *Experimental cell research*, 351(2), 163-172.

Chen, G. F., Xu, T. H., Yan, Y., Zhou, Y. R., Jiang, Y., Melcher, K., & Xu, H. E. (2017). Amyloid beta: structure, biology and structure-based therapeutic development. *Acta Pharmacologica Sinica*, 38(9), 1205-1235.

Cheng, K., Samimi, R., Xie, G., Shant, J., Drachenberg, C., Wade, M., ... & Raufman, J. P. (2008). Acetylcholine release by human colon cancer cells mediates autocrine stimulation of cell proliferation. *American Journal of Physiology-Gastrointestinal and Liver Physiology*, 295(3), G591-G597.

Chen, H. S., Wang, Y. F., Rayudu, P. V., Edgecomb, P., Neill, J. C., Segal, M. M., ... & Jensen, F. E. (1998). Neuroprotective concentrations of the N-methyl-D-aspartate open-channel blocker memantine are effective without cytoplasmic vacuolation following post-ischemic administration and do not block maze learning or long-term potentiation. *Neuroscience*, 86(4), 1121-1132.

Chen, J., Wei, H., Cheng, J., Xie, B., Wang, B., Yi, J., ... & Zhang, Z. (2018). Characteristics of doxorubicin-selected multidrug-resistant human leukemia HL-60 cells with tolerance to arsenic trioxide and contribution of leukemia stem cells. *Oncology letters*, 15(1), 1255-1262.

Chen, L., Willis, S. N., Wei, A., Smith, B. J., Fletcher, J. I., Hinds, M. G., ... & Huang, D. C. (2005). Differential targeting of prosurvival Bcl-2 proteins by their BH3-only ligands allows complementary apoptotic function. *Molecular cell*, 17(3), 393-403.

Cheong, J. W., Kim, Y., Eom, J. I., Jeung, H. K., & Min, Y. H. (2016). Enhanced autophagy in cytarabine arabinoside-resistant U937 leukemia cells and its potential as a target for overcoming resistance. *Molecular Medicine Reports*, 13(4), 3433-3440.

Cheung, Y. T., Khan, R. B., Liu, W., Brinkman, T. M., Edelman, M. N., Reddick, W. E., ... & Krull, K. R. (2018). Association of cerebrospinal fluid biomarkers of central nervous system injury with neurocognitive and brain imaging outcomes in children receiving chemotherapy for acute lymphoblastic leukemia. *JAMA oncology*, 4(7), e180089-e180089.

Chiba, A., Toya, T., Mizuno, H., Tokushige, J., Nakamura, F., Nakazaki, K., & Kurokawa, M. (2018). Chronic myelogenous leukemia presenting with central nervous system infiltration, successfully treated with central nervous system-directed chemotherapy followed by allogeneic stem cell transplantation. *International journal of hematology*, 108(6), 640-646.

Childs, A. C., Phaneuf, S. L., Dirks, A. J., Phillips, T., & Leeuwenburgh, C. (2002). Doxorubicin treatment in vivo causes cytochrome C release and cardiomyocyte apoptosis, as well as increased mitochondrial efficiency, superoxide dismutase activity, and Bcl-2: Bax ratio. *Cancer research*, 62(16), 4592-4598.

Choi, W., Kim, M., Lim, J., Han, K., Lee, S., Lee, J. W., ... & Kim, Y. (2014). Four cases of chronic myelogenous leukemia in mixed phenotype blast phase at initial presentation mimicking mixed phenotype acute leukemia with t (9; 22). *Annals of laboratory medicine*, 34(1), 60.

Chomel, J. C., Bonnet, M. L., Sorel, N., Bertrand, A., Meunier, M. C., Fichelson, S., ... & Turhan, A. G. (2011). Leukemic stem cell persistence in chronic myeloid leukemia patients with sustained undetectable molecular residual disease. *Blood*, 118(13), 3657-3660.

Chu, S., Li, L., Singh, H., & Bhatia, R. (2007). BCR-tyrosine 177 plays an essential role in Ras and Akt activation and in human hematopoietic progenitor transformation in chronic myelogenous leukemia. *Cancer research*, 67(14), 7045-7053.

Chu, S., McDonald, T., Lin, A., Chakraborty, S., Huang, Q., Snyder, D. S., & Bhatia, R. (2011). Persistence of leukemia stem cells in chronic myelogenous leukemia patients in prolonged remission with imatinib treatment. *Blood, The Journal of the American Society of Hematology*, 118(20), 5565-5572.

Ciechomska, I. A., Goemans, G. C., Skepper, J. N., & Tolkovsky, A. M. (2009). Bcl-2 complexed with Beclin-1 maintains full anti-apoptotic function. *Oncogene*, 28(21), 2128-2141.

Clarke, C. J., & Holyoake, T. L. (2017). Preclinical approaches in chronic myeloid leukemia: from cells to systems. *Experimental hematology*, 47, 13-23.

Collett, V. J., & Collingridge, G. L. (2004). Interactions between NMDA receptors and mGlu5 receptors expressed in HEK293 cells. *British journal of pharmacology*, 142(6), 991-1001.

Colovic, M. B., Krstic, D. Z., Lazarevic-Pasti, T. D., Bondzic, A. M., & Vasic, V. M. (2013). Acetylcholinesterase inhibitors: pharmacology and toxicology. *Current neuropharmacology*, 11(3), 315-335.

Cooper, J. K., Schilling, G., Peters, M. F., Herring, W. J., Sharp, A. H., Kaminsky, Z., ... & Dawson, V. L. (1998). Truncated N-terminal fragments of huntingtin with expanded glutamine repeats form nuclear and cytoplasmic aggregates in cell culture. *Human molecular genetics*, 7(5), 783-790.

Corbin, A. S., Agarwal, A., Loriaux, M., Cortes, J., Deininger, M. W., & Druker, B. J. (2011). Human chronic myeloid leukemia stem cells are insensitive to imatinib despite inhibition of BCR-ABL activity. *The Journal of clinical investigation*, 121(1), 396-409.

Cortes, J. E., Hochhaus, A., Kim, D. W., Shah, N. P., Mayer, J., Rowlings, P., ... & Saglio, G. (2013). Four-year (Yr) follow-up of patients (Pts) with newly diagnosed chronic myeloid leukemia in chronic phase (CML-CP) receiving dasatinib or imatinib: efficacy based on early response.

Cortes, J. E., Kim, D. W., Kantarjian, H. M., Brümmendorf, T. H., Dyagil, I., Griskevicius, L., ... & Gambacorti-Passerini, C. (2012). Bosutinib versus imatinib in newly diagnosed chronic-phase chronic myeloid leukemia: results from the BELA trial. *Journal of Clinical Oncology*, 30(28), 3486.

Cortes, J. E., Kim, D. W., Pinilla-Ibarz, J. L., Le Coutre, P., Paquette, R., Chuah, C., ... & DiPersio, J. (2013). A phase 2 trial of ponatinib in Philadelphia chromosome-positive leukemias. *New England Journal of Medicine*, 369(19), 1783-1796.

Cortes, J., & Kantarjian, H. (2003, January). Advanced-phase chronic myeloid leukemia. In *Seminars in hematology* (Vol. 40, No. 1, pp. 79-86). WB Saunders.

Cortes, J., Kantarjian, H., O'Brien, S., Robertson, L. E., Pierce, S., & Talpaz, M. (1996). Results of interferon-alpha therapy in patients with chronic myelogenous leukemia 60 years of age and older. *The American journal of medicine*, 100(4), 452-455.

Cortes, J., & Lang, F. (2021). Third-line therapy for chronic myeloid leukemia: current status and future directions. *Journal of Hematology & Oncology*, 14(1), 1-18.

Cortes, J., Silver, R. T., & Kantarjian, H. M. (2016). Chronic myeloid leukemia. *Holland-Frei Cancer Medicine*, 1-11.

Cosan, D., Soyocak, A., Tekedereli, I., Gacar, G., Karaoz, E., & Ozpolat, B. (2010). Doxorubicin-induced autophagy functions as a pro-survival pathway in breast cancer cells.

Coyle, D. E., Li, J., & Baccei, M. (2011). Regional differentiation of retinoic acid-induced human pluripotent embryonic carcinoma stem cell neurons. *PLoS One*, 6(1), e16174.

Creeley, C., Wozniak, D. F., Labruyere, J., Taylor, G. T., & Olney, J. W. (2006). Low doses of memantine disrupt memory in adult rats. *Journal of Neuroscience*, 26(15), 3923-3932.

Crismon, M. L. (1994). Tacrine: first drug approved for Alzheimer's disease. *Annals of Pharmacotherapy*, 28(6), 744-751.

Cusick, J. K., Mustian, A., Goldberg, K., & Reyland, M. E. (2010). RELT induces cellular death in HEK 293 epithelial cells. *Cellular immunology*, 261(1), 1-8.

Daniel, F., Legrand, A., Pessayre, D., Vadrot, N., Descatoire, V., & Bernuau, D. (2006). Partial Beclin 1 silencing aggravates doxorubicin-and Fas-induced apoptosis in HepG2 cells. *World Journal of Gastroenterology: WJG*, 12(18), 2895.

Davies, S. P., Helps, N. R., Cohen, P. T., & Hardie, D. G. (1995). 5'-AMP inhibits dephosphorylation, as well as promoting phosphorylation, of the AMP-activated protein kinase. Studies using bacterially expressed human protein phosphatase-2C α and native bovine protein phosphatase-2AC. *FEBS letters*, 377(3), 421-425.

Davis, S. E., Roth, J. R., Aljabi, Q., Hakim, A. R., Savell, K. E., Day, J. J., & Arrant, A. E. (2021). Delivering progranulin to neuronal lysosomes protects against excitotoxicity. *Journal of Biological Chemistry*, 297(3).

Degenhardt, K., Mathew, R., Beaudoin, B., Bray, K., Anderson, D., Chen, G., ... & Nelson, D. A. (2006). Autophagy promotes tumor cell survival and restricts necrosis, inflammation, and tumorigenesis. *Cancer cell*, 10(1), 51-64.

Delou, J., Biasoli, D., & Borges, H. L. (2016). The complex link between apoptosis and autophagy: a promising new role for RB. *Anais da Academia Brasileira de Ciências*, 88(4), 2257-2275.

Delphine, R., Gautier, J. F., Breccia, M., Saglio, G., Hughes, T. P., Kantarjian, H. M., ... & Hochhaus, A. (2012). Incidence of hyperglycemia by 3 years in patients (Pts) with newly diagnosed chronic myeloid leukemia in chronic phase (CML-CP) treated with nilotinib (NIL) or imatinib (IM) in ENESTnd.

Demehri, S., O'Hare, T., Eide, C. A., Smith, C. A., Tyner, J. W., Druker, B. J., & Deininger, M. W. N. (2010). The function of the pleckstrin homology domain in BCR-ABL-mediated leukemogenesis. *Leukemia*, 24(1), 226-229.

Deming, P. B., Schafer, Z. T., Tashker, J. S., Potts, M. B., Deshmukh, M., & Kornbluth, S. (2004). Bcr-Abl-mediated protection from apoptosis downstream of mitochondrial cytochrome c release. *Molecular and cellular biology*, 24(23), 10289-10299.

Department of Economic and Social Affairs of the United Nations (DESA) (2019). United Nations Department of Economic and Social Affairs/Population Division (2019). *World Population Prospects 2019: Highlights*. ST/ESA/SER.A/423.

Derderian, P. M., Kantarjian, H. M., Talpaz, M., O'Brien, S., Cork, A., Estey, E., ... & Keating, M. (1993). Chronic myelogenous leukemia in the lymphoid blastic phase: characteristics, treatment response, and prognosis. *The American journal of medicine*, 94(1), 69-74.

De Sarno, P., Shestopal, S. A., King, T. D., Zmijewska, A., Song, L., & Jope, R. S. (2003). Muscarinic receptor activation protects cells from apoptotic effects of DNA damage, oxidative stress, and mitochondrial inhibition. *Journal of Biological Chemistry*, 278(13), 11086-11093.

Deveraux, Q. L., Roy, N., Stennicke, H. R., Van Arsdale, T., Zhou, Q., Srinivasula, S. M., ... & Reed, J. C. (1998). IAPs block apoptotic events induced by caspase-8 and cytochrome c by direct inhibition of distinct caspases. *The EMBO journal*, 17(8), 2215-2223.

Ding, W. X., Ni, H. M., Gao, W., Hou, Y. F., Melan, M. A., Chen, X., ... & Yin, X. M. (2007). Differential effects of endoplasmic reticulum stress-induced autophagy on cell survival. *Journal of Biological Chemistry*, 282(7), 4702-4710.

Diomedea, L., Bizzi, A., Magistrelli, A., Modest, E. J., Salmona, M., & Nosedà, A. (1990). Role of cell cholesterol in modulating antineoplastic ether lipid uptake, membrane effects and cytotoxicity. *International journal of cancer*, 46(2), 341-346.

Dobrovinskaya, O., Valencia-Cruz, G., Castro-Sánchez, L., Bonales-Alatorre, E. O., Liñan-Rico, L., & Pottosin, I. (2016). Cholinergic machinery as relevant target in acute lymphoblastic T leukemia. *Frontiers in pharmacology*, 7, 290.

Dölker, N., Górna, M. W., Sutto, L., Torralba, A. S., Superti-Furga, G., & Gervasio, F. L. (2014). The SH2 domain regulates c-Abl kinase activation by a cyclin-like mechanism and remodulation of the hinge motion. *PLoS computational biology*, 10(10), e1003863.

Drexler, H. G. (1994). Leukemia cell lines: in vitro models for the study of chronic myeloid leukemia. *Leukemia research*, 18(12), 919-927.

Druker, B. J., Guilhot, F., O'Brien, S. G., Gathmann, I., Kantarjian, H., Gattermann, N., ... & Cervantes, F. (2006). Five-year follow-up of patients receiving imatinib for chronic myeloid leukemia. *New England Journal of Medicine*, 355(23), 2408-2417.

Druker, B. J., Sawyers, C. L., Kantarjian, H., Resta, D. J., Reese, S. F., Ford, J. M., ... & Talpaz, M. (2001). Activity of a specific inhibitor of the BCR-ABL tyrosine kinase in the blast crisis of chronic myeloid leukemia and acute lymphoblastic leukemia with the Philadelphia chromosome. *New England Journal of Medicine*, 344(14), 1038-1042.

Druker, B. J., Talpaz, M., Resta, D. J., Peng, B., Buchdunger, E., Ford, J. M., ... & Sawyers, C. L. (2001). Efficacy and safety of a specific inhibitor of the BCR-ABL tyrosine kinase in chronic myeloid leukemia. *New England Journal of Medicine*, 344(14), 1031-1037.

Druker, B. J. (2008). Translation of the Philadelphia chromosome into therapy for CML. *Blood, The Journal of the American Society of Hematology*, 112(13), 4808-4817.

Drullion, C., Trégoat, C., Lagarde, V., Tan, S., Gioia, R., Priault, M., ... & Pasquet, J. M. (2012). Apoptosis and autophagy have opposite roles on imatinib-induced K562 leukemia cell senescence. *Cell death & disease*, 3(8), e373-e373.

Drummond, E., & Wisniewski, T. (2017). Alzheimer's disease: experimental models and reality. *Acta neuropathologica*, 133(2), 155-175.

Eagger, S. A., Levy, R., & Sahakian, B. J. (1991). Tacrine in Alzheimer's disease. *The Lancet*, 337(8748), 989-992.

Ebert, E. C., & Hagspiel, K. D. (2012). Gastrointestinal manifestations of leukemia. *Journal of gastroenterology and hepatology*, 27(3), 458-463.

Egan, D., Kim, J., Shaw, R. J., & Guan, K. L. (2011). The autophagy initiating kinase ULK1 is regulated via opposing phosphorylation by AMPK and mTOR. *Autophagy*, 7(6), 643-644.

Elmaagacli, A. H., Beelen, D. W., Opalka, B., Seeber, S., & Schaefer, U. W. (2000). The amount of BCR-ABL fusion transcripts detected by the real-time quantitative polymerase chain reaction method in patients with Philadelphia chromosome positive chronic myeloid leukemia correlates with the disease stage. *Annals of hematology*, 79(8), 424-431.

Engidawork, E., Gulesserian, T., Seidl, R., Cairns, N., & Lubec, G. (2001). Expression of apoptosis related proteins in brains of patients with Alzheimer's disease. *Neuroscience letters*, 303(2), 79-82.

Ertmer, A., Huber, V., Gilch, S., Yoshimori, T., Erfle, V., Duyster, J., ... & Schätzl, H. M. (2007). The anticancer drug imatinib induces cellular autophagy. *Leukemia*, 21(5), 936-942.

Evans, A. E., Gilbert, E. S., & Zandstra, R. (1970). The increasing incidence of central nervous system leukemia in children.(Children's Cancer Study Group A). *Cancer*, 26(2), 404-409.

Evans, D. B., Rank, K. B., Bhattacharya, K., Thomsen, D. R., Gurney, M. E., & Sharma, S. K. (2000). Tau phosphorylation at serine 396 and serine 404 by human recombinant tau protein kinase II inhibits tau's ability to promote microtubule assembly. *Journal of Biological Chemistry*, 275(32), 24977-24983.

Faderl, S., Talpaz, M., Estrov, Z., O'Brien, S., Kurzrock, R., & Kantarjian, H. M. (1999). The biology of chronic myeloid leukemia. *New England Journal of Medicine*, 341(3), 164-172.

Fainstein, E., Marcelle, C., Rosner, A., Canaani, E., Gale, R. P., Drazan, O., ... & Croce, C. M. (1987). A new fused transcript in Philadelphia chromosome positive acute lymphocytic leukaemia. *Nature*, 330(6146), 386-388.

Fantini, J., Di Scala, C., Yahi, N., Troadec, J. D., Sadelli, K., Chahinian, H., & Garmy, N. (2014). Bexarotene blocks calcium-permeable ion channels formed by neurotoxic Alzheimer's β -amyloid peptides. *ACS chemical neuroscience*, 5(3), 216-224.

Feng, Y., Wang, X. P., Yang, S. G., Wang, Y. J., Zhang, X., Du, X. T., ... & Liu, R. T. (2009). Resveratrol inhibits beta-amyloid oligomeric cytotoxicity but does not prevent oligomer formation. *Neurotoxicology*, 30(6), 986-995.

Ferrero, J., Williams, L., Stella, H., Leitermann, K., Mikulskis, A., O'Gorman, J., & Sevigny, J. (2016). First-in-human, double-blind, placebo-controlled, single-dose escalation study of aducanumab (BIIB037) in mild-to-moderate Alzheimer's disease. *Alzheimer's & Dementia: Translational Research & Clinical Interventions*, 2(3), 169-176.

Florou, D., Patsis, C., Ardavanis, A., & Scorilas, A. (2013). Effect of doxorubicin, oxaliplatin, and methotrexate administration on the transcriptional activity of BCL-2 family gene members in stomach cancer cells. *Cancer biology & therapy*, 14(7), 587-596.

Fraczkowska, K., Bacia, M., Przybyło, M., Drabik, D., Kaczorowska, A., Rybka, J., ... & Wrobel, T. (2018). Alterations of biomechanics in cancer and normal cells induced by doxorubicin. *Biomedicine & Pharmacotherapy*, 97, 1195-1203.

Franz, W. M., Berger, P., & Wang, J. Y. (1989). Deletion of an N-terminal regulatory domain of the c-abl tyrosine kinase activates its oncogenic potential. *The EMBO Journal*, 8(1), 137-147.

Freedman, D. M., Wu, J., Chen, H., Kuncel, R. W., Enewold, L. R., Engels, E. A., ... & Pfeiffer, R. M. (2016). Associations between cancer and Alzheimer's disease in a US Medicare population. *Cancer medicine*, 5(10), 2965-2976.

Furuya, D., Tsuji, N., Yagihashi, A., & Watanabe, N. (2005). Beclin 1 augmented cis-diamminedichloroplatinum induced apoptosis via enhancing caspase-9 activity. *Experimental cell research*, 307(1), 26-40.

Gambacorti-Passerini, C., Le Coutre, P., Mologni, L., Fanelli, M., Bertazzoli, C., Marchesi, E., ... & Lydon, N. B. (1997). Inhibition of the ABL kinase activity blocks the proliferation of BCR/ABL+ leukemic cells and induces apoptosis. *Blood Cells, Molecules, and Diseases*, 23(3), 380-394.

Gamen, S., Anel, A., Pérez-Galán, P., Lasierra, P., Johnson, D., Piñeiro, A., & Naval, J. (2000). Doxorubicin treatment activates a Z-VAD-sensitive caspase, which causes $\Delta\Psi_m$ loss, caspase-9 activity, and apoptosis in Jurkat cells. *Experimental cell research*, 258(1), 223-235.

Gao, M., Huang, Z. L., Tao, K., Xiao, Q., Wang, X., Cao, W. X., ... & Feng, W. L. (2017). Depression of oncogenicity by dephosphorylating and degrading BCR-ABL. *Oncotarget*, 8(2), 3304.

Ghahramanyan, N., Danelyan, S., Meliksetyan, K., & Hakobyan, Y. (2019). Chronic Myeloid Leukemia with Primary Blast Crisis: Experience of Hematology Center in Armenia. *Clinical Lymphoma, Myeloma and Leukemia*, 19, S296.

Gorantla, N. V., & Chinnathambi, S. (2021). Autophagic pathways to clear the tau aggregates in Alzheimer's disease. *Cellular and Molecular Neurobiology*, 41(6), 1175-1181.

Gordon, J., Amini, S., & White, M. K. (2013). General overview of neuronal cell culture. In *Neuronal Cell Culture* (pp. 1-8). Humana Press, Totowa, NJ.

Gorre, M. E., Mohammed, M., Ellwood, K., Hsu, N., Paquette, R., Rao, P. N., & Sawyers, C. L. (2001). Clinical resistance to STI-571 cancer therapy caused by BCR-ABL gene mutation or amplification. *Science*, 293(5531), 876-880.

Goussetis, D. J., Gounaris, E., Wu, E. J., Vakana, E., Sharma, B., Bogyo, M., ... & Platanias, L. C. (2012). Autophagic degradation of the BCR-ABL oncoprotein and generation of antileukemic responses by arsenic trioxide. *Blood, The Journal of the American Society of Hematology*, 120(17), 3555-3562.

Graham, F. L., Smiley, J., Russell, W. C., & Nairn, R. (1977). Characteristics of a human cell line transformed by DNA from human adenovirus type 5. *Journal of General Virology*, 36(1), 59-72.

Grant, E. R., Bacskai, B. J., Pleasure, D. E., Pritchett, D. B., Gallagher, M. J., Kendrick, S. J., ... & Lynch, D. R. (1997). N-methyl-D-aspartate receptors expressed in a nonneuronal cell line mediate subunit-specific increases in free intracellular calcium. *Journal of Biological Chemistry*, 272(1), 647-656.

Gratwohl, A. (2016). The role of hematopoietic stem cell transplantation in chronic myeloid leukemia. In *Chronic Myeloid Leukemia* (pp. 177-196). Springer, Cham.

Gresch, O., & Altrogge, L. (2012). Transfection of difficult-to-transfect primary mammalian cells. In *Protein Expression in Mammalian Cells* (pp. 65-74). Humana Press.

Greshock, J., Nathanson, K., Martin, A. M., Zhang, L., Coukos, G., Weber, B. L., & Zaks, T. Z. (2007). Cancer cell lines as genetic models of their parent histology: analyses based on array comparative genomic hybridization. *Cancer research*, 67(8), 3594-3600.

Griffin W. (2006) Inflammation and neurodegenerative diseases. *Am J Clin Nutr* 3(Suppl.): 470–474.

Gross, A. W., Zhang, X., & Ren, R. (1999). Bcr-Abl with an SH3 deletion retains the ability to induce a myeloproliferative disease in mice, yet c-Abl activated by an SH3 deletion induces only lymphoid malignancy. *Molecular and cellular biology*, 19(10), 6918.

Grossberg, G. T., Manes, F., Allegri, R. F., Gutiérrez-Robledo, L. M., Gloger, S., Xie, L., ... & Graham, S. M. (2013). The safety, tolerability, and efficacy of once-daily memantine (28 mg): a multinational, randomized, double-blind, placebo-controlled trial in patients with moderate-to-severe Alzheimer's disease taking cholinesterase inhibitors. *CNS drugs*, 27(6), 469-478.

Grundke-Iqbal, I., Iqbal, K., Tung, Y. C., Quinlan, M., Wisniewski, H. M., & Binder, L. I. (1986). Abnormal phosphorylation of the microtubule-associated protein tau (tau) in Alzheimer cytoskeletal pathology. *Proceedings of the National Academy of Sciences*, 83(13), 4913-4917.

Gu, J., Fan, Y. Q., Zhang, H. L., Pan, J. A., Yu, J. Y., Zhang, J. F., & Wang, C. Q. (2018). Resveratrol suppresses doxorubicin-induced cardiotoxicity by disrupting E2F1 mediated autophagy inhibition and apoptosis promotion. *Biochemical pharmacology*, 150, 202-213.

Gunthorpe, M., Smith, G., Davis, J., & Randall, A. (2001). Characterisation of a human acid-sensing ion channel (hASIC1a) endogenously expressed in HEK293 cells. *Pflügers Archiv*, 442(5), 668-674.

Haass, C., Hung, A. Y., Schlossmacher, M. G., Oltersdorf, T., Teplow, D. B., & Selkoe, D. J. (1993). Normal Cellular Processing of the β -Amyloid Precursor Protein Results in the Secretion of the Amyloid β Peptide and Related Molecules. *Annals of the New York Academy of Sciences*, 695(1), 109-116.

Haass, C., & Selkoe, D. J. (1993). Cellular processing of β -amyloid precursor protein and the genesis of amyloid β -peptide. *Cell*, 75(6), 1039-1042.

Hamacher-Brady, A., Brady, N. R., & Gottlieb, R. A. (2006). Enhancing macroautophagy protects against ischemia/reperfusion injury in cardiac myocytes. *Journal of Biological Chemistry*, 281(40), 29776-29787.

Han, B., Zhao, Y., Lin, Y., Fu, S., Wang, L., Zhang, M., ... & Yu, J. (2017). Hydroxychloroquine sensitizes chronic myeloid leukemia cells to V γ 9V δ 2 T cell-mediated lysis independent of autophagy. *International Journal of Oncology*, 50(5), 1810-1820.

Hansen, R. A., Gartlehner, G., Webb, A. P., Morgan, L. C., Moore, C. G., & Jonas, D. E. (2008). Efficacy and safety of donepezil, galantamine, and rivastigmine for the treatment of Alzheimer's disease: a systematic review and meta-analysis. *Clinical interventions in aging*, 3(2), 211.

Hantschel, O., Nagar, B., Guettler, S., Kretschmar, J., Dorey, K., Kuriyan, J., & Superti-Furga, G. (2003). A myristoyl/phosphotyrosine switch regulates c-Abl. *Cell*, 112(6), 845-857.

Hantschel, O. (2012). Structure, regulation, signaling, and targeting of abl kinases in cancer. *Genes & cancer*, 3(5-6), 436-446.

Harb, J. G., Neviani, P., Chyla, B. J., Ellis, J. J., Ferencak, G. J., Oaks, J. J., ... & Perrotti, D. (2013). Bcl-xL anti-apoptotic network is dispensable for development and maintenance of CML but is required for disease progression where it represents a new therapeutic target. *Leukemia*, 27(10), 1996-2005.

Hayes, C. D., Dey, D., Palavicini, J. P., Wang, H., Patkar, K. A., Minond, D., ... & Lakshmana, M. K. (2013). Striking reduction of amyloid plaque burden in an Alzheimer's mouse model after chronic administration of carmustine. *BMC medicine*, 11(1), 81.

Healey, M. A., Allendorf, D. J., Borate, U., & Madan, A. (2021). CNS Involvement in a Patient with Chronic Myeloid Leukemia. *Case Reports in Hematology*, 2021.

Hehlmann, R., Anger, B., Messerer, D., Zankovich, R., Bergmann, L., Kolb, H. J., ... & Heimpele, H. (1988). Randomized study on the treatment of chronic myeloid leukemia (CML) in chronic phase with busulfan versus hydroxyurea versus interferon-alpha. *Blut*, 56(2), 87-91.

Hengartner, M. O. (2000). The biochemistry of apoptosis. *Nature*, 407(6805), 770-776.

Herholz, K. (2008). Acetylcholine esterase activity in mild cognitive impairment and Alzheimer's disease. *European journal of nuclear medicine and molecular imaging*, 35(1), 25-29.

Hermans, André, Nora Heisterkamp, Marieke von Lindern, Sjozef van Baal, Dies Meijer, Dorien van der Plas, Leanne M. Wiedemann, John Groffen, Dirk Bootsma, and Gerard Grosveld. "Unique fusion of bcr and c-abl genes in Philadelphia chromosome positive acute lymphoblastic leukemia." *Cell* 51, no. 1 (1987): 33-40.

Hinz, S., Trauzold, A., Boenicke, L., Sandberg, C., Beckmann, S., Bayer, E., ... & Ungefroren, H. (2000). Bcl-X L protects pancreatic adenocarcinoma cells against CD95-and TRAIL-receptor-mediated apoptosis. *Oncogene*, 19(48), 5477-5486.

Hirata, Y., Yamamoto, H., Atta, M. S. M., Mahmoud, S., Oh-hashii, K., & Kiuchi, K. (2011). Chloroquine inhibits glutamate-induced death of a neuronal cell line by reducing reactive oxygen species through sigma-1 receptor. *Journal of neurochemistry*, 119(4), 839-847.

Hochhaus, A., Baccarani, M., Silver, R. T., Schiffer, C., Apperley, J. F., Cervantes, F., ... & Hehlmann, R. (2020). European LeukemiaNet 2020 recommendations for treating chronic myeloid leukemia. *Leukemia*, 34(4), 966-984.

Hockenbery, D. M., Zutter, M., Hickey, W., Nahm, M., & Korsmeyer, S. J. (1991). BCL2 protein is topographically restricted in tissues characterized by apoptotic cell death. *Proceedings of the National Academy of Sciences*, 88(16), 6961-6965.

Holliday, R. (1996). The urgency of research on ageing. *BioEssays*, 18(2), 89-90.

Houshmand, M., Simonetti, G., Circosta, P., Gaidano, V., Cignetti, A., Martinelli, G., ... & Gale, R. P. (2019). Chronic myeloid leukemia stem cells. *Leukemia*, 33(7), 1543-1556.

Huang, X., Li, Y., Shou, L., Li, L., Chen, Z., Ye, X., & Qian, W. (2019). The molecular mechanisms underlying BCR/ABL degradation in chronic myeloid leukemia cells promoted by Beclin1-mediated autophagy. *Cancer Management and Research*, 11, 5197.

Huang, X., Qi, Q., Hua, X., Li, X., Zhang, W., Sun, H., ... & Li, B. (2014). Beclin 1, an autophagy-related gene, augments apoptosis in U87 glioblastoma cells. *Oncology reports*, 31(4), 1761-1767.

Hughes, D., Edwardson, J. A., Rima, B. K., & Allsop, D. (1994). Human IMR-32 neuroblastoma cells as a model cell line in Alzheimer's disease research. *Journal of neuroscience research*, 39(4), 482-493.

Hu, Y., Benedict, M. A., Ding, L., & Núñez, G. (1999). Role of cytochrome c and dATP/ATP hydrolysis in Apaf-1-mediated caspase-9 activation and apoptosis. *The EMBO journal*, 18(13), 3586-3595.

Ikami, Y., Terasawa, K., Sakamoto, K., Ohtake, K., Harada, H., Watabe, T., ... & Hara-Yokoyama, M. (2022). The two-domain architecture of LAMP2A regulates its interaction with Hsc70. *Experimental cell research*, 411(1), 112986.

Ilaria, R. L., & Van Etten, R. A. (1996). P210 and P190BCR/ABL induce the tyrosine phosphorylation and DNA binding activity of multiple specific STAT family members. *Journal of Biological Chemistry*, 271(49), 31704-31710.

Inagaki, S., Funato, M., Nakamura, S., Shimazawa, M., Kaneko, H., & Hara, H. (2019). Donepezil, an anti-Alzheimer's disease drug has the neuroprotective effect on RGCs derived from familial glaucoma patients' iPS cells. *Investigative Ophthalmology & Visual Science*, 60(9), 626-626.

Inoki, K., Zhu, T., & Guan, K. L. (2003). TSC2 mediates cellular energy response to control cell growth and survival. *Cell*, 115(5), 577-590.

Iqbal, K., Del Alonso, A. C., Gondal, J. A., Gong, C. X., Haque, N., Khatoon, S., ... & Grundke-Iqbal, I. (2000). Mechanism of neurofibrillary degeneration and pharmacologic therapeutic approach. In *Advances in Dementia Research* (pp. 213-222). Springer, Vienna.

Jäättelä, M., Wissing, D., Kokholm, K., Kallunki, T., & Egeblad, M. (1998). Hsp70 exerts its anti-apoptotic function downstream of caspase-3-like proteases. *The EMBO journal*, 17(21), 6124-6134.

Jabbour, E., & Kantarjian, H. (2018). Chronic myeloid leukemia: 2018 update on diagnosis, therapy and monitoring. *American journal of hematology*, 93(3), 442-459.

Jabbour, E., & Kantarjian, H. (2020). Chronic myeloid leukemia: 2020 update on diagnosis, therapy and monitoring. *American journal of hematology*, 95(6), 691-709.

Jabbour, E., Kantarjian, H., O'Brien, S., Rios, M. B., Abruzzo, L., Verstovsek, S., ... & Cortes, J. (2006). Sudden blastic transformation in patients with chronic myeloid leukemia treated with imatinib mesylate. *Blood*, 107(2), 480-482.

Jain, A., Lamark, T., Sjøttem, E., Larsen, K. B., Awuh, J. A., Øvervatn, A., ... & Johansen, T. (2010). p62/SQSTM1 is a target gene for transcription factor NRF2 and creates a positive feedback loop by inducing antioxidant response element-driven gene transcription. *Journal of Biological Chemistry*, 285(29), 22576-22591.

Jain, P., Kantarjian, H. M., Ghorab, A., Sasaki, K., Jabbour, E. J., Nogueras Gonzalez, G., ... & Deltasala, S. (2017). Prognostic factors and survival outcomes in patients with chronic myeloid leukemia in blast phase in the tyrosine kinase inhibitor era: cohort study of 477 patients. *Cancer*, 123(22), 4391-4402.

Jakubowska, J., Stasiak, M., Szulawska, A., Bednarek, A., & Czyz, M. (2007). Combined effects of doxorubicin and STI571 on growth, differentiation and apoptosis of CML cell line K562. *Acta Biochimica Polonica*, 54(4), 839-846.

Jan, R. (2019). Understanding apoptosis and apoptotic pathways targeted cancer therapeutics. *Advanced pharmaceutical bulletin*, 9(2), 205.

Jantas, D., & Lason, W. (2009). Protective effect of memantine against Doxorubicin toxicity in primary neuronal cell cultures: influence a development stage. *Neurotoxicity research*, 15(1), 24-37.

Jantas, D., Pytel, M., Mozrzymas, J. W., Leskiewicz, M., Regulska, M., Antkiewicz-Michaluk, L., & Lason, W. (2008). The attenuating effect of memantine on staurosporine-, salsolinol- and doxorubicin-induced apoptosis in human neuroblastoma SH-SY5Y cells. *Neurochemistry international*, 52(4-5), 864-877.

Jaul, E., & Barron, J. (2017). Age-related diseases and clinical and public health implications for the 85 years old and over population. *Frontiers in public health*, 5, 335.

Jeon, S. M., Chandel, N. S., & Hay, N. (2012). AMPK regulates NADPH homeostasis to promote tumour cell survival during energy stress. *Nature*, 485(7400), 661-665.

Jin, Z., Li, Y., Pitti, R., Lawrence, D., Pham, V. C., Lill, J. R., & Ashkenazi, A. (2009). Cullin3-based polyubiquitination and p62-dependent aggregation of caspase-8 mediate extrinsic apoptosis signaling. *Cell*, 137(4), 721-735.

Johnson, J. R., Bross, P., Cohen, M., Rothmann, M., Chen, G., Zajicek, A., ... & Pazdur, R. (2003). Approval summary: imatinib mesylate capsules for treatment of adult patients with newly diagnosed Philadelphia chromosome-positive chronic myelogenous leukemia in chronic phase. *Clinical Cancer Research*, 9(6), 1972-1979.

Johnson, R., Shabalala, S., Louw, J., Kappo, A. P., & Muller, C. J. F. (2017). Aspalathin reverts doxorubicin-induced cardiotoxicity through increased autophagy and decreased expression of p53/mTOR/p62 signaling. *Molecules*, 22(10), 1589.

Ju, W. K., Kim, K. Y., Angert, M., Duong-Polk, K. X., Lindsey, J. D., Ellisman, M. H., & Weinreb, R. N. (2009). Memantine blocks mitochondrial OPA1 and cytochrome c release and subsequent apoptotic cell death in glaucomatous retina. *Investigative ophthalmology & visual science*, 50(2), 707-716.

Kabeya, Y., Mizushima, N., Ueno, T., Yamamoto, A., Kirisako, T., Noda, T., ... & Yoshimori, T. (2000). LC3, a mammalian homologue of yeast Apg8p, is localized in autophagosome membranes after processing. *The EMBO journal*, 19(21), 5720-5728.

Kafi, H., Salamzadeh, J., Beladimoghadam, N., Sistanizad, M., & Kouchek, M. (2014). Study of the neuroprotective effects of memantine in patients with mild to moderate ischemic stroke. *Iranian journal of pharmaceutical research: IJPR*, 13(2), 591.

Kakinuma, Y., Ando, M., Kuwabara, M., Katare, R. G., Okudela, K., Kobayashi, M., & Sato, T. (2005). Acetylcholine from vagal stimulation protects cardiomyocytes against ischemia and hypoxia involving additive non-hypoxic induction of HIF-1 α . *FEBS letters*, 579(10), 2111-2118.

Kale, J., Osterlund, E. J., & Andrews, D. W. (2018). BCL-2 family proteins: changing partners in the dance towards death. *Cell Death & Differentiation*, 25(1), 65-80.

Kamal, T., Green, T. N., Morel-Kopp, M. C., Ward, C. M., McGregor, A. L., McGlashan, S. R., ... & Skerry, T. M. (2015). Inhibition of glutamate regulated calcium entry into leukemic megakaryoblasts reduces cell proliferation and supports differentiation. *Cellular signalling*, 27(9), 1860-1872.

Kamthan, A. G., Lind, M. J., Thatcher, N., Steward, W. P., Bronchud, M. H., Ranson, M. R., & Stout, R. (1990). Ifosfamide, doxorubicin and etoposide in small cell lung cancer patients with poor prognosis. *European Journal of Cancer and Clinical Oncology*, 26(6), 691-694.

Kang, Z. J., Liu, Y. F., Xu, L. Z., Long, Z. J., Huang, D., Yang, Y., ... & Liu, Q. (2016). The Philadelphia chromosome in leukemogenesis. *Chinese journal of cancer*, 35(1), 48.

Kantarjian, H. M., Dixon, D., Keating, M. J., Talpaz, M., Walters, R. S., McCredie, K. B., & Freireich, E. J. (1988). Characteristics of accelerated disease in chronic myelogenous leukemia. *Cancer*, 61(7), 1441-1446.

Kantarjian, H. M., O'Brien, S., Smith, T. L., Cortes, J., Giles, F. J., Beran, M., ... & Freireich, E. J. (2000). Results of treatment with hyper-CVAD, a dose-intensive regimen, in adult acute lymphocytic leukemia. *Journal of Clinical Oncology*, 18(3), 547-547.

Kantarjian, H., Sawyers, C., Hochhaus, A., Guilhot, F., Schiffer, C., Gambacorti-Passerini, C., ... & Druker, B. (2002). Hematologic and cytogenetic responses to imatinib mesylate in chronic myelogenous leukemia. *New England Journal of Medicine*, 346(9), 645-652.

Karbowski, M., Norris, K. L., Cleland, M. M., Jeong, S. Y., & Youle, R. J. (2006). Role of Bax and Bak in mitochondrial morphogenesis. *Nature*, 443(7112), 658-662.

Kato, M., Kolotuev, I., Cunha, A., Gharib, S., & Sternberg, P. W. (2021). Extrasynaptic acetylcholine signaling through a muscarinic receptor regulates cell migration. *Proceedings of the National Academy of Sciences*, 118(1).

Kawamata, T., Horie, T., Matsunami, M., Sasaki, M., & Ohsumi, Y. (2017). Zinc starvation induces autophagy in yeast. *Journal of Biological Chemistry*, 292(20), 8520-8530.

Khalidi, H. S., Brynes, R. K., Medeiros, L. J., Chang, K. L., Slovak, M. L., Snyder, D. S., & Arber, D. A. (1998). The immunophenotype of blast transformation of chronic myelogenous leukemia: a high frequency of mixed lineage phenotype in "lymphoid" blasts and A comparison of morphologic, immunophenotypic, and molecular findings. *Modern pathology: an official journal of the United States and Canadian Academy of Pathology, Inc*, 11(12), 1211-1221.

Kim, J. K., & Park, S. U. (2017). Pharmacological aspects of galantamine for the treatment of Alzheimer's disease. *EXCLI journal*, 16, 35.

Kim, J. L., Lee, D. H., Jeong, S., Kim, B. R., Na, Y. J., Park, S. H., ... & Oh, S. C. (2019). Imatinib-induced apoptosis of gastric cancer cells is mediated by endoplasmic reticulum stress. *Oncology Reports*, 41(3), 1616-1626.

King, A., Bodi, I., & Troakes, C. (2020). The neuropathological diagnosis of Alzheimer's disease—the challenges of pathological mimics and concomitant pathology. *Brain sciences*, 10(8), 479.

Kirchner, P., Bourdenx, M., Madrigal-Matute, J., Tiano, S., Diaz, A., Bartholdy, B. A., ... & Cuervo, A. M. (2019). Proteome-wide analysis of chaperone-mediated autophagy targeting motifs. *PLoS biology*, 17(5), e3000301.

Kitaoka, K., Shimizu, N., Ono, K., Chikahisa, S., Nakagomi, M., Shudo, K., ... & Yoshizaki, K. (2013). The retinoic acid receptor agonist Am80 increases hippocampal ADAM10 in aged SAMP8 mice. *Neuropharmacology*, 72, 58-65.

Ki, Y. S., Park, E. Y., Lee, H. W., Oh, M. S., Cho, Y. W., Kwon, Y. K. I., ... & Lee, K. T. (2010). Donepezil, a potent acetylcholinesterase inhibitor, induces caspase-dependent apoptosis in human promyelocytic leukemia HL-60 cells. *Biological and Pharmaceutical Bulletin*, 33(6), 1054-1059.

Klein, E., Vánky, F., Ben-Bassat, H., Neumann, H., Ralph, P., Zeuthen, J., & Polliack, A. (1976). Properties of the K562 cell line, derived from a patient with chronic myeloid leukemia. *International journal of cancer*, 18(4), 421-431.

Komatsu, M., Waguri, S., Koike, M., Sou, Y. S., Ueno, T., Hara, T., ... & Hamazaki, J. (2007). Homeostatic levels of p62 control cytoplasmic inclusion body formation in autophagy-deficient mice. *Cell*, 131(6), 1149-1163.

Kønig, S. M., Rissler, V., Terkelsen, T., Lambrugh, M., & Papaleo, E. (2019). Alterations of the interactome of Bcl-2 proteins in breast cancer at the transcriptional, mutational and structural level. *PLoS computational biology*, 15(12), e1007485.

Kovalevich, J., & Langford, D. (2013). Considerations for the use of SH-SY5Y neuroblastoma cells in neurobiology. In *Neuronal Cell Culture* (pp. 9-21). Humana Press, Totowa, NJ.

Krishan, A., Ganapathi, R. N., & Israel, M. (1978). Effect of adriamycin and analogs on the nuclear fluorescence of propidium iodide-stained cells. *Cancer research*, 38(11 Part 1), 3656-3662.

Ku, B., Liang, C., Jung, J. U., & Oh, B. H. (2011). Evidence that inhibition of BAX activation by BCL-2 involves its tight and preferential interaction with the BH3 domain of BAX. *Cell research*, 21(4), 627-641.

Kubonishi, I., & Miyoshi, I. (1983). Establishment of a Ph1 chromosome-positive cell line from chronic myelogenous leukemia in blast crisis. *The International Journal of Cell Cloning*, 1(2), 105-117.

Kuchibhotla, K. V., Goldman, S. T., Lattarulo, C. R., Wu, H. Y., Hyman, B. T., & Bacskai, B. J. (2008). A β plaques lead to aberrant regulation of calcium homeostasis in vivo resulting in structural and functional disruption of neuronal networks. *Neuron*, 59(2), 214-225.

Kuwana, T., Mackey, M. R., Perkins, G., Ellisman, M. H., Latterich, M., Schneider, R., ... & Newmeyer, D. D. (2002). Bid, Bax, and lipids cooperate to form supramolecular openings in the outer mitochondrial membrane. *Cell*, 111(3), 331-342.

Laane, E., Tamm, K. P., Buentke, E., Ito, K., Khahariza, P., Oscarsson, J., ... & Heyman, M. (2009). Cell death induced by dexamethasone in lymphoid leukemia is mediated through initiation of autophagy. *Cell Death & Differentiation*, 16(7), 1018-1029.

Lahiri, D. K., Lewis, S., & Farlow, M. R. (1994). Tacrine alters the secretion of the beta-amyloid precursor protein in cell lines. *Journal of neuroscience research*, 37(6), 777-787.

Lahoti, T.S, Patel, D., Thekkemadom, V., Beckett, R., & D Ray, S. (2012). Doxorubicin-induced in vivo nephrotoxicity involves oxidative stress-mediated multiple pro-and anti-apoptotic signaling pathways. *Current neurovascular research*, 9(4), 282-295.

Laker, R. C., Drake, J. C., Wilson, R. J., Lira, V. A., Lewellen, B. M., Ryall, K. A., ... & Kundu, M. (2017). Ampk phosphorylation of Ulk1 is required for targeting of mitochondria to lysosomes in exercise-induced mitophagy. *Nature communications*, 8(1), 548.

Laroche-Clary, A., Larrue, A., & Robert, J. (2000). Down-regulation of bcr-abl and bcl-X1 expression in a leukemia cell line and its doxorubicin-resistant variant by topoisomerase II inhibitors. *Biochemical pharmacology*, 60(12), 1823-1828.

Larson, R. A., Kim, D. W., Jootar, S., Pasquini, R., Clark, R. E., Lobo, C., ... & Hughes, T. P. (2014). ENESTnd 5-year (y) update: Long-term outcomes of patients (pts) with chronic myeloid leukemia in chronic phase (CML-CP) treated with frontline nilotinib (NIL) versus imatinib (IM).

Lazova, R., Camp, R. L., Klump, V., Siddiqui, S. F., Amaravadi, R. K., & Pawelek, J. M. (2012). Punctate LC3B expression is a common feature of solid tumors and associated with proliferation, metastasis, and poor outcome. *Clinical cancer research*, 18(2), 370-379.

Lebrecht, D., Setzer, B., Rohrbach, R., & Walker, U. A. (2004). Mitochondrial DNA and its respiratory chain products are defective in doxorubicin nephrosis. *Nephrology Dialysis Transplantation*, 19(2), 329-336.

Lee, Y. L., Chen, C. W., Liu, F. H., Huang, Y. W., & Huang, H. M. (2013). Aclacinomycin A sensitizes K562 chronic myeloid leukemia cells to imatinib through p38MAPK-mediated erythroid differentiation. *PLoS One*, 8(4).

Leis, J. F., Stepan, D. E., Curtin, P. T., Ford, J. M., Peng, B., Schubach, S., ... & Maziarz, R. T. (2004). Central nervous system failure in patients with chronic myelogenous leukemia lymphoid blast crisis and Philadelphia chromosome positive acute lymphoblastic leukemia treated with imatinib (STI-571). *Leukemia & lymphoma*, 45(4), 695-698.

Leprivier, G., Remke, M., Rotblat, B., Dubuc, A., Mateo, A. R. F., Kool, M., ... & Faubert, B. (2013). The eEF2 kinase confers resistance to nutrient deprivation by blocking translation elongation. *Cell*, 153(5), 1064-1079.

Leung, L. K., & Wang, T. T. (1999). Differential effects of chemotherapeutic agents on the Bcl-2/Bax apoptosis pathway in human breast cancer cell line MCF-7. *Breast cancer research and treatment*, 55(1), 73-83.

Liang, X. H., Kleeman, L. K., Jiang, H. H., Gordon, G., Goldman, J. E., Berry, G., ... & Levine, B. (1998). Protection against fatal Sindbis virus encephalitis by beclin, a novel Bcl-2-interacting protein. *Journal of virology*, 72(11), 8586-8596.

Li, D. L., Wang, Z. V., Ding, G., Tan, W., Luo, X., Criollo, A., ... & Schneider, J. W. (2016). Doxorubicin blocks cardiomyocyte autophagic flux by inhibiting lysosome acidification. *Circulation*, 133(17), 1668-1687.

Li, J., Liu, W., Hao, H., Wang, Q., & Xue, L. (2019). Rapamycin enhanced the antitumor effects of doxorubicin in myelogenous leukemia K562 cells by downregulating the mTOR/p70S6K pathway. *Oncology letters*, 18(3), 2694-2703.

Li, L., & Hanahan, D. (2013). Hijacking the neuronal NMDAR signaling circuit to promote tumor growth and invasion. *Cell*, 153(1), 86-100.

Li, L., You, L. S., Mao, L. P., Jin, S. H., Chen, X. H., & Qian, W. B. (2018). Combing oncolytic adenovirus expressing Beclin-1 with chemotherapy agent doxorubicin synergistically enhances cytotoxicity in human CML cells in vitro. *Acta Pharmacologica Sinica*, 39(2), 251-260.

Li, L., Zeng, Q., Bhutkar, A., Galván, J. A., Karamitopoulou, E., Noordermeer, D., ... & Hanahan, D. (2018). GKAP acts as a genetic modulator of NMDAR signaling to govern invasive tumor growth. *Cancer Cell*, 33(4), 736-751.

Lin, C. L., Chen, T. F., Chiu, M. J., Way, T. D., & Lin, J. K. (2009). Epigallocatechin gallate (EGCG) suppresses β -amyloid-induced neurotoxicity through inhibiting c-Abl/FE65 nuclear translocation and GSK3 β activation. *Neurobiology of aging*, 30(1), 81-92.

Linder, B., & Kögel, D. (2019). Autophagy in Cancer Cell Death. *Biology*, 8(4), 82. <https://doi.org/10.3390/biology8040082>.

Lin, Q., Mao, L., Shao, L., Zhu, L., Han, Q., Zhu, H., ... & You, L. (2020). Global, Regional, and National Burden of Chronic Myeloid Leukemia, 1990–2017: A Systematic Analysis for the Global Burden of Disease Study 2017. *Frontiers in oncology*, 10, 2789.

Lin, W. J., & Kuang, H. Y. (2014). Oxidative stress induces autophagy in response to multiple noxious stimuli in retinal ganglion cells. *Autophagy*, 10(10), 1692-1701.

Li, P., Shi, M., Maique, J., Shaffer, J., Yan, S., Moe, O. W., & Hu, M. C. (2020). Beclin 1/Bcl-2 complex-dependent autophagy activity modulates renal susceptibility to ischemia-reperfusion injury and mediates renoprotection by Klotho. *American Journal of Physiology-Renal Physiology*, 318(3), F772-F792.

Li, S., Ilaria Jr, R. L., Million, R. P., Daley, G. Q., & Van Etten, R. A. (1999). The P190, P210, and P230 forms of the BCR/ABL oncogene induce a similar chronic myeloid leukemia-like syndrome in mice but have different lymphoid leukemogenic activity. *The Journal of experimental medicine*, 189(9), 1399-1412.

Liu, D. Z., & Ander, B. P. (2012). Cell cycle inhibition without disruption of neurogenesis is a strategy for treatment of aberrant cell cycle diseases: an update. *The Scientific World Journal*, 2012.

Liu, J., Ren, H., Liu, B., Zhang, Q., Li, M., & Zhu, R. (2016). Diosmetin inhibits cell proliferation and induces apoptosis by regulating autophagy via the mammalian target of rapamycin pathway in hepatocellular carcinoma HepG2 cells. *Oncology letters*, 12(6), 4385-4392.

Liu, J., Zhou, Y., Yuan, Q., & Xiao, M. (2020). Myeloid Blast Crisis of Chronic Myeloid Leukemia Followed by Lineage Switch to B-Lymphoblastic Leukemia: A Case Report. *OncoTargets and therapy*, 13, 3259.

Liu, R., Meng, F., Zhang, L., Liu, A., Qin, H., Lan, X., ... & Du, G. (2011). Luteolin isolated from the medicinal plant *Elsholtzia rugulosa* (Labiatae) prevents copper-mediated toxicity in β -amyloid precursor protein Swedish mutation overexpressing SH-SY5Y cells. *Molecules*, 16(3), 2084-2096.

Lomonosova, E., & Chinnadurai, G. (2008). BH3-only proteins in apoptosis and beyond: an overview. *Oncogene*, 27(1), S2-S19.

Loreto, C., La Rocca, G., Anzalone, R., Caltabiano, R., Vespasiani, G., Castorina, S., ... & Sansalone, S. (2014). The role of intrinsic pathway in apoptosis activation and progression in Peyronie's disease. *BioMed research international*, 2014.

Lozzio, C. B., & Lozzio, B. B. (1975). Human chronic myelogenous leukemia cell-line with positive Philadelphia chromosome.

Lu, L., Wu, W., Yan, J., Li, X., Yu, H., & Yu, X. (2009). Adriamycin-induced autophagic cardiomyocyte death plays a pathogenic role in a rat model of heart failure. *International journal of cardiology*, 134(1), 82-90.

Luo, D., Cheng, S. C. S., Xie, H., & Xie, Y. (2000). Effects of Bcl-2 and Bcl-XL protein levels on chemoresistance of hepatoblastoma HepG2 cell line. *Biochemistry and Cell Biology*, 78(2), 119-126.

Luo, S., & Rubinsztein, D. C. (2010). Apoptosis blocks Beclin 1-dependent autophagosome synthesis: an effect rescued by Bcl-xL. *Cell Death & Differentiation*, 17(2), 268-277.

Maiuri, M. C., Le Toumelin, G., Criollo, A., Rain, J. C., Gautier, F., Juin, P., ... & Hickman, J. A. (2007). Functional and physical interaction between Bcl-XL and a BH3-like domain in Beclin-1. *The EMBO journal*, 26(10), 2527-2539.

Marquez, R. T., & Xu, L. (2012). Bcl-2: Beclin 1 complex: multiple, mechanisms regulating autophagy/apoptosis toggle switch. *American journal of cancer research*, 2(2), 214.

Marum, J. E., Wang, P. P., Stangl, D., Yeung, D. T., Mueller, M. C., Dietz, C. T., ... & Ross, D. M. (2016). Novel fusion genes at CML diagnosis reveal a complex pattern of genomic rearrangements and sequence inversions associated with the Philadelphia chromosome in patients with early blast crisis.

Mathew, R., Kongara, S., Beaudoin, B., Karp, C. M., Bray, K., Degenhardt, K., ... & White, E. (2007). Autophagy suppresses tumor progression by limiting chromosomal instability. *Genes & development*, 21(11), 1367-1381.

Matsui, Y., Takagi, H., Qu, X., Abdellatif, M., Sakoda, H., Asano, T., ... & Sadoshima, J. (2007). Distinct roles of autophagy in the heart during ischemia and reperfusion: roles of AMP-activated protein kinase and Beclin 1 in mediating autophagy. *Circulation research*, 100(6), 914-922.

Ma, T., Tan, M. S., Yu, J. T., & Tan, L. (2014). Resveratrol as a therapeutic agent for Alzheimer's disease. *BioMed research international*.

Matsuda, M., Morita, Y., Shimada, T., Miyatake, J., Hirase, C., Tanaka, M., ... & Kanamaru, A. (2005). Extramedullary blast crisis derived from 2 different clones in the central nervous system and neck during complete cytogenetic remission of chronic myelogenous leukemia treated with imatinib mesylate. *International journal of hematology*, 81(4), 307-309.

Matutes, E., Pickl, W. F., Van't Veer, M., Morilla, R., Swansbury, J., Strobl, H., ... & Ludwig, W. D. (2011). Mixed-phenotype acute leukemia: clinical and laboratory features and outcome in 100 patients defined according to the WHO 2008 classification. *Blood, The Journal of the American Society of Hematology*, 117(11), 3163-3171.

Maurel, J., Martins, A. S., Poveda, A., López-Guerrero, J. A., Cubedo, R., Casado, A., ... & Garcia del Muro, X. (2010). Imatinib plus low-dose doxorubicin in patients with advanced gastrointestinal stromal tumors refractory to high-dose imatinib: A phase I-II study by the Spanish group for research on sarcomas. *Cancer*, 116(15), 3692-3701.

Mauthe, M., Orhon, I., Rocchi, C., Zhou, X., Luhr, M., Hijlkema, K. J., ... & Reggiori, F. (2018). Chloroquine inhibits autophagic flux by decreasing autophagosome-lysosome fusion. *Autophagy*, 14(8), 1435-1455.

Maycotte, P., Aryal, S., Cummings, C. T., Thorburn, J., Morgan, M. J., & Thorburn, A. (2012). Chloroquine sensitizes breast cancer cells to chemotherapy independent of autophagy. *Autophagy*, 8(2), 200-212.

Mayer, B. J., & Baltimore, D. (1994). Mutagenic analysis of the roles of SH2 and SH3 domains in regulation of the Abl tyrosine kinase. *Molecular and cellular biology*, 14(5), 2883-2894.

McKnight, N. C., & Yue, Z. (2013). Beclin 1, an essential component and master regulator of PI3K-III in health and disease. *Current pathobiology reports*, 1(4), 231-238.

McKnight, N. C., Zhong, Y., Wold, M. S., Gong, S., Phillips, G. R., Dou, Z., ... & Yue, Z. (2014). Beclin 1 is required for neuron viability and regulates endosome pathways via the UVRAG-VPS34 complex. *PLoS Genet*, 10(10), e1004626.

McMurtray, A., Clark, D. G., Christine, D., & Mendez, M. F. (2006). Early-onset dementia: frequency and causes compared to late-onset dementia. *Dementia and geriatric cognitive disorders*, 21(2), 59-64.

Medeiros, B. C., Possick, J., & Fradley, M. (2018). Cardiovascular, pulmonary, and metabolic toxicities complicating tyrosine kinase inhibitor therapy in chronic myeloid leukemia: Strategies for monitoring, detecting, and managing. *Blood reviews*, 32(4), 289-299.

Mehdizadeh, K., Ataei, F., & Hosseinkhani, S. (2020). Effects of doxorubicin and docetaxel on susceptibility to apoptosis in high expression level of survivin in HEK and HEK-S cell lines as in vitro models. *Biochemical and Biophysical Research Communications*, 532(1), 139-144.

Mendez, M. F. (2019). Early-onset Alzheimer disease and its variants. *Continuum (Minneapolis, Minn.)*, 25(1), 34.

Mendizabal, A. M., Younes, N., & Levine, P. H. (2016). Geographic and income variations in age at diagnosis and incidence of chronic myeloid leukemia. *International journal of hematology*, 103(1), 70-78.

Menon, M. B., & Dhamija, S. (2018). Beclin 1 phosphorylation—at the center of autophagy regulation. *Frontiers in cell and developmental biology*, 6, 137.

Meriwether, W. D., & Bachur, N. R. (1972). Inhibition of DNA and RNA metabolism by daunorubicin and adriamycin in L1210 mouse leukemia. *Cancer research*, 32(6), 1137-1142.

Meyer-Luehmann, M., Spires-Jones, T. L., Prada, C., Garcia-Alloza, M., De Calignon, A., Rozkalne, A., ... & Hyman, B. T. (2008). Rapid appearance and local toxicity of amyloid- β plaques in a mouse model of Alzheimer's disease. *Nature*, 451(7179), 720-724.

Mietelska-Porowska, A., Wasik, U., Goras, M., Filipek, A., & Niewiadomska, G. (2014). Tau protein modifications and interactions: their role in function and dysfunction. *International journal of molecular sciences*, 15(3), 4671-4713.

Miki, A., Otori, Y., Morimoto, T., Okada, M., & Tano, Y. (2006). Protective effect of donepezil on retinal ganglion cells in vitro and in vivo. *Current eye research*, 31(1), 69-77.

Minn, A. J., Rudin, C. M., Boise, L. H., & Thompson, C. B. (1995). Expression of bcl-xL can confer a multidrug resistance phenotype.

Minowada, J., Tsubota, T., Greaves, M. F., & Walters, T. R. (1977). A non-T, non-B human leukemia cell line (NALM-1): establishment of the cell line and presence of leukemia-associated antigens. *Journal of the National Cancer Institute*, 59(1), 83-87.

Mizushima, N. (2018). A brief history of autophagy from cell biology to physiology and disease. *Nature cell biology*, 20(5), 521-527.

Mizushima, N., Yoshimori, T., & Levine, B. (2010). Methods in mammalian autophagy research. *Cell*, 140(3), 313-326.

Momparler, R. L., Karon, M., Siegel, S. E., & Avila, F. (1976). Effect of adriamycin on DNA, RNA, and protein synthesis in cell-free systems and intact cells. *Cancer research*, 36(8), 2891-2895.

Mori, H., Takio, K., Ogawara, M., & Selkoe, D. J. (1992). Mass spectrometry of purified amyloid beta protein in Alzheimer's disease. *Journal of Biological Chemistry*, 267(24), 17082-17086.

Morimoto, B. H., & Koshland Jr, D. E. (1990). Induction and expression of long-and short-term neurosecretory potentiation in a neural cell line. *Neuron*, 5(6), 875-880.

Mortazavian, S. M., Parsaee, H., Mousavi, S. H., Tayarani-Najaran, Z., Ghorbani, A., & Sadeghnia, H. R. (2013). Acetylcholinesterase inhibitors promote angiogenesis in chick chorioallantoic membrane and inhibit apoptosis of endothelial cells. *International journal of Alzheimer's disease*, 2013.

Moschovi, M., & Kelaidi, C. (2021). Chronic Myeloid Leukemia in Children and Adolescents: The Achilles Heel of Oncogenesis and Tyrosine Kinase Inhibitors. *International Journal of Molecular Sciences*, 22(15), 7806.

Müller, I., Jenner, A., Bruchelt, G., Niethammer, D., & Halliwell, B. (1997). Effect of concentration on the cytotoxic mechanism of doxorubicin—apoptosis and oxidative DNA damage. *Biochemical and biophysical research communications*, 230(2), 254-257.

Muresan, V., & Muresan, Z. L. (2015). Amyloid- β precursor protein: multiple fragments, numerous transport routes and mechanisms. *Experimental cell research*, 334(1), 45-53.

Murphy, M. P., & LeVine, H. (2010). Alzheimer's Disease and the β -Amyloid Peptide. *Journal of Alzheimer's Disease : JAD*, 19(1), 311.

Musiwaro, P., Smith, M., Manifava, M., Walker, S. A., & Ktistakis, N. T. (2013). Characteristics and requirements of basal autophagy in HEK 293 cells. *Autophagy*, 9(9), 1407-1417.

Myung Park, J., Huang, S., Wu, T. T., Foster, N. R., & Sinicrope, F. A. (2013). Prognostic impact of Beclin 1, p62/sequestosome 1 and LC3 protein expression in colon carcinomas from patients receiving 5-fluorouracil as adjuvant chemotherapy. *Cancer biology & therapy*, 14(2), 100-107.

Narayanan, A. S., Reyes, S. B., Um, K., McCarty, J. H., & Tolia, K. F. (2013). The Rac-GAP Bcr is a novel regulator of the Par complex that controls cell polarity. *Molecular biology of the cell*, 24(24), 3857-3868.

National Center for Biotechnology Information (NCBI) (2021). ABL1 ABL proto-oncogene 1, non-receptor tyrosine kinase [Homo sapiens (human)] - Gene. Retrieved 10 November 2021, from <https://www.ncbi.nlm.nih.gov/gene?Db=gene&Cmd=DetailsSearch&Term=25>

National Center for Biotechnology Information (NCBI) (2021). BCR BCR activator of RhoGEF and GTPase [Homo sapiens (human)] - Gene. Retrieved 10 November 2021, from <https://www.ncbi.nlm.nih.gov/gene/613>

National Health Service (NHS) (2021). Alzheimer's disease - Diagnosis. Retrieved 3 August 2021, from <https://www.nhs.uk/conditions/alzheimers-disease/diagnosis/>

National Health Service (NHS) (2021). Alzheimer's disease. Retrieved 31 October 2021, from <https://www.nhs.uk/conditions/alzheimers-disease/>

National Health Service (NHS) (2021). Chronic myeloid leukaemia. Retrieved 31 October 2021, from <https://www.nhs.uk/conditions/chronic-myeloid-leukaemia/>

National Institute for Health and Care Excellence (NICE) (2011) 'Donepezil, galantamine, rivastigmine and memantine for the treatment of Alzheimer's disease. NICE Guideline (TA217)'. Available at: <https://www.nice.org.uk/guidance/ta217>.

NIHR (National Institute for Health and Care Research) (2019). Clinical Trials Guide. Retrieved 29 April 2022, from <https://www.nihr.ac.uk/documents/clinical-trials-guide/20595>

National Institute on Aging (NIA) (2021). How Is Alzheimer's Disease Diagnosed? Retrieved 3 August 2021, from <https://www.nia.nih.gov/health/how-alzheimers-disease-diagnosed>

Negrin, R. S., & Schiffer, C. A. Interferon alfa for the treatment of chronic myeloid leukemia. UpToDate, Waltham, MA. (Accessed on May 14, 2016.) PubMed.

Neill, D., Hughes, D., Edwardson, J. A., Rima, B. K., & Allsop, D. (1994). Human IMR-32 neuroblastoma cells as a model cell line in Alzheimer's disease research. *Journal of neuroscience research*, 39(4), 482-493.

Neri, L. M., Cani, A., Martelli, A. M., Simioni, C., Junghanss, C., Tabellini, G., ... & Capitani, S. (2014). Targeting the PI3K/Akt/mTOR signaling pathway in B-precursor acute lymphoblastic leukemia and its therapeutic potential. *Leukemia*, 28(4), 739-748.

New York Times (NYT) (1993). "ALZHEIMER'S DRUG APPROVED BY F.D.A." The, 10 Sept. 1993, www.nytimes.com/1993/09/10/us/alzheimer-s-drug-approved-by-fda.html.

Nikoletopoulou, V., Markaki, M., Palikaras, K. and Tavernarakis, N., (2013) 'Crosstalk between apoptosis, necrosis and autophagy'. *Biochimica et Biophysica Acta (BBA)-Molecular Cell Research*, 1833(12), pp.3448-3459.

Nilsson, P., Loganathan, K., Sekiguchi, M., Matsuba, Y., Hui, K., Tsubuki, S., ... & Saido, T. C. (2013). A β secretion and plaque formation depend on autophagy. *Cell reports*, 5(1), 61-69.

Nixon, R. A., Wegiel, J., Kumar, A., Yu, W. H., Peterhoff, C., Cataldo, A., & Cuervo, A. M. (2005). Extensive involvement of autophagy in Alzheimer disease: an immuno-electron microscopy study. *Journal of Neuropathology & Experimental Neurology*, 64(2), 113-122.

Noh, M. Y., Koh, S. H., Kim, Y., Kim, H. Y., Cho, G. W., & Kim, S. H. (2009). Neuroprotective effects of donepezil through inhibition of GSK-3 activity in amyloid- β -induced neuronal cell death. *Journal of neurochemistry*, 108(5), 1116-1125.

Nordberg, A., & Svensson, A. L. (1998). Cholinesterase inhibitors in the treatment of Alzheimer's disease. *Drug safety*, 19(6), 465-480.

Nylén, U., Baral, E., Svane, G., & Rutqvist, L. E. (1989). Weekly doxorubicin in the treatment of metastatic breast carcinoma. *Acta Oncologica*, 28(4), 515-517.

Oakhill, J. S., Chen, Z. P., Scott, J. W., Steel, R., Castelli, L. A., Ling, N., ... & Kemp, B. E. (2010). β -Subunit myristoylation is the gatekeeper for initiating metabolic stress sensing by AMP-activated protein kinase (AMPK). *Proceedings of the National Academy of Sciences*, 107(45), 19237-19241.

Oberstein, A., Jeffrey, P. D., & Shi, Y. (2007). Crystal structure of the Bcl-XL-Beclin 1 peptide complex: Beclin 1 is a novel BH3-only protein. *Journal of Biological Chemistry*, 282(17), 13123-13132.

O'Brien, M. E., Wigler, N., Inbar, M. C. B. C. S. G., Rosso, R., Grischke, E., Santoro, A., ... & CAELYX Breast Cancer Study Group. (2004). Reduced cardiotoxicity and comparable efficacy in a phase III trial of pegylated liposomal doxorubicin HCl (CAELYX™/Doxil®) versus conventional doxorubicin for first-line treatment of metastatic breast cancer. *Annals of oncology*, 15(3), 440-449.

O'Brien, R. J., & Wong, P. C. (2011). Amyloid precursor protein processing and Alzheimer's disease. *Annual review of neuroscience*, 34, 185-204.

Ohkubo, T., Kamamoto, T., Kita, K., Hiraoka, A., Yoshida, Y., & Uchino, H. (1985). A novel Ph1 chromosome positive cell line established from a patient with chronic myelogenous leukemia in blastic crisis. *Leukemia research*, 9(7), 921-926.

Ohnishi, A., Mihara, M., Kamakura, H., Tomono, Y., Hasegawa, J., Yamazaki, K., ... & Tanaka, T. (1993). Comparison of the pharmacokinetics of E2020, a new compound for Alzheimer's disease, in healthy young and elderly subjects. *The Journal of Clinical Pharmacology*, 33(11), 1086-1091.

Ohnishi, T., Tamai, I., Sakanaka, K., Sakata, A., Yamashima, T., Yamashita, J., & Tsuji, A. (1995). In vivo and in vitro evidence for ATP-dependency of P-glycoprotein-mediated efflux of doxorubicin at the blood-brain barrier. *Biochemical pharmacology*, 49(10), 1541-1544.

Oltval, Z. N., Milliman, C. L., & Korsmeyer, S. J. (1993). Bcl-2 heterodimerizes in vivo with a conserved homolog, Bax, that accelerates programmed cell death. *cell*, 74(4), 609-619.

Ongnok, B., Khuanjing, T., Chunchai, T., Pantiya, P., Kerdphoo, S., Arunsak, B., ... & Chattipakorn, S. C. (2021). Donepezil protects against doxorubicin-induced chemobrain in rats via attenuation of inflammation and oxidative stress without interfering with doxorubicin efficacy. *Neurotherapeutics*, 18(3), 2107-2125.

Oral, E. A., Reilly, S. M., Gomez, A. V., Meral, R., Butz, L., Ajluni, N., ... & Rus, D. (2017). Inhibition of IKK ϵ and TBK1 improves glucose control in a subset of patients with type 2 diabetes. *Cell metabolism*, 26(1), 157-170.

Ozretic, P., Alvir, I., Sarcevic, B., Vujaskovic, Z., Rendic-Miocevic, Z., Roguljic, A., & Beketic-Oreskovic, L. (2018). Apoptosis regulator Bcl-2 is an independent prognostic marker for worse overall survival in triple-negative breast cancer patients. *The International journal of biological markers*, 33(1), 109-115.

Pabón, M. A., Patino, E., Bhatia, D., Rojas-Quintero, J., Ma, K. C., Finkelsztein, E. J., ... & Ryter, S. W. (2018). Beclin-1 regulates cigarette smoke-induced kidney injury in a murine model of chronic obstructive pulmonary disease. *JCI insight*, 3(18).

Palamà, I. E., Cortese, B., D'Amone, S., Arcadio, V., & Gigli, G. (2015). Coupled delivery of imatinib mesylate and doxorubicin with nanoscaled polymeric vectors for a sustained downregulation of BCR-ABL in chronic myeloid leukemia. *Biomaterials science*, 3(2), 361-372.

Palandri, F., Castagnetti, F., Testoni, N., Luatti, S., Marzocchi, G., Bassi, S., ... & Rosti, G. (2008). Chronic myeloid leukemia in blast crisis treated with imatinib 600 mg: outcome of the patients alive after a 6-year follow-up. *Haematologica*, 93(12), 1792-1796.

Panaretakis, T., Pokrovskaja, K., Shoshan, M. C., & Grandér, D. (2002). Activation of Bak, Bax, and BH3-only proteins in the apoptotic response to doxorubicin. *Journal of Biological Chemistry*, 277(46), 44317-44326.

Pane, F., Frigeri, F., Sindona, M., Luciano, L., Ferrara, F., Cimino, R., ... & Rotoli, B. (1996). Neutrophilic-chronic myeloid leukemia: a distinct disease with a specific molecular marker (BCR/ABL with C3/A2 junction).

Pankiv, S., Clausen, T. H., Lamark, T., Brech, A., Bruun, J. A., Outzen, H., ... & Johansen, T. (2007). p62/SQSTM1 binds directly to Atg8/LC3 to facilitate degradation of ubiquitinated protein aggregates by autophagy. *Journal of biological chemistry*, 282(33), 24131-24145.

Pan, Y., Gao, Y., Chen, L., Gao, G., Dong, H., Yang, Y., ... & Chen, X. (2011). Targeting autophagy augments in vitro and in vivo antimyeloma activity of DNA-damaging chemotherapy. *Clinical Cancer Research*, 17(10), 3248-3258.

Park, S. Y., Kim, H. S., Cho, E. K., Kwon, B. Y., Phark, S., Hwang, K. W., & Sul, D. (2008). Curcumin protected PC12 cells against beta-amyloid-induced toxicity through the inhibition of oxidative damage and tau hyperphosphorylation. *Food and Chemical Toxicology*, 46(8), 2881-2887.

Parsons, C. G., Danysz, W., & Quack, G. (1999). Memantine is a clinically well tolerated N-methyl-D-aspartate (NMDA) receptor antagonist—a review of preclinical data. *Neuropharmacology*, 38(6), 735-767.

Parsons, C. G., Rammes, G., & Danysz, W. (2008). Pharmacodynamics of memantine: an update. *Current neuropharmacology*, 6(1), 55-78.

Pattingre, S., Tassa, A., Qu, X., Garuti, R., Liang, X. H., Mizushima, N., ... & Levine, B. (2005). Bcl-2 antiapoptotic proteins inhibit Beclin 1-dependent autophagy. *Cell*, 122(6), 927-939.

Pendergast, A. M., Muller, A. J., Havlik, M. H., Maru, Y., & Witte, O. N. (1991). BCR sequences essential for transformation by the BCR-ABL oncogene bind to the ABL SH2 regulatory domain in a non-phosphotyrosine-dependent manner. *Cell*, 66(1), 161-171.

Peng, X. X., Shi, Z., Huang, X. C., Kruh, G., Wu, H. C., Parmar, S., ... & Chen, Z. S. (2007). Characterization of chronic myeloid leukemia cell lines with acquired drug resistance to 6-mercaptopurine and imatinib.

Peng, Y., Huang, Z., Zhou, F., Wang, T., Mou, K., & Feng, W. (2021). Effect of HSP90AB1 and CC domain interaction on Bcr-Abl protein cytoplasm localization and function in chronic myeloid leukemia cells. *Cell Communication and Signaling*, 19(1), 1-14.

Perl, D. P. (2010). Neuropathology of Alzheimer's Disease. *The Mount Sinai Journal of Medicine*, New York, 77(1), 32-42.

Perry, J. M., Tao, F., Roy, A., Lin, T., He, X. C., Chen, S., ... & Li, L. (2020). Overcoming Wnt- β -catenin dependent anticancer therapy resistance in leukaemia stem cells. *Nature cell biology*, 1-12.

Peters, I., Igbavboa, U., Schütt, T., Haidari, S., Hartig, U., Rosello, X., ... & Wood, W. G. (2009). The interaction of beta-amyloid protein with cellular membranes stimulates its own production. *Biochimica et Biophysica Acta (BBA)-Biomembranes*, 1788(5), 964-972.

Pfeiffer, A., Jaeckel, M., Lewerenz, J., Noack, R., Pouya, A., Schacht, T., ... & Methner, A. (2014). Mitochondrial function and energy metabolism in neuronal HT22 cells resistant to oxidative stress. *British journal of pharmacology*, 171(8), 2147-2158.

Pilco-Ferreto, N., & Calaf, G. M. (2016). Influence of doxorubicin on apoptosis and oxidative stress in breast cancer cell lines. *International journal of oncology*, 49(2), 753-762.

Pistritto, G., Trisciuglio, D., Ceci, C., Garufi, A., & D'Orazi, G. (2016). Apoptosis as anticancer mechanism: function and dysfunction of its modulators and targeted therapeutic strategies. *Aging (Albany NY)*, 8(4), 603.

Pluk, H., Dorey, K., & Superti-Furga, G. (2002). Autoinhibition of c-Abl. *Cell*, 108(2), 247-259.

Polli, J. E. (2008). In vitro studies are sometimes better than conventional human pharmacokinetic in vivo studies in assessing bioequivalence of immediate-release solid oral dosage forms. *The AAPS journal*, 10(2), 289-299.

Prakash, A. V., Sivakolundu, K. P., Savage, N. M., Kota, V. K., & Shoukier, M. (2021). Sudden Blast Crisis After Excellent Initial Response in Chronic Myeloid Leukemia. *Cureus*, 13(9).

Prince, M., Knapp, M., Guerchet, M., McCrone, P., Prina, M., Comas-Herrera, A., ... & Rehill, A. (2014). Dementia UK: update. *Alzheimer's Society*.

Puil, L., Liu, J. I. A. X. I. N., Gish, G., Mbamalu, G., Bowtell, D., Pelicci, P. G., ... & Pawson, T. (1994). Bcr-Abl oncoproteins bind directly to activators of the Ras signalling pathway. *The EMBO journal*, 13(4), 764-773.

Qian, H., & Yang, Y. (2009). Alterations of cellular organelles in human liver-derived hepatoma G2 cells induced by adriamycin. *Anti-cancer drugs*, 20(9), 779-786.

Qin, H., Srinivasula, S. M., Wu, G., Fernandes-Alnemri, T., Alnemri, E. S., & Shi, Y. (1999). Structural basis of procaspase-9 recruitment by the apoptotic protease-activating factor 1. *Nature*, 399(6736), 549-557.

Quintás-Cardama, A., Kantarjian, H., Garcia-Manero, G., O'Brien, S., Faderl, S., Estrov, Z., ... & Cortes, J. (2007). Phase I/II study of subcutaneous homoharringtonine in patients with chronic myeloid leukemia who have failed prior therapy. *Cancer*, 109(2), 248-255.

Qu, X., Yu, J., Bhagat, G., Furuya, N., Hibshoosh, H., Troxel, A., ... & Cattoretti, G. (2003). Promotion of tumorigenesis by heterozygous disruption of the beclin 1 autophagy gene. *The Journal of clinical investigation*, 112(12), 1809-1820.

Radhika, N., Minakshi, M., Rajesh, M., Manas, B. R., & Kumar, M. D. (2011). Central nervous system blast crisis in chronic myeloid leukemia on imatinib mesylate therapy: report of two cases. *Indian Journal of Hematology and Blood Transfusion*, 27(1), 51-54.

Rafiei, A., Mian, A. A., Döring, C., Metodieva, A., Oancea, C., Thalheimer, F. B., ... & Ruthardt, M. (2015). The functional interplay between the t (9; 22)-associated fusion proteins BCR/ABL and ABL/BCR in Philadelphia chromosome-positive acute lymphatic leukemia. *PLoS Genet*, 11(4), e1005144.

Ramaker, J. M., Cargill, R. S., Swanson, T. L., Quirindongo, H., Cassar, M., Kretschmar, D., & Copenhaver, P. F. (2016). Amyloid precursor proteins are dynamically trafficked and processed during neuronal development. *Frontiers in molecular neuroscience*, 9, 130.

Rao, R. R., & Kisaalita, W. S. (2002). Biochemical and electrophysiological differentiation profile of a human neuroblastoma (IMR-32) cell line. *In Vitro Cellular & Developmental Biology-Animal*, 38(8), 450-456.

Rissman, R. A., Poon, W. W., Blurton-Jones, M., Oddo, S., Torp, R., Vitek, M. P., ... & Cotman, C. W. (2004). Caspase-cleavage of tau is an early event in Alzheimer disease tangle pathology. *The Journal of clinical investigation*, 114(1), 121-130.

Ristic, B., Bosnjak, M., Arsikin, K., Mircic, A., Suzin-Zivkovic, V., Bogdanovic, A., ... & Trajkovic, V. (2014). Idarubicin induces mTOR-dependent cytotoxic autophagy in leukemic cells. *Experimental cell research*, 326(1), 90-102.

Robert, G., Jacquet, A., & Auberger, P. (2019). Chaperone-mediated autophagy and its emerging role in hematological malignancies. *Cells*, 8(10), 1260.

Robert, V. (2004). BACE1: The beta-Secretase Enzyme in Alzheimer's Disease. *Journal of Molecular Neuroscience*, 23(1-2), 1-2.

Rocchi, A., Yamamoto, S., Ting, T., Fan, Y., Sadleir, K., Wang, Y., ... & He, C. (2017). A *Becl1* mutation mediates hyperactive autophagic sequestration of amyloid oligomers and improved cognition in Alzheimer's disease. *PLoS genetics*, 13(8), e1006962.

Ross, R. A., Spengler, B. A., & Biedler, J. L. (1983). Coordinate morphological and biochemical interconversion of human neuroblastoma cells. *Journal of the National Cancer Institute*, 71(4), 741-747.

Rubinstein, A. D., & Kimchi, A. (2012). Life in the balance—a mechanistic view of the crosstalk between autophagy and apoptosis. *Journal of cell science*, 125(22), 5259-5268.

Rubio, J., Dang, H., Gong, M., Liu, X., Chen, S. L., & Gonzales, G. F. (2007). Aqueous and hydroalcoholic extracts of Black Maca (*Lepidium meyenii*) improve scopolamine-induced memory impairment in mice. *Food and chemical toxicology*, 45(10), 1882-1890.

Runwal, G., Stamatakou, E., Siddiqi, F., Puri, C., Zhu, Y., & Rubinsztein, D. (2019). LC3-positive structures are prominent in autophagy-deficient cells.

Russell, R. C., Tian, Y., Yuan, H., Park, H. W., Chang, Y. Y., Kim, J., ... & Guan, K. L. (2013). ULK1 induces autophagy by phosphorylating Beclin-1 and activating VPS34 lipid kinase. *Nature cell biology*, 15(7), 741-750.

Rzeski, W., Turski, L., & Ikonomidou, C. (2001). Glutamate antagonists limit tumor growth. *Proceedings of the National Academy of Sciences*, 98(11), 6372-6377.

Sacha, T., Hochhaus, A., Hanfstein, B., Müller, M. C., Rudzki, Z., Czopek, J., ... & Skotnicki, A. B. (2003). ABL-kinase domain point mutation as a cause of imatinib (STI571) resistance in CML patient who progress to myeloid blast crisis. *Leukemia research*, 27(12), 1163-1166.

Sadeghi-Aliabadi, H., Minaiyan, M., & Dabestan, A. (2010). Cytotoxic evaluation of doxorubicin in combination with simvastatin against human cancer cells. *Research in pharmaceutical sciences*, 5(2), 127.

Saglio, G., Guerrasio, A., Rosso, C., Zaccaria, A., Tassinari, A., Serra, A., ... & Gavosto, F. (1990). New type of Bcr/Abl junction in Philadelphia chromosome-positive chronic myelogenous leukemia.

Sahay, S., Pannucci, N. L., Mahon, G. M., Rodriguez, P. L., Megjugorac, N. J., Kostenko, E. V., ... & Whitehead, I. P. (2008). The RhoGEF domain of p210 Bcr-Abl activates RhoA and is required for transformation. *Oncogene*, 27(14), 2064-2071.

Sakuma, Y., Matsukuma, S., Nakamura, Y., Yoshihara, M., Koizume, S., Sekiguchi, H., ... & Oguni, S. (2013). Enhanced autophagy is required for survival in EGFR-independent EGFR-mutant lung adenocarcinoma cells. *Laboratory investigation*, 93(10), 1137-1146.

Sales, L. D. O., Mesquita, F. P., PORTILHO, A. J. D. S., De Moraes Filho, M. O., DE MORAES, M. E. A., Montenegro, R. C., & Moreira-Nunes, C. A. (2019). Comparison of BCR-ABL Transcript Variants Between Patients With Chronic Myeloid Leukaemia and Leukaemia Cell Lines. *in vivo*, 33(4), 1119-1124.

Samaddar, J. S., Gaddy, V. T., Duplantier, J., Thandavan, S. P., Shah, M., Smith, M. J., ... & Schoenlein, P. V. (2008). A role for macroautophagy in protection against 4-hydroxytamoxifen-induced cell death and the development of antiestrogen resistance. *Molecular cancer therapeutics*, 7(9), 2977-2987.

Sardi, I., Fantappiè, O., la Marca, G., Giovannini, M. G., Iorio, A. L., da Ros, M., ... & Mazzanti, R. (2014). Delivery of doxorubicin across the blood-brain barrier by ondansetron pretreatment: a study in vitro and in vivo. *Cancer letters*, 353(2), 242-247.

Sarkar, B., Dhiman, M., Mittal, S., & Mantha, A. K. (2017). Curcumin revitalizes Amyloid beta (25-35)-induced and organophosphate pesticides pestered neurotoxicity in SH-SY5Y and IMR-32 cells via activation of APE1 and Nrf2. *Metabolic brain disease*, 32(6), 2045-2061.

Sasaki, K., Strom, S. S., O'Brien, S., Jabbour, E., Ravandi, F., Konopleva, M., ... & Pierce, S. (2015). Relative survival in patients with chronic-phase chronic myeloid leukaemia in the

tyrosine-kinase inhibitor era: analysis of patient data from six prospective clinical trials. *The Lancet Haematology*, 2(5), e186-e193.

Sato, K., Yamanaka, Y., Asakura, Y., & Nedachi, T. (2016). Glutamate levels control HT22 murine hippocampal cell death by regulating biphasic patterns of Erk1/2 activation: role of metabolic glutamate receptor 5. *Bioscience, biotechnology, and biochemistry*, 80(4), 712-718.

Sato, T., Hanada, M., Bodrug, S., Irie, S., Iwama, N., Boise, L. H., ... & Wang, H. G. (1994). Interactions among members of the Bcl-2 protein family analyzed with a yeast two-hybrid system. *Proceedings of the National Academy of Sciences*, 91(20), 9238-9242.

Satpute, S., Shingare, V., & Mehta, M. (2015). PHARMACOTHERAPY OF ALZHEIMER'S DISEASE: A REVIEW. *International Journal of Pharmaceutical Sciences and Research*, 6(12), 5000.

Sattler, M., Salgia, R., Okuda, K., Uemura, N., Durstin, M. A., Pisick, E., ... & Griffin, J. D. (1996). The proto-oncogene product p120CBL and the adaptor proteins CRKL and c-CRK link c-ABL, p190BCR/ABL and p210BCR/ABL to the phosphatidylinositol-3'kinase pathway. *Oncogene*, 12(4), 839-846.

Sawyers, C. L. (1999). Chronic myeloid leukemia. *New England Journal of Medicine*, 340(17), 1330-1340.

Sawyers, C. L., Hochhaus, A., Feldman, E., Goldman, J. M., Miller, C. B., Ottmann, O. G., ... & Druker, B. J. (2002). Imatinib induces hematologic and cytogenetic responses in patients with chronic myelogenous leukemia in myeloid blast crisis: results of a phase II study Presented in part at the 43rd Annual Meeting of The American Society of Hematology, Orlando, FL, December 11, 2001. *Blood*, 99(10), 3530-3539.

Schlereth, T., Birklein, F., Haack, K., Schiffmann, S., Kilbinger, H., Kirkpatrick, C. J., & Wessler, I. (2006). In vivo release of non-neuronal acetylcholine from the human skin as measured by dermal microdialysis: effect of botulinum toxin. *British journal of pharmacology*, 147(2), 183-187.

Schmitz, K. J., Ademi, C., Bertram, S., Schmid, K. W., & Baba, H. A. (2016). Prognostic relevance of autophagy-related markers LC3, p62/sequestosome 1, Beclin-1 and ULK1 in colorectal cancer patients with respect to KRAS mutational status. *World journal of surgical oncology*, 14(1), 1-13.

Schneider, L. S., & Sano, M. (2009). Current Alzheimer's disease clinical trials: Methods and placebo outcomes. *Alzheimer's & Dementia: The Journal of the Alzheimer's Association*, 5(5), 388–397.

Score, J., Calasanz, M. J., Ottman, O., Pane, F., Yeh, R. F., Sobrinho-Simões, M. A., ... & Grand, F. H. (2010). Analysis of genomic breakpoints in p190 and p210 BCR–ABL indicate distinct mechanisms of formation. *Leukemia*, 24(10), 1742-1750.

Seidlitz, E. P., Sharma, M. K., Saikali, Z., Ghert, M., & Singh, G. (2009). Cancer cell lines release glutamate into the extracellular environment. *Clinical & experimental metastasis*, 26(7), 781.

Seifabadi, S., Vaseghi, G., Javanmard, S. H., Omid, E., Tajadini, M., & Zarrin, B. (2017). The cytotoxic effect of memantine and its effect on cytoskeletal proteins expression in metastatic breast cancer cell line. *Iranian journal of basic medical sciences*, 20(1), 41.

Selkoe, D. J. (2001). Alzheimer's Disease: Genes, Proteins, and Therapy. *Physiological reviews*, 81(2), 741-766.

Sevigny, J., Chiao, P., Bussi re, T., Weinreb, P. H., Williams, L., Maier, M., ... & Sandrock, A. (2016). The antibody aducanumab reduces A β plaques in Alzheimer's disease. *Nature*, 537(7618), 50-56.

Shacka, J. J., Klocke, B. J., Shibata, M., Uchiyama, Y., Datta, G., Schmidt, R. E., & Roth, K. A. (2006). Bafilomycin A1 inhibits chloroquine-induced death of cerebellar granule neurons. *Molecular pharmacology*, 69(4), 1125-1136.

Shacka, J. J., Lu, J., Xie, Z. L., Uchiyama, Y., Roth, K. A., & Zhang, J. (2007). Kainic acid induces early and transient autophagic stress in mouse hippocampus. *Neuroscience letters*, 414(1), 57-60.

Shah, N. P., Nicoll, J. M., Nagar, B., Gorre, M. E., Paquette, R. L., Kuriyan, J., & Sawyers, C. L. (2002). Multiple BCR-ABL kinase domain mutations confer polyclonal resistance to the tyrosine kinase inhibitor imatinib (STI571) in chronic phase and blast crisis chronic myeloid leukemia. *Cancer cell*, 2(2), 117-125.

Sharifipour, M., Izadpanah, E., Nikkhoo, B., Zare, S., Abdolmaleki, A., Hassanzadeh, K., ... & Hassanzadeh, K. (2014). A new pharmacological role for donepezil: attenuation of morphine-induced tolerance and apoptosis in rat central nervous system. *Journal of biomedical science*, 21(1), 6.

Shaw, G., Morse, S., Ararat, M., & Graham, F. L. (2002). Preferential transformation of human neuronal cells by human adenoviruses and the origin of HEK 293 cells. *The FASEB journal*, 16(8), 869-871.

Shen, C., Gu, M., Song, C., Miao, L., Hu, L., Liang, D., & Zheng, C. (2008). The tumorigenicity diversification in human embryonic kidney 293 cell line cultured in vitro. *Biologicals*, 36(4), 263-268.

Sherrington, R., Froelich, S., Sorbi, S., Campion, D., Chi, H., Rogaeva, E. A., ... & Ikeda, M. (1996). Alzheimer's disease associated with mutations in presenilin 2 is rare and variably penetrant. *Human molecular genetics*, 5(7), 985-988.

Shamas-Din, A., Kale, J., Leber, B., & Andrews, D. W. (2013). Mechanisms of action of Bcl-2 family proteins. *Cold Spring Harbor perspectives in biology*, 5(4), a008714.

Shi, C., Wu, F., Xu, J., & Zou, J. (2011). Bilobalide regulates soluble amyloid precursor protein release via phosphatidyl inositol 3 kinase-dependent pathway. *Neurochemistry international*, 59(1), 59-64.

Shimizu, S., Kanaseki, T., Mizushima, N., Mizuta, T., Arakawa-Kobayashi, S., Thompson, C. B., & Tsujimoto, Y. (2004). Role of Bcl-2 family proteins in a non-apoptotic programmed cell death dependent on autophagy genes. *Nature cell biology*, 6(12), 1221-1228.

Shi, Y., Su, X., Cui, H., Yu, L., Du, H., & Han, Y. (2019). Combination of quercetin and Adriamycin effectively suppresses the growth of refractory acute leukemia. *Oncology letters*, 18(1), 153-160.

Sillaber, C., Gesbert, F., Frank, D. A., Sattler, M., & Griffin, J. D. (2000). STAT5 activation contributes to growth and viability in Bcr/Abl-transformed cells. *Blood, The Journal of the American Society of Hematology*, 95(6), 2118-2125.

Sishi, B. J., Loos, B., van Rooyen, J., & Engelbrecht, A. M. (2013). Autophagy upregulation promotes survival and attenuates doxorubicin-induced cardiotoxicity. *Biochemical pharmacology*, 85(1), 124-134.

Sloane, P. D., Zimmerman, S., Suchindran, C., Reed, P., Wang, L., Boustani, M., & Sudha, S. (2002). The public health impact of Alzheimer's disease, 2000–2050: potential implication of treatment advances. *Annual review of public health*, 23(1), 213-231.

Slupianek, A., Schmutte, C., Tomblin, G., Nieborowska-Skorska, M., Hoser, G., Nowicki, M. O., ... & Skorski, T. (2001). BCR/ABL regulates mammalian RecA homologs, resulting in drug resistance. *Molecular cell*, 8(4), 795-806.

Smith, K. M., Yacobi, R., & Van Etten, R. A. (2003). Autoinhibition of Bcr-Abl through its SH3 domain. *Molecular cell*, 12(1), 27-37.

Song, C., Han, Y., Luo, H., Qin, Z., Chen, Z., Liu, Y., ... & Zhou, C. (2019). HOXA10 induces BCL2 expression, inhibits apoptosis, and promotes cell proliferation in gastric cancer. *Cancer Medicine*, 8(12), 5651-5661.

Song, G., Li, Y., Lin, L., & Cao, Y. (2015). Anti-autophagic and anti-apoptotic effects of memantine in a SH-SY5Y cell model of Alzheimer's disease via mammalian target of rapamycin-dependent and-independent pathways. *Molecular medicine reports*, 12(5), 7615-7622.

Song, P., Sekhon, H. S., Jia, Y., Keller, J. A., Blusztajn, J. K., Mark, G. P., & Spindel, E. R. (2003). Acetylcholine is synthesized by and acts as an autocrine growth factor for small cell lung carcinoma. *Cancer research*, 63(1), 214-221.

Song, X., Lee, D. H., Dilly, A. K., Lee, Y. S., Choudry, H. A., Kwon, Y. T., ... & Lee, Y. J. (2018). Crosstalk between apoptosis and autophagy is regulated by the arginylated BiP/Beclin-1/p62 complex. *Molecular Cancer Research*, 16(7), 1077-1091.

Sonneveld, P., Mulder, J. A., & Van Bekkum, D. W. (1981). Cytotoxicity of doxorubicin for normal hematopoietic and acute myeloid leukemia cells of the rat. *Cancer chemotherapy and pharmacology*, 5(3), 167-173.

Soverini, S., Martinelli, G., Rosti, G., Bassi, S., Amabile, M., Poerio, A., ... & Luatti, S. (2005). ABL mutations in late chronic phase chronic myeloid leukemia patients with up-front cytogenetic resistance to imatinib are associated with a greater likelihood of progression to blast crisis and shorter survival: a study by the GIMEMA Working Party on Chronic Myeloid Leukemia. *Journal of clinical oncology*, 23(18), 4100-4109.

Srdic-Rajic, T., Tisma-Miletic, N., Cavic, M., Kanjer, K., Savikin, K., Galun, D., ... & Zoranovic, T. (2016). Sensitization of K562 leukemia cells to doxorubicin by the *Viscum album* extract. *Phytotherapy Research*, 30(3), 485-495.

Stagno, F., Stella, S., Berretta, S., Massimino, M., Antolino, A., Giustolisi, R., ... & Vigneri, P. (2007). Sequential mutations causing resistance to both Imatinib Mesylate and Dasatinib in a chronic myeloid leukaemia patient progressing to lymphoid blast crisis. *Leukemia research*, 32(4), 673-674.

Sukumaran, P., Nascimento Da Conceicao, V., Sun, Y., Ahamad, N., Saraiva, L. R., Selvaraj, S., & Singh, B. B. (2021). Calcium signaling regulates autophagy and apoptosis. *Cells*, 10(8), 2125.

Stone, R. M. (2004). Optimizing treatment of chronic myeloid leukemia: a rational approach. *The oncologist*, 9(3), 259-270.

Strong, L. M., Chang, C., Riley, J. F., Boecker, C. A., Flower, T. G., Buffalo, C. Z., ... & Hurley, J. H. (2021). Structural basis for membrane recruitment of ATG16L1 by WIPI2 in autophagy. *Elife*, 10, e70372.

Su, J. H., Zhao, M., Anderson, A. J., Srinivasan, A., & Cotman, C. W. (2001). Activated caspase-3 expression in Alzheimer's and aged control brain: correlation with Alzheimer pathology. *Brain research*, 898(2), 350-357.

Sumimoto, H., Tsujimura, H., Ise, M., Mimura, N., Sakai, C., Takagi, T., & Kumagai, K. (2010). Blast phase of chronic myeloid leukemia presenting lymphoid phenotype with a chronic phase of extremely short duration. *Internal Medicine*, 49(13), 1297-1301.

Sung, H., Ferlay, J., Siegel, R. L., Laversanne, M., Soerjomataram, I., Jemal, A., & Bray, F. (2021). Global cancer statistics 2020: GLOBOCAN estimates of incidence and mortality worldwide for 36 cancers in 185 countries. *CA: a cancer journal for clinicians*, 71(3), 209-249.

Sun, X., Chen, W. D., & Wang, Y. D. (2015). β -Amyloid: the key peptide in the pathogenesis of Alzheimer's disease. *Frontiers in pharmacology*, 6, 221.

Swain, S. M., Whaley, F. S., Gerber, M. C., Ewer, M. S., Bianchine, J. R., & Gams, R. A. (1997). Delayed administration of dexrazoxane provides cardioprotection for patients with advanced breast cancer treated with doxorubicin-containing therapy. *Journal of clinical oncology*, 15(4), 1333-1340.

Synowiec, E., Hoser, G., Bialkowska-Warzecha, J., Pawlowska, E., Skorski, T., & Blasiak, J. (2015). Doxorubicin differentially induces apoptosis, expression of mitochondrial apoptosis-related genes, and mitochondrial potential in BCR-ABL1-expressing cells sensitive and resistant to imatinib. *BioMed research international*, 2015.

Tadwalkar, S. (2017). The global incidence and prevalence of chronic myeloid leukemia over the next ten years (2017–2027). In *Abstr. International Conference on Hematology and Oncology*, Bangkok, June.

Takayama, N., Sato, N., O'Brien, S. G., Ikeda, Y., & Okamoto, S. I. (2002). Imatinib mesylate has limited activity against the central nervous system involvement of Philadelphia chromosome-positive acute lymphoblastic leukaemia due to poor penetration into cerebrospinal fluid. *British journal of haematology*, 119(1), 106-108.

Talpaz, M., Silver, R. T., Druker, B. J., Goldman, J. M., Gambacorti-Passerini, C., Guilhot, F., ... & Sawyers, C. L. (2002). Imatinib induces durable hematologic and cytogenetic responses in patients with accelerated phase chronic myeloid leukemia: results of a phase 2 study. *Blood, The Journal of the American Society of Hematology*, 99(6), 1928-1937.

Talukdar, R., Sareen, A., Zhu, H., Yuan, Z., Dixit, A., Cheema, H., ... & Saluja, A. K. (2016). Release of cathepsin B in cytosol causes cell death in acute pancreatitis. *Gastroenterology*, 151(4), 747-758.

Tang, J. M., Yuan, J., Li, Q., Wang, J. N., Kong, X., Zheng, F., ... & Chen, S. Y. (2012). Acetylcholine induces mesenchymal stem cell migration via Ca²⁺/PKC/ERK1/2 signal pathway. *Journal of cellular biochemistry*, 113(8), 2704-2713.

Tanner, E. A., Blute, T. A., Brachmann, C. B., & McCall, K. (2011). Bcl-2 proteins and autophagy regulate mitochondrial dynamics during programmed cell death in the *Drosophila* ovary. *Development*, 138(2), 327-338.

Tanzi, R. E., & Bertram, L. (2005). Twenty years of the Alzheimer's disease amyloid hypothesis: a genetic perspective. *Cell*, 120(4), 545-555.

The Guardian (2021). FDA approves first new Alzheimer's drug in almost 20 years. Retrieved 10 June 2021, from <https://www.theguardian.com/society/2021/jun/07/fda-announce-decision-new-alzheimers-drug-aducanumab>

The Surveillance, Epidemiology, and End Results (SEER) Program (2019). Cancer Stat Facts: Cancer of Any Site. National Cancer Institute (NCI). Bethesda, MD, Retrieved 20 October 2021, from <https://seer.cancer.gov/statfacts/html/all.html>

Thiele, J., Kvasnicka, H. M., Schmitt-Graeff, A., Bundschuh, S., Biermann, T., Roessler, G., ... & Schaefer, H. E. (2000). Effects of chemotherapy (busulfan-hydroxyurea) and interferon-alfa on bone marrow morphologic features in chronic myelogenous leukemia: histochemical and morphometric study on sequential trephine biopsy specimens with special emphasis on dynamic features. *American journal of clinical pathology*, 114(1), 57-65.

Thinakaran, G., & Koo, E. H. (2008). Amyloid precursor protein trafficking, processing, and function. *Journal of Biological Chemistry*, 283(44), 29615-29619.

Thomas, P., & Smart, T. G. (2005). HEK293 cell line: a vehicle for the expression of recombinant proteins. *Journal of pharmacological and toxicological methods*, 51(3), 187-200.

Tinklenberg, J. R., Kraemer, H. C., Yaffe, K., Ross, L., Sheikh, J., Ashford, J. W., ... & Taylor, J. L. (2007). Donepezil treatment and Alzheimer disease: can the results of randomized clinical trials be applied to Alzheimer disease patients in clinical practice?. *The American Journal of Geriatric Psychiatry*, 15(11), 953-960.

Tomlinson, B. E., Blessed, G., & Roth, M. (1970). Observations on the brains of demented old people. *Journal of the neurological sciences*, 11(3), 205-242.

Tong, Y., You, L., Liu, H., Li, L., Meng, H., Qian, Q., & Qian, W. (2013). Potent antitumor activity of oncolytic adenovirus expressing Beclin-1 via induction of autophagic cell death in leukemia. *Oncotarget*, 4(6), 860.

Townsend, P. A., Kozhevnikova, M. V., Cexus, O. N., Zamyatnin, A. A., & Soond, S. M. (2021). BH3-mimetics: recent developments in cancer therapy. *Journal of Experimental & Clinical Cancer Research*, 40(1), 1-33.

Trauzold, A., Schmiedel, S., Röder, C., Tams, C., Christgen, M., Oestern, S., ... & Kalthoff, H. (2003). Multiple and synergistic deregulations of apoptosis-controlling genes in pancreatic carcinoma cells. *British journal of cancer*, 89(9), 1714-1721.

Trialists, C. M. L. (1997). Collaborative Group. Interferon alfa versus chemotherapy for chronic myeloid leukemia: a meta-analysis of seven randomized trials. *J Natl Cancer Inst*, 89(1616), 20.

Ueno, M., Kakinuma, Y., Yuhki, K. I., Murakoshi, N., Iemitsu, M., Miyauchi, T., & Yamaguchi, I. (2006). Doxorubicin induces apoptosis by activation of caspase-3 in cultured cardiomyocytes in vitro and rat cardiac ventricles in vivo. *Journal of pharmacological sciences*, 0606090013-0606090013.

U.S. Food and Drug Administration (FDA) (2021). FDA's Decision to Approve New Treatment for Alzheimer's Disease. [online] Available at: <https://www.fda.gov/drugs/news-events-human-drugs/fdas-decision-approve-new-treatment-alzheimers-disease> [Accessed 7 June 2021].

U.S. Food and Drug Administration (FDA) (2018). FDA requires multiple new safety measures for leukemia drug Iclusig. (2021). Retrieved 21 November 2021, from <https://www.fda.gov/drugs/drug-safety-and-availability/fda-drug-safety-communication-fda-requires-multiple-new-safety-measures-leukemia-drug-iclusig>

Valderas, J. M., Starfield, B., Sibbald, B., Salisbury, C., & Roland, M. (2009). Defining comorbidity: implications for understanding health and health services. *The Annals of Family Medicine*, 7(4), 357-363.

Vallejos, C. S., Trujillo, J. M., Cork, A., Bodey, G. P., McCredie, K. B., & Freireich, E. J. (1974). Blastic crisis in chronic granulocytic leukemia: Experience in 39 patients. *Cancer*, 34(5), 1806-1812.

Van Rhee, F., Szydlo, R. M., Hermans, J., Devergie, A., Frassoni, F., Arcese, W., ... & Gratwohl, A. (1997). Long-term results after allogeneic bone marrow transplantation for chronic myelogenous leukemia in chronic phase: a report from the Chronic Leukemia Working Party of the European Group for Blood and Marrow Transplantation. *Bone marrow transplantation*, 20(7), 553-560.

Vara-Ciruelos, D., Russell, F. M., & Hardie, D. G. (2019). The strange case of AMPK and cancer: Dr Jekyll or Mr Hyde?. *Open biology*, 9(7), 190099.

Verma, A. K., Bharti, P. S., Rafat, S., Bhatt, D., Goyal, Y., Pandey, K. K., ... & Dev, K. (2021). Autophagy paradox of cancer: Role, regulation, and duality. *Oxidative Medicine and Cellular Longevity*, 2021.

Verrma, S. P., Dutta, T. K., Vinod, K. V., Dubashi, B., & Ariga, K. K. (2014). Philadelphia chromosome positive pre-T cell acute lymphoblastic leukemia: a rare case report and short review. *Indian Journal of Hematology and Blood Transfusion*, 30(1), 177-179.

Verschoor, A. J., Litière, S., Marréaud, S., Judson, I., Toulmonde, M., Wardelmann, E., ... & Gelderblom, H. (2020). Survival of soft tissue sarcoma patients after completing six cycles of first-line anthracycline containing treatment: an EORTC-STBSG database study. *Clinical sarcoma research*, 10(1), 1-9.

Von Bubnoff, N., Manley, P. W., Mestan, J., Sanger, J., Peschel, C., & Duyster, J. (2006). Bcr-Abl resistance screening predicts a limited spectrum of point mutations to be associated with clinical resistance to the Abl kinase inhibitor nilotinib (AMN107). *Blood*, 108(4), 1328-1333.

Vu, M., Kassouf, N., Ofili, R., Lund, T., Bell, C., & Appiah, S. (2020). Doxorubicin selectively induces apoptosis through the inhibition of a novel isoform of Bcl-2 in acute myeloid leukaemia MOLM-13 cells with reduced Beclin 1 expression. *International Journal of Oncology*, 57(1), 113-121.

Wang, F., Chen, J., Zhang, Z., Yi, J., Yuan, M., Wang, M., ... & Wang, L. (2017). Differences of basic and induced autophagic activity between K562 and K562/ADM cells. *Intractable & rare diseases research*, 6(4), 281-290.

Wang, J. Z., Xia, Y. Y., Grundke-Iqbal, I., & Iqbal, K. (2013). Abnormal hyperphosphorylation of tau: sites, regulation, and molecular mechanism of neurofibrillary degeneration. *Journal of Alzheimer's Disease*, 33(s1), S123-S139.

Wang, S., Konorev, E. A., Kotamraju, S., Joseph, J., Kalivendi, S., & Kalyanaraman, B. (2004). Doxorubicin induces apoptosis in normal and tumor cells via distinctly different mechanisms intermediacy of H₂O₂-and p53-dependent pathways. *Journal of Biological Chemistry*, 279(24), 25535-25543.

Wang, X., Wang, X. L., Chen, H. L., Wu, D., Chen, J. X., Wang, X. X., ... & Wei, Y. Q. (2014). Ghrelin inhibits doxorubicin cardiotoxicity by inhibiting excessive autophagy through AMPK and p38-MAPK. *Biochemical pharmacology*, 88(3), 334-350.

Wang, Y., & Mandelkow, E. (2016). Tau in physiology and pathology. *Nature reviews neuroscience*, 17(1), 22-35.

Wang, Y., Wei, S., Wang, J., Fang, Q., & Chai, Q. (2014). Phenethyl isothiocyanate inhibits growth of human chronic myeloid leukemia K562 cells via reactive oxygen species generation and caspases. *Molecular medicine reports*, 10(1), 543-549.

Wang, Z., Xu, F., Yuan, N., Niu, Y., Lin, W., Cao, Y., ... & Zhao, W. (2014). Rapamycin inhibits pre-B acute lymphoblastic leukemia cells by downregulating DNA and RNA polymerases. *Leukemia research*, 38(8), 940-947.

Watt, P. M., & Hickson, I. D. (1994). Structure and function of type II DNA topoisomerases. *Biochemical Journal*, 303(Pt 3), 681.

Weingarten, M. D., Lockwood, A. H., Hwo, S. Y., & Kirschner, M. W. (1975). A protein factor essential for microtubule assembly. *Proceedings of the National Academy of Sciences*, 72(5), 1858-1862.

Wenkstetten-Holub, A., Fangmeyer-Binder, M., & Fasching, P. (2021). Prevalence of comorbidities in elderly cancer patients. *memo-Magazine of European Medical Oncology*, 14(1), 15-19.

Westerink, R. H. S., & Ewing, A. G. (2008). The PC12 cell as model for neurosecretion. *Acta Physiologica*, 192(2), 273-285

White, C., Li, C., Yang, J., Petrenko, N. B., Madesh, M., Thompson, C. B., & Foskett, J. K. (2005). The endoplasmic reticulum gateway to apoptosis by Bcl-XL modulation of the InsP3R. *Nature cell biology*, 7(10), 1021-1028.

Wittenberg, R., Hu, B., Barraza-Araiza, L., & Rehill, A. (2020). Projections of older people with dementia and costs of dementia care in the United Kingdom, 2019–2040. Retrieved 13 April 2020, from https://www.alzheimers.org.uk/sites/default/files/2019-11/cpec_report_november_2019.pdf

Wolff, N. C., Richardson, J. A., Egorin, M., & Ilaria Jr, R. L. (2003). The CNS is a sanctuary for leukemic cells in mice receiving imatinib mesylate for Bcr/Abl-induced leukemia. *Blood*, 101(12), 5010-5013.

Won, K. Y., Kim, G. Y., Kim, Y. W., Song, J. Y., & Lim, S. J. (2010). Clinicopathologic correlation of beclin-1 and bcl-2 expression in human breast cancer. *Human pathology*, 41(1), 107-112.

World Health Organisation (WHO) (2022). Ageing and health. (2022). Retrieved 25 February 2022, from <https://www.who.int/news-room/fact-sheets/detail/ageing-and-health>

World Health Organisation (WHO) (2021). Dementia. Retrieved 25 November 2021, from <https://www.who.int/news-room/fact-sheets/detail/dementia>

Wu, D. H., Jia, C. C., Chen, J., Lin, Z. X., Ruan, D. Y., Li, X., ... & Chen, Z. H. (2014). Autophagic LC3B overexpression correlates with malignant progression and predicts a poor prognosis in hepatocellular carcinoma. *Tumor Biology*, 35(12), 12225-12233.

Wuilleme-Toumi, S., Robillard, N., Gomez, P., Moreau, P., Le Gouill, S., Avet-Loiseau, H., ... & Bataille, R. (2005). Mcl-1 is overexpressed in multiple myeloma and associated with relapse and shorter survival. *Leukemia*, 19(7), 1248-1252.

Wunderlich, M., Mizukawa, B., Chou, F. S., Sexton, C., Shrestha, M., Sauntharajah, Y., & Mulloy, J. C. (2013). AML cells are differentially sensitive to chemotherapy treatment in a human xenograft model. *Blood, The Journal of the American Society of Hematology*, 121(12), e90-e97.

Xu, H. D., & Qin, Z. H. (2019). Beclin 1, Bcl-2 and autophagy. *Autophagy: Biology and Diseases*, 109-126.

Xu, X., Chen, K., Kobayashi, S., Timm, D., & Liang, Q. (2012). Resveratrol attenuates doxorubicin-induced cardiomyocyte death via inhibition of p70 S6 kinase 1-mediated autophagy. *Journal of pharmacology and experimental therapeutics*, 341(1), 183-195.

Yang, X., & Qian, K. (2017). Protein O-GlcNAcylation: emerging mechanisms and functions. *Nature reviews Molecular cell biology*, 18(7), 452-465.

Yang, Y. H., Li, D. L., Bi, X. Y., Sun, L., Yu, X. J., Fang, H. L., ... & Zang, W. J. (2015). Acetylcholine inhibits LPS-induced MMP-9 production and cell migration via the $\alpha 7$ nAChR-JAK2/STAT3 pathway in RAW264. 7 cells. *Cellular Physiology and Biochemistry*, 36(5), 2025-2038.

Yazdankhah, M., Farioli-Vecchioli, S., Tonchev, A. B., Stoykova, A., & Cecconi, F. (2014). The autophagy regulators Ambra1 and Beclin 1 are required for adult neurogenesis in the brain subventricular zone. *Cell death & disease*, 5(9), e1403-e1403.

Ye, Z. C., & Sontheimer, H. (1999). Glioma cells release excitotoxic concentrations of glutamate. *Cancer research*, 59(17), 4383-4391.

Yiannopoulou, K. G., & Papageorgiou, S. G. (2013). Current and future treatments for Alzheimer's disease. *Therapeutic advances in neurological disorders*, 6(1), 19-33.

Yi, M., Zhang, L., Liu, Y., Livingston, M. J., Chen, J. K., Nahman Jr, N. S., ... & Dong, Z. (2017). Autophagy is activated to protect against podocyte injury in adriamycin-induced nephropathy. *American Journal of Physiology-Renal Physiology*, 313(1), F74-F84

Yin, S., Wang, R., Zhou, F., Zhang, H., & Jing, Y. (2011). Bcl-xL is a dominant antiapoptotic protein that inhibits homoharringtonine-induced apoptosis in leukemia cells. *Molecular pharmacology*, 79(6), 1072-1083.

Yonekawa, T., & Thorburn, A. (2013). Autophagy and cell death. *Essays in biochemistry*, 55, 105.

Yoon, W. S., Yeom, M. Y., Kang, E. S., Chung, Y. A., Chung, D. S., & Jeun, S. S. (2017). Memantine induces NMDAR1-mediated autophagic cell death in malignant glioma cells. *Journal of Korean Neurosurgical Society*, 60(2), 130.

Yoon, Y. H., Cho, K. S., Hwang, J. J., Lee, S. J., Choi, J. A., & Koh, J. Y. (2010). Induction of lysosomal dilatation, arrested autophagy, and cell death by chloroquine in cultured ARPE-19 cells. *Investigative ophthalmology & visual science*, 51(11), 6030-6037.

Yu, C., Gorantla, S. P., Müller-Rudorf, A., Müller, T. A., Kreutmair, S., Albers, C., ... & Follo, M. (2020). Phosphorylation of Beclin-1 by BCR-ABL suppresses autophagy in chronic myeloid leukemia. *haematologica*, 105(5), 1285-1293.

Yung, L. Y., Lam, W. S., Ho, M. K., Hu, Y., Ip, F. C., Pang, H., ... & Wong, Y. H. (2012). Astragaloside IV and cycloastragenol stimulate the phosphorylation of extracellular signal-regulated protein kinase in multiple cell types. *Planta medica*, 78(02), 115-121.

Yu, R., Shtil, A. A., Tan, T. H., Roninson, I. B., & Kong, A. N. T. (1996). Adriamycin activates c-jun N-terminal kinase in human leukemia cells: a relevance to apoptosis. *Cancer letters*, 107(1), 73-81.

Yu, Y., Yang, L., Zhao, M., Zhu, S., Kang, R., Vernon, P., ... & Cao, L. (2012). Targeting microRNA-30a-mediated autophagy enhances imatinib activity against human chronic myeloid leukemia cells. *Leukemia*, 26(8), 1752-1760.

Zare-shahabadi, A., Masliah, E., Johnson, G. V., & Rezaei, N. (2015). Autophagy in Alzheimer's disease. *Reviews in the neurosciences*, 26(4), 385-395.

Zaretsky, J. Z., & Wreschner, D. H. (2008). Protein multifunctionality: principles and mechanisms. *Translational oncogenomics*, 3, 99.

Zhang, J., Wang, J. C., Han, Y. H., Ji, S. P., Liu, S. X., Liu, X. P., & Yao, L. B. (2005). High expression of bcl-xL in K562 cells and its role in the low sensitivity of K562 to realgar-induced apoptosis. *Acta haematologica*, 113(4), 247-254.

Zhang, L. J., Gan, Y. M., & Yu, L. (2015). Occurrence of BCR/ABL fusion gene in a patient with acute promyelocytic leukemia. *Medical Oncology*, 32(1), 382.

Zhang, L., Ming, L., & Yu, J. (2007). BH3 mimetics to improve cancer therapy; mechanisms and examples. *Drug Resistance Updates*, 10(6), 207-217.

Zhao, D., Yuan, H., Yi, F., Meng, C., & Zhu, Q. (2014). Autophagy prevents doxorubicin-induced apoptosis in osteosarcoma. *Molecular medicine reports*, 9(5), 1975-1981.

Zhao, L., & Zhang, B. (2017). Doxorubicin induces cardiotoxicity through upregulation of death receptors mediated apoptosis in cardiomyocytes. *Scientific reports*, 7(1), 1-11.

Zhao, Y., Bhattacharjee, S., Jones, B. M., Dua, P., Alexandrov, P. N., Hill, J. M., & Lukiw, W. J. (2013). Regulation of TREM2 expression by an NF- κ B-sensitive miRNA-34a. *Neuroreport*, 24(6), 318.

Zheng, H., & Koo, E. H. (2011). Biology and pathophysiology of the amyloid precursor protein. *Molecular neurodegeneration*, 6(1), 27.

Zhou, A., Wu, H., Pan, J., Wang, X., Li, J., Wu, Z., & Hui, A. (2015). Synthesis and evaluation of paeonol derivatives as potential multifunctional agents for the treatment of Alzheimer's disease. *Molecules*, 20(1), 1304-1318.

Zhou, Y., Chen, E., Tang, Y., Mao, J., Shen, J., Zheng, X., ... & Zhi, X. (2019). miR-223 overexpression inhibits doxorubicin-induced autophagy by targeting FOXO3a and reverses chemoresistance in hepatocellular carcinoma cells. *Cell death & disease*, 10(11), 1-13.

Zhu, F., Wu, F., Ma, Y., Liu, G., Li, Z., Sun, Y. A., & Pei, Z. (2011). Decrease in the production of beta-amyloid by berberine inhibition of the expression of beta-secretase in HEK293 cells. *BMC neuroscience*, 12(1), 125.

Appendices

Appendix I: Statistical analyses for the viability of K-562 and HEK293T cells using CyQUANT® Direct assay

A) Media vs 0.05% DMSO at 0, 24, 48 and 72 h (HEK293T cells)

Protein Sample	N	Mean	StDev	SE Mean	T-Value	DF	P-Value
0 h HEK Media	3	100.017	0.323	0.19	0.40	4	0.707
0 h HEK DMSO	3	99.67	1.47	0.85			
24 h HEK Media	3	92.48	2.15	1.2	-1.02	4	0.365
24 h HEK DMSO	3	94.61	2.9	1.7			
48 h HEK Media	3	94.1	12.7	7.3	0.21	4	0.84
48 h HEK DMSO	3	92.16	9.64	5.6			
72 h HEK Media	3	116.3	12.4	7.2	0.46	4	0.669
72 h HEK DMSO	3	112.19	9.09	5.3			

B) Media vs 0.05% DMSO at 24, 48 and 72 h (K-562 cells)

Protein Sample	N	Mean	StDev	SE Mean	T-Value	DF	P-Value
0 h K-562 Media	3	100.284	0.736	0.43	0.15	4	0.888
0 h K-562 DMSO	3	100.00	3.18	1.8			
24 h K-562 Media	3	95.47	1.44	0.83	0.78	4	0.479
24 h K-562 DMSO	3	94.24	2.32	1.3			
48 h K-562 Media	3	98.54	1.95	1.1	0.37	4	0.731
48 h K-562 DMSO	3	97.45	4.74	2.7			
72 h K-562 Media	3	106.68	3.30	1.9	-0.67	4	0.537
72 h K-562 DMSO	3	109.26	5.73	3.3			

C) K-562 and HEK293T (Control vs cells incubated for 24, 48 and 72 h)

Protein Sample	N	Mean	StDev	SE Mean	T-Value	DF	P-Value
0 h HEK Media	3	100.017	0.323	0.19	5.46	4	0.005
24 h HEK Media	3	92.67	2.31	1.3			
0 h HEK Media	3	100.017	0.323	0.19	0.81	4	0.465
48 h HEK Media	3	94.1	12.7	7.3			
0 h HEK Media	3	100.017	0.323	0.19	-2.28	4	0.085
72 h HEK Media	3	116.3	12.3	7.1			
0 h HEK DMSO	3	99.67	1.47	0.85	2.55	4	0.063
24 h HEK DMSO	3	94.67	3.06	1.8			
0 h HEK DMSO	3	99.67	1.47	0.85	1.35	4	0.249
48 h HEK DMSO	3	92.12	9.60	5.5			
0 h HEK DMSO	3	99.67	1.47	0.85	-2.36	4	0.078
72 h HEK DMSO	3	112.26	9.12	5.3			
0 h K-562 Media	3	100.284	0.736	0.43	5.16	4	0.007
24 h K-562 Media	3	95.47	1.44	0.83			

0 h K-562 Media	3	100.284	0.736	0.43	1.45	4	0.220
48 h K-562 Media	3	98.54	1.95	1.1			
0 h K-562 Media	3	100.284	0.736	0.43	-3.27	4	0.031
72 h K-562 Media	3	106.68	3.30	1.9			
0 h K-562 DMSO	3	100.00	3.18	1.8	2.54	4	0.064
24 h K-562 DMSO	3	94.24	2.32	1.3			
0 h K-562 DMSO	3	100.00	3.18	1.8	0.77	4	0.483
48 h K-562 DMSO	3	97.45	4.74	2.7			
0 h K-562 DMSO	3	100.00	3.18	1.8	-2.45	4	0.071
72 h K-562 DMSO	3	109.26	5.73	3.3			

D) Dox vs control and the various concentration of Dox treatments at 24 and 48 h

Tukey Simultaneous Tests for Differences of Means					
Difference of Levels	Difference of Means	SE of Difference	95% CI	T-Value	Adjusted P-Value
DX1 H24 - Ctrl H24	-54.83	4.52	(-68.46, -41.21)	-12.12	0
DX5 H24 - Ctrl H24	-76.17	4.52	(-89.79, -62.54)	-16.84	0
DX10 H24 - Ctrl H24	-84.5	4.52	(-98.12, -70.88)	-18.68	0
DX5 H24 - DX1 H24	-21.33	5.22	(-37.06, -5.60)	-4.09	0.008
DX10 H24 - DX1 H24	-29.67	5.22	(-45.40, -13.94)	-5.68	0.001
DX10 H24 - DX5 H24	-8.33	5.22	(-24.06, 7.40)	-1.6	0.42
Individual confidence level = 98.82%					

Tukey Simultaneous Tests for Differences of Means					
Difference of Levels	Difference of Means	SE of Difference	95% CI	T-Value	Adjusted P-Value
DX1 H48 - Ctrl H48	-63.6	5.44	(-79.75, -47.46)	-11.7	0
DX5 H48 - Ctrl H48	-88.45	5.44	(-104.59, -72.30)	-16.27	0
DX10 H48 - Ctrl H48	-93.05	5.44	(-109.19, -76.90)	-17.11	0
DX5 H48 - DX1 H48	-24.84	6.43	(-43.95, -5.74)	-3.86	0.011
DX10 H48 - DX1 H48	-29.44	6.43	(-48.55, -10.34)	-4.58	0.003
DX10 H48 - DX5 H48	-4.6	6.43	(-23.70, 14.50)	-0.72	0.889
Individual confidence level = 98.83%					

E) Memantine vs control and the various concentration (1, 5, 10 μ M) of Memantine treatments at 24 and 48 h

Tukey Simultaneous Tests for Differences of Means					
Difference of Levels	Difference of Means	SE of Difference	95% CI	T-Value	Adjusted P-Value
M1 H24 - Ctrl H24	40.2	11.2	(6.5, 73.8)	3.59	0.019
M5 H24 - Ctrl H24	10.8	11.2	(-22.8, 44.5)	0.97	0.769
M10 H24 - Ctrl H24	7.5	11.2	(-26.2, 41.2)	0.67	0.906
M5 H24 - M1 H24	-29.3	12.9	(-68.2, 9.5)	-2.27	0.164

M10 H24 - M1 H24	-32.7	12.9	(-71.5, 6.2)	-2.53	0.109
M10 H24 - M5 H24	-3.3	12.9	(-42.2, 35.5)	-0.26	0.994
Individual confidence level = 98.82%					

Tukey Simultaneous Tests for Differences of Means					
Difference of Levels	Difference of Means	SE of Difference	95% CI	T-Value	Adjusted P-Value
M1 H48 - Ctrl H48	20.69	8.69	(-5.11, 46.48)	2.38	0.134
M5 H48 - Ctrl H48	2.92	8.69	(-22.88, 28.72)	0.34	0.986
M10 H48 - Ctrl H48	2.79	8.69	(-23.01, 28.58)	0.32	0.988
M5 H48 - M1 H48	-17.8	10.3	(-48.3, 12.8)	-1.73	0.352
M10 H48 - M1 H48	-17.9	10.3	(-48.4, 12.6)	-1.74	0.346
M10 H48 - M5 H48	-0.1	10.3	(-30.7, 30.4)	-0.01	1
Individual confidence level = 98.83%					

F) Donepezil vs control and the various concentration of Donepezil treatments (1, 5, 10 μ M) at 24 and 48 h

Tukey Simultaneous Tests for Differences of Means					
Difference of Levels	Difference of Means	SE of Difference	95% CI	T-Value	Adjusted P-Value
DP1 H24 - Ctrl H24	-48.8	28	(-133.1, 35.4)	-1.75	0.004
DP5 H24 - Ctrl H24	-19.8	28	(-104.1, 64.4)	-0.71	0.891
DP10 H24 - Ctrl H24	-11.2	28	(-95.4, 73.1)	-0.4	0.977
DP5 H24 - DP1 H24	29	32.3	(-68.3, 126.3)	0.9	0.806
DP10 H24 - DP1 H24	37.7	32.3	(-59.6, 135.0)	1.17	0.659
DP10 H24 - DP5 H24	8.7	32.3	(-88.6, 106.0)	0.27	0.993
Individual confidence level = 98.82%					

Tukey Simultaneous Tests for Differences of Means					
Difference of Levels	Difference of Means	SE of Difference	95% CI	T-Value	Adjusted P-Value
DP1 H48 - Ctrl H48	-43.45	8.47	(-68.59, -18.30)	-5.13	0.001
DP5 H48 - Ctrl H48	17.12	8.47	(-8.03, 42.27)	2.02	0.234
DP10 H48 - Ctrl H48	25.22	8.47	(0.07, 50.37)	2.98	0.049
DP5 H48 - DP1 H48	60.6	10	(30.8, 90.3)	6.05	0
DP10 H48 - DP1 H48	68.7	10	(38.9, 98.4)	6.85	0
DP10 H48 - DP5 H48	8.1	10	(-21.7, 37.9)	0.81	0.849
Individual confidence level = 98.83%					

Where,

DX1= Dox 1 μ M, DX5= Dox 5 μ M, DX10= Dox 10 μ M;

DP1= Donepezil 1 μ M, DP5= Donepezil 5 μ M, DP10= Donepezil 10 μ M

M1= Memantine 1 μ M, M5= Memantine 5 μ M, M10= Memantine 10 μ M

H24= 24 h, H48= 48 h, Ctrl- Control

Appendix II: Drug effects comparison amongst Dox, Memantine and Donepezil (1, 5 and 10 μ M) on the cell viability of HEK293T cells using CyQUANT® Direct assay

A) Bar chart data representation showing the drug effects comparison between:

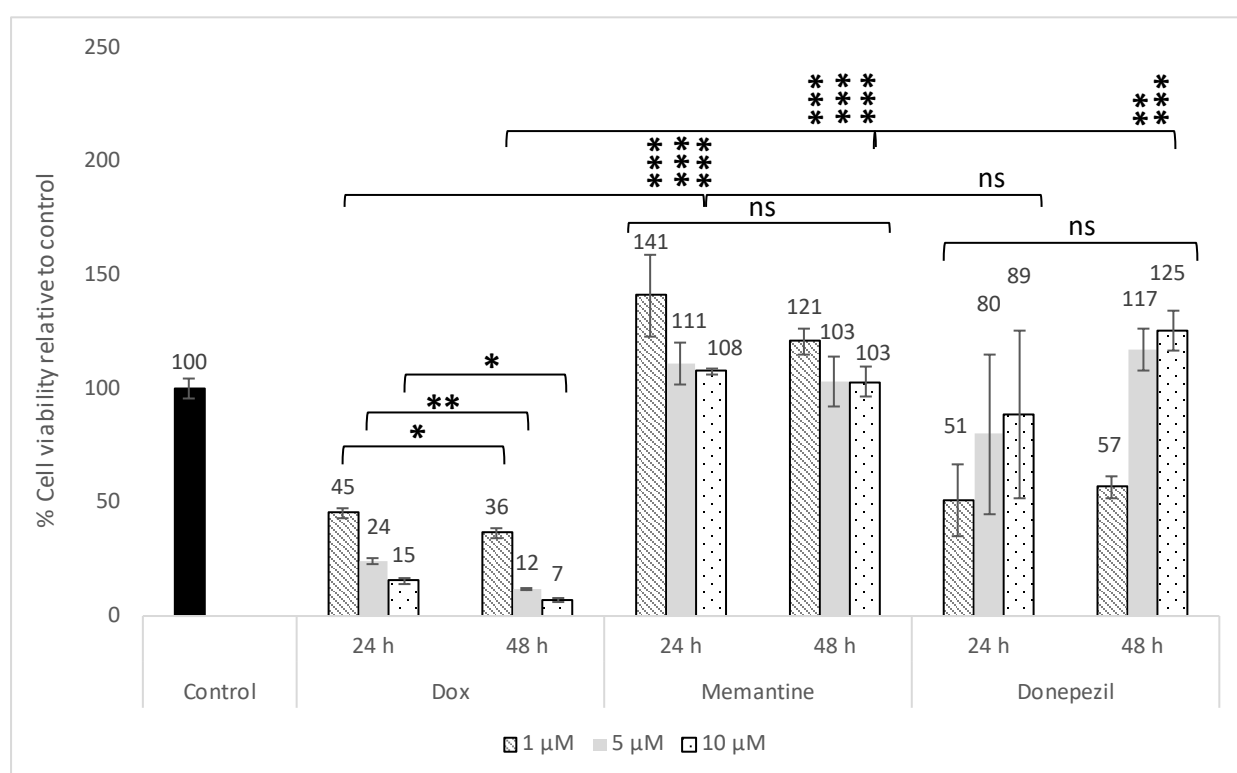
Dox 1, 5 and 10 μ M vs Mem 1, 5 and 10 μ M (at their common time points)

Dox 1, 5 and 10 μ M vs Donepezil 1, 5 and 10 μ M (at their common time points)

Dox 1, 5 and 10 μ M vs Dox 1, 5 and 10 μ M (24 and 48 h)

Memantine 1, 5 and 10 μ M vs Memantine 1, 5 and 10 μ M (24 and 48 h)

Donepezil 1, 5 and 10 μ M vs Donepezil 1, 5 and 10 μ M (24 and 48 h)



Appendix IIA: Effect of Dox, Memantine and Donepezil on the viability of HEK293T cells using CyQUANT® Direct assay. Figure shows the difference between Dox vs each AD drugs and each drug, at various times tested. No significant difference amongst the Memantine doses as well as Donepezil doses tested at 24 h vs 48 h. Experiments were repeated at least three times, and data are expressed as mean \pm SE. Statistical analysis was performed using one-way ANOVA, Tukey test and the statistical differences between the treatments and control were accepted as: *, $p \leq 0.05$; **, $p \leq 0.01$; ***, $p \leq 0.001$; ns= not significant.

B) Minitab statistical analysis output showing the p-values for the compared drug effects between:

1) Dox 1, 5 and 10 μM vs Mem 1, 5 and 10 μM (at their common time points)

Tukey Simultaneous Tests for Differences of Means					
Difference of Levels	Difference of Means	SE of Difference	95% CI	T-Value	Adjusted P-Value
M1 H24 - DX1 H24	95	10.1	(58.7, 131.3)	9.45	0
M5 H24 - DX5 H24	87	10.1	(50.7, 123.3)	8.65	0
M10 H24 - DX10 H24	92	10.1	(55.7, 128.3)	9.15	0
M1 H48 - DX1 H48	84.3	10.1	(48.0, 120.6)	8.38	0
M5 H48 - DX5 H48	91.4	10.1	(55.1, 127.6)	9.09	0
M10 H48 - DX10 H48	95.8	10.1	(59.6, 132.1)	9.53	0
Individual confidence level = 99.86%					

2) Dox 1, 5 and 10 μM vs Donepezil 1, 5 and 10 μM (at their common time points)

Tukey Simultaneous Tests for Differences of Means					
Difference of Levels	Difference of Means	SE of Difference	95% CI	T-Value	Adjusted P-Value
DP1 H24 - DX1 H24	6	22.4	(-74.7, 86.7)	0.27	1
DP5 H24 - DX5 H24	56.3	22.4	(-24.3, 137.0)	2.52	0.375
DP10 H24 - DX10 H24	73.3	22.4	(-7.3, 154.0)	3.28	0.099
DP1 H48 - DX1 H48	20.2	22.4	(-60.5, 100.8)	0.9	0.998
DP5 H48 - DX5 H48	105.6	22.4	(24.9, 186.2)	4.72	0.004
DP10 H48 - DX10 H48	118.3	22.4	(37.6, 198.9)	5.29	0.001
Individual confidence level = 99.86%					

3) Dox 1, 5 and 10 μM vs Dox 1, 5 and 10 μM (24 and 48 h)

Tukey Simultaneous Tests for Differences of Means					
Difference of Levels	Difference of Means	SE of Difference	95% CI	T-Value	Adjusted P-Value
DX1 H48 - DX1 H24	-8.92	2.27	(-16.54, -1.31)	-3.94	0.019
DX5 H48 - DX5 H24	-12.43	2.27	(-20.05, -4.82)	-5.48	0.002
DX10 H48 - DX10 H24	-8.7	2.27	(-16.32, -1.08)	-3.84	0.022
Individual confidence level = 99.43%					

4) Memantine 1, 5 and 10 μM vs Memantine 1, 5 and 10 μM (24 and 48 h)

Tukey Simultaneous Tests for Differences of Means					
Difference of Levels	Difference of Means	SE of Difference	95% CI	T-Value	Adjusted P-Value
M1 H48 - M1 H24	-19.6	14	(-66.8, 27.5)	-1.4	0.728
M5 H48 - M5 H24	-8.1	14	(-55.2, 39.1)	-0.57	0.991
M10 H48 - M10 H24	-4.9	14	(-52.0, 42.3)	-0.35	0.999
Individual confidence level = 99.43%					

5) Donepezil 1, 5 and 10 μM vs Donepezil 1, 5 and 10 μM (24 and 48 h)

Tukey Simultaneous Tests for Differences of Means					
Difference of Levels	Difference of Means	SE of Difference	95% CI	T-Value	Adjusted P-Value
DP1 H48 - DP1 H24	5.2	31.6	(-100.8, 111.2)	0.17	1
DP5 H48 - DP5 H24	36.8	31.6	(-69.2, 142.8)	1.17	0.844
DP10 H48 - DP10 H24	36.2	31.6	(-69.8, 142.2)	1.15	0.852
Individual confidence level = 99.43%					

Where,

DX1= Dox 1 μM , DX5= Dox 5 μM , DX10= Dox 10 μM ;

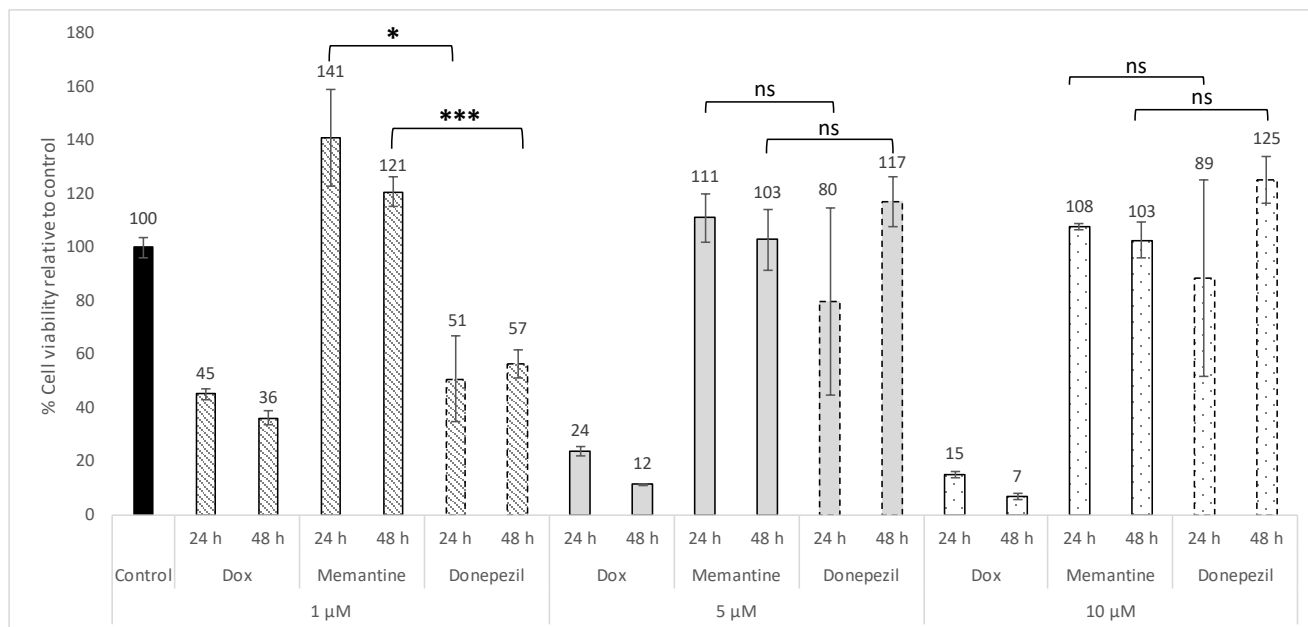
DP1= Donepezil 1 μM , DP5= Donepezil 5 μM , DP10= Donepezil 10 μM

M1= Memantine 1 μM , M5= Memantine 5 μM , M10= Memantine 10 μM

H24= 24 h, H48= 48 h

Appendix III: Comparison of the cell viability effects between Memantine and Donepezil (1, 5 and 10 μM) at 24 and 48 h treatments using CyQUANT® Direct assay

A) Bar chart data representation showing the drug effect differences between Memantine and Donepezil (1, 5 and 10 μM) at their common time points of 24 and 48 h.



Appendix IIIA: Effect of Dox, Memantine and Donepezil on the viability of HEK293T cells using CyQUANT® Direct assay. Figure shows the difference between Memantine and Donepezil (1, 5 and 10 μM) 24 and 48 h treatments. Experiments were repeated at least three times, and data are expressed as mean \pm SE. Basic statistical analysis was performed using 2-sample t-test and significant difference shown as: *, $p \leq 0.05$; ***, $p \leq 0.001$; ns= not significant.

B) Minitab statistical analysis output showing the p-values for the comparison between Memantine and Donepezil (1, 5 and 10 μM) at their common time points of 24 and 48 h.

Tukey Simultaneous Tests for Differences of Means					
Difference of Levels	Difference of Means	SE of Difference	95% CI	T-Value	Adjusted P-Value
M1 H24 - DP1 H24	89	24.4	(0.9, 177.1)	3.64	0.046
M5 H24 - DP5 H24	30.7	24.4	(-57.4, 118.7)	1.26	0.977
M10 H24 - DP10 H24	18.7	24.4	(-69.4, 106.7)	0.76	1
Individual confidence level = 99.86%					
M1 H48 - DP1 H48	64.1	11.3	(26.1, 102.2)	5.66	0.001
M5 H48 - DP5 H48	-14.2	11.3	(-52.3, 23.9)	-1.25	0.804
M10 H48 - DP10 H48	-22.4	11.3	(-60.5, 15.6)	-1.98	0.406
Individual confidence level = 99.43%					

Where,

DP1= Donepezil 1 μM , DP5= Donepezil 5 μM , DP10= Donepezil 10 μM

M1= Memantine 1 μM , M5= Memantine 5 μM , M10= Memantine 10 μM

H24= 24 h, H48= 48 h

Appendix IV: Statistical analyses for the cell death effect of Dox, Imatinib, Donepezil and Memantine on K-562 and HEK293T cells using flow cytometer

Below is the 2-sample t-test results from Minitab showing the significant difference (p-value) between treatments:

A) HEK293T vs control

Sample	N	Mean	StDev	SE Mean	T-Value	DF	P-Value
Ctrl H48	2	97.632	0.145	0.1	14.66	2	0.005
DX1 H48	2	63.08	3.33	2.4			
Ctrl H48	2	97.632	0.145	0.1	36.35	2	0.001
DX5 H48	2	42.98	2.12	1.5			
Ctrl H48	2	97.632	0.145	0.1	1.52	2	0.268
DP1 H48	2	96.47	1.07	0.76			
Ctrl H48	2	97.632	0.145	0.1	-2.55	2	0.126
DP5 H48	2	97.953	0.103	0.073			
Ctrl H48	2	97.632	0.145	0.1	-3.03	2	0.094
DP10 H48	2	98.55	0.403	0.28			
Ctrl H48	2	97.632	0.145	0.1	-3.12	2	0.089
M1 H48	2	99.323	0.753	0.53			
Ctrl H48	2	97.632	0.145	0.1	-7.42	2	0.018
M5 H48	2	98.683	0.138	0.098			
Ctrl H48	2	97.632	0.145	0.1	-6.66	2	0.022
M10 H48	2	98.87	0.219	0.16			

B) K-562 cells vs control

Sample	N	Mean	StDev	SE Mean	T-Value	DF	P-Value
Ctrl H48	2	88.03	1.73	1.2	4.72	1	0.042
Imat1 H48	2	77.08	2.79	2			
Ctrl H48	2	88.03	1.73	1.2	9.4	2	0.011
DX1 H48	2	74.07	1.19	0.84			
Ctrl H48	2	88.03	1.73	1.2	-1.14	2	0.372
M1 H48	2	89.69	1.12	0.79			
Ctrl H48	2	88.03	1.73	1.2	0.29	2	0.798

M5 H48	2	87.06	4.4	3.1			
Ctrl H48	2	88.03	1.73	1.2	-0.71	2	0.549
M10 H48	2	88.91	0.262	0.19			

C) HEK293T vs K-562 cells

Cell line; Sample	N	Mean	StDev	SE Mean	T-Value	DF	P-Value
HEK293T; M1 H48	2	99.323	0.753	0.53	10.11	2	0.01
K-562; M1 H48	2	89.69	1.12	0.79			
HEK293T; M5 H48	2	98.683	0.138	0.098	3.74	2	0.065
K-562; M5 H48	2	87.06	4.4	3.1			
HEK293T; M10 H48	2	98.87	0.219	0.16	41.27	2	0.001
K-562; M10 H48	2	88.91	0.262	0.19			
HEK293T; DX1 H48	2	63.08	3.33	2.4	-4.39	2	0.048
K-562; DX1 H48	2	74.07	1.19	0.84			

Where,

DX1= Dox 1 μ M, DX5= Dox 5 μ M

DP1= Donepezil 1 μ M, DP5= Donepezil 5 μ M, DP10= Donepezil 10 μ M

M1= Memantine 1 μ M, M5= Memantine 5 μ M, M10= Memantine 10 μ M

H48= 48 h, Ctrl- Negative control

Appendix V. Flow cytometry analyses of the cell population of viable and non-viable K-562 and HEK293T cells exhibiting different cell death types following 48 h drug treatments

A) In K-562 cells

Cell population of viable and non-viable K-562 cells exhibiting different cell death types following 48 h drug treatments

Treatments	Viable cells	Non-viable cells		
		Early apoptosis	Late apoptosis	Necrosis
Untreated	88.0 ± 1.22	7.08 ± 1.260	4.11 ± 0.025	0.79 ± 0.013
Imatinib 1 μM	77.1 ± 1.97*	12.02 ± 0.443	6.99 ± 0.583	3.91 ± 0.948
Dox 1 μM	74.1 ± 0.84*	2.79 ± 0.098	7.15 ± 1.075	15.99 ± 1.82
Memantine 10 μM	88.9 ± 0.19	8.44 ± 0.238	2.32 ± 0.010	0.33 ± 0.042
Memantine 5 μM	87.1 ± 3.11	10.12 ± 3.233	2.41 ± 0.155	0.41 ± 0.033
Memantine 1 μM	89.7 ± 0.79	6.80 ± 0.478	2.73 ± 0.150	0.78 ± 0.163

The results are presented as the mean cell population (%) ± standard error. *, $p \leq 0.05$ when compared to untreated cells

B) In HEK293T cells

Cell population of viable and non-viable HEK293T cells exhibiting different cell death types following 48 h drug treatments

Treatments	Viable cells	Non-viable cells		
		Early apoptosis	Late apoptosis	Necrosis
Untreated	97.6 ± 0.10	2.03 ± 0.103	0.12 ± 0.008	0.21 ± 0.007
Dox 5 μM	43.0 ± 1.50***	44.19 ± 2.90	7.85 ± 0.65	4.98 ± 0.750
Dox 1 μM	63.1 ± 2.36**	30.95 ± 4.097	3.15 ± 1.383	2.82 ± 0.360
Donepezil 10 μM	98.6 ± 0.28	0.66 ± 0.092	0.20 ± 0.037	0.59 ± 0.155
Donepezil 5 μM	98.0 ± 0.07	1.82 ± 0.128	0.06 ± 0.008	0.17 ± 0.048
Donepezil 1 μM	96.5 ± 0.76	2.90 ± 0.575	0.17 ± 0.085	0.46 ± 0.268
Memantine 10 μM	98.9 ± 0.16	0.63 ± 0.090	0.14 ± 0.013	0.36 ± 0.052
Memantine 5 μM	98.7 ± 0.10	1.18 ± 0.028	0.04 ± 0.038	0.10 ± 0.033
Memantine 1 μM	99.3 ± 0.53	0.23 ± 0.130	0.07 ± 0.058	0.38 ± 0.345

The results are presented as the mean cell population (%) ± standard error. **, $p \leq 0.01$; ***, $p \leq 0.001$ when compared to untreated cells

Appendix VI: Statistical analyses for the measurement of the basal levels of protein in HEK293T vs K-562 cells using Western blot

Below is the 2-sample t test results using Minitab showing the significant difference (p-value) between protein levels in both cell lines compared:

Protein Sample	N	Mean	StDev	SE Mean	T-Value	DF	P-Value
Bcl-2 H48	3	0.385	0.014	0.008	-12.01		0
Bcl-2 K48	3	0	0	0			
Bcl-xL H48	3	0.415	0.114	0.066	-4.11	4	0.01
Bcl-xL K48	3	1.543	0.462	0.27			
Bak H48	3	1.1366	0.0874	0.05	10.02	4	0.001
Bak K48	3	0.6049	0.0285	0.016			
Bax H48	3	0.3505	0.0438	0.025	13.63	4	0
Bax K48	3	0.00531	0.00197	0.0011			
Cyto c H48	3	0.936	0.0693	0.04	19.53	4	0
Cyto c K48	3	0.117	0.0216	0.012			
Beclin-1 H48	3	7.02	1.55	0.89	4.89	4	0.008
Beclin-1 K48	3	2.456	0.469	0.27			
p62 H48	3	0.1242	0.0135	0.0078	-42.11	4	0
p62 K48	3	1.0314	0.0348	0.02			
LC3-II/LC3-I H48	3	0.1793	0.0472	0.027	3.65	4	0.022
LC3-II/LC3-I K48	3	0.0694	0.0223	0.013			

Where, H48= HEK293T cells treated for 48 h
K48= K-562 cells treated for 48 h

Appendix VII: Statistical analyses for the protein expression level in single drug-treated HEK293T vs K-562 cells using Western blot

Shown below is the Minitab outputs of the significant difference (p-value) for treatments between:

A) HEK293T versus control and K-562 cells versus control

Difference of Levels	Difference of Means	SE of Difference	95% CI	T-Value	Adjusted P-Value
		Bcl-2			
D 1 H48 - Media H48	0.6482	0.0321	(0.5228, 0.7735)	20.22	0
D 5 H48 - Media H48	0.105	0.0321	(-0.0204, 0.2303)	3.27	0.007
D 10 H48 - Media H48	0.4175	0.0321	(0.2921, 0.5428)	13.02	0
M 50 H48 - Media H48	-0.0139	0.0321	(-0.1393, 0.1114)	-0.43	1
M 30 H48 - Media H48	-0.0484	0.0321	(-0.1738, 0.0769)	-1.51	0.999
M 20 H48 - Media H48	-0.0549	0.0321	(-0.1803, 0.0704)	-1.71	0.993
M 10 H48 - Media H48	0.2419	0.0321	(0.1165, 0.3672)	7.54	0.002
M 5 H48 - Media H48	0.3568	0.0321	(0.2314, 0.4822)	11.13	0
M 1 H48 - Media H48	1.1711	0.0321	(1.0457, 1.2965)	36.53	0
DX 1 H48 - Media H48	0.0463	0.0321	(-0.0790, 0.1717)	1.45	0.999
Imat 1 H48 - Media H48	1.1692	0.0321	(1.0439, 1.2946)	36.47	0
D 1 K48 - Media K48	0.0263	0.0321	(-0.0991, 0.1517)	0.82	1
D 5 K48 - Media K48	0.0184	0.0321	(-0.1070, 0.1437)	0.57	1
D 10 K48 - Media K48	0.0152	0.0321	(-0.1102, 0.1405)	0.47	1
M 50 K48 - Media K48	0.0246	0.0321	(-0.1008, 0.1499)	0.77	1
M 30 K48 - Media K48	0.0236	0.0321	(-0.1017, 0.1490)	0.74	1
M 20 K48 - Media K48	0.0295	0.0321	(-0.0959, 0.1549)	0.92	1
M 10 K48 - Media K48	0.043	0.0321	(-0.0824, 0.1684)	1.34	1
M 5 K48 - Media K48	0.0492	0.0321	(-0.0762, 0.1745)	1.53	0.999
M 1 K48 - Media K48	0.0487	0.0321	(-0.0767, 0.1741)	1.52	0.999
DX 1 K48 - Media K48	0.0253	0.0321	(-0.1001, 0.1507)	0.79	1
Imat 1 K48 - Media K48	0.027	0.0321	(-0.0984, 0.1524)	0.84	1
		Bcl-xL			
D 1 H48 - Media H48	1.608	0.248	(0.637, 2.580)	6.47	0.014
D 5 H48 - Media H48	1.034	0.248	(0.063, 2.005)	4.16	0.106
D 10 H48 - Media H48	1.197	0.248	(0.226, 2.168)	4.82	0.059
M 50 H48 - Media H48	-0.304	0.248	(-1.275, 0.668)	-1.22	0.96
M 30 H48 - Media H48	-0.253	0.248	(-1.224, 0.718)	-1.02	0.983
M 20 H48 - Media H48	-0.247	0.248	(-1.218, 0.724)	-0.99	0.985
M 10 H48 - Media H48	2.677	0.248	(1.705, 3.648)	10.78	0
M 5 H48 - Media H48	1.5	0.248	(0.528, 2.471)	6.04	0.006
M 1 H48 - Media H48	1.7	0.248	(0.729, 2.672)	6.85	0.002
DX 1 H48 - Media H48	-0.343	0.248	(-1.315, 0.628)	-1.38	0.007
Imat 1 H48 - Media H48	0.781	0.248	(-0.191, 1.752)	3.14	0.01

	Bcl-xL cont'd				
D 1 K48 - Media K48	0.247	0.248	(-0.724, 1.219)	1	1
D 5 K48 - Media K48	-0.209	0.248	(-1.181, 0.762)	-0.84	1
D 10 K48 - Media K48	-0.122	0.248	(-1.094, 0.849)	-0.49	1
M 50 K48 - Media K48	-0.224	0.248	(-1.195, 0.747)	-0.9	1
M 30 K48 - Media K48	-0.242	0.248	(-1.213, 0.730)	-0.97	1
M 20 K48 - Media K48	-0.178	0.248	(-1.150, 0.793)	-0.72	1
M 10 K48 - Media K48	0.371	0.248	(-0.600, 1.342)	1.49	0.999
M 5 K48 - Media K48	-0.098	0.248	(-1.069, 0.874)	-0.39	1
M 1 K48 - Media K48	-0.536	0.248	(-1.508, 0.435)	-2.16	0.914
DX 1 K48 - Media K48	-1.366	0.248	(-2.337, -0.395)	-5.5	0.007
Imat 1 K48 - Media K48	-1.113	0.248	(-2.084, -0.142)	-4.48	0.009
		Bak			
D 1 H48 - Media H48A	7.96	0.803	(4.819, 11.100)	9.91	0
D 5 H48 - Media H48A	4.469	0.803	(1.328, 7.609)	5.56	0.011
D 10 H48 - Media H48A	6.488	0.803	(3.347, 9.628)	8.08	0.001
M 50 H48 - Media H48A	0.966	0.803	(-2.174, 4.106)	1.2	0.977
M 30 H48 - Media H48A	0.723	0.803	(-2.418, 3.863)	0.9	0.995
M 20 H48 - Media H48A	2.613	0.803	(-0.527, 5.753)	3.25	0.325
M 10 H48 - Media H48A	12.272	0.803	(9.131, 15.412)	15.28	0
M 5 H48 - Media H48A	4.224	0.803	(1.084, 7.365)	5.26	0.032
M 1 H48 - Media H48A	9.653	0.803	(6.512, 12.793)	12.02	0
DX 1 H48 - Media H48A	0.082	0.803	(-3.059, 3.222)	0.1	0.04
Imat 1 H48 h - Media H48A	10.462	0.803	(7.322, 13.602)	13.03	0.001
D 1 K48 - Media K48	0.124	0.803	(-3.017, 3.264)	0.15	0.252
D 5 K48 - Media K48	0.176	0.803	(-2.965, 3.316)	0.22	0.078
D 10 K48 - Media K48	0.158	0.803	(-2.982, 3.298)	0.2	0.117
M 50 K48 - Media K48	0.251	0.803	(-2.889, 3.391)	0.31	0.2
M 30 K48 - Media K48	0.114	0.803	(-3.027, 3.254)	0.14	0.892
M 20 K48 - Media K48	0.257	0.803	(-2.883, 3.398)	0.32	0.18
M 10 K48 - Media K48	0.528	0.803	(-2.612, 3.669)	0.66	0.001
M 5 K48 - Media K48	0.097	0.803	(-3.043, 3.238)	0.12	0.944
M 1 K48 - Media K48	0.055	0.803	(-3.085, 3.195)	0.07	0.997
DX 1 K48 - Media K48	-0.293	0.803	(-3.433, 2.848)	-0.36	0
Imat 1 K48 - Media K48	0.197	0.803	(-2.943, 3.338)	0.25	0.011
		Cytochrome c			
D 1 H48 - Media H48A	0.3664	0.0974	(-0.0145, 0.7473)	3.76	0.022
D 5 H48 - Media H48A	-0.2035	0.0974	(-0.5844, 0.1774)	-2.09	0.053
D 10 H48 - Media H48A	0.4603	0.0974	(0.0794, 0.8412)	4.73	0.002
M 50 H48 - Media H48A	-0.5459	0.0974	(-0.9268, -0.1650)	-5.6	0.001
M 30 H48 - Media H48A	-0.4846	0.0974	(-0.8655, -0.1037)	-4.97	0.002
M 20 H48 - Media H48A	-0.676	0.0974	(-1.0569, -0.2951)	-6.94	0
M 10 H48 - Media H48A	-0.146	0.0974	(-0.5270, 0.2349)	-1.5	0.715

	Cytochrome c cont'd				
M 5 H48 - Media H48A	0.3393	0.0974	(-0.0417, 0.7202)	3.48	0.036
M 1 H48 - Media H48A	0.1333	0.0974	(-0.2476, 0.5142)	1.37	0.788
DX 1 H48 - Media H48A	0.2697	0.0974	(-0.1112, 0.6506)	2.77	0.032
Imat 1 H48 h - Media H48A	-0.0633	0.0974	(-0.4442, 0.3176)	-0.65	0.409
D 1 K48 - Media K48	0.4673	0.0974	(0.0863, 0.8482)	4.8	0.003
D 5 K48 - Media K48	0.9051	0.0974	(0.5242, 1.2861)	9.29	0
D 10 K48 - Media K48	0.8746	0.0974	(0.4937, 1.2556)	8.98	0
M 50 K48 - Media K48	0.2531	0.0974	(-0.1278, 0.6341)	2.6	0
M 30 K48 - Media K48	0.3142	0.0974	(-0.0667, 0.6951)	3.23	0
M 20 K48 - Media K48	0.1374	0.0974	(-0.2435, 0.5183)	1.41	0.001
M 10 K48 - Media K48	0.0857	0.0974	(-0.2952, 0.4666)	0.88	0.056
M 5 K48 - Media K48	0.1722	0.0974	(-0.2087, 0.5531)	1.77	0
M 1 K48 - Media K48	0.2071	0.0974	(-0.1738, 0.5881)	2.13	0
DX 1 K48 - Media K48	0.9327	0.0974	(0.5518, 1.3137)	9.57	0.001
Imat 1 K48 - Media K48	1.2711	0.0974	(0.8902, 1.6520)	13.05	0.001
		Bax			
D 1 H48 - Media H48A	0.689	0.317	(-0.549, 1.928)	2.18	0.296
D 5 H48 - Media H48A	0.808	0.317	(-0.431, 2.046)	2.55	0.192
D 10 H48 - Media H48A	0.75	0.317	(-0.488, 1.989)	2.37	0.238
M 50 H48 - Media H48A	-0.171	0.317	(-1.409, 1.068)	-0.54	1
M 30 H48 - Media H48A	-0.212	0.317	(-1.451, 1.026)	-0.67	0.999
M 20 H48 - Media H48A	-0.254	0.317	(-1.493, 0.984)	-0.8	0.998
M 10 H48 - Media H48A	1.121	0.317	(-0.118, 2.359)	3.54	0.311
M 5 H48 - Media H48A	0.237	0.317	(-1.002, 1.475)	0.75	0.999
M 1 H48 - Media H48A	1.486	0.317	(0.247, 2.724)	4.69	0.096
DX 1 H48 - Media H48A	-0.255	0.317	(-1.494, 0.983)	-0.81	0.008
Imat 1 H48 h - Media H48A	1.266	0.317	(0.028, 2.505)	4	0.131
D 1 K48 - Media K48	0.021	0.317	(-1.217, 1.260)	0.07	0.104
D 5 K48 - Media K48	0.027	0.317	(-1.212, 1.265)	0.08	0.039
D 10 K48 - Media K48	0.037	0.317	(-1.202, 1.275)	0.12	0.007
M 50 K48 - Media K48	0.099	0.317	(-1.140, 1.337)	0.31	0.532
M 30 K48 - Media K48	0.126	0.317	(-1.112, 1.365)	0.4	0.273
M 20 K48 - Media K48	0.068	0.317	(-1.171, 1.306)	0.21	0.848
M 10 K48 - Media K48	0.048	0.317	(-1.190, 1.287)	0.15	0.964
M 5 K48 - Media K48	0.031	0.317	(-1.207, 1.270)	0.1	0.996
M 1 K48 - Media K48	0.025	0.317	(-1.213, 1.264)	0.08	0.999
DX 1 K48 - Media K48	-0.005	0.317	(-1.244, 1.233)	-0.02	1
Imat 1 K48 - Media K48	0.501	0.317	(-0.737, 1.740)	1.58	0.998

		p62			
D 1 H48 - Media H48A	1.37	0.191	(0.623, 2.118)	7.17	0.003
D 5 H48 - Media H48A	2.048	0.191	(1.300, 2.795)	10.71	0
D 10 H48 - Media H48A	1.352	0.191	(0.604, 2.100)	7.07	0.003
M 50 H48 - Media H48A	-0.047	0.191	(-0.794, 0.701)	-0.24	1
M 30 H48 - Media H48A	-0.029	0.191	(-0.777, 0.718)	-0.15	1
M 20 H48 - Media H48A	0.013	0.191	(-0.735, 0.760)	0.07	1
M 10 H48 - Media H48A	3.315	0.191	(2.568, 4.063)	17.34	0
M 5 H48 - Media H48A	1.101	0.191	(0.353, 1.848)	5.76	0.002
M 1 H48 - Media H48A	2.098	0.191	(1.351, 2.846)	10.97	0
DX 1 H48 - Media H48A	1.203	0.191	(0.455, 1.951)	6.29	0
Imat 1 H48 h - Media H48A	0.86	0.191	(0.113, 1.608)	4.5	0
D 1 K48 - Media K48	0.032	0.191	(-0.716, 0.779)	0.17	0.977
D 5 K48 - Media K48	-0.034	0.191	(-0.782, 0.714)	-0.18	0.972
D 10 K48 - Media K48	-0.268	0.191	(-1.015, 0.480)	-1.4	0.039
M 50 K48 - Media K48	2.558	0.191	(1.810, 3.306)	13.38	0
M 30 K48 - Media K48	0.079	0.191	(-0.668, 0.827)	0.41	1
M 20 K48 - Media K48	0.277	0.191	(-0.471, 1.024)	1.45	0.999
M 10 K48 - Media K48	0.781	0.191	(0.034, 1.529)	4.09	0.036
M 5 K48 - Media K48	0.509	0.191	(-0.239, 1.256)	2.66	0.626
M 1 K48 - Media K48	1.577	0.191	(0.829, 2.324)	8.25	0
DX 1 K48 - Media K48	-1.031	0.191	(-1.779, -0.284)	-5.39	0.001
Imat 1 K48 - Media K48	-0.56	0.191	(-1.308, 0.188)	-2.93	0
		Beclin-1			
D 1 H48 - Media H48A	-4.959	0.449	(-6.716, -3.202)	-11.04	0
D 5 H48 - Media H48A	-4.409	0.449	(-6.166, -2.652)	-9.81	0.001
D 10 H48 - Media H48A	-4.954	0.449	(-6.711, -3.197)	-11.03	0
M 50 H48 - Media H48A	-4.173	0.449	(-5.930, -2.416)	-9.29	0
M 30 H48 - Media H48A	-4.544	0.449	(-6.301, -2.787)	-10.11	0
M 20 H48 - Media H48A	-4.447	0.449	(-6.204, -2.690)	-9.9	0
M 10 H48 - Media H48A	-2.96	0.449	(-4.717, -1.203)	-6.59	0.005
M 5 H48 - Media H48A	-2.836	0.449	(-4.592, -1.079)	-6.31	0.007
M 1 H48 - Media H48A	-3.678	0.449	(-5.435, -1.921)	-8.19	0.001
DX 1 H48 - Media H48A	-3.566	0.449	(-5.323, -1.809)	-7.94	0.016
Imat 1 H48 h - Media H48A	-1.399	0.449	(-3.156, 0.358)	-3.11	0.211
D 1 K48 - Media K48	-1.403	0.449	(-3.160, 0.354)	-3.12	0.001
D 5 K48 - Media K48	-1.133	0.449	(-2.890, 0.624)	-2.52	0.004
D 10 K48 - Media K48	-1.725	0.449	(-3.482, 0.032)	-3.84	0
M 50 K48 - Media K48	-0.996	0.449	(-2.753, 0.761)	-2.22	0.001
M 30 K48 - Media K48	-1.035	0.449	(-2.792, 0.722)	-2.3	0
M 20 K48 - Media K48	-1.138	0.449	(-2.895, 0.619)	-2.53	0
M 10 K48 - Media K48	-1.225	0.449	(-2.982, 0.532)	-2.73	0
M 5 K48 - Media K48	-1.274	0.449	(-3.031, 0.483)	-2.84	0
M 1 K48 - Media K48	-1.469	0.449	(-3.226, 0.288)	-3.27	0

	Beclin-1 cont'd				
DX 1 K48 - Media K48	1.002	0.45	(-0.759, 2.763)	2.23	0.025
Imat 1 K48 - Media K48	-0.544	0.449	(-2.301, 1.213)	-1.21	0.146
		LC3-II/LC3-I			
D 1 H48 - Media H48A	0.3587	0.0686	(0.0906, 0.6268)	5.23	0
D 5 H48 - Media H48A	0.2469	0.0686	(-0.0212, 0.5150)	3.6	0.002
D 10 H48 - Media H48A	0.0656	0.0686	(-0.2025, 0.3337)	0.96	0.44
M 50 H48 - Media H48A	-0.0977	0.0686	(-0.3658, 0.1704)	-1.42	0.361
M 30 H48 - Media H48A	-0.1136	0.0686	(-0.3817, 0.1545)	-1.66	0.217
M 20 H48 - Media H48A	-0.1142	0.0686	(-0.3823, 0.1539)	-1.67	0.213
M 10 H48 - Media H48A	0.0734	0.0686	(-0.1947, 0.3415)	1.07	0.662
M 5 H48 - Media H48A	-0.0078	0.0686	(-0.2759, 0.2603)	-0.11	1
M 1 H48 - Media H48A	0.1964	0.0686	(-0.0717, 0.4645)	2.86	0.009
DX 1 H48 - Media H48A	-0.089	0.0686	(-0.3571, 0.1791)	-1.3	0.052
Imat 1 H48 - Media H48A	-0.0186	0.0686	(-0.2867, 0.2495)	-0.27	0.733
D 1 K48 - Media K48	0.2482	0.0686	(-0.0199, 0.5163)	3.62	0.39
D 5 K48 - Media K48	0.035	0.0686	(-0.2331, 0.3031)	0.51	0.995
D 10 K48 - Media K48	0.0316	0.0686	(-0.2365, 0.2998)	0.46	0.996
M 50 K48 - Media K48	1.8151	0.0686	(1.5470, 2.0832)	26.47	0
M 30 K48 - Media K48	0.3008	0.0686	(0.0326, 0.5689)	4.39	0.001
M 20 K48 - Media K48	0.2126	0.0686	(-0.0555, 0.4807)	3.1	0.013
M 10 K48 - Media K48	0.0918	0.0686	(-0.1763, 0.3599)	1.34	0.566
M 5 K48 - Media K48	0.0109	0.0686	(-0.2572, 0.2790)	0.16	1
M 1 K48 - Media K48	0.1479	0.0686	(-0.1202, 0.4160)	2.16	0.121
DX 1 K48 - Media K48	0.2661	0.0686	(-0.0020, 0.5342)	3.88	0
Imat 1 K48 - Media K48	0.2517	0.0686	(-0.0164, 0.5198)	3.67	0.001

B) HEK293T versus K-562 cells

Difference of Levels	Difference of Means	SE of Difference	95% CI	T-Value	Adjusted P-Value
		Bcl-2			
D 1 K48 - D 1 H48	-1.007	0.0321	(-1.1324, -0.8816)	-31.41	0
D 5 K48 - D 5 H48	-0.4717	0.0321	(-0.5971, -0.3464)	-14.71	0
D 10 K48 - D 10 H48	-0.7874	0.0321	(-0.9128, -0.6621)	-24.56	0
M 50 K48 - M 50 H48	-0.3466	0.0321	(-0.4720, -0.2213)	-10.81	0
M 30 K48 - M 30 H48	-0.3131	0.0321	(-0.4384, -0.1877)	-9.76	0
M 20 K48 - M 20 H48	-0.3007	0.0321	(-0.4261, -0.1753)	-9.38	0
M 10 K48 - M 10 H48	-0.584	0.0321	(-0.7094, -0.4586)	-18.21	0
M 5 K48 - M 5 H48	-0.6928	0.0321	(-0.8181, -0.5674)	-21.61	0
M 1 K48 - M 1 H48	-1.5075	0.0321	(-1.6329, -1.3822)	-47.02	0
DX 1 K48 - DX 1 H48	-0.4062	0.0321	(-0.5315, -0.2808)	-12.67	0
Imat 1 K48 - Imat 1 H48	-1.5274	0.0321	(-1.6528, -1.4020)	-47.64	0

		Bcl-xL			
D 1 K48 - D 1 H48	-0.233	0.248	(-1.204, 0.739)	-0.94	0.594
D 5 K48 - D 5 H48	-0.115	0.248	(-1.086, 0.856)	-0.46	0.733
D 10 K48 - D 10 H48	-0.191	0.248	(-1.162, 0.781)	-0.77	0.495
M 50 K48 - M 50 H48	1.208	0.248	(0.236, 2.179)	4.86	0
M 30 K48 - M 30 H48	1.14	0.248	(0.169, 2.111)	4.59	0
M 20 K48 - M 20 H48	1.197	0.248	(0.226, 2.168)	4.82	0
M 10 K48 - M 10 H48	-1.177	0.248	(-2.149, -0.206)	-4.74	0.106
M 5 K48 - M 5 H48	-0.469	0.248	(-1.440, 0.502)	-1.89	0.047
M 1 K48 - M 1 H48	-1.108	0.248	(-2.080, -0.137)	-4.46	0.01
DX 1 K48 - DX 1 H48	0.106	0.248	(-0.866, 1.077)	0.43	0.001
Imat 1 K48 - Imat 1 H48	-0.765	0.248	(-1.737, 0.206)	-3.08	0.008
		Bak			
D 1 K48 - D 1 H48	-8.368	0.803	(-11.508, -5.227)	-10.42	0
D 5 K48 - D 5 H48	-4.824	0.803	(-7.965, -1.684)	-6.01	0.001
D 10 K48 - D 10 H48	-6.862	0.803	(-10.002, -3.721)	-8.54	0.006
M 50 K48 - M 50 H48	-1.247	0.803	(-4.387, 1.894)	-1.55	0.001
M 30 K48 - M 30 H48	-1.141	0.803	(-4.281, 2.000)	-1.42	0
M 20 K48 - M 20 H48	-2.887	0.803	(-6.028, 0.253)	-3.6	0.006
M 10 K48 - M 10 H48	-12.275	0.803	(-15.415, -9.135)	-15.28	0.003
M 5 K48 - M 5 H48	-4.659	0.803	(-7.799, -1.518)	-5.8	0
M 1 K48 - M 1 H48	-10.13	0.803	(-13.270, -6.989)	-12.61	0
DX 1 K48 - DX 1 H48	-0.906	0.803	(-4.047, 2.234)	-1.13	0
Imat 1 K48 - Imat 1 H48 h	-10.796	0.803	(-13.937, -7.656)	-13.44	0.001
		Cytochrome c			
D 1 K48 - D 1 H48	-0.7181	0.0974	(-1.0990, -0.3372)	-7.37	0.003
D 5 K48 - D 5 H48	0.2897	0.0974	(-0.0912, 0.6706)	2.97	0.066
D 10 K48 - D 10 H48	-0.4046	0.0974	(-0.7855, -0.0237)	-4.15	0.016
M 50 K48 - M 50 H48	-0.0199	0.0974	(-0.4008, 0.3610)	-0.2	0.302
M 30 K48 - M 30 H48	-0.0202	0.0974	(-0.4011, 0.3607)	-0.21	0.019
M 20 K48 - M 20 H48	-0.0055	0.0974	(-0.3864, 0.3754)	-0.06	0.899
M 10 K48 - M 10 H48	-0.5872	0.0974	(-0.9681, -0.2063)	-6.03	0.024
M 5 K48 - M 5 H48	-0.986	0.0974	(-1.3669, -0.6051)	-10.12	0
M 1 K48 - M 1 H48	-0.7451	0.0974	(-1.1260, -0.3642)	-7.65	0
DX 1 K48 - DX 1 H48	-0.1559	0.0974	(-0.5368, 0.2250)	-1.6	0.43
Imat 1 K48 - Imat 1 H48 h	0.5155	0.0974	(0.1345, 0.8964)	5.29	0.022
		Bax			
D 1 K48 - D 1 H48	-1.013	0.317	(-2.252, 0.225)	-3.2	0.015
D 5 K48 - D 5 H48	-1.126	0.317	(-2.365, 0.112)	-3.56	0.019
D 10 K48 - D 10 H48	-1.058	0.317	(-2.297, 0.180)	-3.34	0.034
M 50 K48 - M 50 H48	-0.076	0.317	(-1.315, 1.162)	-0.24	0.001

	Bax cont'd				
M 30 K48 - M 30 H48	-0.007	0.317	(-1.245, 1.232)	-0.02	0.948
M 20 K48 - M 20 H48	-0.023	0.317	(-1.261, 1.216)	-0.07	0.637
M 10 K48 - M 10 H48	-1.418	0.317	(-2.656, -0.179)	-4.48	0.119
M 5 K48 - M 5 H48	-0.551	0.317	(-1.789, 0.688)	-1.74	0.05
M 1 K48 - M 1 H48	-1.806	0.317	(-3.044, -0.567)	-5.7	0.027
DX 1 K48 - DX 1 H48	-0.095	0.317	(-1.334, 1.143)	-0.3	0
Imat 1 K48 - Imat 1 H48 h	-1.11	0.317	(-2.349, 0.128)	-3.51	0.096
		p62			
D 1 K48 - D 1 H48	-0.432	0.191	(-1.179, 0.316)	-2.26	0.227
D 5 K48 - D 5 H48	-1.174	0.191	(-1.922, -0.427)	-6.14	0.002
D 10 K48 - D 10 H48	-0.712	0.191	(-1.460, 0.035)	-3.73	0.008
M 50 K48 - M 50 H48	3.512	0.191	(2.764, 4.260)	18.37	0
M 30 K48 - M 30 H48	1.016	0.191	(0.268, 1.764)	5.31	0
M 20 K48 - M 20 H48	1.171	0.191	(0.424, 1.919)	6.13	0
M 10 K48 - M 10 H48	-1.627	0.191	(-2.375, -0.879)	-8.51	0.013
M 5 K48 - M 5 H48	0.315	0.191	(-0.433, 1.063)	1.65	0.188
M 1 K48 - M 1 H48	0.386	0.191	(-0.362, 1.133)	2.02	0.274
DX 1 K48 - DX 1 H48	-1.327	0.191	(-2.075, -0.580)	-6.94	0
Imat 1 K48 - Imat 1 H48	-0.513	0.191	(-1.261, 0.235)	-2.68	0.002
		Beclin-1			
D 1 K48 - D 1 H48	-1.008	0.449	(-2.765, 0.749)	-2.24	0.001
D 5 K48 - D 5 H48	-1.288	0.449	(-3.045, 0.469)	-2.87	0.001
D 10 K48 - D 10 H48	-1.335	0.449	(-3.092, 0.422)	-2.97	0
M 50 K48 - M 50 H48	-1.387	0.449	(-3.144, 0.370)	-3.09	0.005
M 30 K48 - M 30 H48	-1.055	0.449	(-2.812, 0.702)	-2.35	0.001
M 20 K48 - M 20 H48	-1.255	0.449	(-3.012, 0.502)	-2.79	0.002
M 10 K48 - M 10 H48	-2.829	0.449	(-4.586, -1.072)	-6.3	0.005
M 5 K48 - M 5 H48	-3.003	0.449	(-4.760, -1.246)	-6.68	0
M 1 K48 - M 1 H48	-2.355	0.449	(-4.112, -0.598)	-5.24	0.004
DX 1 K48 - DX 1 H48	0.003	0.45	(-1.757, 1.764)	0.01	0.98
Imat 1 K48 - Imat 1 H48 h	-3.709	0.449	(-5.466, -1.952)	-8.26	0
		LC3-II/LC3-I			
D 1 K48 - D 1 H48	-0.2204	0.0686	(-0.4885, 0.0477)	-3.21	0.347
D 5 K48 - D 5 H48	-0.3218	0.0686	(-0.5899, -0.0537)	-4.69	0.001
D 10 K48 - D 10 H48	-0.1439	0.0686	(-0.4120, 0.1242)	-2.1	0.22
M 50 K48 - M 50 H48	1.8029	0.0686	(1.5348, 2.0710)	26.29	0
M 30 K48 - M 30 H48	0.3045	0.0686	(0.0364, 0.5726)	4.44	0.001
M 20 K48 - M 20 H48	0.2169	0.0686	(-0.0512, 0.4850)	3.16	0.004
M 10 K48 - M 10 H48	-0.0914	0.0686	(-0.3596, 0.1767)	-1.33	0.13
M 5 K48 - M 5 H48	-0.0912	0.0686	(-0.3593, 0.1770)	-1.33	0.004
M 1 K48 - M 1 H48	-0.1584	0.0686	(-0.4265, 0.1097)	-2.31	0.092

	LC3-II/LC3-I cont'd				
DX 1 K48 - DX 1 H48	0.2452	0.0686	(-0.0229, 0.5133)	3.58	0
Imat 1 K48 - Imat 1 H48	0.1604	0.0686	(-0.1077, 0.4285)	2.34	0.031

Where,

H48= HEK293T cells treated for 48 h; K48= K-562 cells treated for 48 h;

DX1= Dox 1 μ M; Imat 1= Imatinib 1 μ M

DP1= Donepezil 1 μ M, DP5= Donepezil 5 μ M, DP10= Donepezil 10 μ M

M1= Memantine 1 μ M, M5= Memantine 5 μ M, M10= Memantine 10 μ M, M20= Memantine 20 μ M, M30= Memantine 30 μ M, M50= Memantine 50 μ M

H48= 48 h, Ctrl- Control

Appendix VIII: Statistical analyses comparing protein expression levels in Dox 1 μ M, CQ10 μ M and Dox 1 + CQ 10 (μ M) drug-treated K-562 cells as detected through Western blot analyses

Shown below is the Minitab outputs of the significant difference (p-value) amongst the drug-treated K-562 cells:

Difference of Levels	Difference of Means	SE of Difference	95% CI	T-Value	Adjusted P-Value
Beclin-1					
DX 1 K48 - Media K48	1.002	0.258	(0.108, 1.897)	3.88	0.031
DX1/CQ10 K48 - Media K48	0.843	0.289	(-0.157, 1.843)	2.92	0.094
CQ10 K48 - Media K48	0.231	0.289	(-0.769, 1.231)	0.8	0.853
DX1/CQ10 K48 - DX 1 K48	-0.159	0.289	(-1.159, 0.841)	-0.55	0.943
CQ10 K48 - DX 1 K48	-0.771	0.289	(-1.771, 0.228)	-2.67	0.127
CQ10 K48 - DX1/CQ10 K48	-0.613	0.316	(-1.708, 0.483)	-1.94	0.306
Individual confidence level = 98.66%					
p62					
DX 1 K48 - Media K48	-1.0314	0.0298	(-1.1346, -0.9283)	-34.64	0
DX1/CQ10 K48 - Media K48	-0.4218	0.0333	(-0.5372, -0.3065)	-12.67	0
CQ10 K48 - Media K48	-0.0979	0.0333	(-0.2133, 0.0174)	-2.94	0.092
DX1/CQ10 K48 - DX 1 K48	0.6096	0.0333	(0.4942, 0.7249)	18.31	0
CQ10 K48 - DX 1 K48	0.9335	0.0333	(0.8182, 1.0488)	28.04	0
CQ10 K48 - DX1/CQ10 K48	0.3239	0.0365	(0.1976, 0.4503)	8.88	0
Individual confidence level = 98.66%					
Bcl-2					
DX 1 K48 - Media K48	0.0253	0.0158	(-0.0295, 0.0801)	1.6	0.444
DX1/CQ10 K48 - Media K48	0.2284	0.0177	(0.1672, 0.2897)	12.92	0
CQ10 K48 - Media K48	0.3214	0.0177	(0.2602, 0.3827)	18.18	0
DX1/CQ10 K48 - DX 1 K48	0.2031	0.0177	(0.1419, 0.2644)	11.49	0
CQ10 K48 - DX 1 K48	0.2961	0.0177	(0.2349, 0.3574)	16.75	0
CQ10 K48 - DX1/CQ10 K48	0.093	0.0194	(0.0259, 0.1601)	4.8	0.012
Individual confidence level = 98.66%					

Cytochrome c					
DX 1 K48 - Media K48	0.9327	0.0774	(0.6646, 1.2008)	12.05	0
DX1/CQ10 K48 - Media K48	0.1114	0.0865	(-0.1884, 0.4111)	1.29	0.602
CQ10 K48 - Media K48	0.2044	0.0865	(-0.0953, 0.5041)	2.36	0.185
DX1/CQ10 K48 - DX 1 K48	-0.8213	0.0865	(-1.1211, -0.5216)	-9.49	0
CQ10 K48 - DX 1 K48	-0.7283	0.0865	(-1.0281, -0.4286)	-8.42	0.001
CQ10 K48 - DX1/CQ10 K48	0.093	0.0948	(-0.2353, 0.4214)	0.98	0.765
Individual confidence level = 98.66%					

Where, K48= K-562 cells treated for 48 h

DX1= Dox 1 μ M; CQ10= CQ 10 μ M;

DX1/CQ10 = Dox 1 μ M + CQ 10 μ M

Appendix IX: Statistical analyses for the measurement of the Bax:Bcl-2 and Bax:Bcl-xL ratios in Donepezil treated HEK293T cells using Western blot

Below is the 2-sample tee test results from Minitab showing the significant difference (p-value):

Protein Sample	N	Mean	StDev	SE Mean	T-Value	DF	P-Value
Bax:Bcl-2-Untreated	3	1	0.0969	0.056	-0.39	4	0.714
Bax:Bcl-2-Donepezil 1 μ M	3	1.104	0.447	0.26			
Bax:Bcl-2-Untreated	3	1	0.0969	0.056	-2.28	4	0.084
Bax:Bcl-2-Donepezil 5 μ M	3	2.61	1.22	0.7			
Bax:Bcl-2-Untreated	3	1	0.0969	0.056	-1.13	4	0.321
Bax:Bcl-2-Donepezil 10 μ M	3	1.497	0.754	0.44			
Bax:Bcl-xL-Untreated	3	1	0.144	0.083	1.73	4	0.159
Bax:Bcl-xL-Donepezil 1 μ M	3	0.633	0.339	0.2			
Bax:Bcl-xL-Untreated	3	1	0.144	0.083	0	4	0.999
Bax:Bcl-xL-Donepezil 5 μ M	3	1.001	0.556	0.32			
Bax:Bcl-xL-Untreated	3	1	0.144	0.083	0.48	4	0.656
Bax:Bcl-xL-Donepezil 10 μ M	3	0.838	0.565	0.33			

Appendix X: Statistical analyses for the protein expression levels in Dox/ Memantine combination-treated HEK293T and K-562 cells using Western blot

Shown below is the Minitab outputs of the significant difference (p-value) for treatments between:

A) HEK293T versus control and K-562 cells versus control

Difference of Levels	Difference of Means	SE of Difference	95% CI	T-Value	Adjusted P-Value
Bcl-2					
M 1 H48 - Media H48	1.1711	0.0321	(1.0457, 1.2965)	36.53	0
DX 1 H48 - Media H48	0.0463	0.0321	(-0.0790, 0.1717)	1.45	0.999
DX-Mem 1 H48 - Media H48	0.5099	0.0321	(0.3846, 0.6353)	15.9	0.001
M 1 K48 - Media K48	0.0487	0.0321	(-0.0767, 0.1741)	1.52	0.999
DX 1 K48 - Media K48	0.0253	0.0321	(-0.1001, 0.1507)	0.79	1
DX-Mem 1 K48 - Media K48	0.0053	0.0321	(-0.1201, 0.1307)	0.17	1
Bcl-xL					
M 1 H48 - Media H48	1.7	0.248	(0.729, 2.672)	6.85	0.002
DX 1 H48 - Media H48	-0.343	0.248	(-1.315, 0.628)	-1.38	0.007
DX-Mem 1 H48 - Media H48	-0.011	0.248	(-0.983, 0.960)	-0.05	0.91
M 1 K48 - Media K48	-0.536	0.248	(-1.508, 0.435)	-2.16	0.914
DX 1 K48 - Media K48	-1.366	0.248	(-2.337, -0.395)	-5.5	0.007
DX-Mem 1 K48 - Media K48	-0.917	0.248	(-1.888, 0.055)	-3.69	0.034
Bak					
M 1 H48 - Media H48A	9.653	0.803	(6.512, 12.793)	12.02	0
DX 1 H48 - Media H48A	0.082	0.803	(-3.059, 3.222)	0.1	0.04
DX-Mem 1 H48 - Media H48A	2.545	0.803	(-0.595, 5.686)	3.17	0.014
M 1 K48 - Media K48	0.055	0.803	(-3.085, 3.195)	0.07	0.997
DX 1 K48 - Media K48	-0.293	0.803	(-3.433, 2.848)	-0.36	0
DX-Mem 1 K48 - Media K48	-0.297	0.803	(-3.438, 2.843)	-0.37	0.008
Cytochrome c					
M 1 H48 - Media H48A	0.1333	0.0974	(-0.2476, 0.5142)	1.37	0.788
DX 1 H48 - Media H48A	0.2697	0.0974	(-0.1112, 0.6506)	2.77	0.032
DX-Mem 1 H48 - Media H48A	-0.0748	0.0974	(-0.4558, 0.3061)	-0.77	0.401
M 1 K48 - Media K48	0.2071	0.0974	(-0.1738, 0.5881)	2.13	0
DX 1 K48 - Media K48	0.9327	0.0974	(0.5518, 1.3137)	9.57	0.001
DX-Mem 1 K48 - Media K48	0.7083	0.0974	(0.3274, 1.0893)	7.27	0
Bax					
M 1 H48 - Media H48A	1.486	0.317	(0.247, 2.724)	4.69	0.096
DX 1 H48 - Media H48A	-0.255	0.317	(-1.494, 0.983)	-0.81	0.008
DX-Mem 1 H48 - Media H48A	-0.194	0.317	(-1.433, 1.045)	-0.61	0.042

		Bax cont'd			
M 1 K48 - Media K48	0.025	0.317	(-1.213, 1.264)	0.08	0.999
DX 1 K48 - Media K48	-0.005	0.317	(-1.244, 1.233)	-0.02	1
DX-Mem 1 K48 - Media K48	-0.005	0.317	(-1.244, 1.233)	-0.02	1
		p62			
M 1 H48 - Media H48A	2.098	0.191	(1.351, 2.846)	10.97	0
DX 1 H48 - Media H48A	1.203	0.191	(0.455, 1.951)	6.29	0
DX-Mem 1 H48 - Media H48A	1.534	0.191	(0.786, 2.281)	8.02	0.001
M 1 K48 - Media K48	1.577	0.191	(0.829, 2.324)	8.25	0
DX 1 K48 - Media K48	-1.031	0.191	(-1.779, -0.284)	-5.39	0.001
DX-Mem 1 K48 - Media K48	-1.031	0.191	(-1.779, -0.284)	-5.39	0.001
		Beclin-1			
M 1 H48 - Media H48A	-3.678	0.449	(-5.435, -1.921)	-8.19	0.001
DX 1 H48 - Media H48A	-3.566	0.449	(-5.323, -1.809)	-7.94	0.016
DX-Mem 1 H48 - Media H48A	-3.216	0.449	(-4.973, -1.459)	-7.16	0.023
M 1 K48 - Media K48	-1.469	0.449	(-3.226, 0.288)	-3.27	0
DX 1 K48 - Media K48	1.002	0.45	(-0.759, 2.763)	2.23	0.025
DX-Mem 1 K48 - Media K48	-0.708	0.449	(-2.465, 1.049)	-1.58	0.04
		LC3-II/LC3-I			
M 1 H48 - Media H48A	0.1964	0.0686	(-0.0717, 0.4645)	2.86	0.009
DX 1 H48 - Media H48A	-0.089	0.0686	(-0.3571, 0.1791)	-1.3	0.052
DX-Mem 1 H48 - Media H48A	-0.0005	0.0686	(-0.2686, 0.2676)	-0.01	0.989
M 1 K48 - Media K48	0.1479	0.0686	(-0.1202, 0.4160)	2.16	0.121
DX 1 K48 - Media K48	0.2661	0.0686	(-0.0020, 0.5342)	3.88	0
DX-Mem 1 K48 - Media K48	0.4483	0.0686	(0.1802, 0.7164)	6.54	0

B) Dox versus Dox/Memantine and Memantine vs Dox/Memantine

Difference of Levels	Difference of Means	SE of Difference	95% CI	T-Value	Adjusted P-Value
		Bcl-2			
DX-Mem 1 H48 - M 1 H48	-0.6612	0.0321	(-0.7865, -0.5358)	-20.62	0.002
DX 1 H48 - DX-Mem 1 H48	-0.4636	0.0321	(-0.5890, -0.3382)	-14.46	0.001
DX 1 K48 - DX-Mem 1 K48	0.02	0.0321	(-0.1054, 0.1454)	0.62	0
DX-Mem 1 K48 - M 1 K48	-0.0434	0.0321	(-0.1688, 0.0820)	-1.35	0.003
		Bcl-xL			
DX-Mem 1 H48 - M 1 H48	-1.712	0.248	(-2.683, -0.741)	-6.89	0.002
DX 1 H48 - DX-Mem 1 H48	-0.332	0.248	(-1.303, 0.639)	-1.34	0.008
DX-Mem 1 K48 - M 1 K48	-0.38	0.248	(-1.352, 0.591)	-1.53	0.031

		Bcl-xL cont'd			
DX 1 K48 - DX-Mem 1 K48	-0.449	0.248	(-1.420, 0.522)	-1.81	0.016
Bak					
DX-Mem 1 H48 - M 1 H48	-7.107	0.803	(-10.248, -3.967)	-8.85	0.003
DX 1 H48 - DX-Mem 1 H48	-2.464	0.803	(-5.604, 0.677)	-3.07	0.017
DX-Mem 1 K48 - M 1 K48	-0.352	0.803	(-3.493, 2.788)	-0.44	0.004
DX 1 K48 - DX-Mem 1 K48	0.004	0.803	(-3.136, 3.145)	0.01	0.945
Cytochrome c					
DX-Mem 1 K48 - M 1 K48	0.5012	0.0974	(0.1203, 0.8821)	5.14	0
DX 1 K48 - DX-Mem 1 K48	0.2244	0.0974	(-0.1565, 0.6053)	2.3	0.095
DX-Mem 1 H48 - M 1 H48	-0.2082	0.0974	(-0.5891, 0.1728)	-2.14	0.921
DX 1 H48 - DX-Mem 1 H48	0.3445	0.0974	(-0.0364, 0.7254)	3.54	0.025
Bax					
DX-Mem 1 H48 - M 1 H48	-1.68	0.317	(-2.918, -0.441)	-5.3	0.034
DX 1 H48 - DX-Mem 1 H48	-0.061	0.317	(-1.300, 1.177)	-0.19	0.462
DX-Mem 1 K48 - M 1 K48	-0.03	0.317	(-1.269, 1.208)	-0.1	1
DX 1 K48 - DX-Mem 1 K48	0	0.317	(-1.239, 1.239)	0	1
p62					
DX-Mem 1 H48 - M 1 H48	-0.565	0.191	(-1.312, 0.183)	-2.95	0.049
DX 1 H48 - DX-Mem 1 H48	-0.33	0.191	(-1.078, 0.417)	-1.73	0.191
DX-Mem 1 K48 - M 1 K48	-2.608	0.191	(-3.356, -1.861)	-13.64	0.002
DX 1 K48 - DX-Mem 1 K48	0.518	0.213	(-0.165, 1.201)	2.43	0.05
Beclin-1					
DX-Mem 1 H48 - M 1 H48	0.462	0.449	(-1.295, 2.219)	1.03	0.024
DX 1 H48 - DX-Mem 1 H48	-0.35	0.449	(-2.107, 1.407)	-0.78	0.011
DX-Mem 1 K48 - M 1 K48	0.761	0.449	(-0.996, 2.518)	1.69	0
DX 1 K48 - DX-Mem 1 K48	1.71	0.45	(-0.050, 3.471)	3.8	0.698
LC3-II/LC3-I					
DX-Mem 1 H48 - M 1 H48	-0.1969	0.0686	(-0.4650, 0.0712)	-2.87	0.039
DX 1 H48 - DX-Mem 1 H48	-0.0885	0.0686	(-0.3566, 0.1796)	-1.29	0.019
DX-Mem 1 K48 - M 1 K48	0.3004	0.0686	(0.0323, 0.5685)	4.38	0.297
DX 1 K48 - DX-Mem 1 K48	-0.1822	0.0686	(-0.4503, 0.0859)	-2.66	0.013

Where,

H48= HEK293T cells treated for 48 h; K48= K-562 cells treated for 48 h;

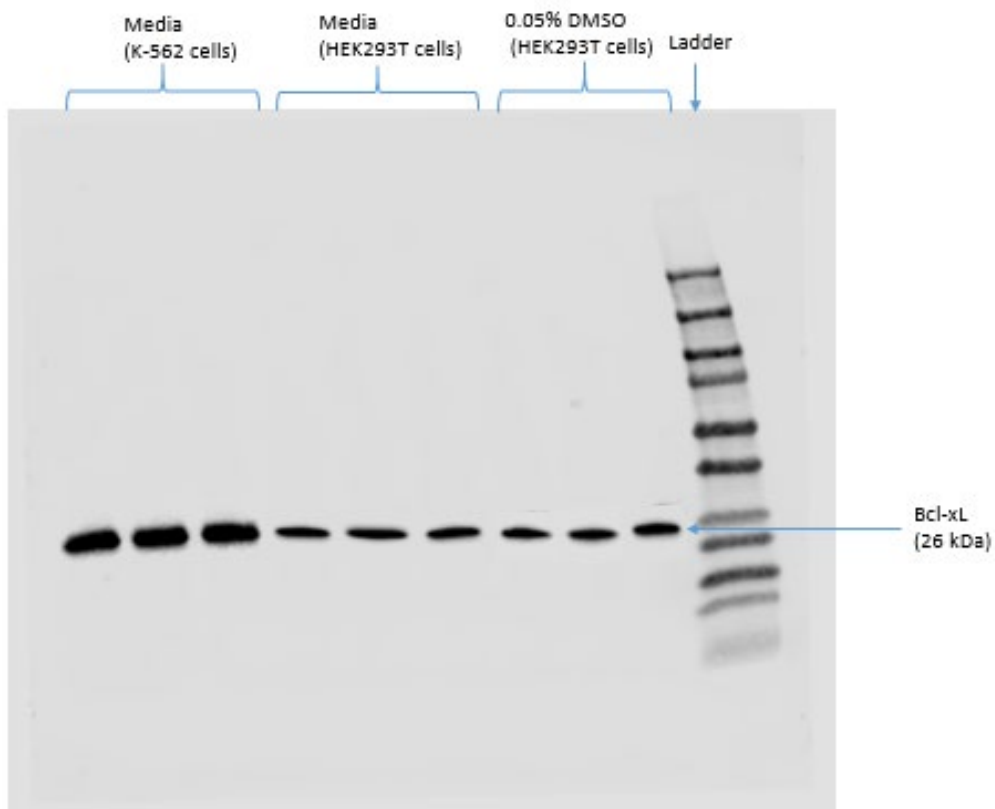
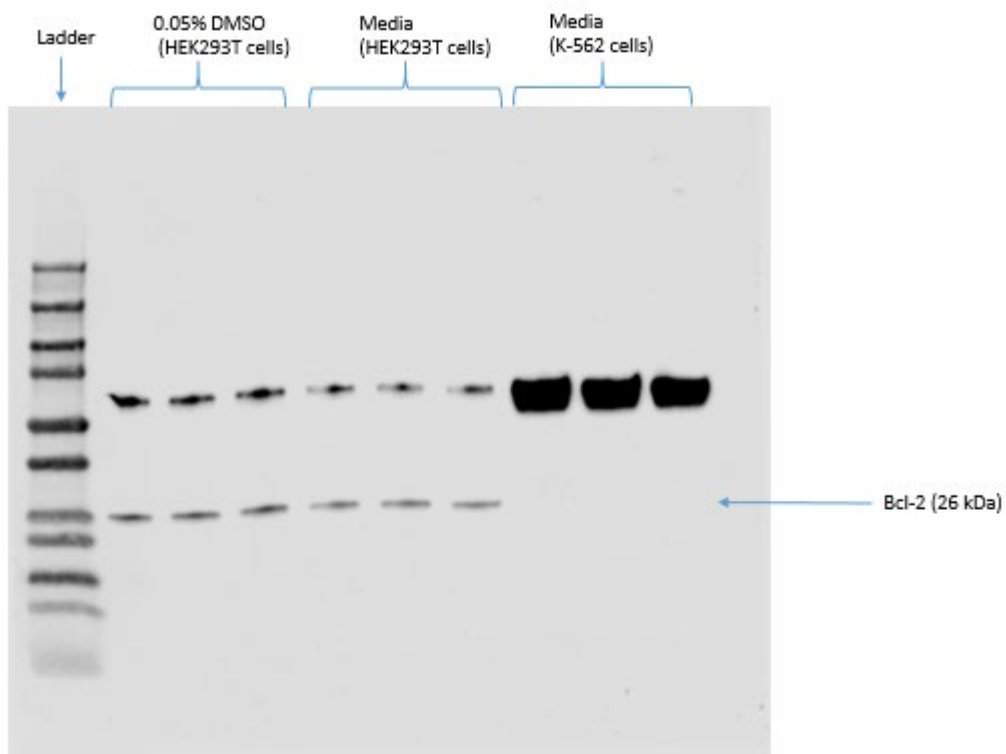
DX 1= Dox 1 μ M; M1= Memantine 1 μ M;

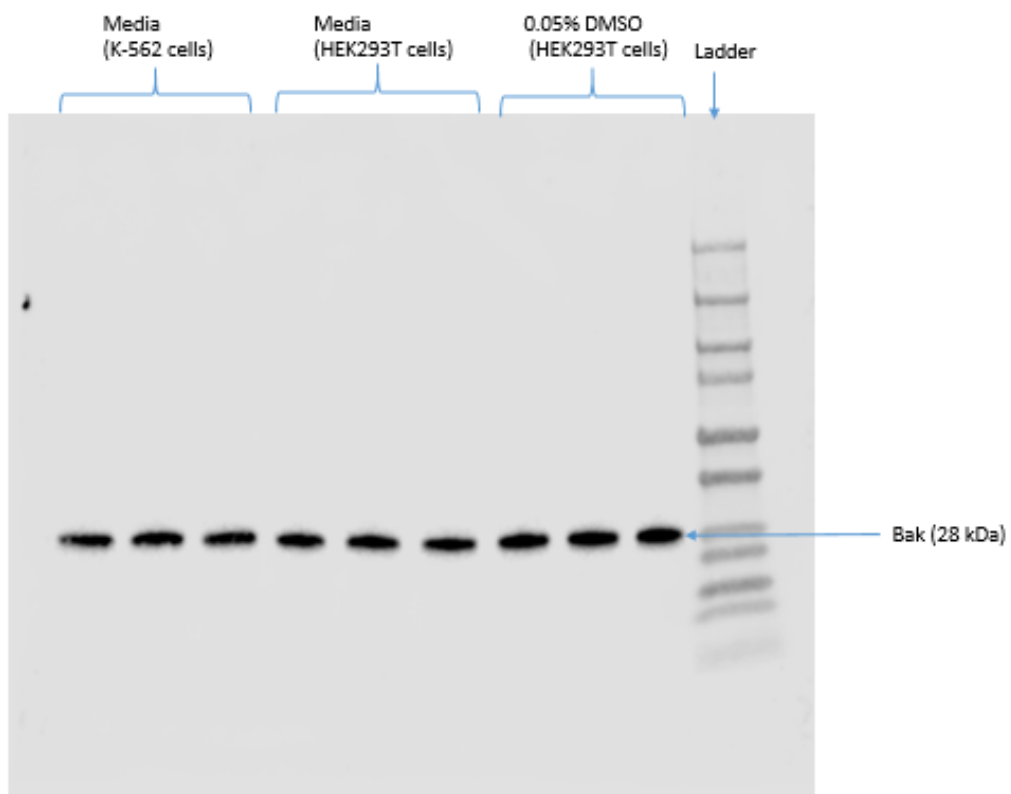
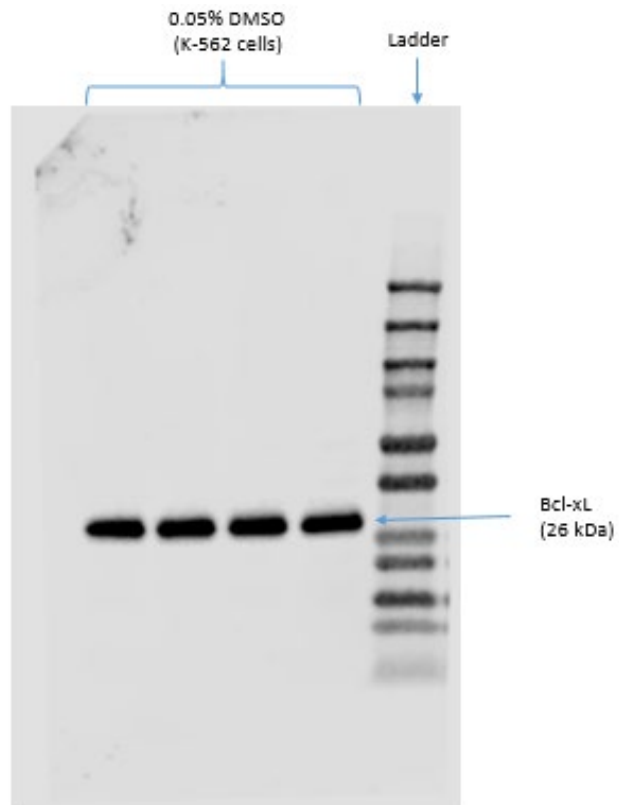
DX-Mem 1= Dox/ Memantine (1 μ M) combination treatment

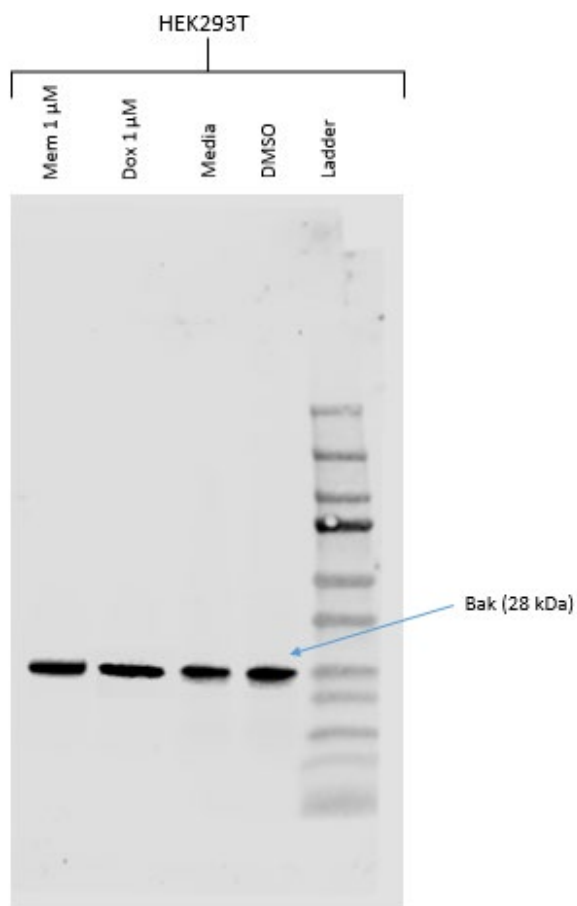
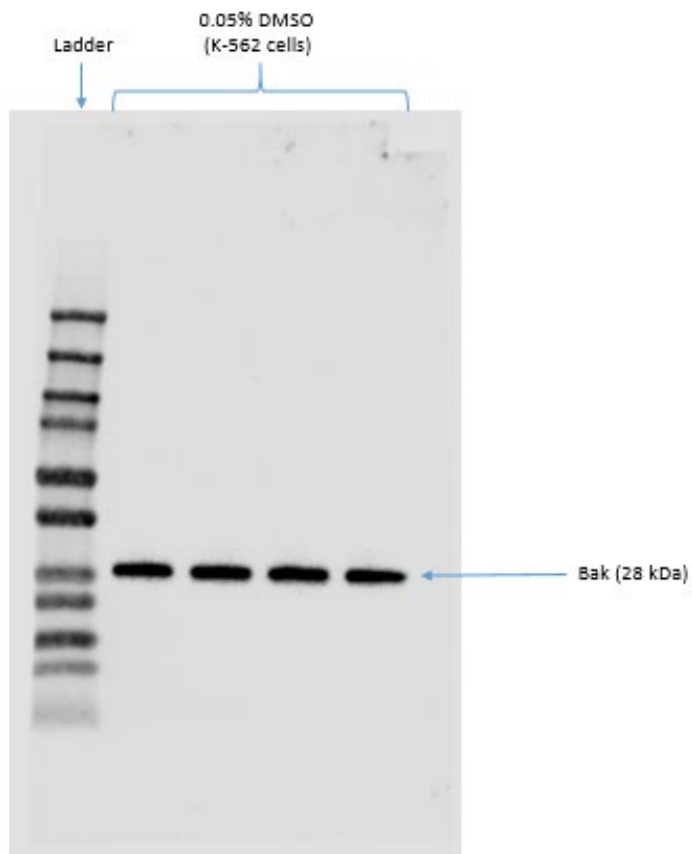
H48= 48 h, Ctrl- Control

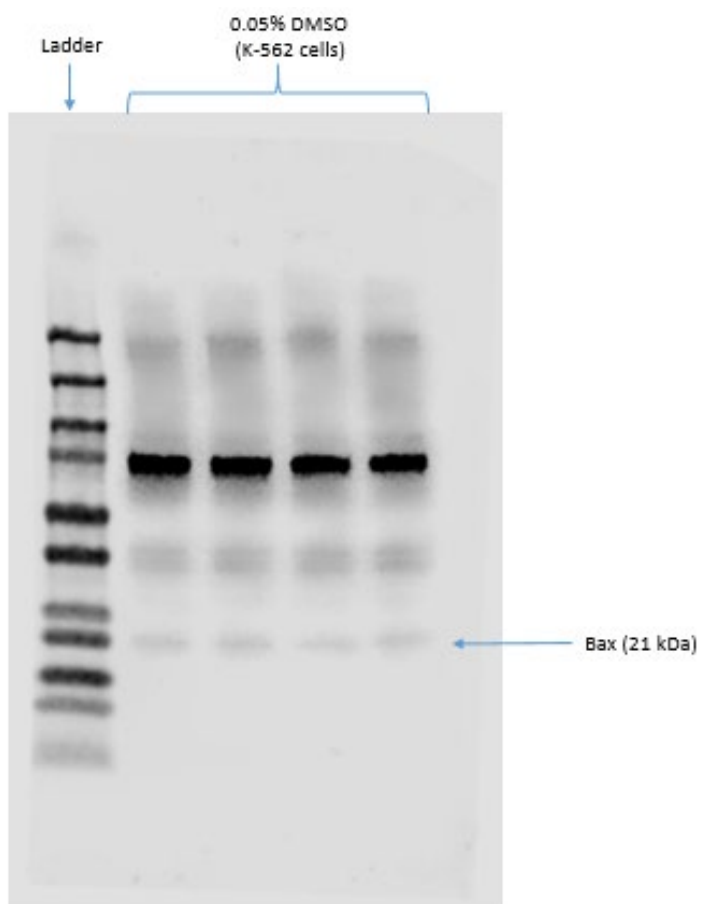
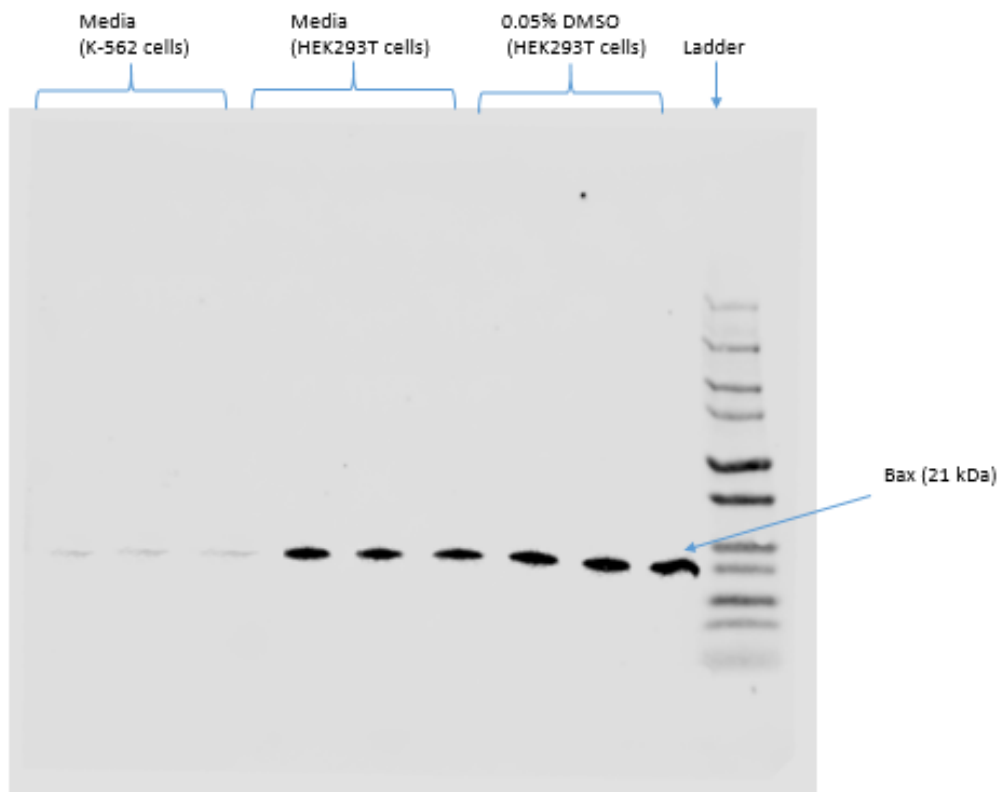
Appendix XI: Representative photos of some of the gels acquired from the Western blot analyses carried out

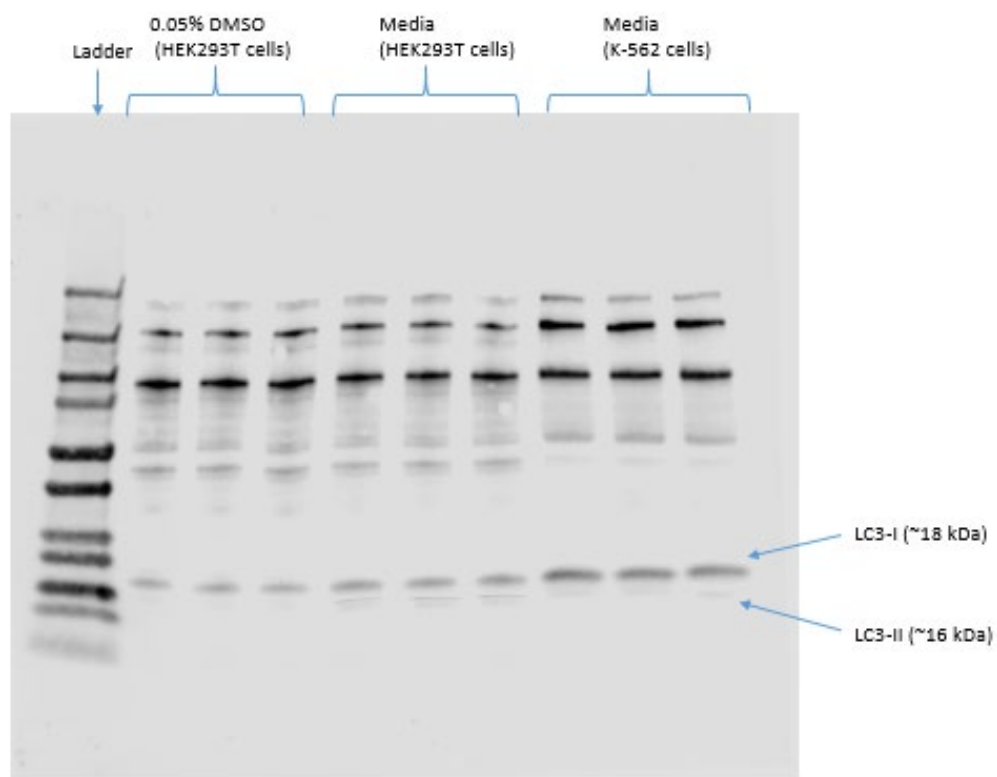
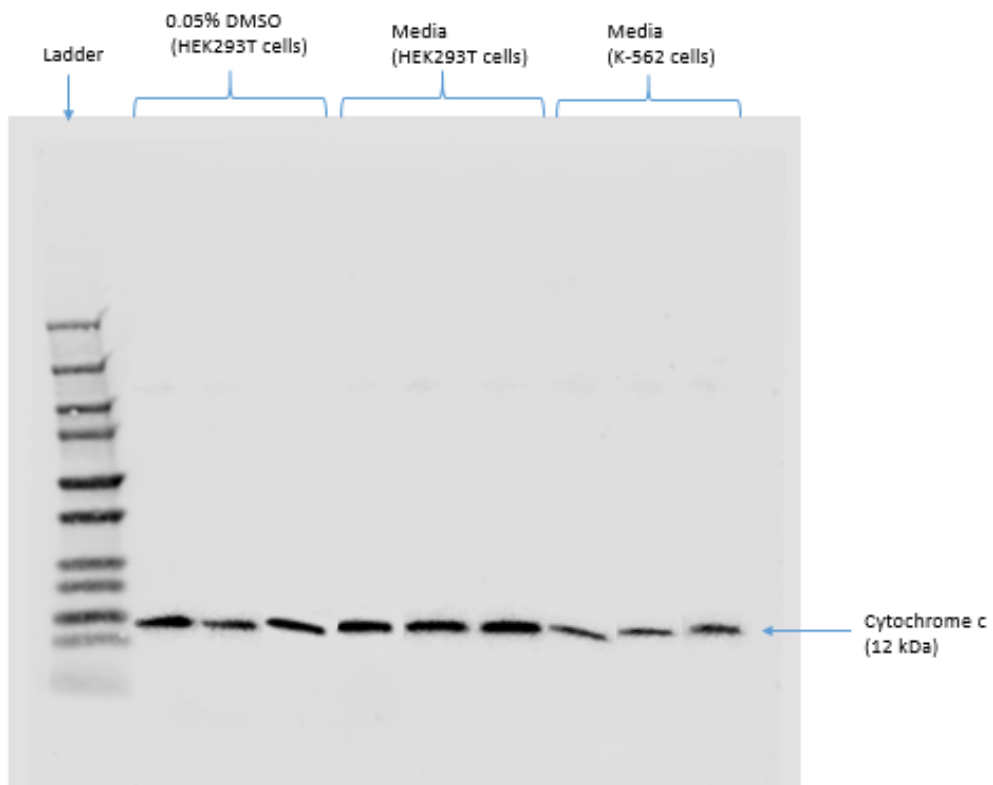
1) DMSO and Media – HEK293T and K-562 cells

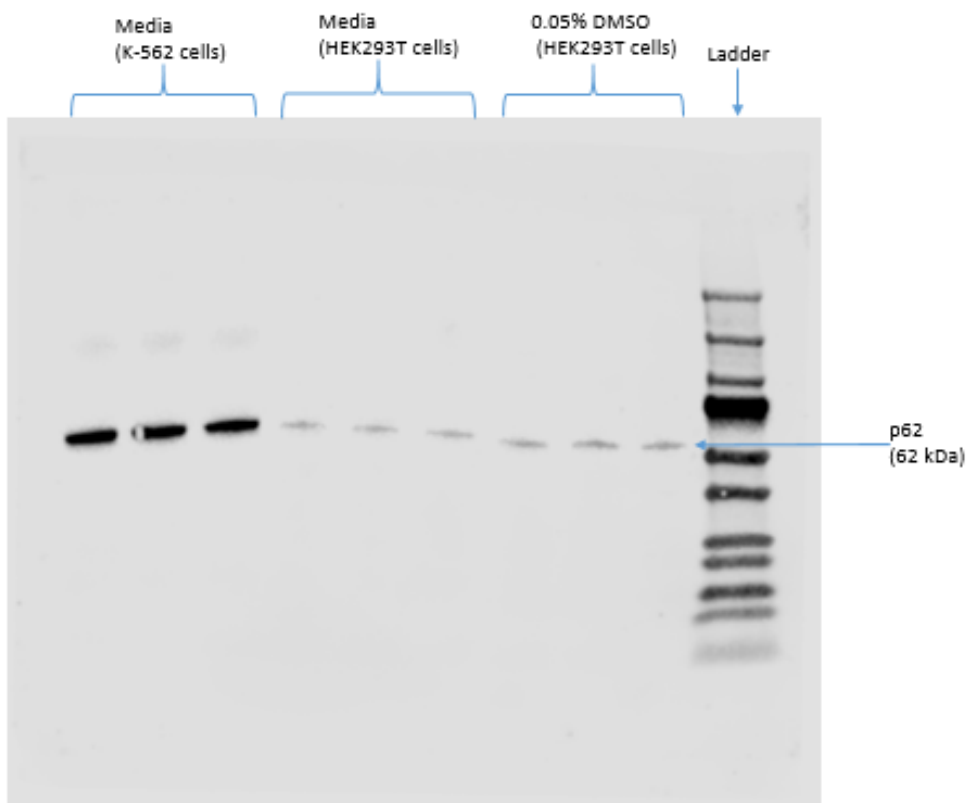
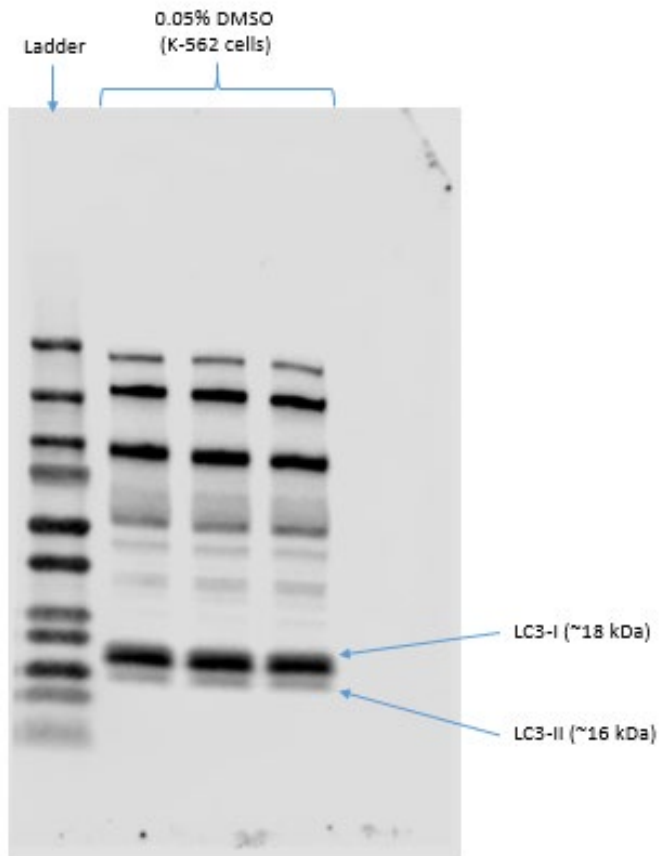


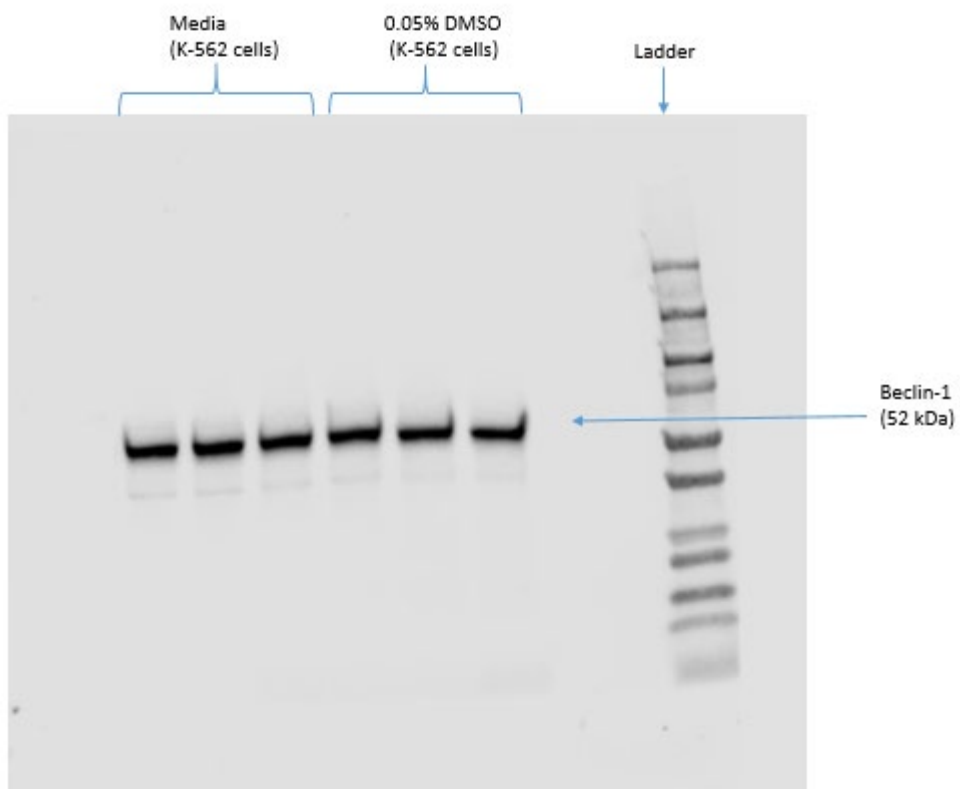
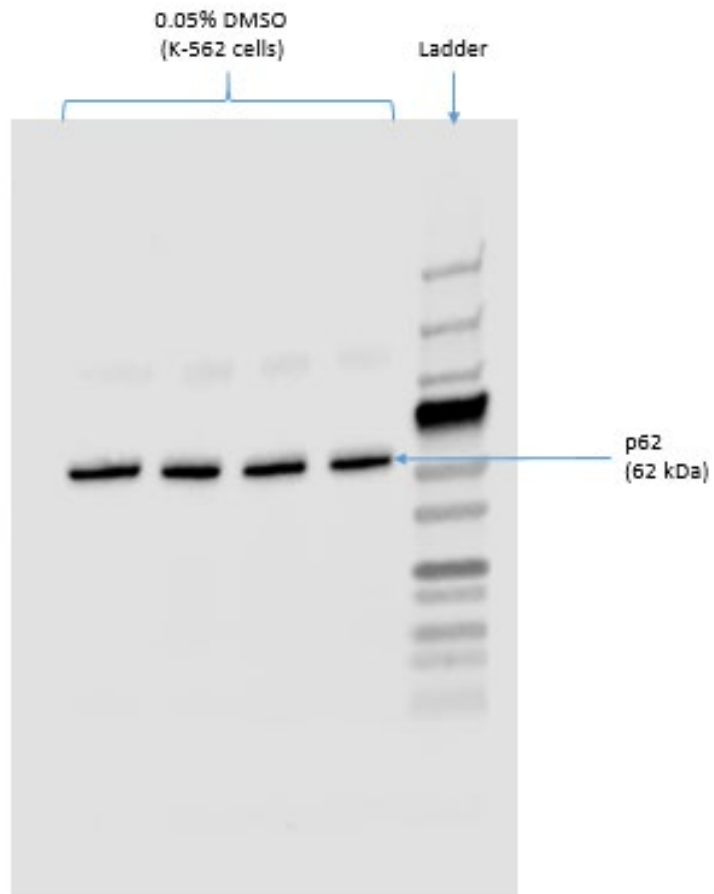


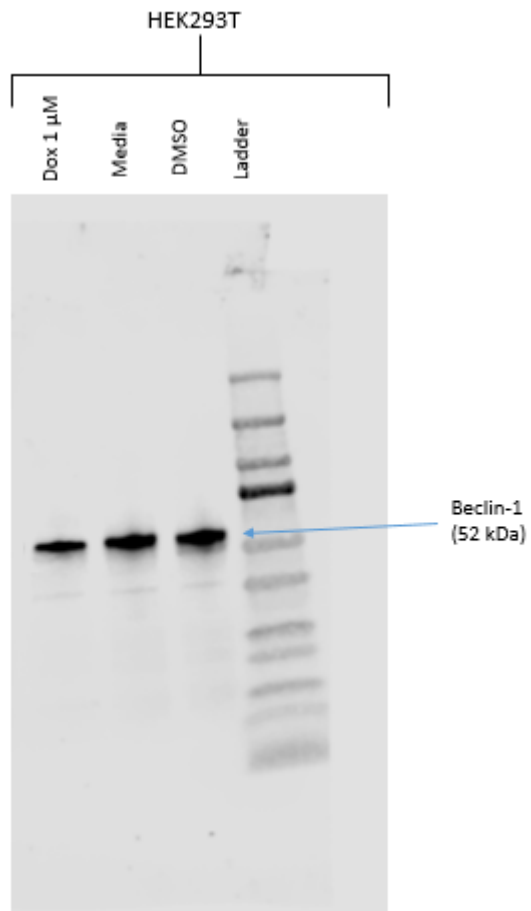




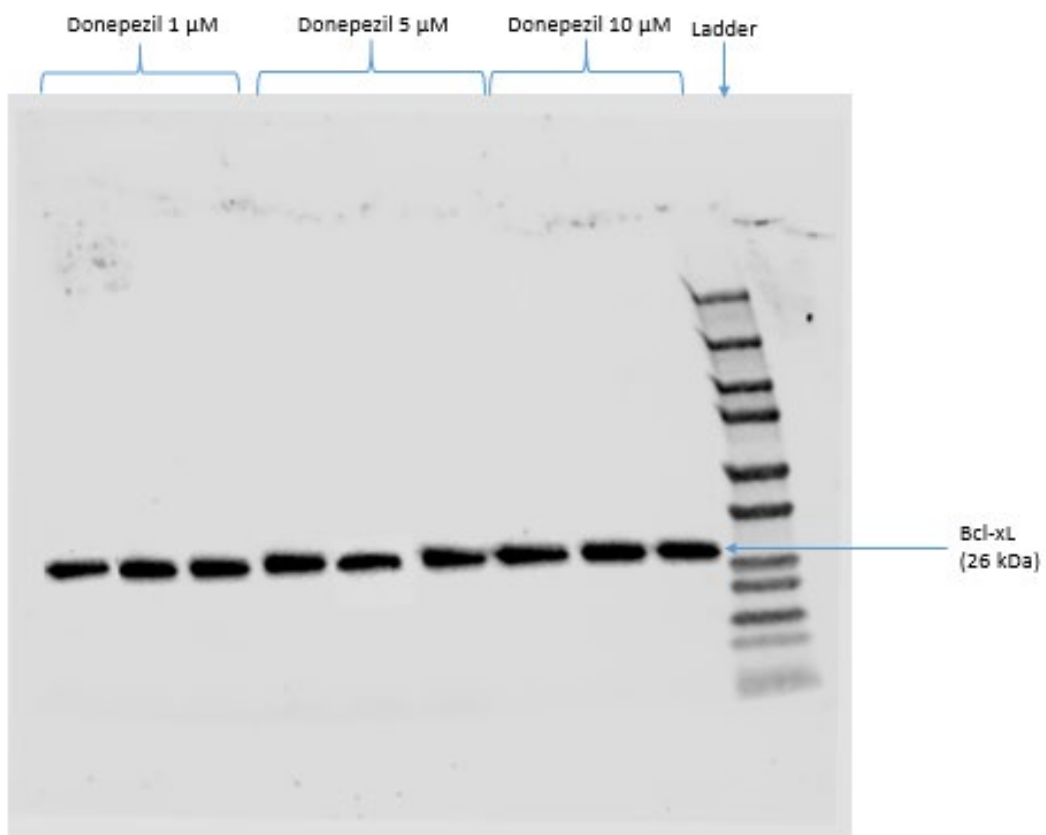
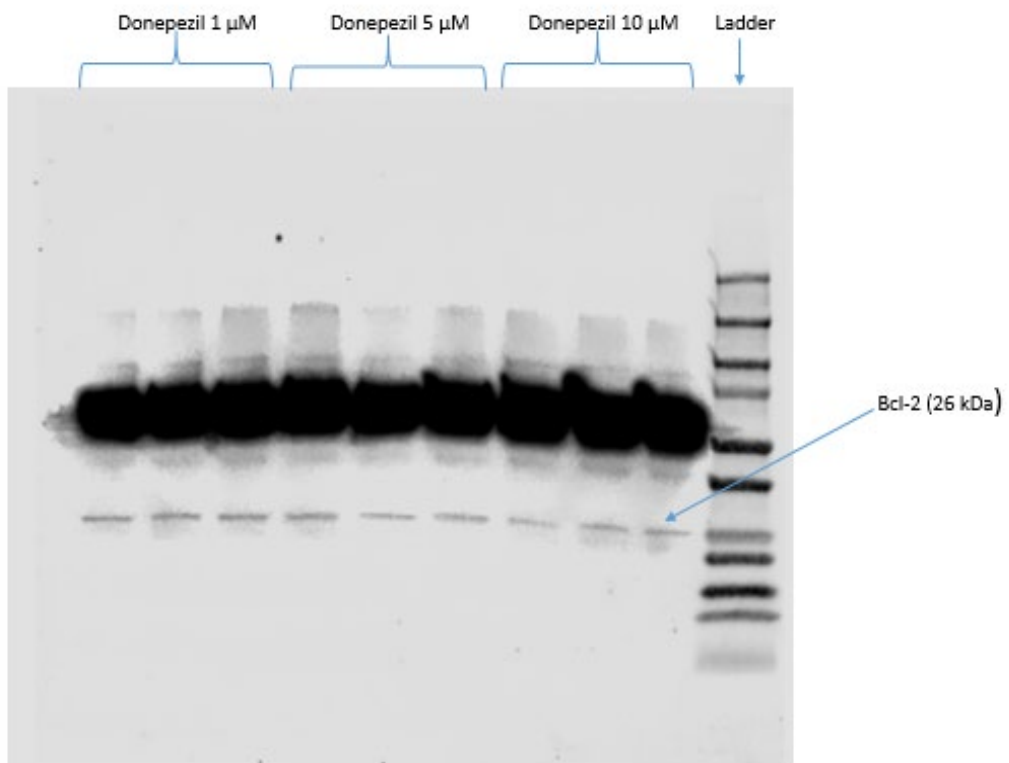


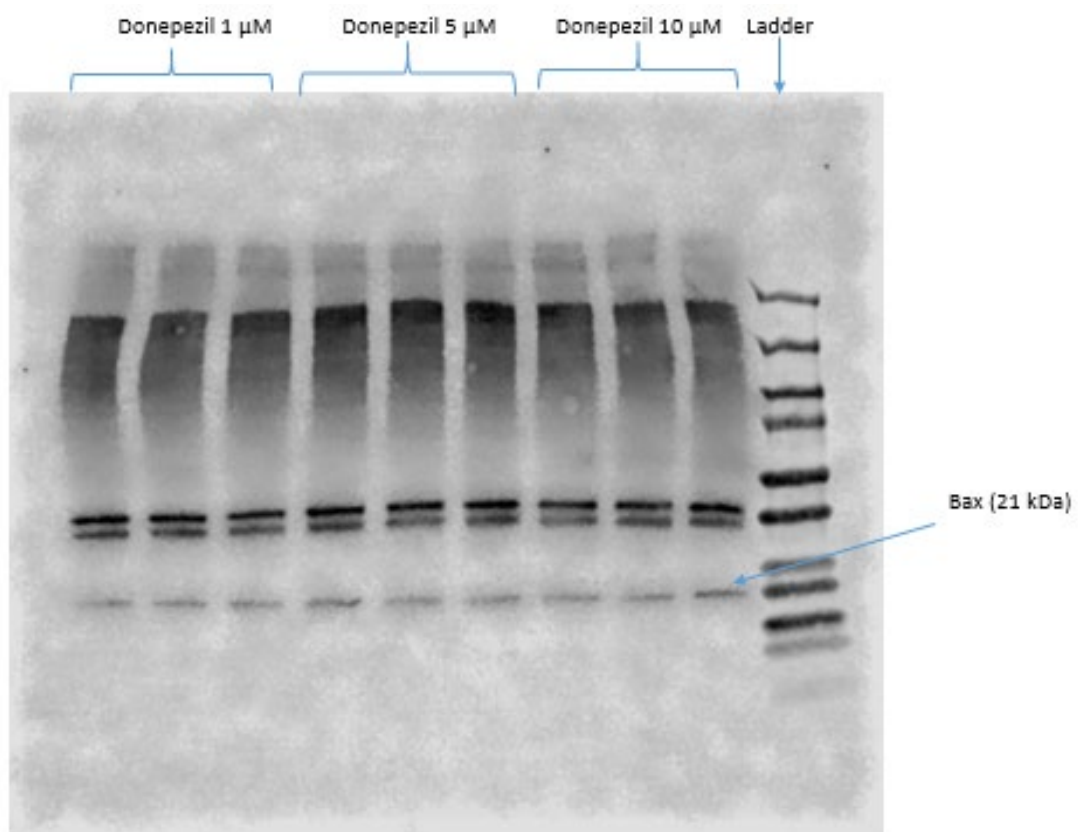
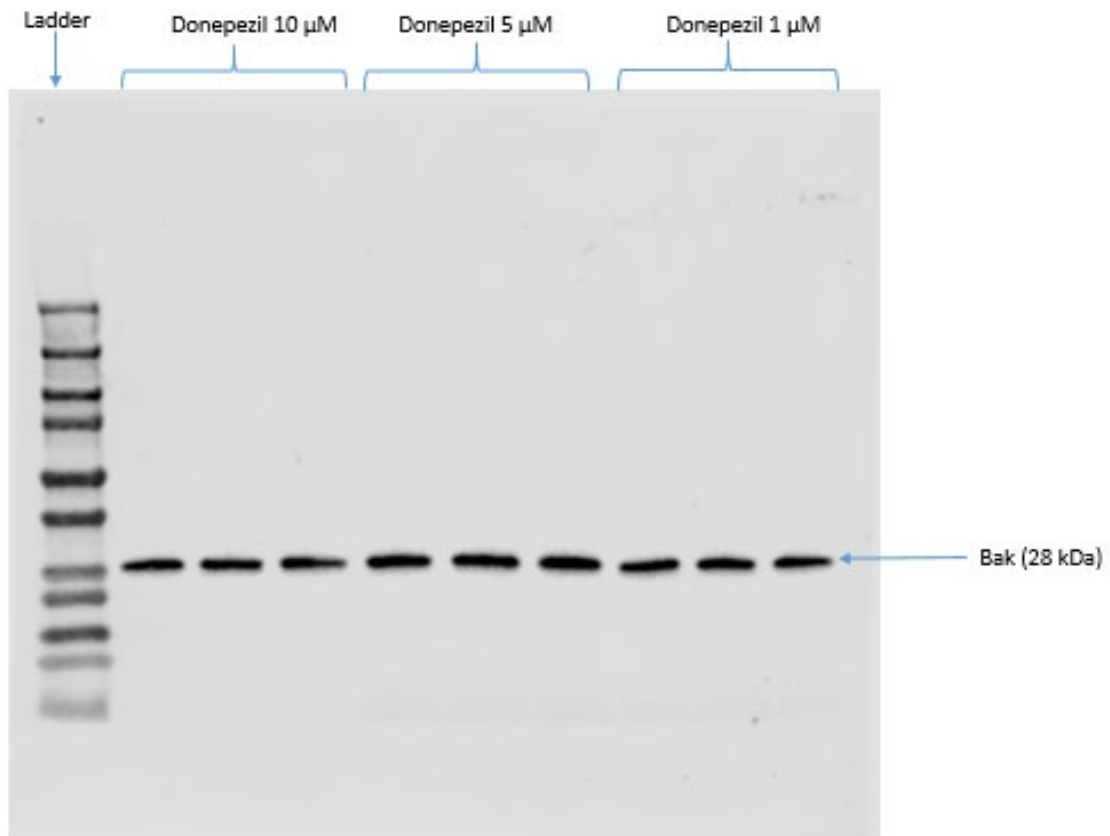


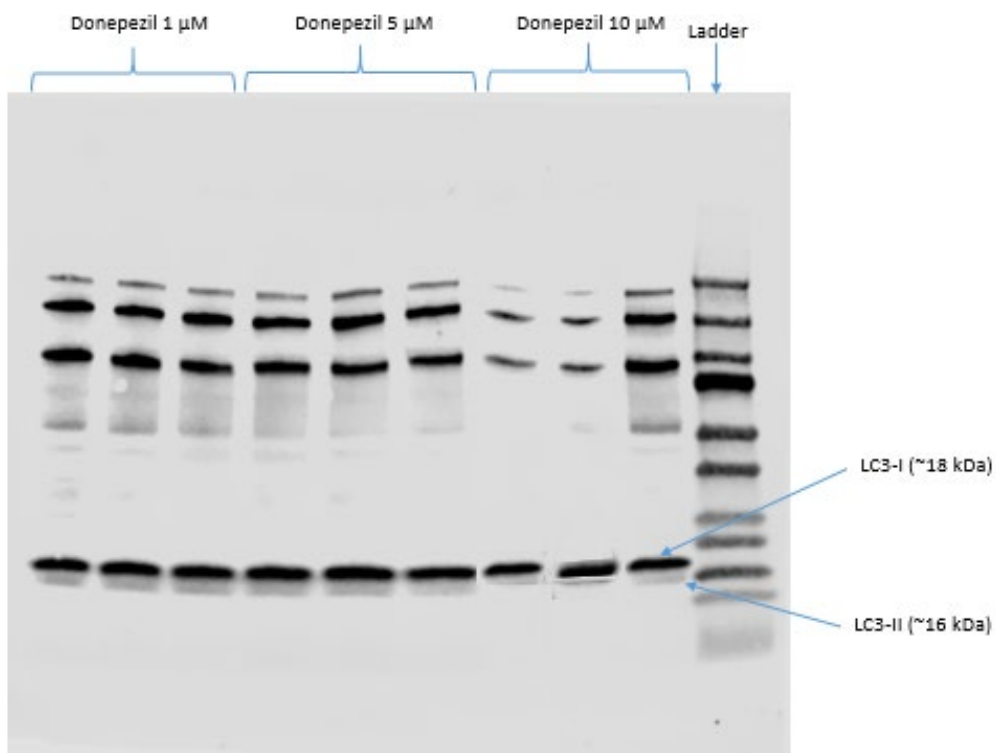
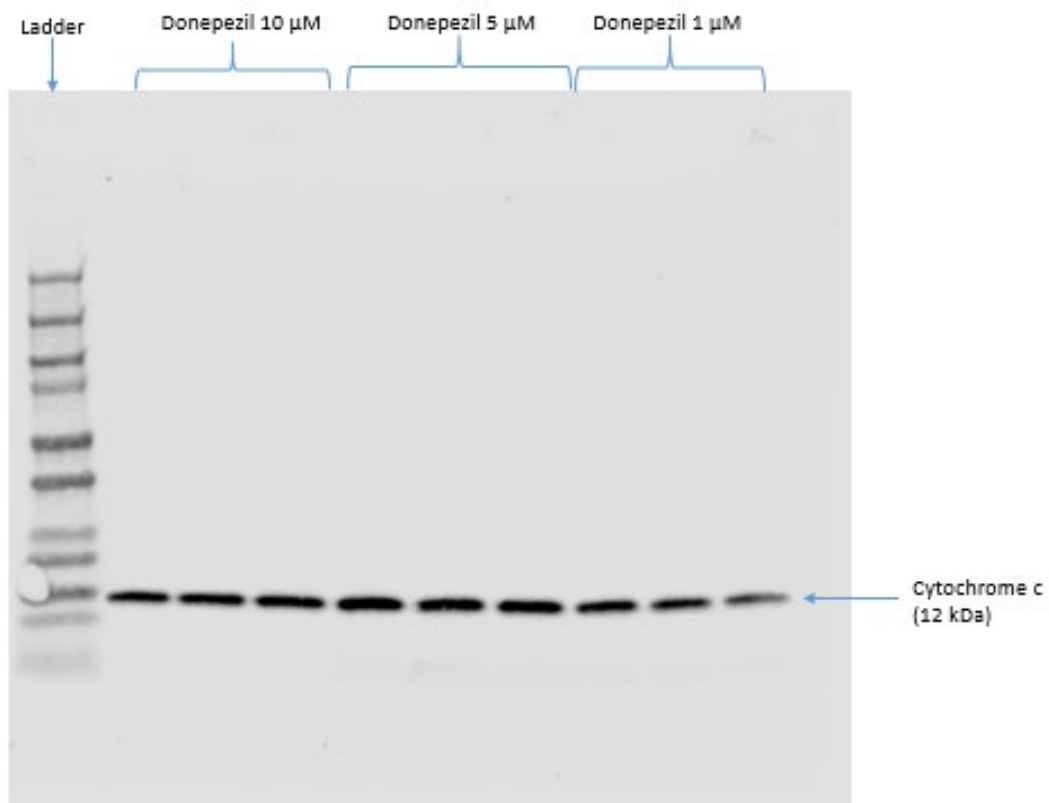


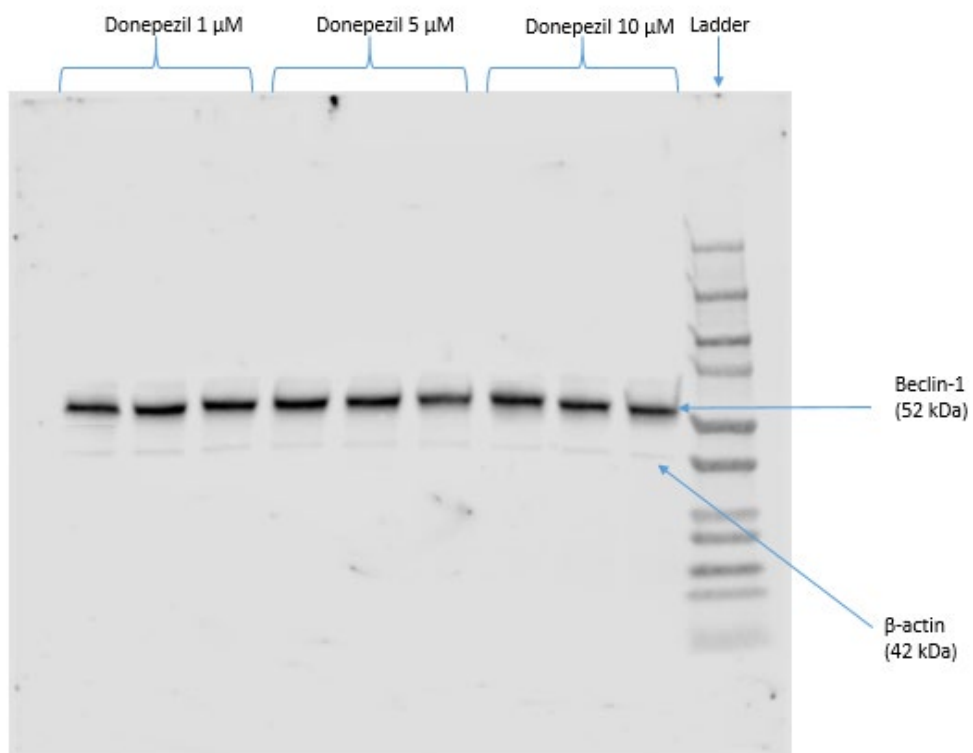
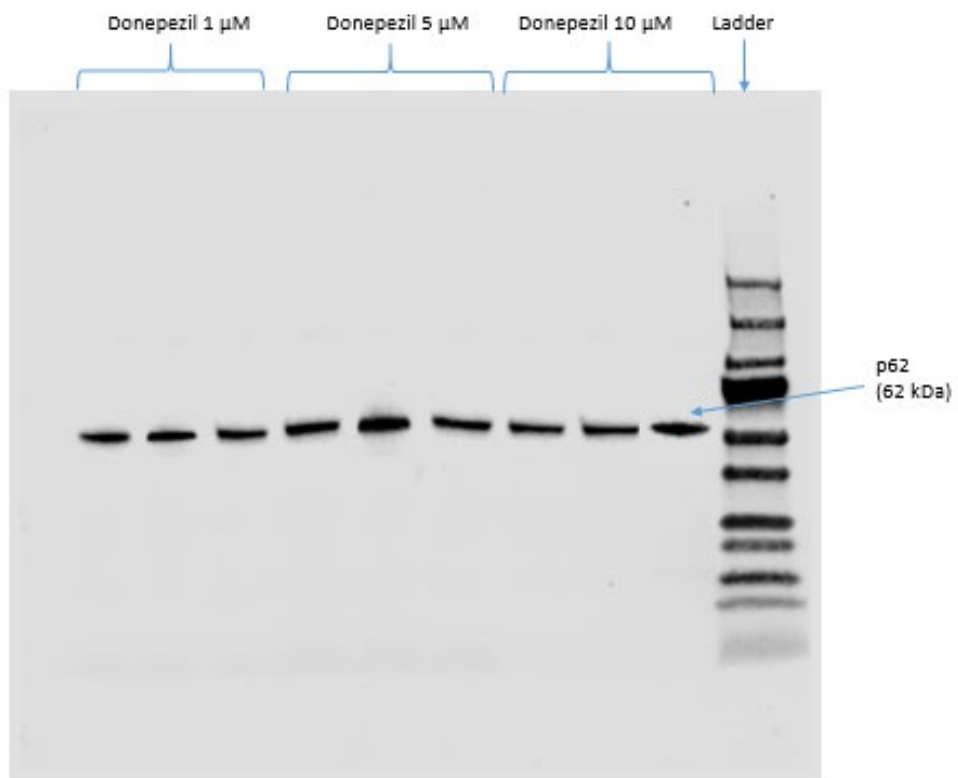


2a) Donepezil 1, 5, 10 μ M (K-562 cells)

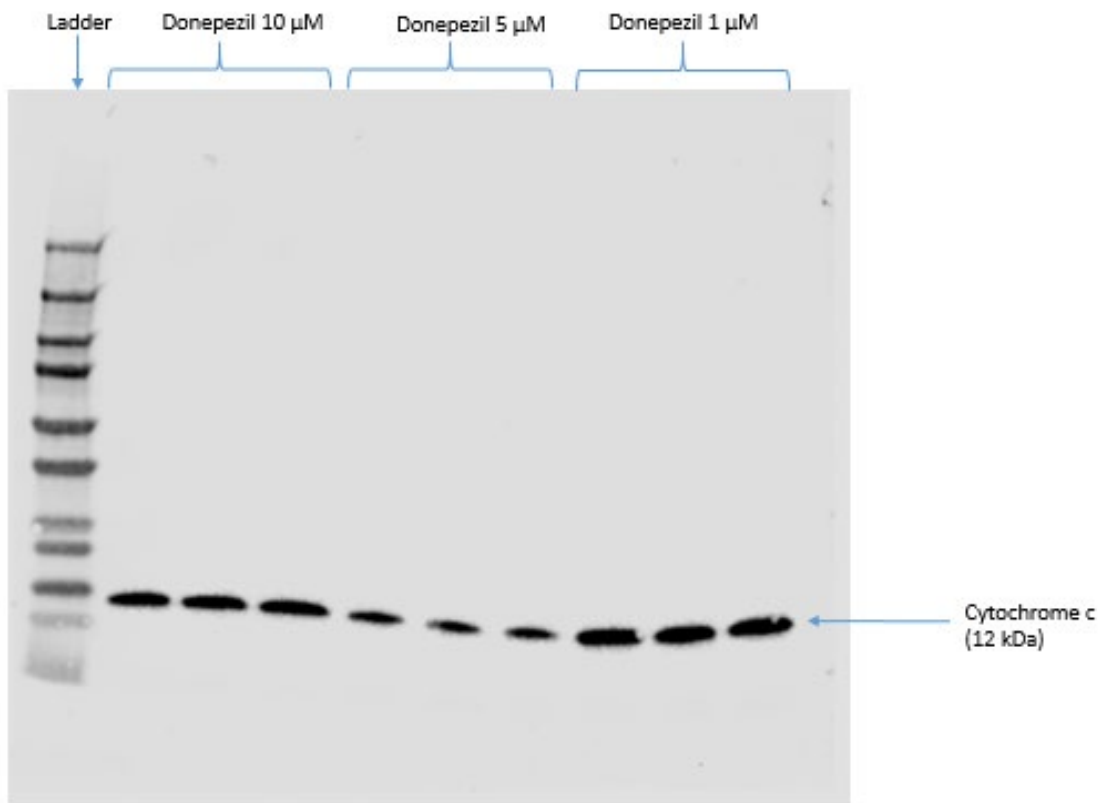
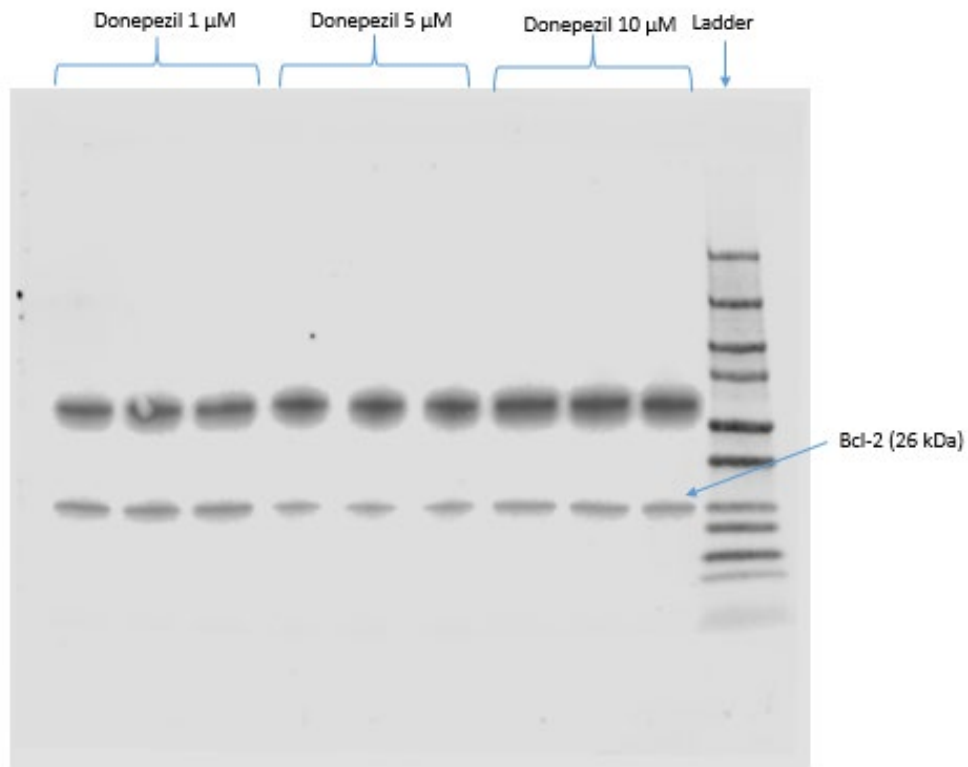


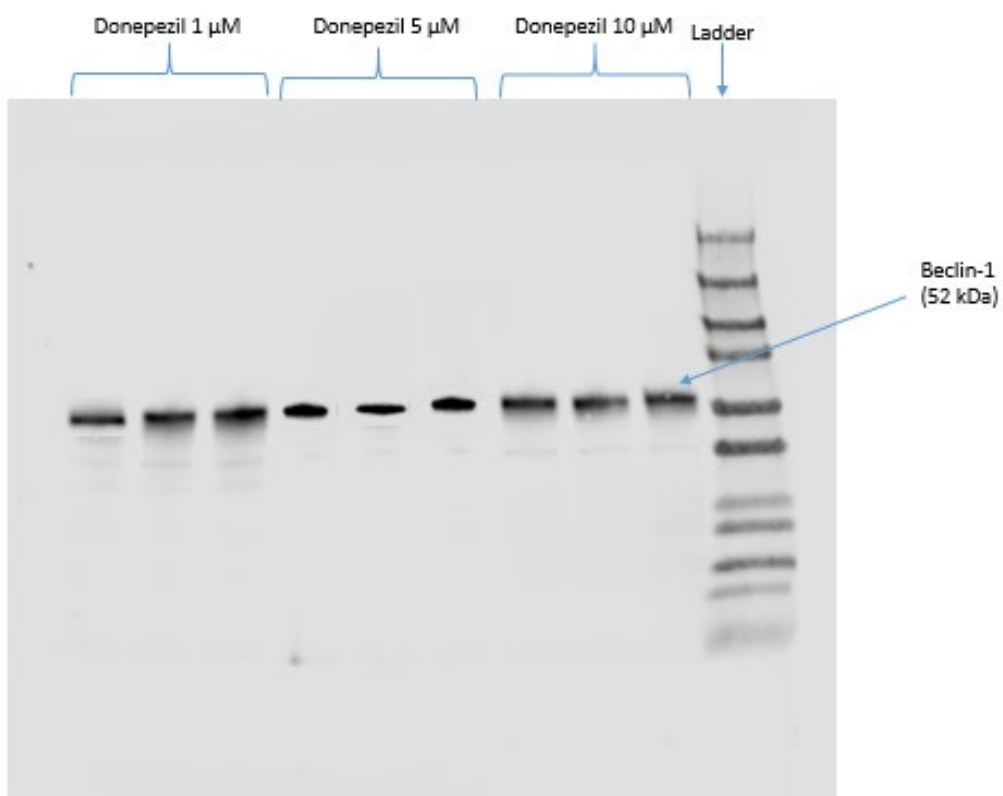
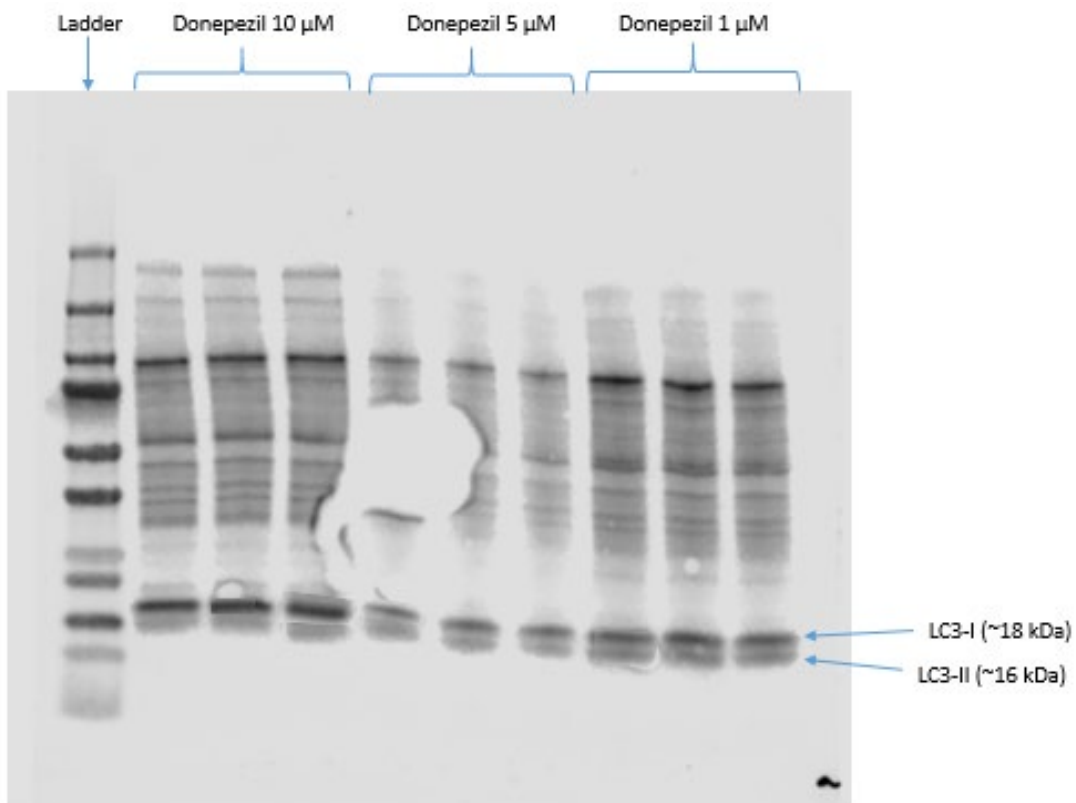




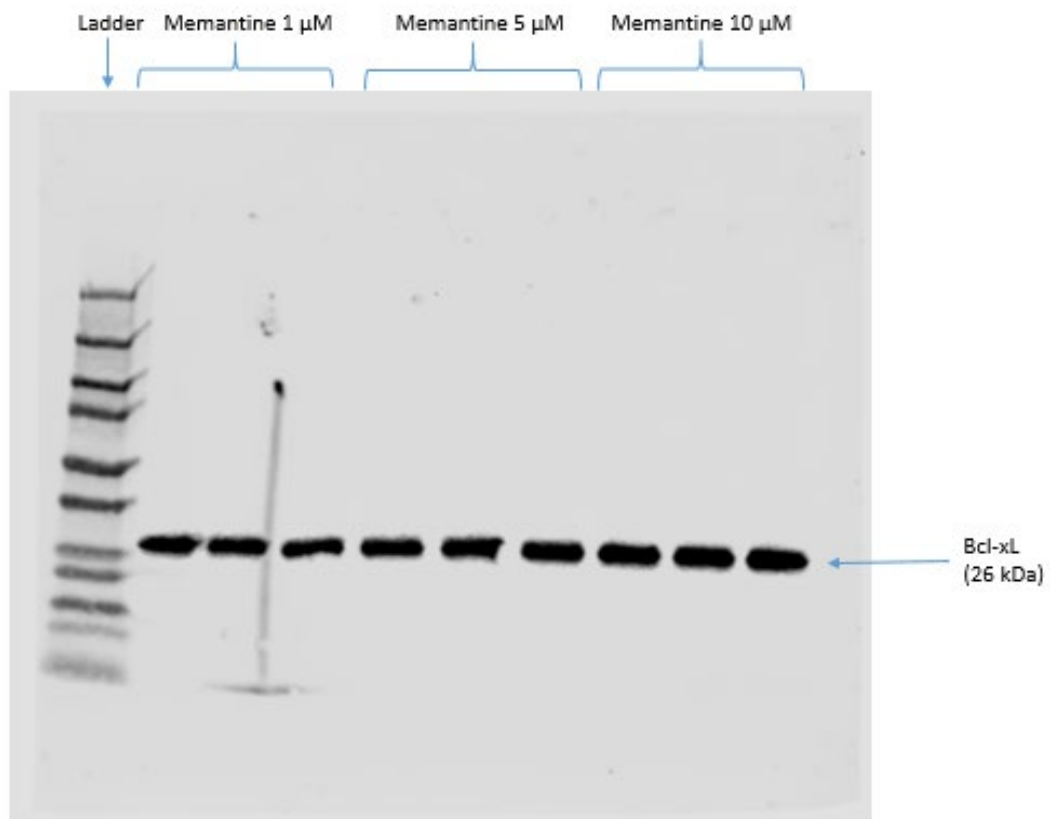
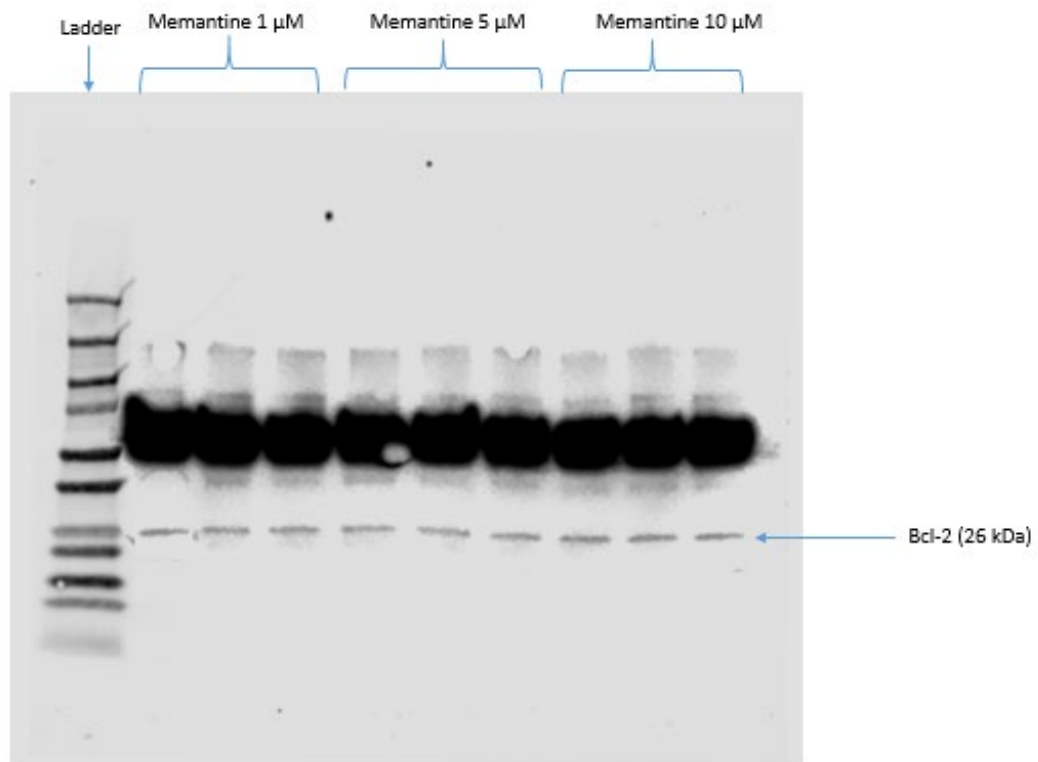


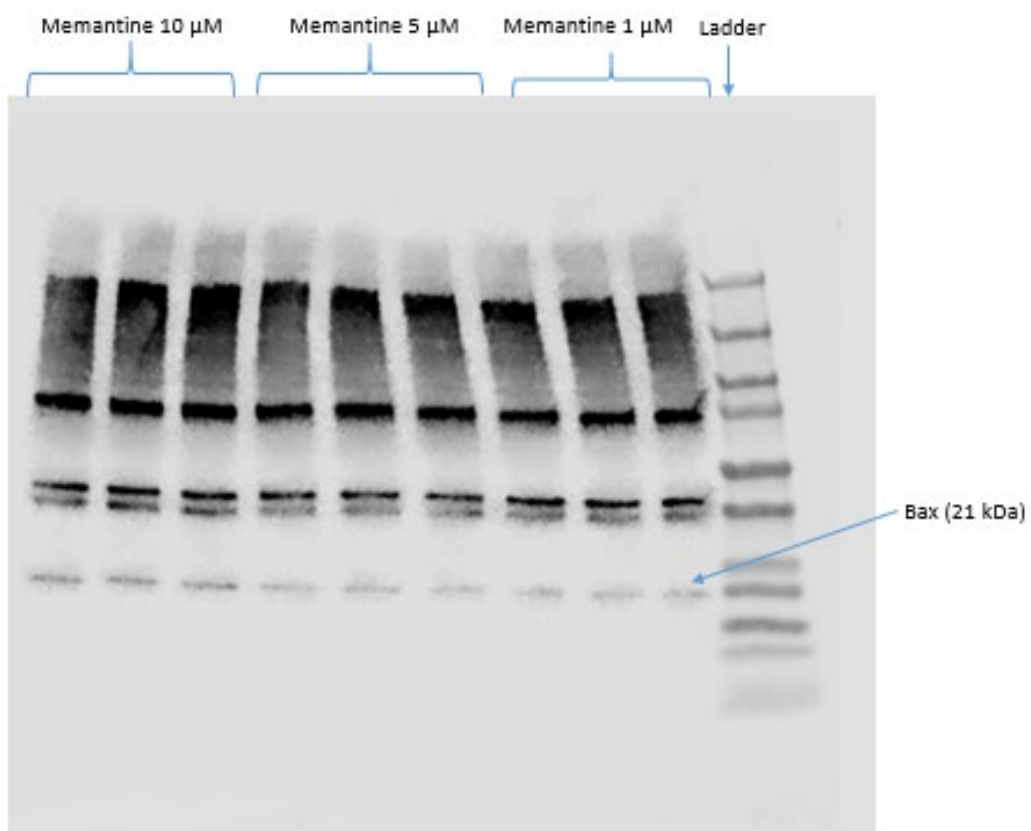
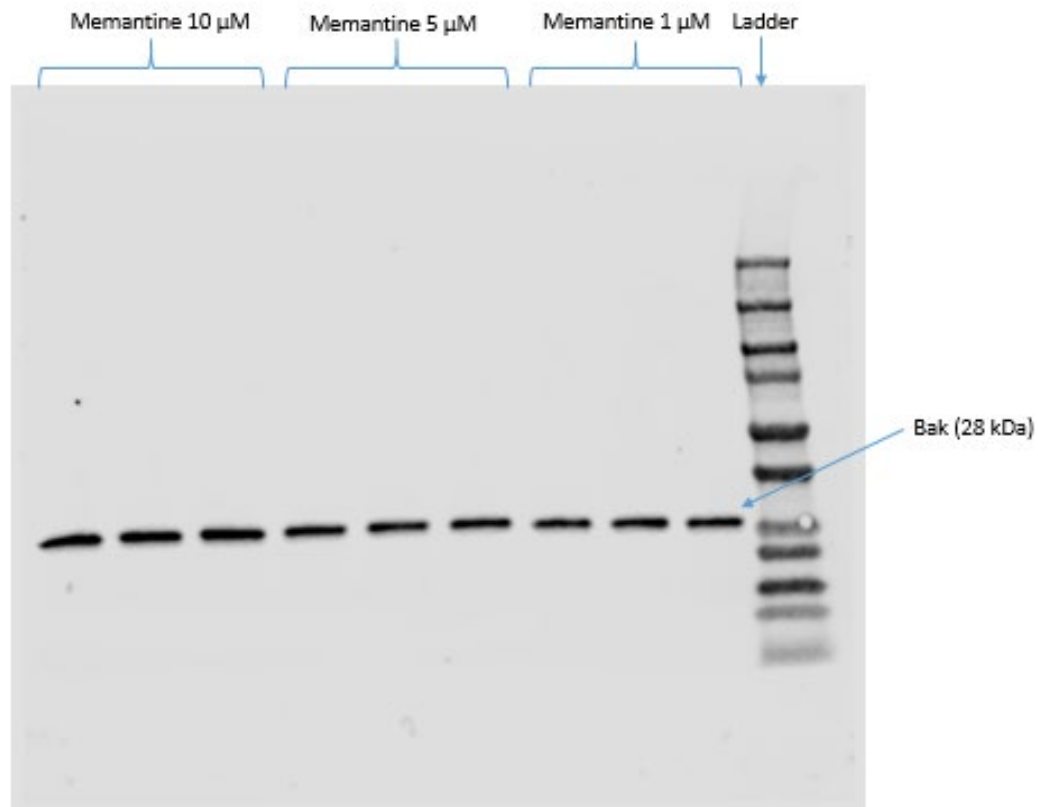
2b) Donepezil 1, 5, 10 μ M (HEK293T cells)

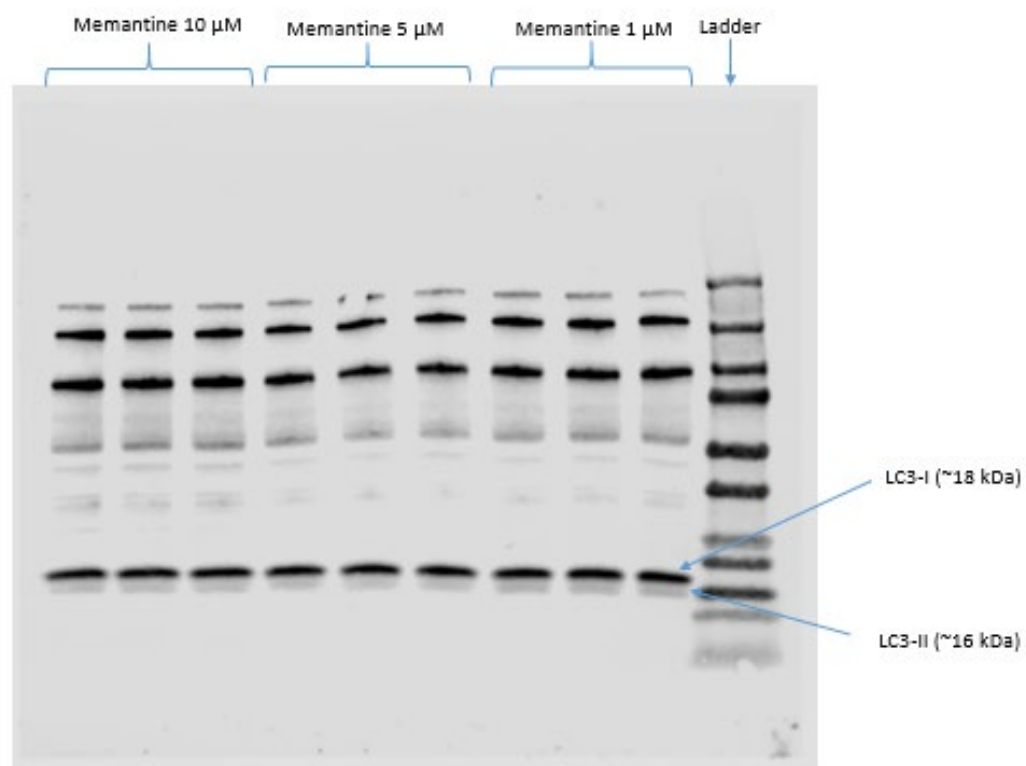
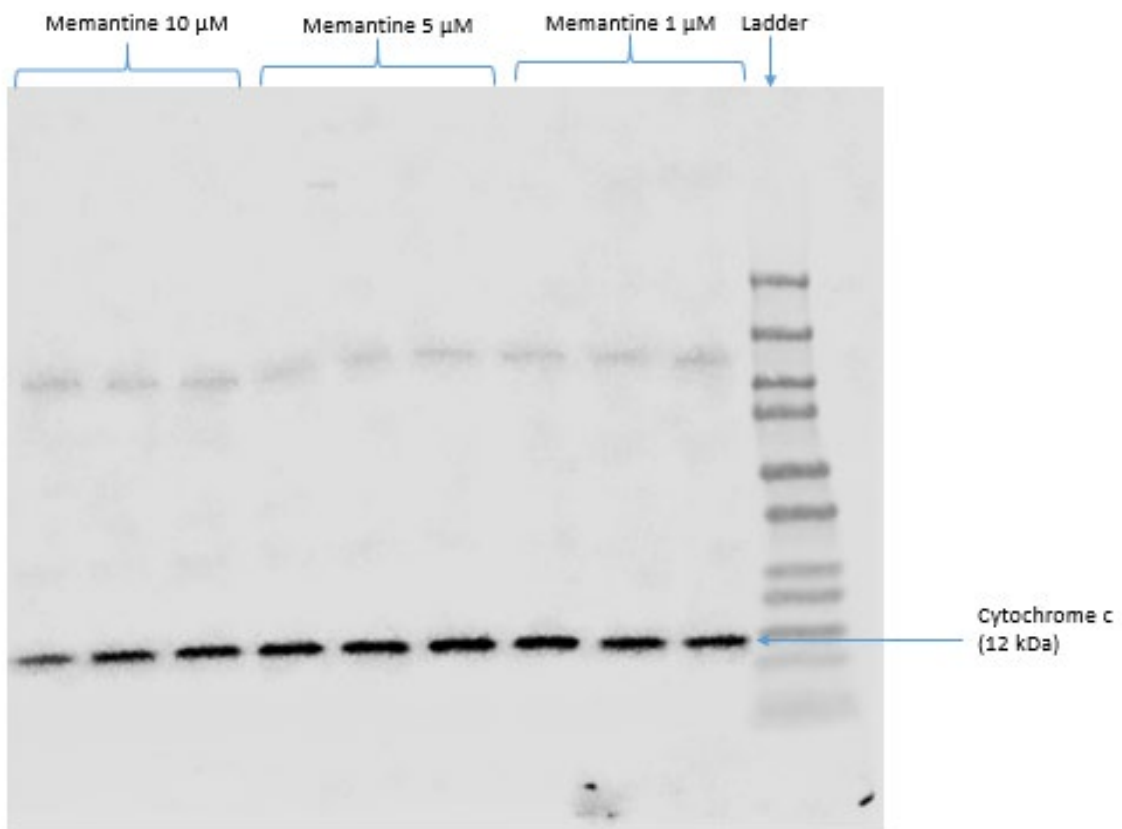


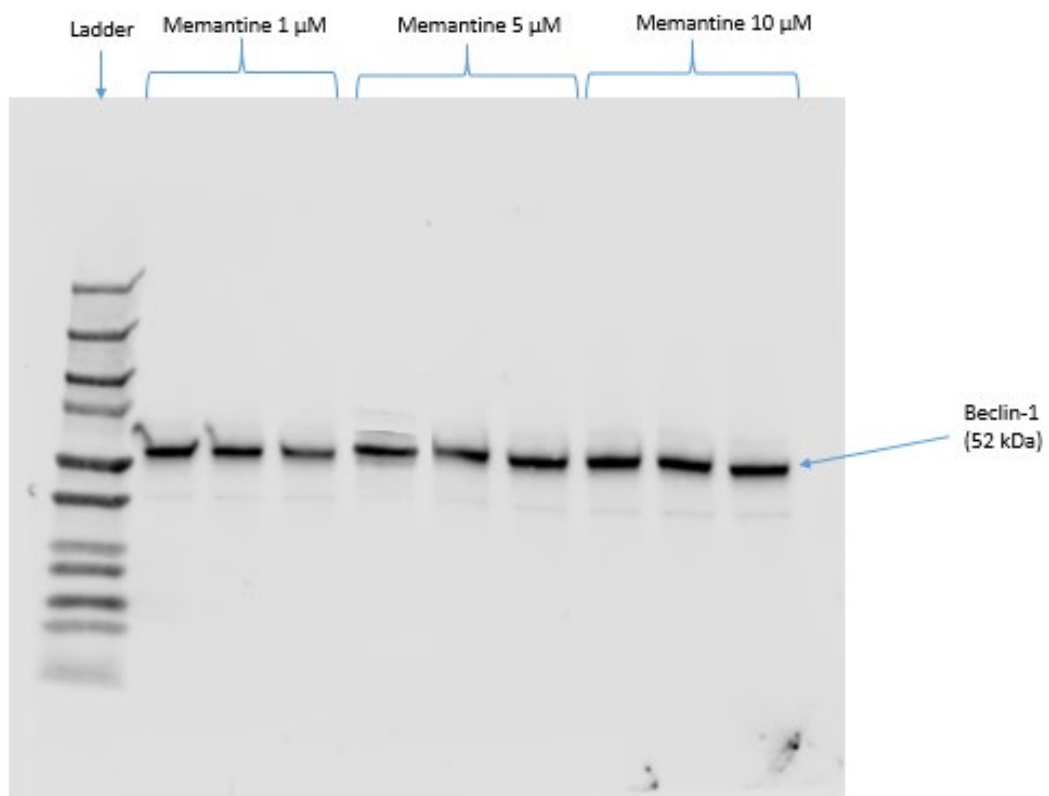
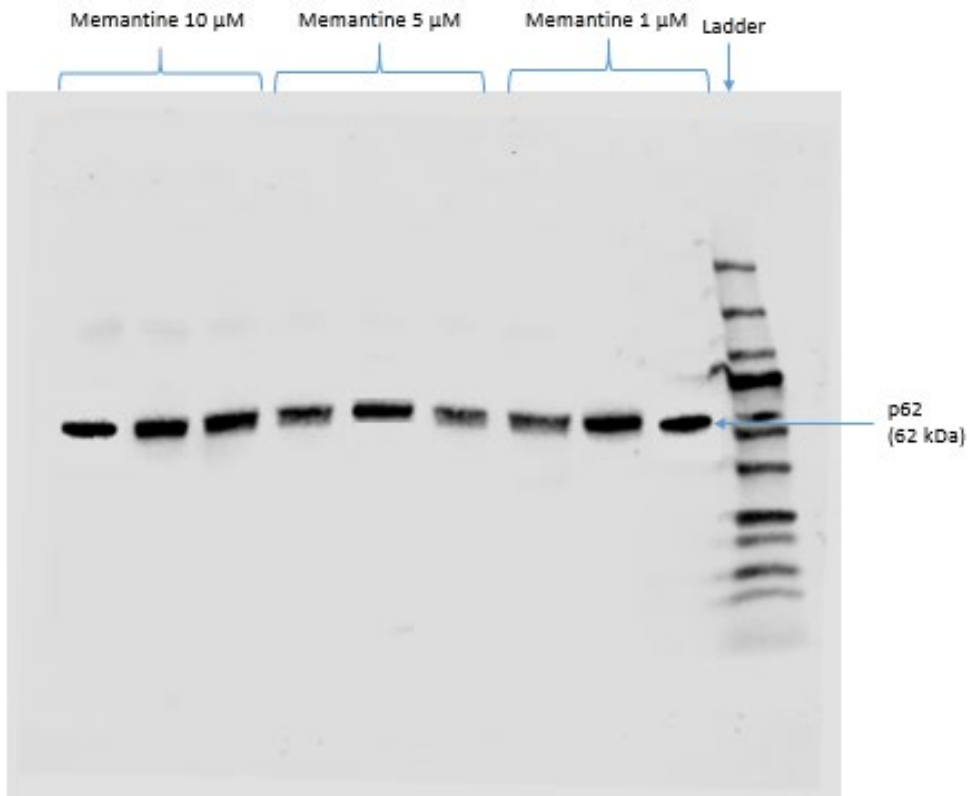


3a) Memantine 1, 5, 10 μ M (K-562 cells)

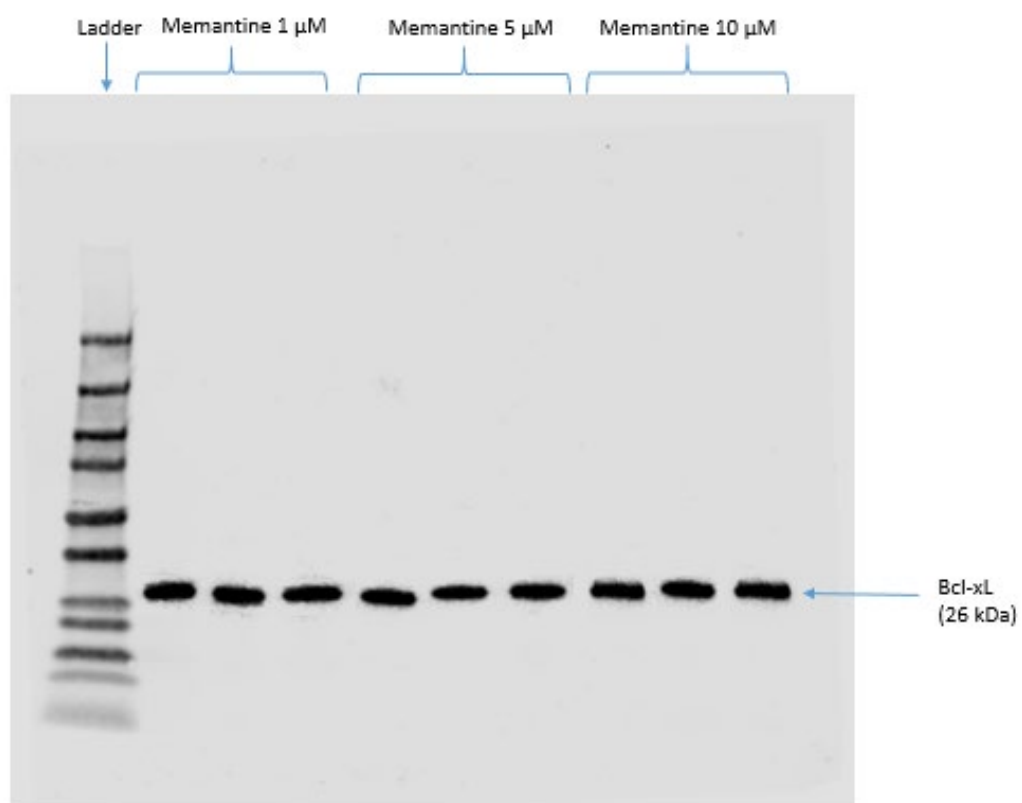
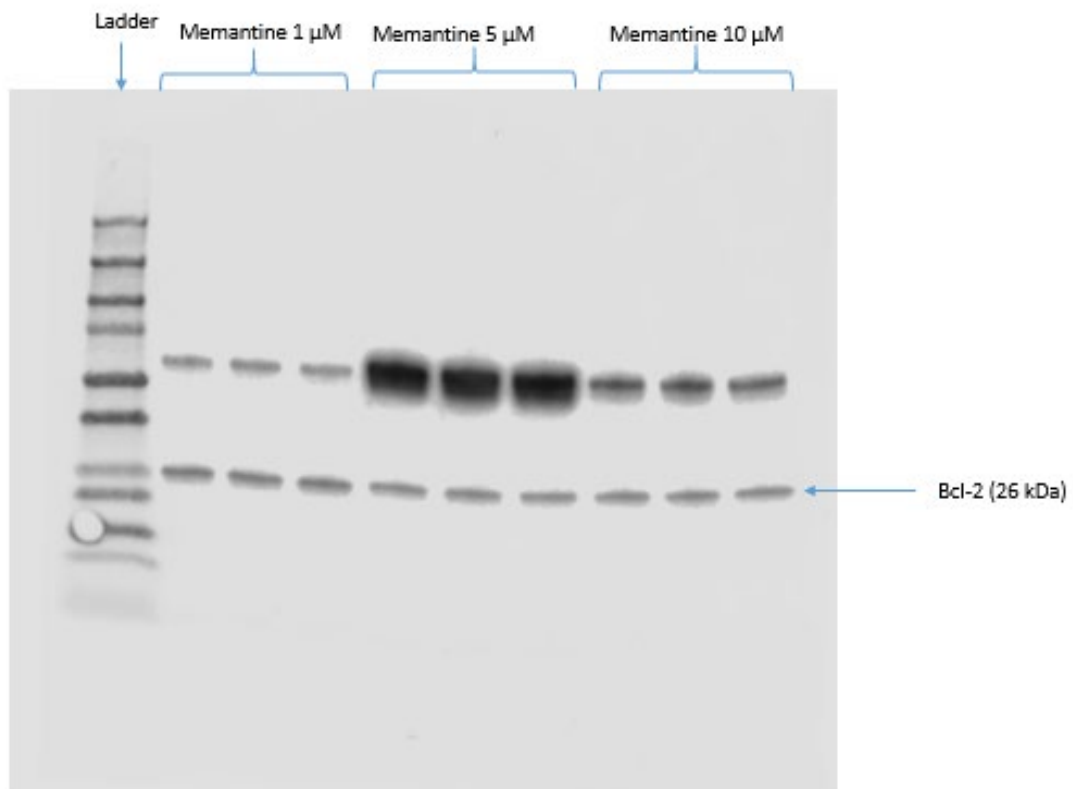


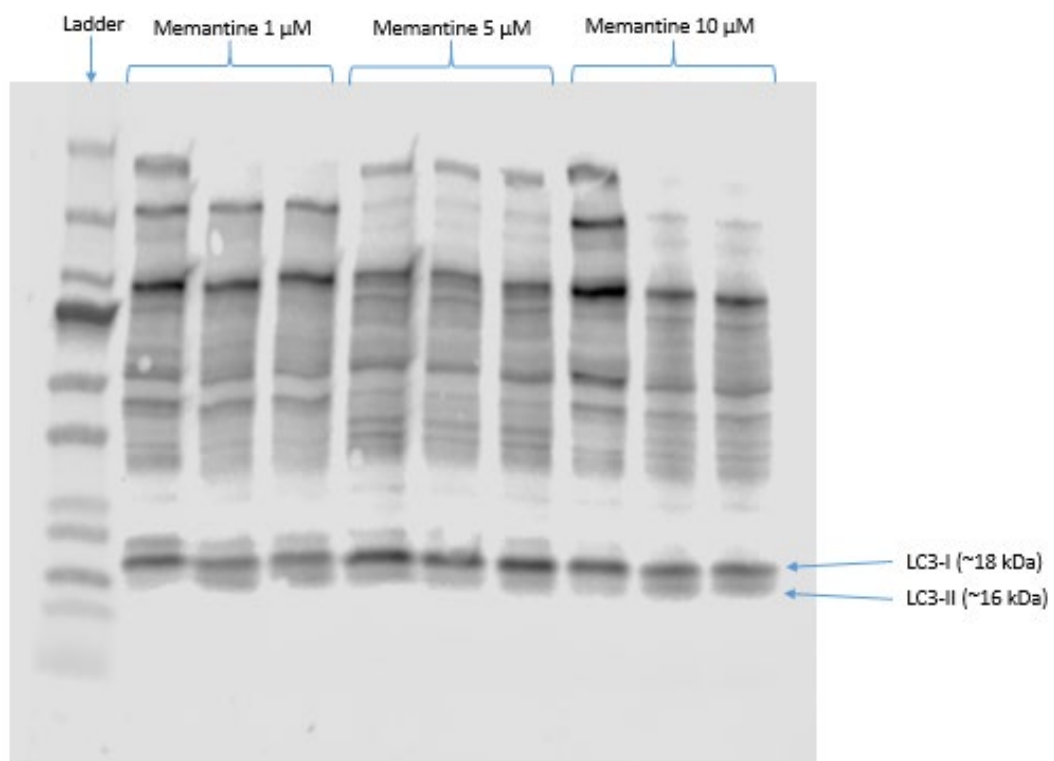
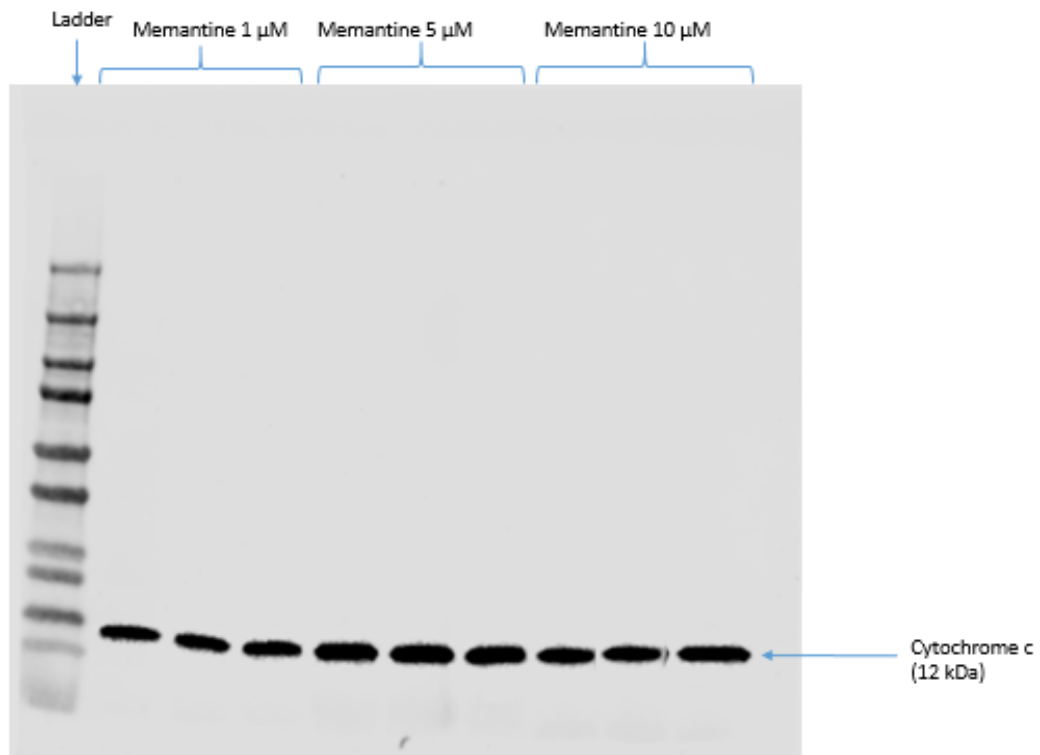


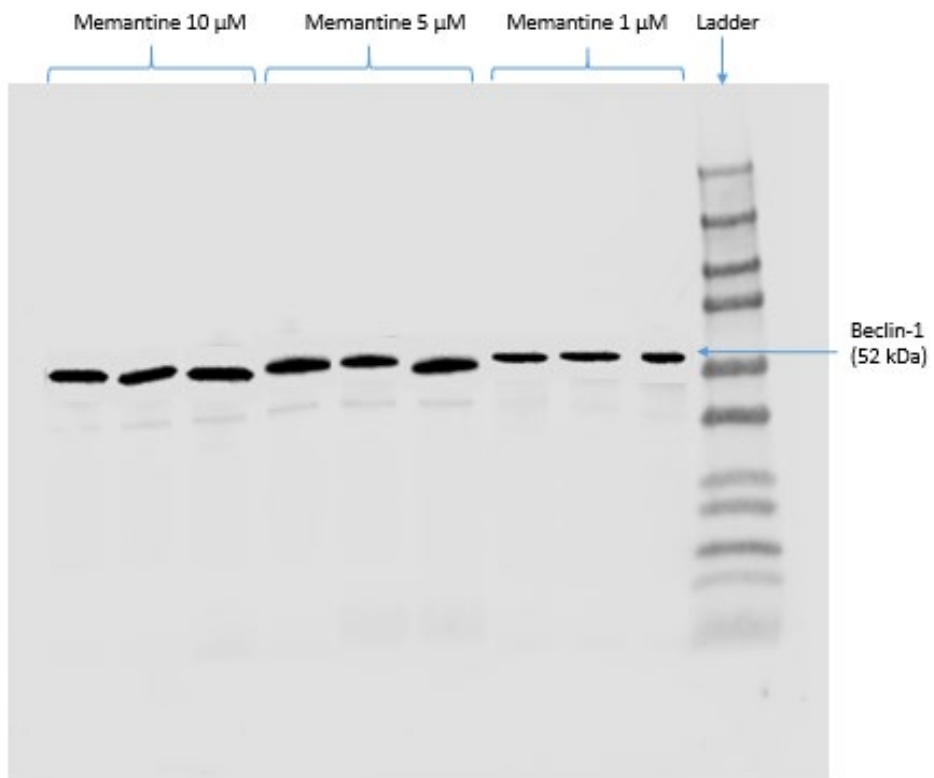




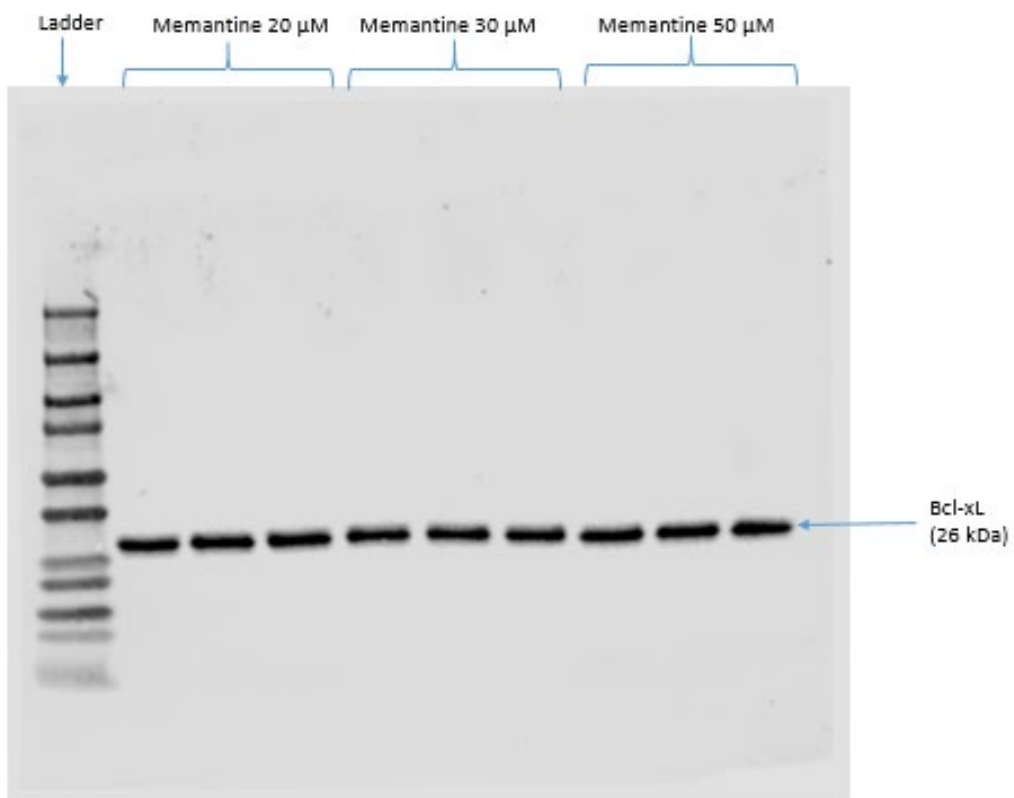
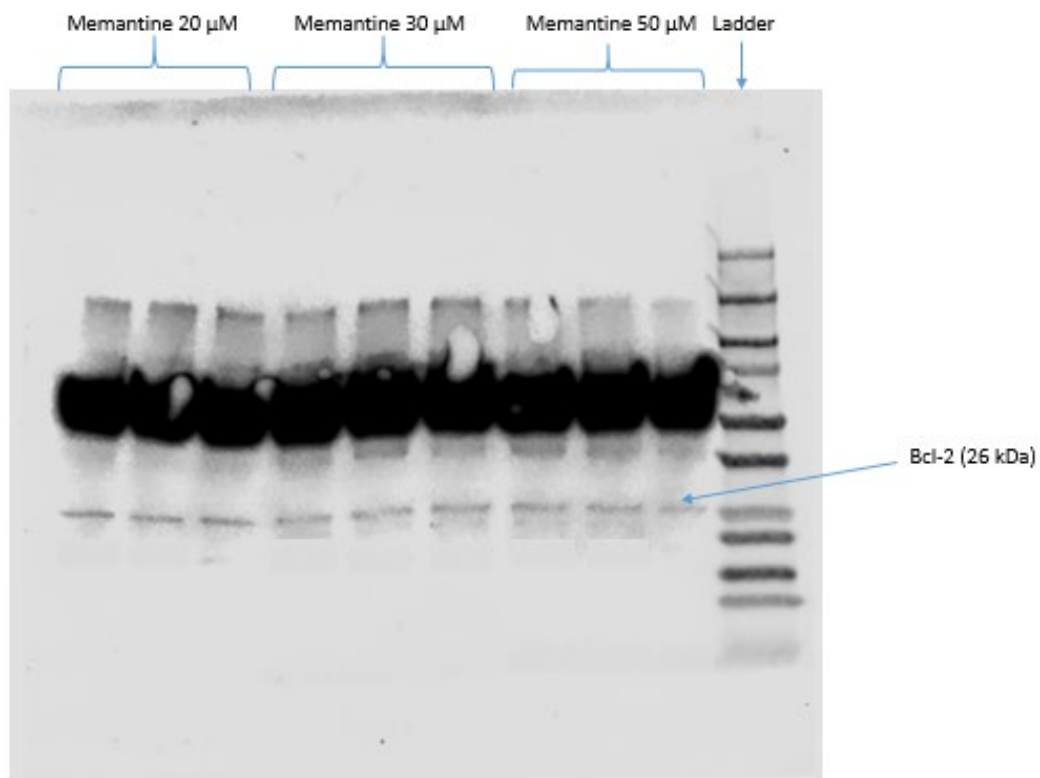
3b) Memantine 1, 5, 10 μ M (HEK293T cells)

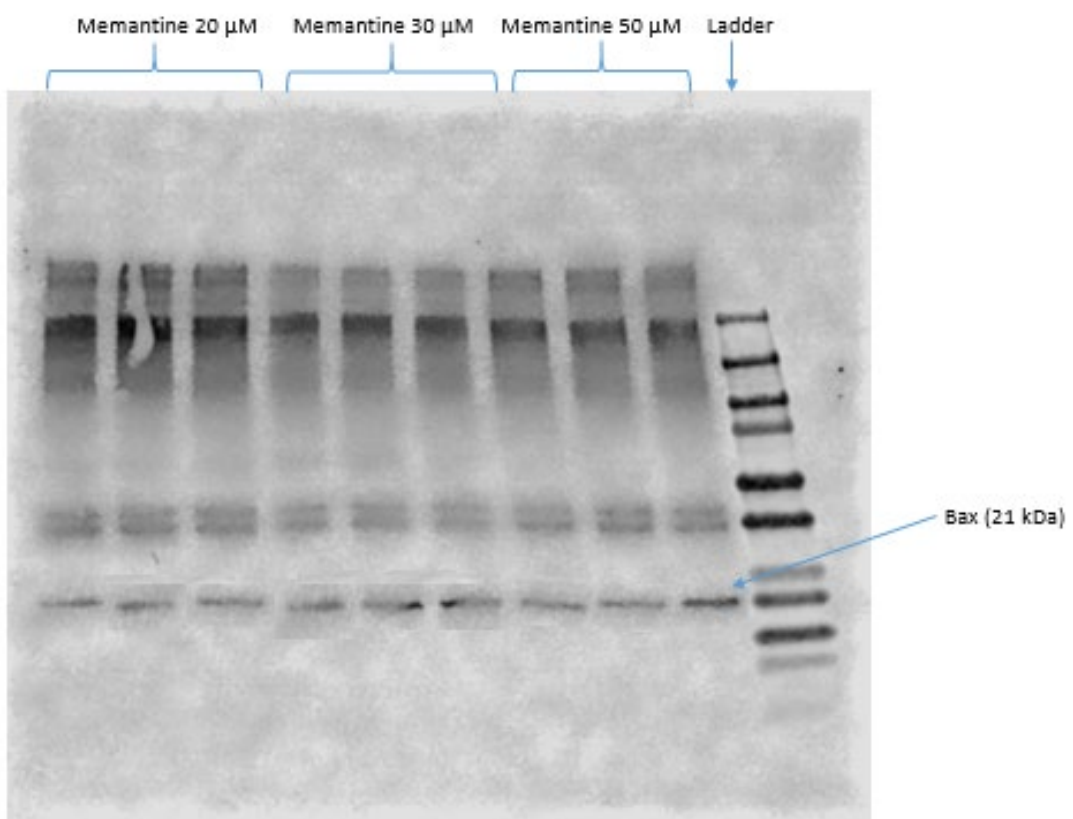
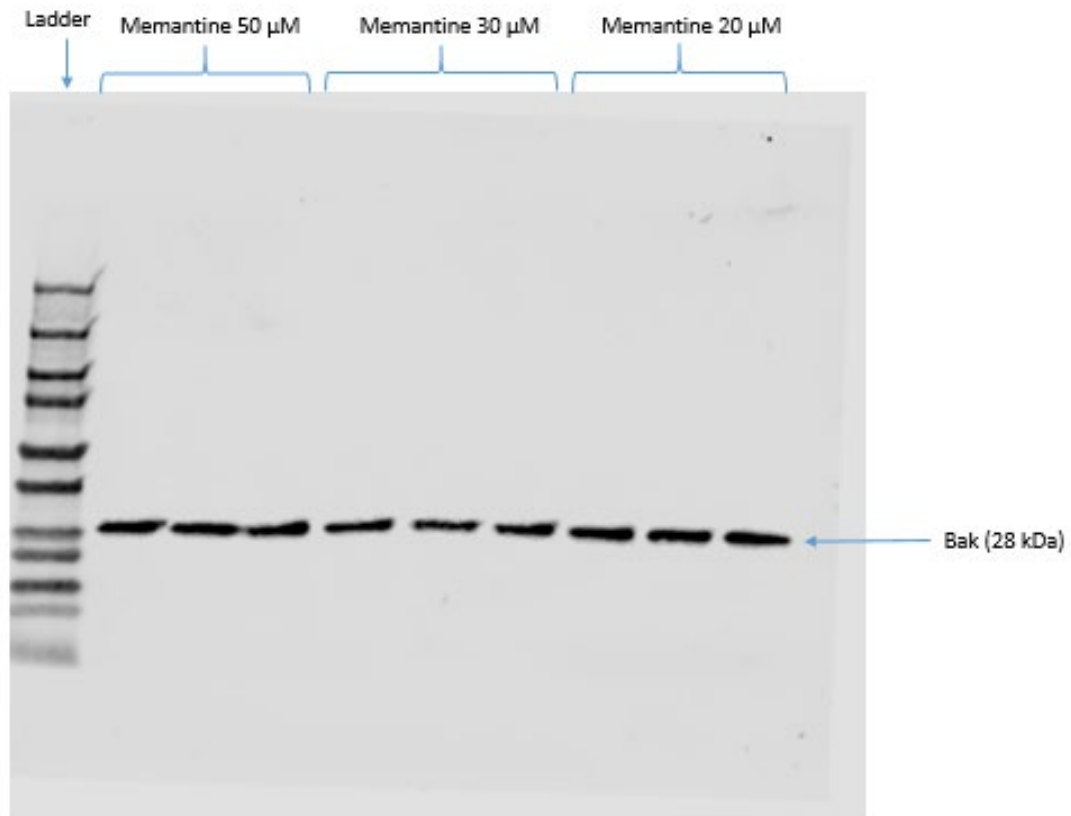


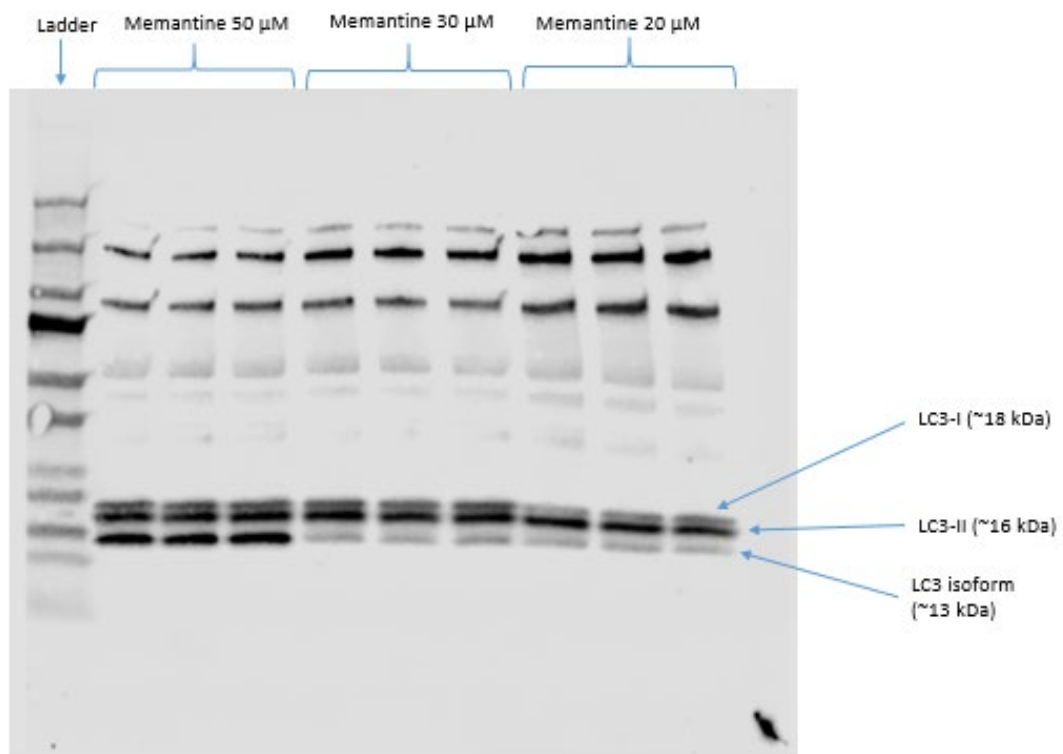
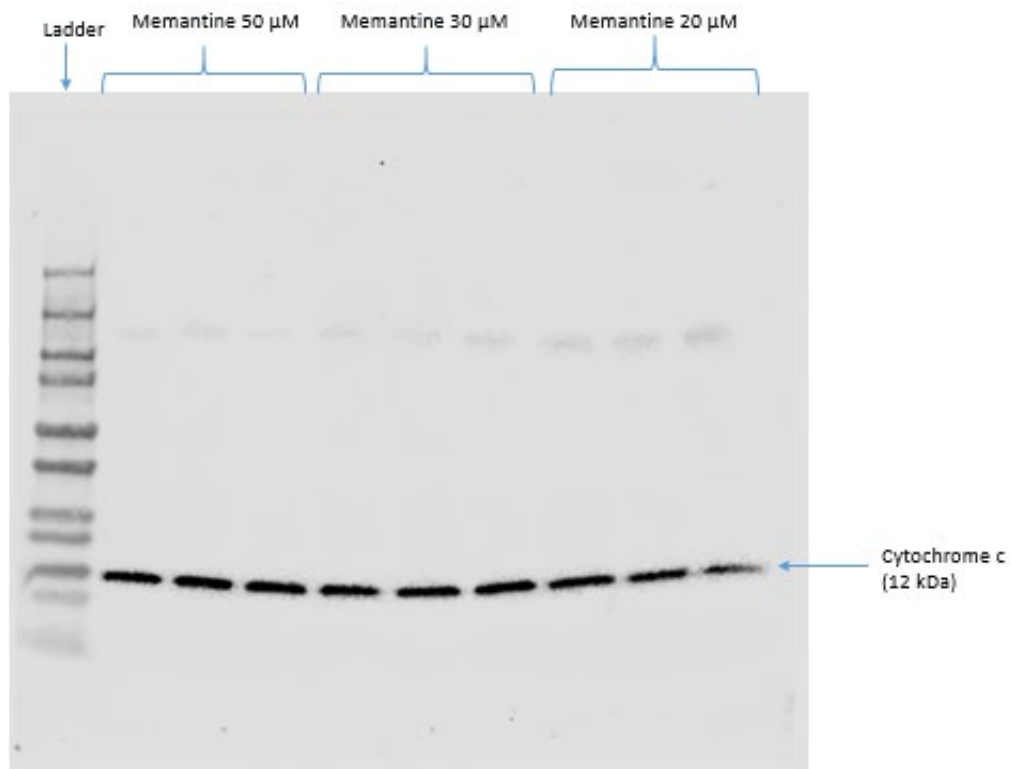


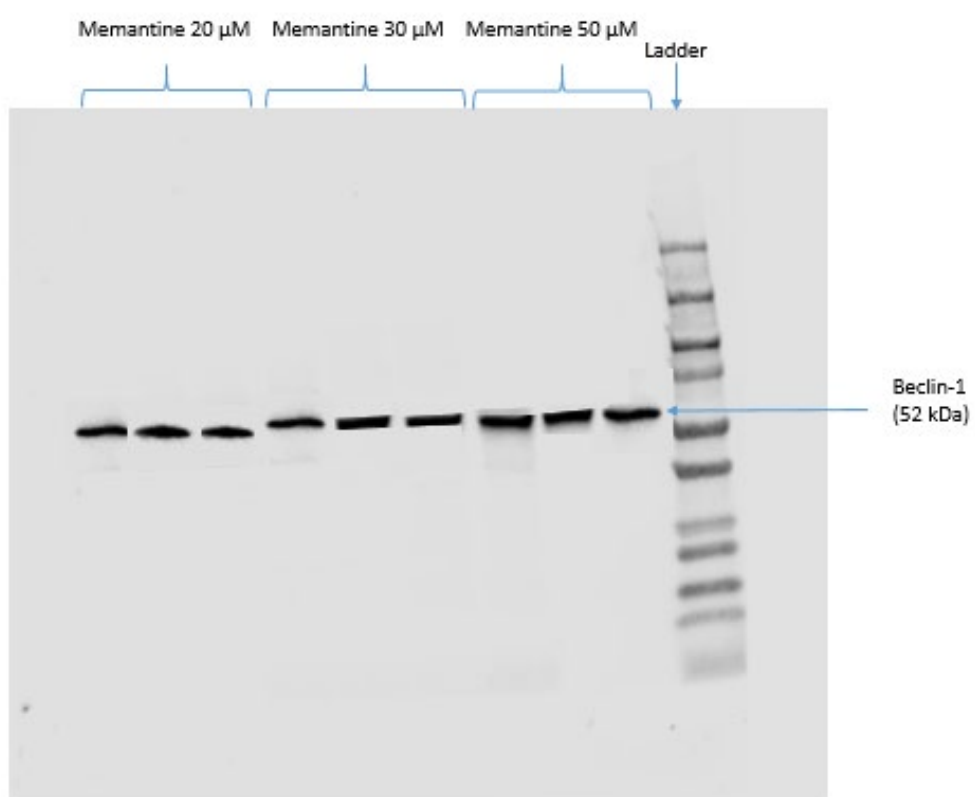
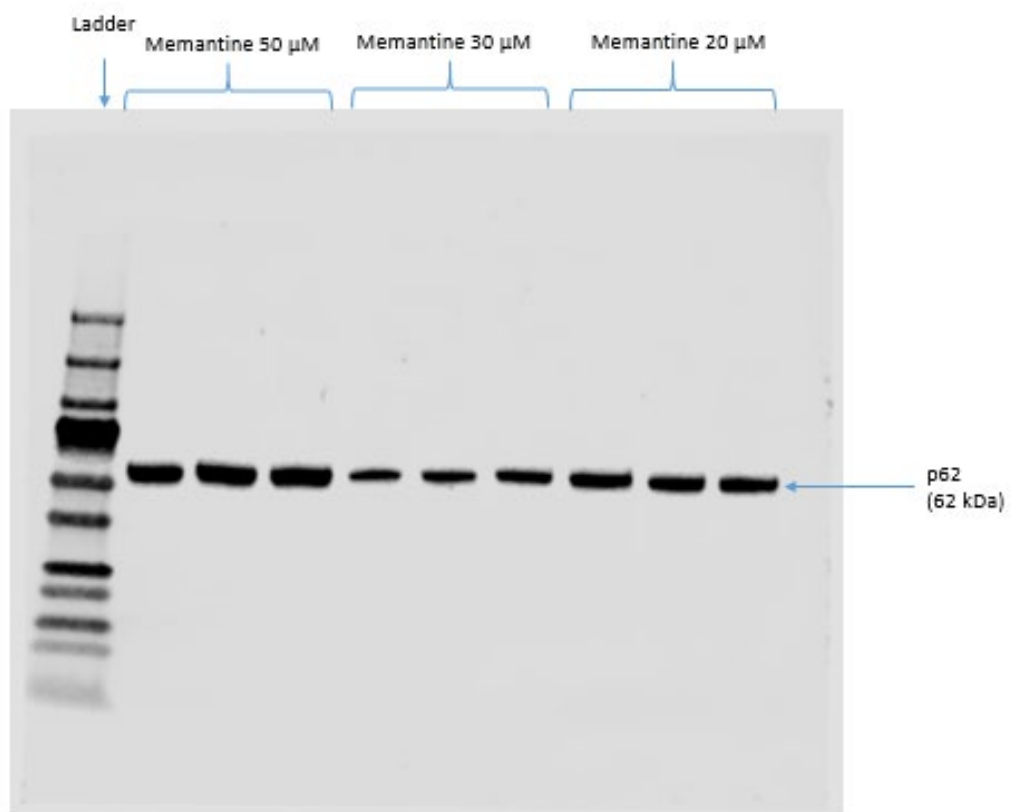


4a) Memantine 20, 30, 50 μ M (K-562 cells)

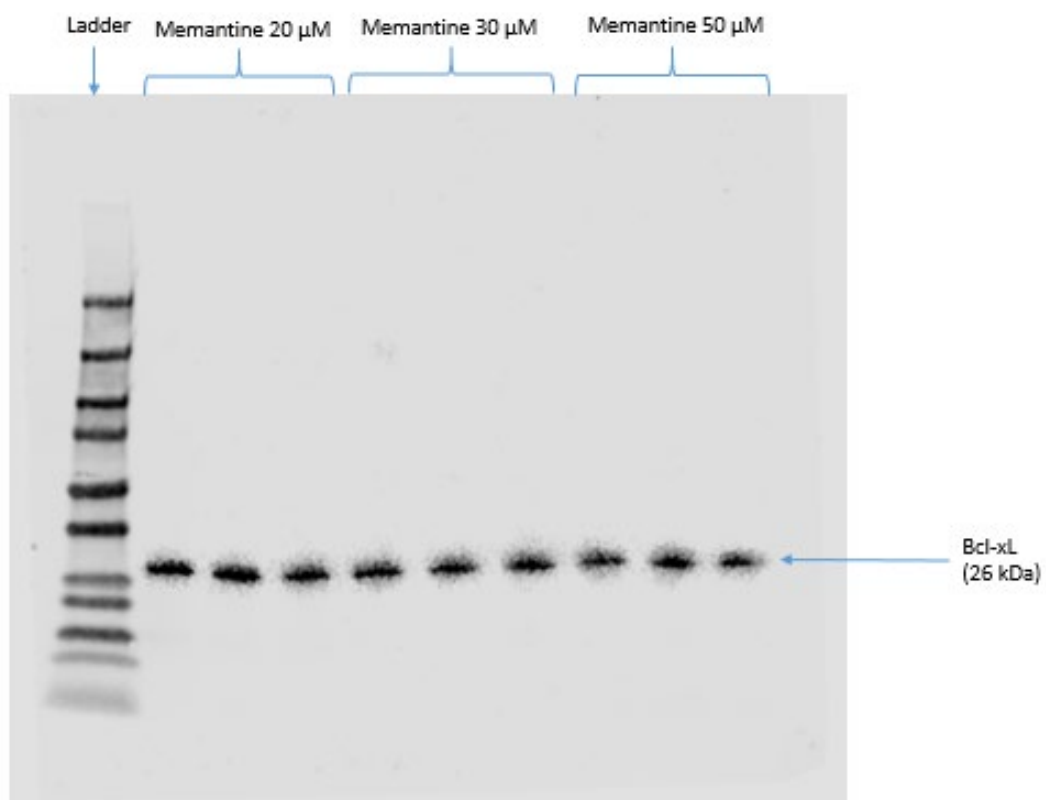
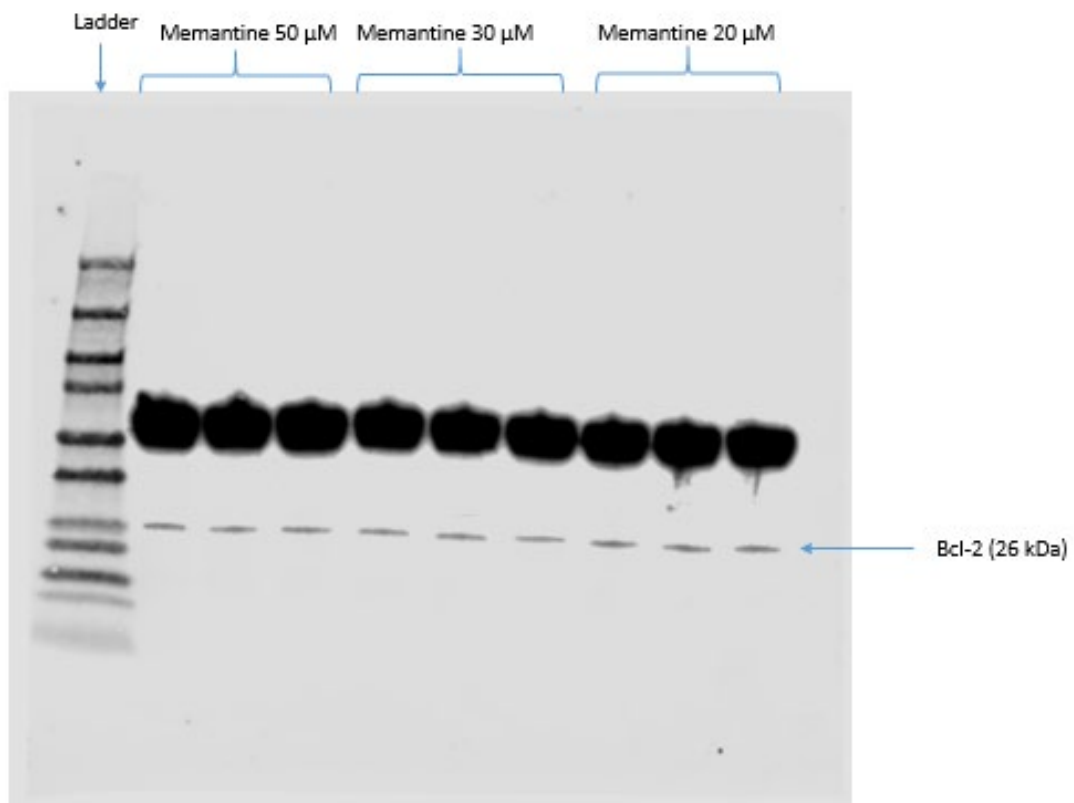


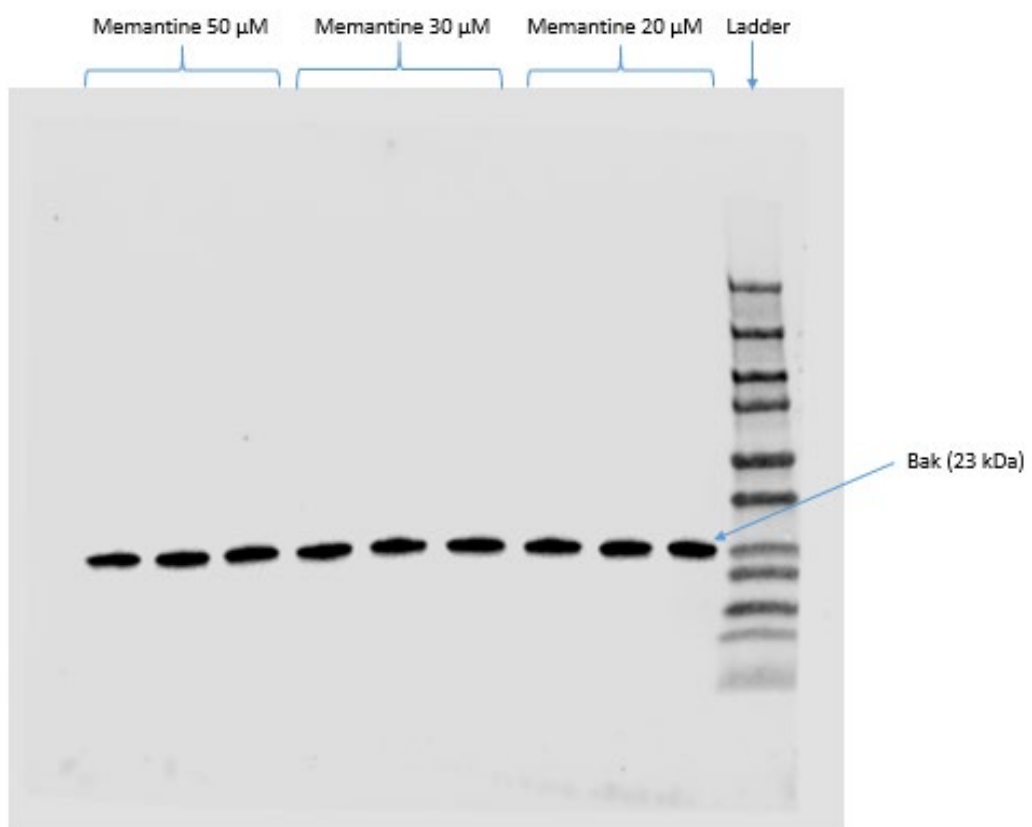
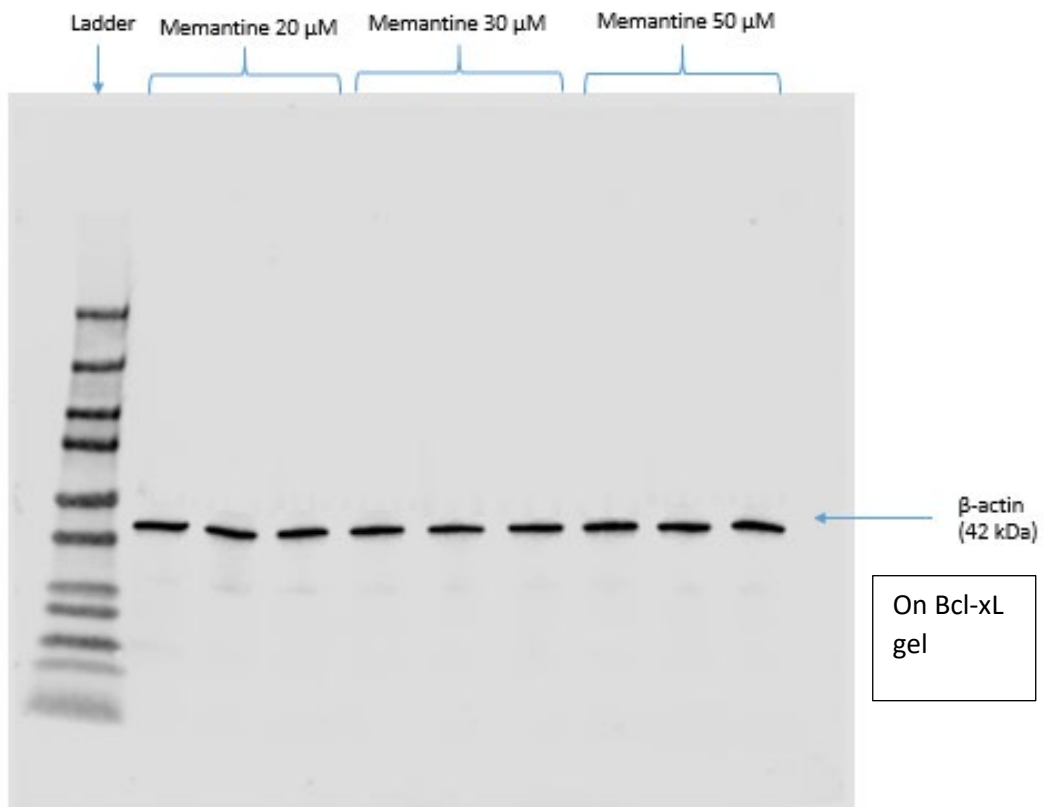


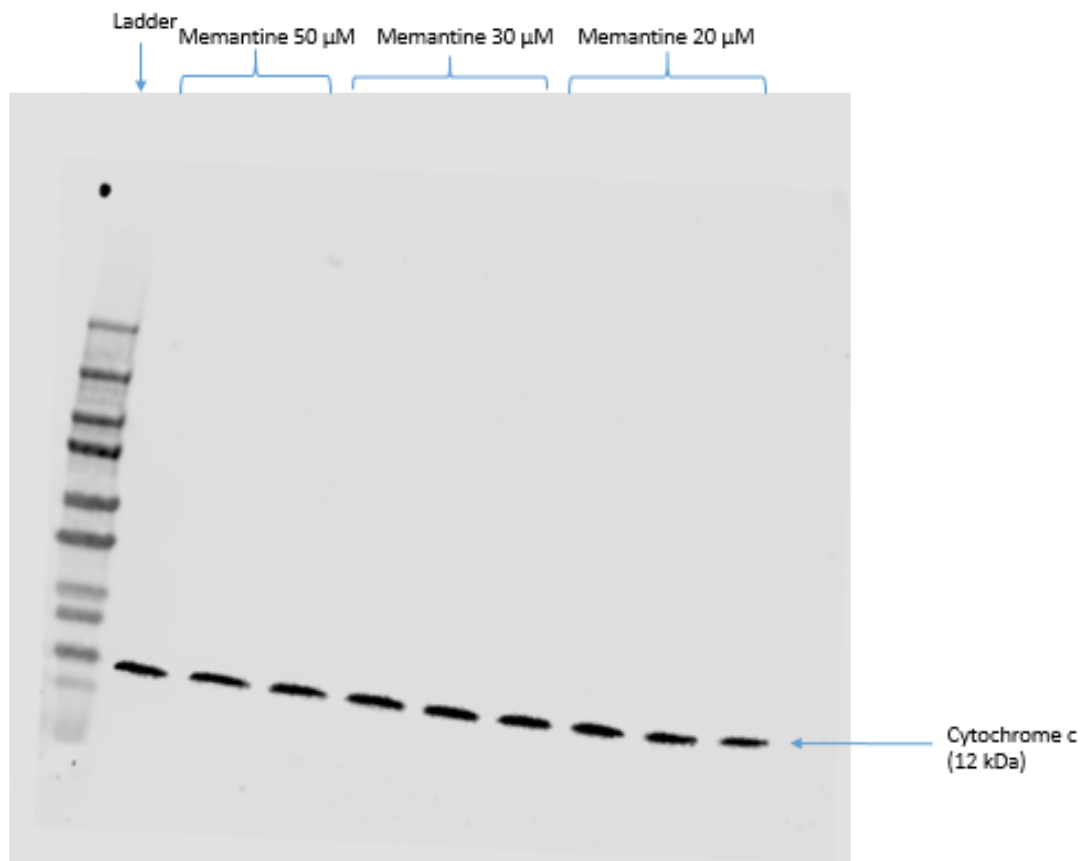
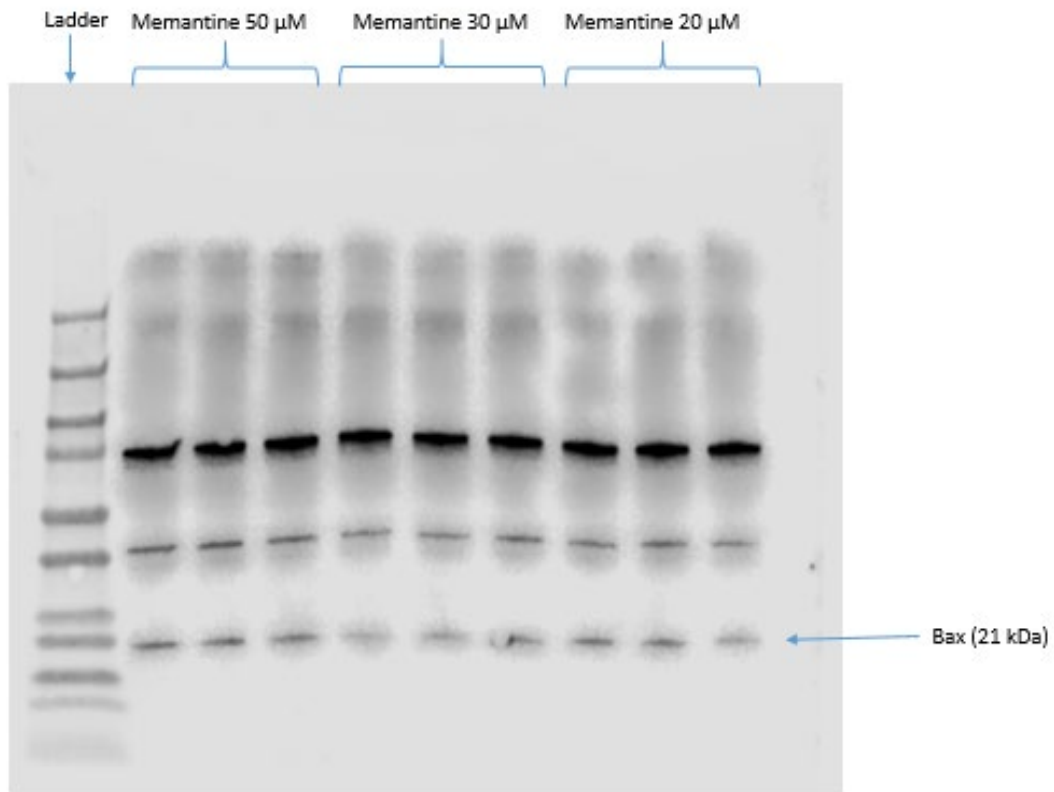


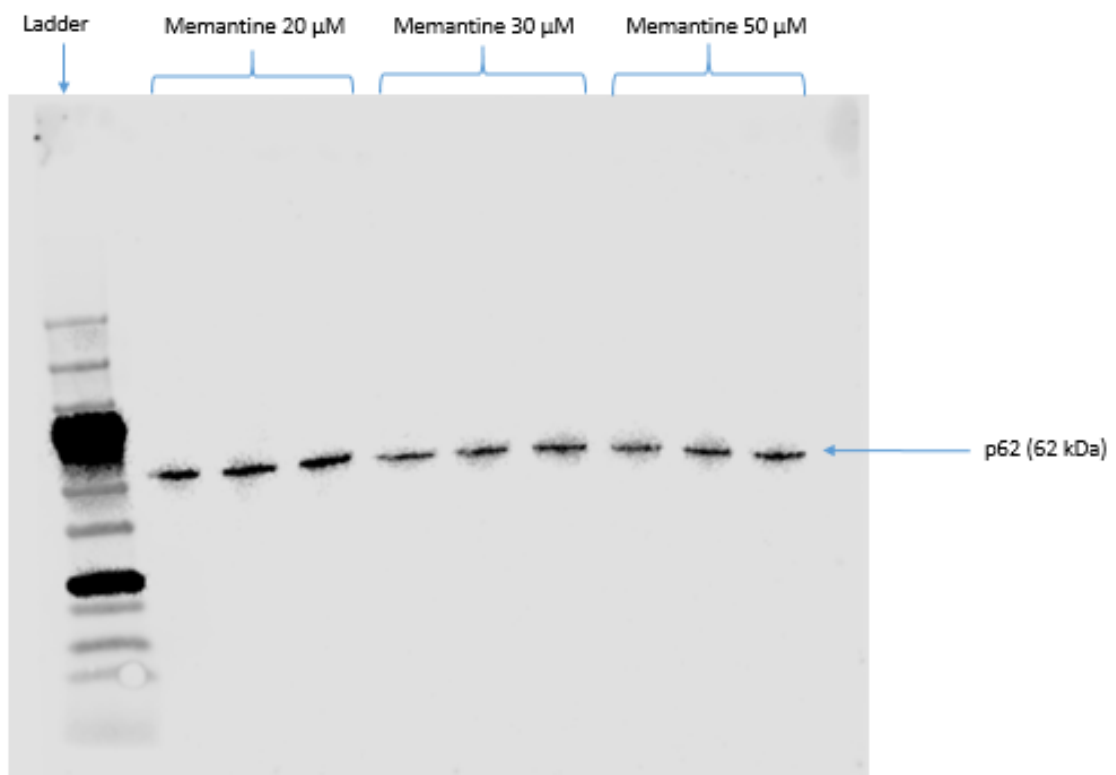
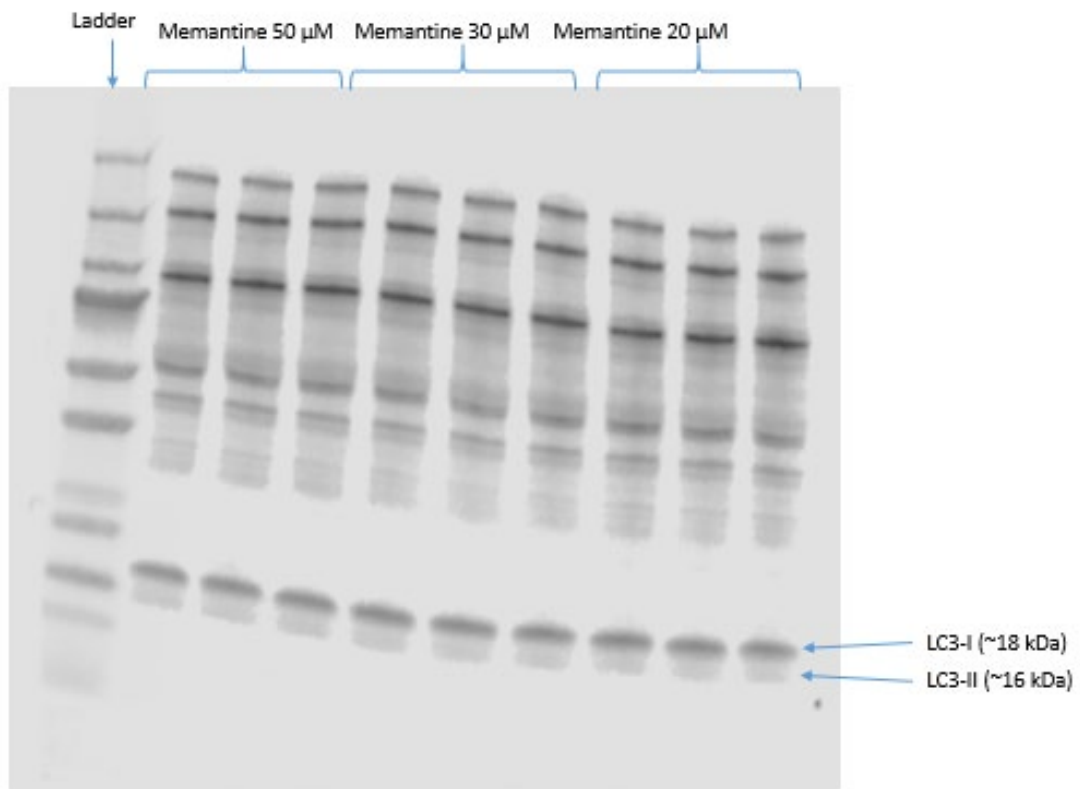


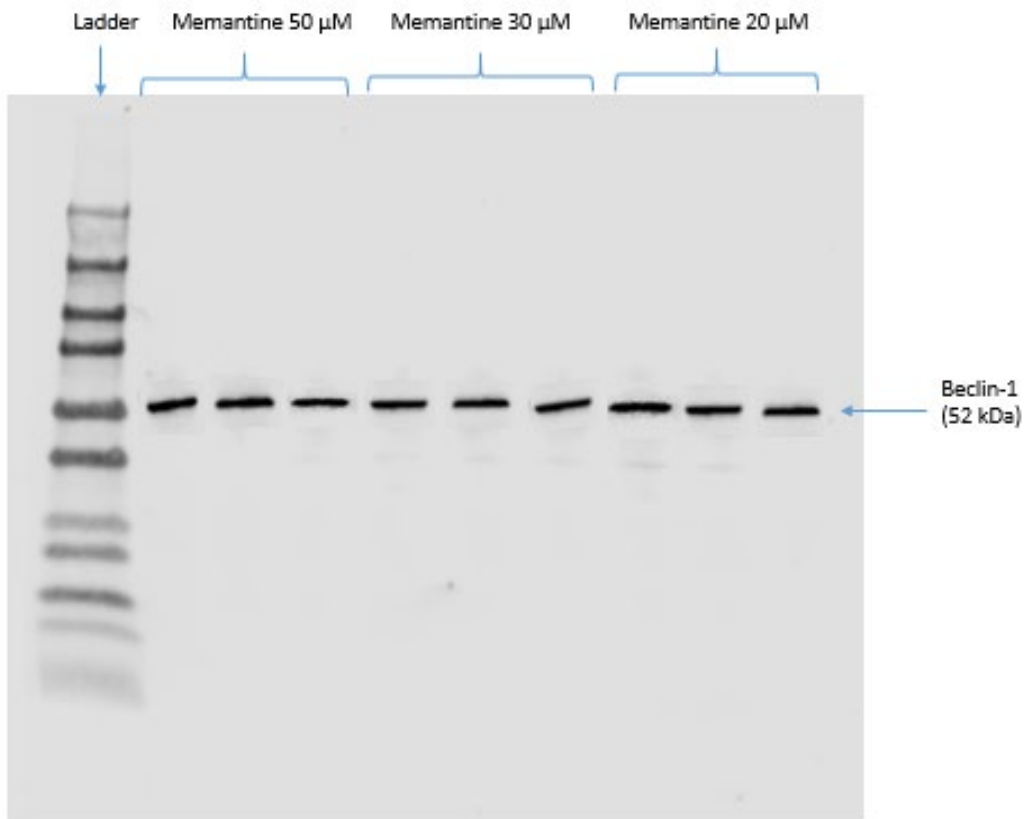
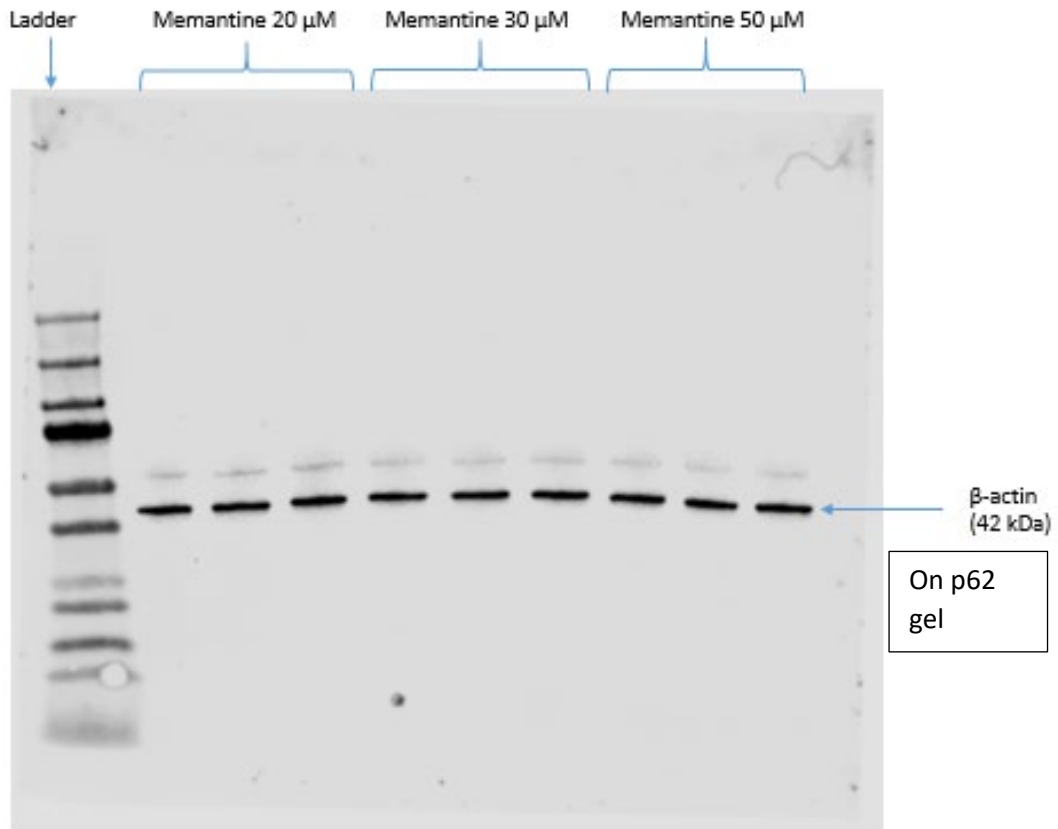
4b) Memantine 20, 30, 50 μ M (HEK293T cells)



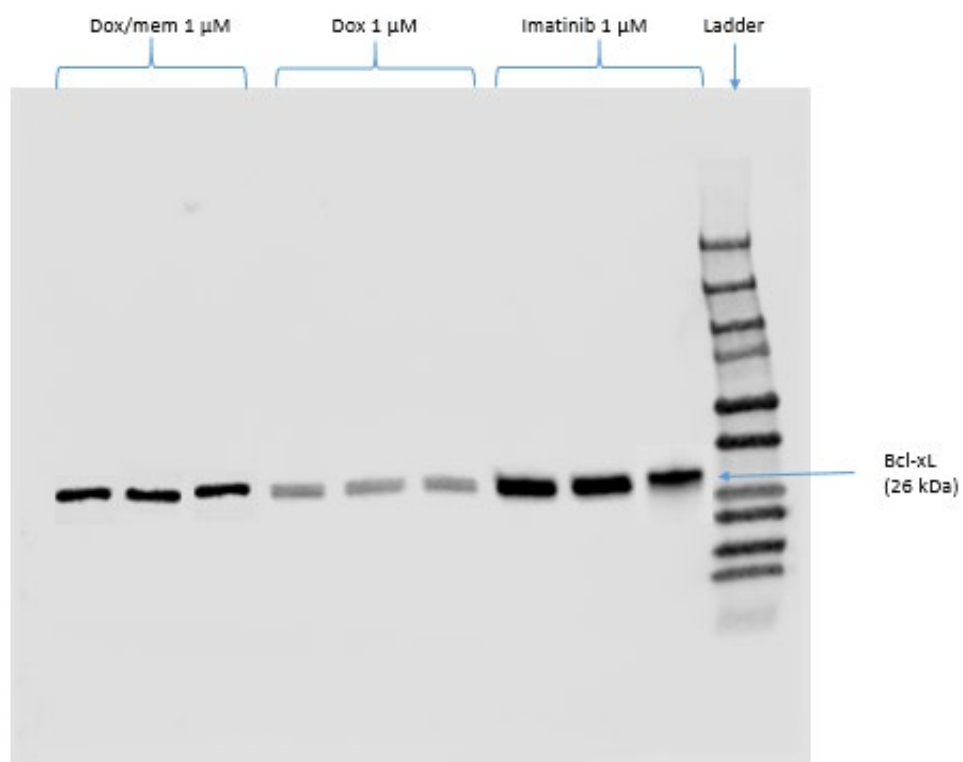
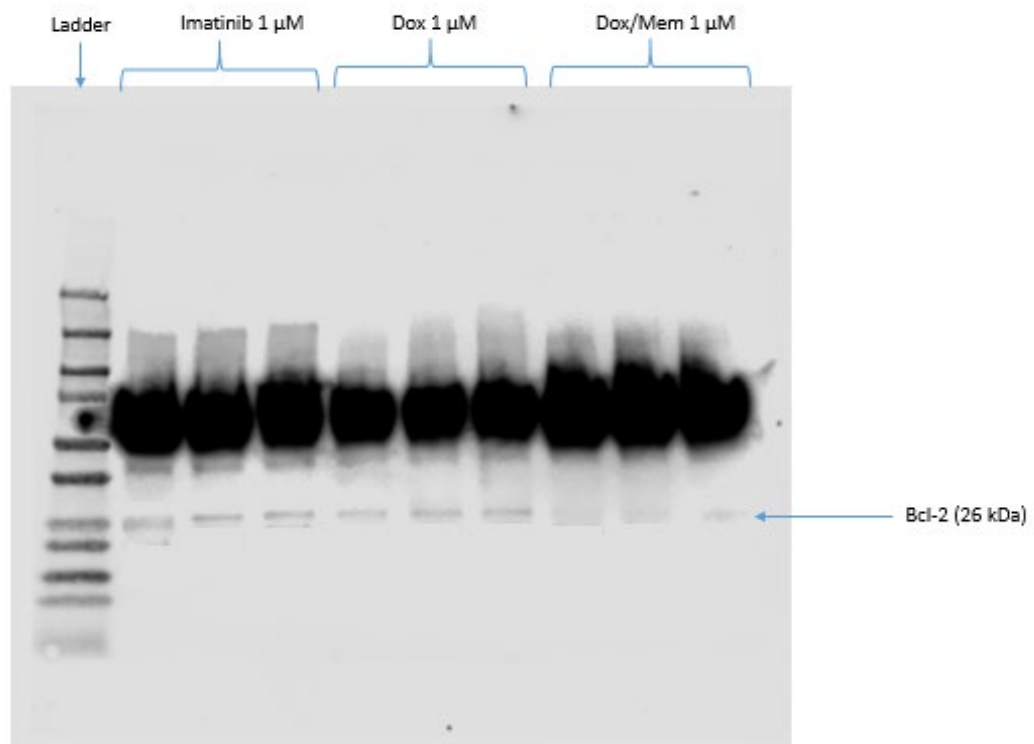


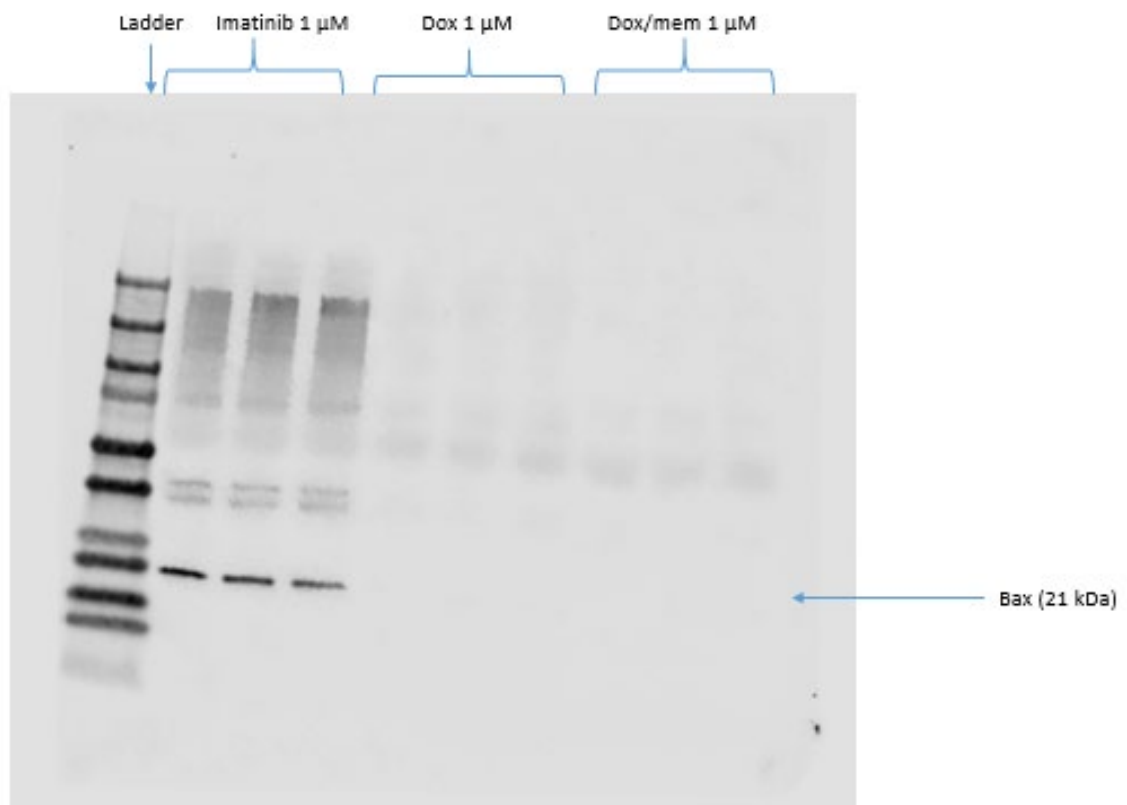
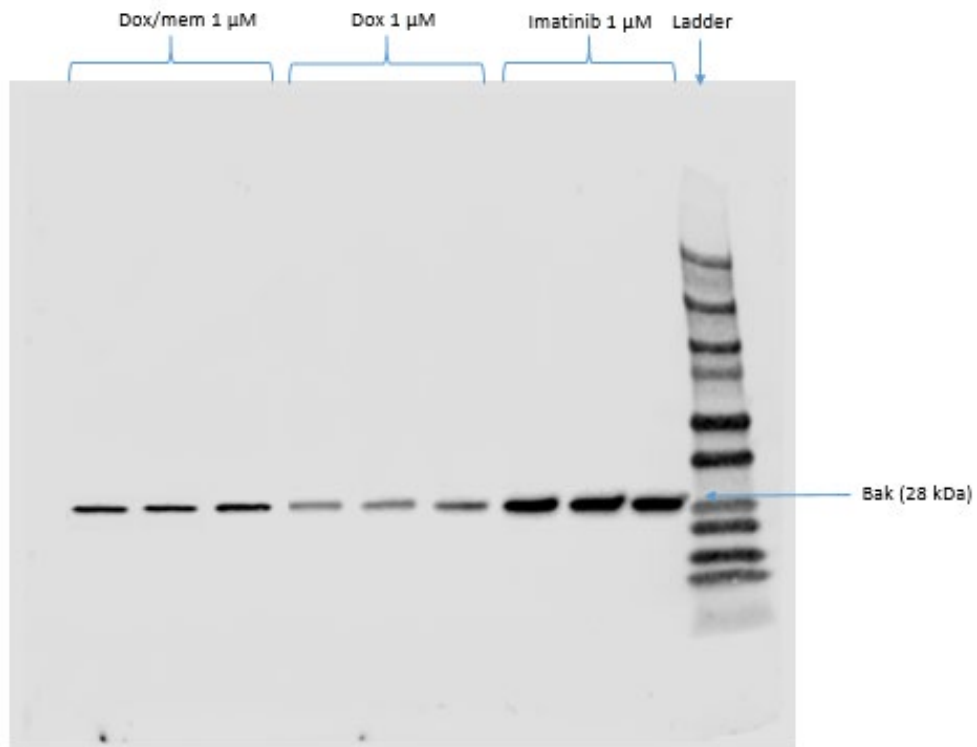


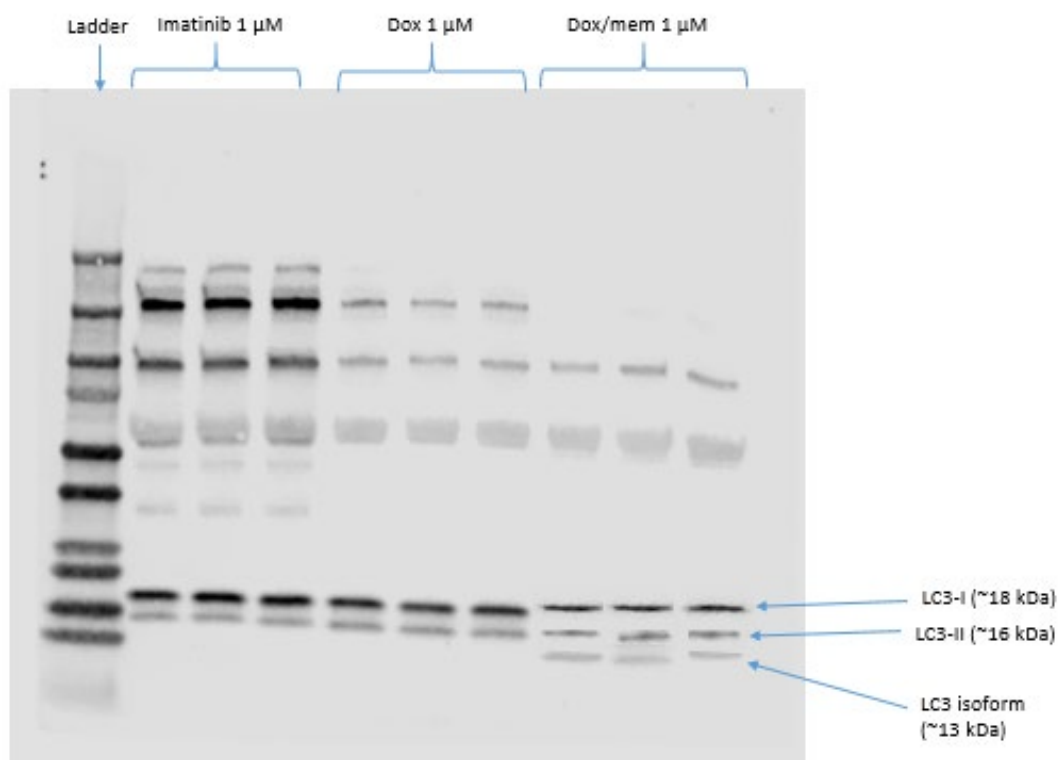
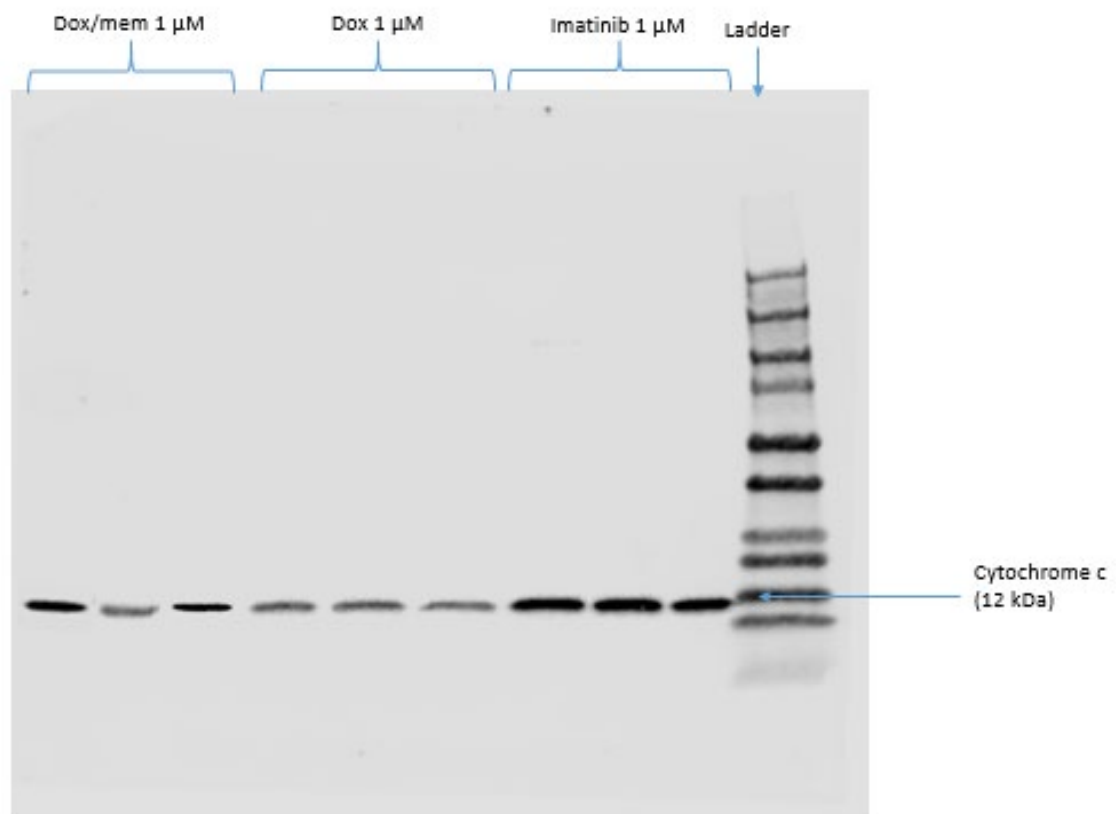


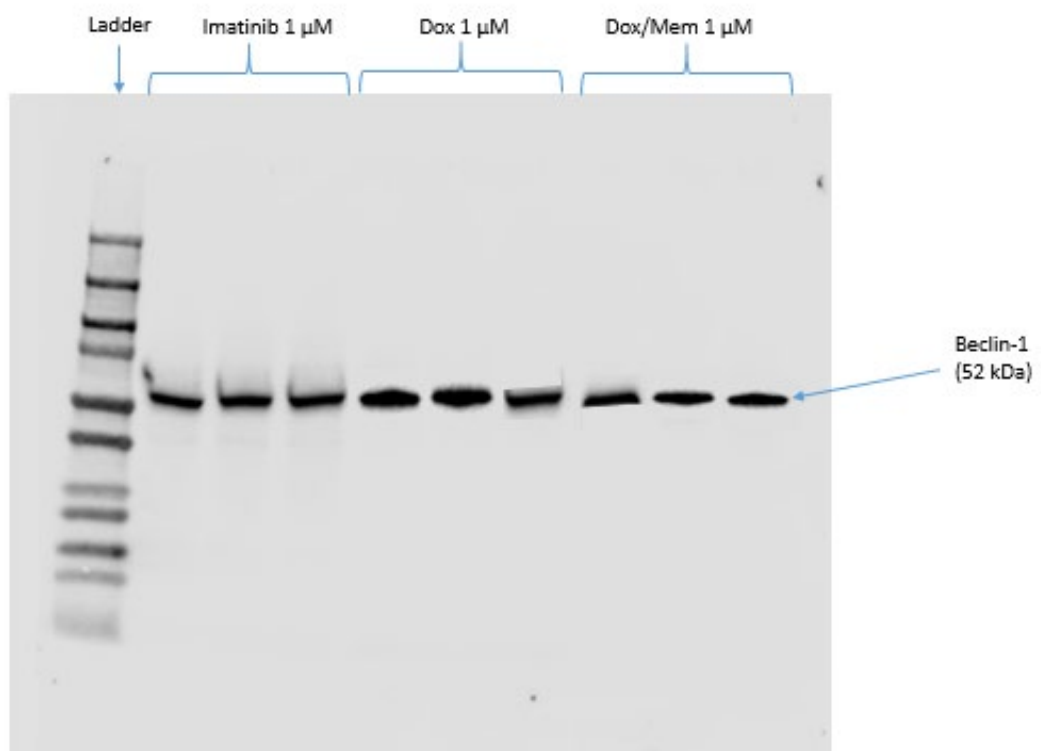
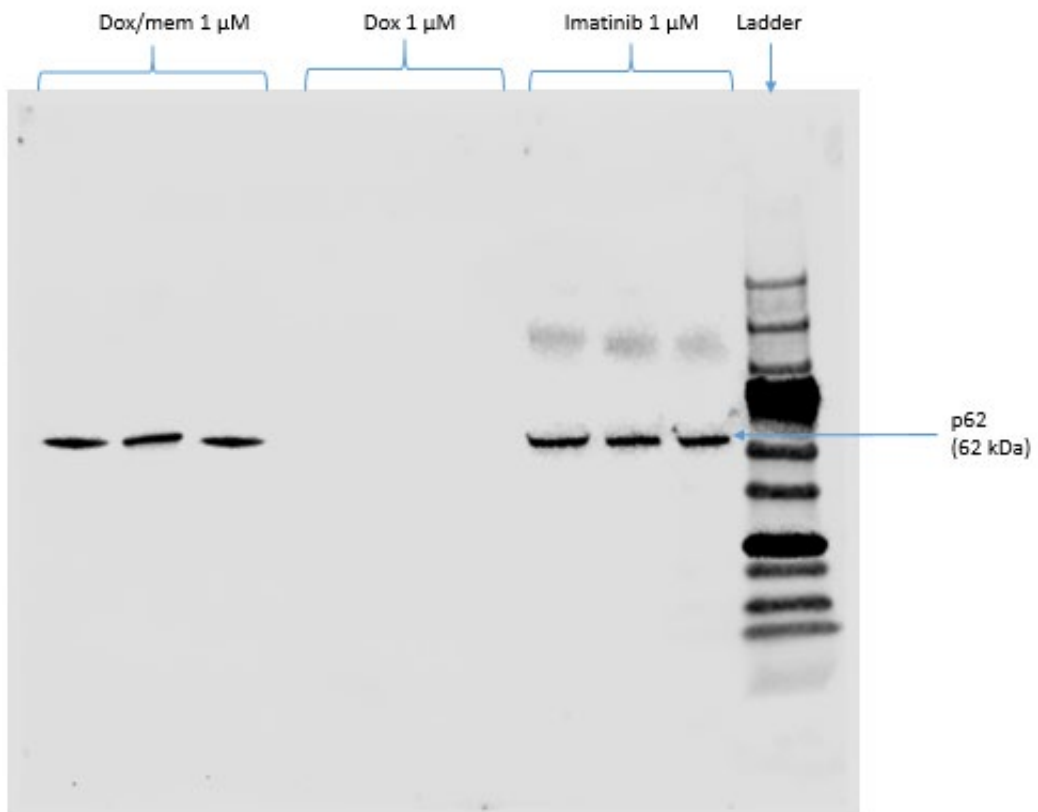


5a) Imatinib 1 μ M, Dox 1 μ M, Dox/Mem 1 μ M (K-562 cells)

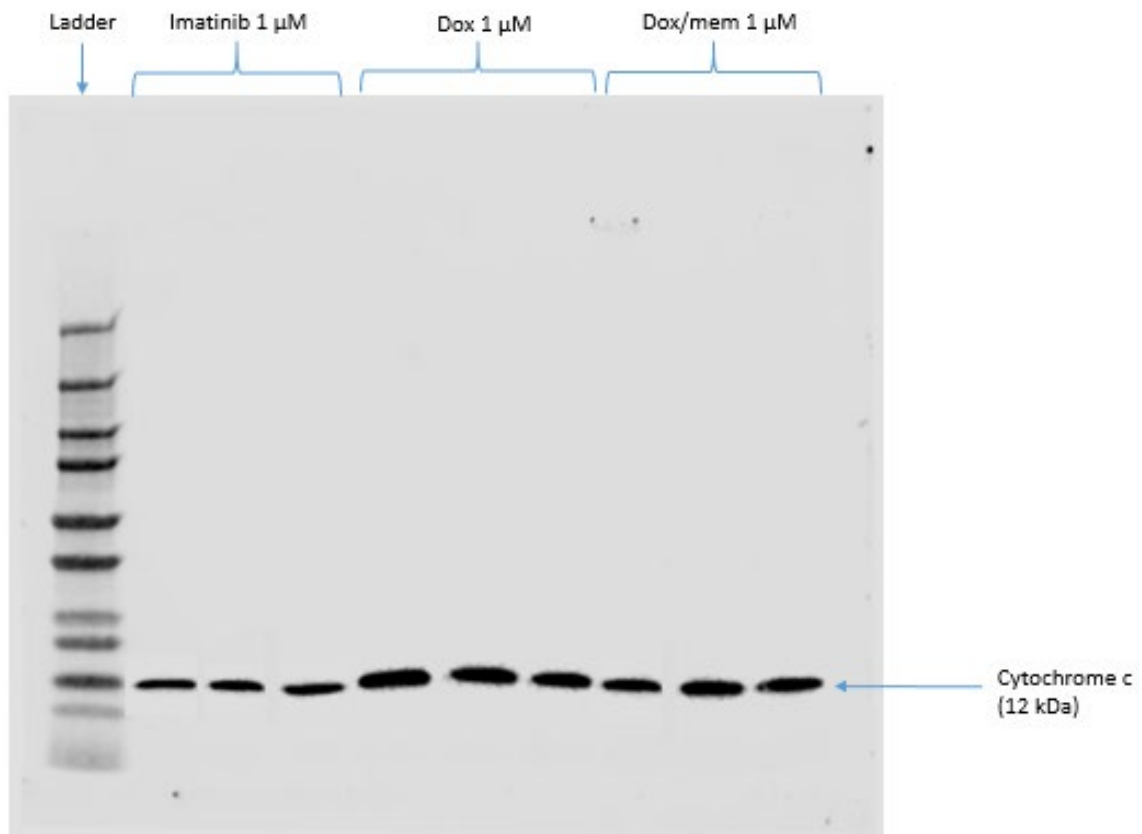
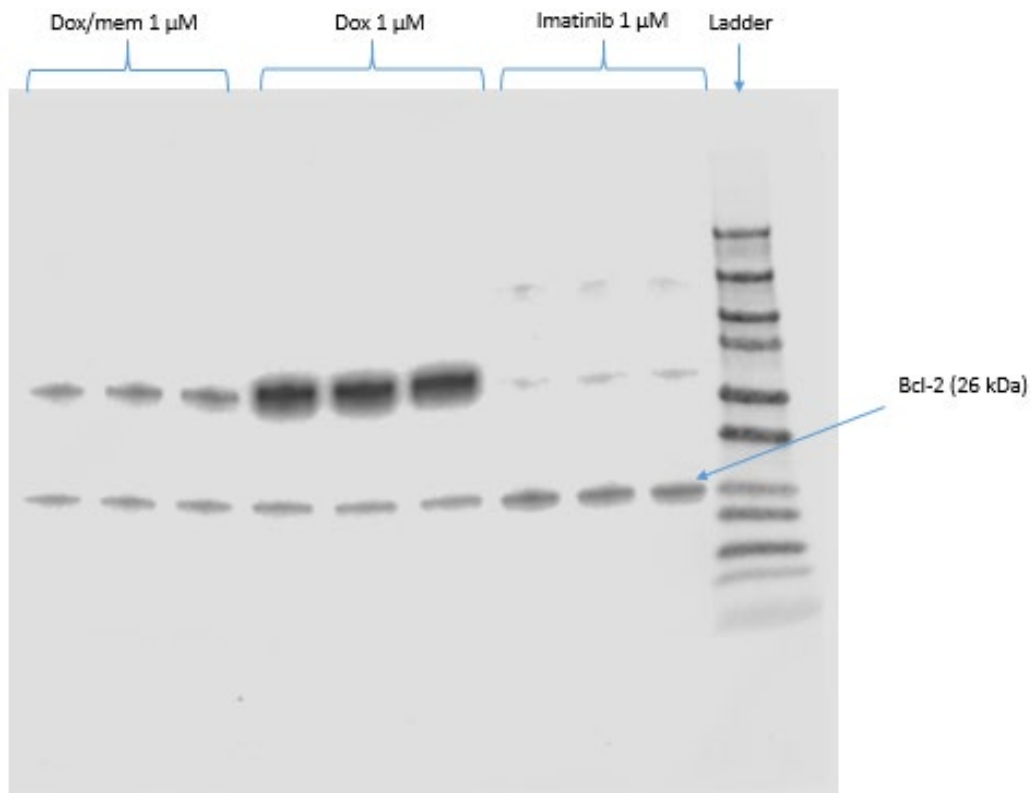


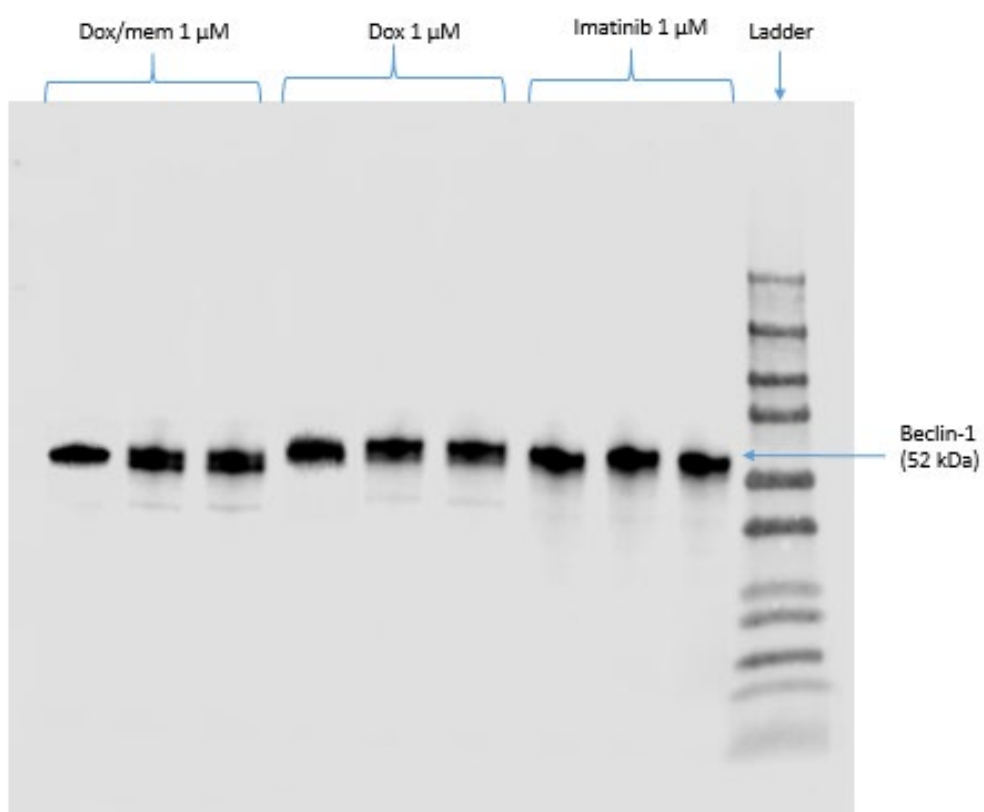
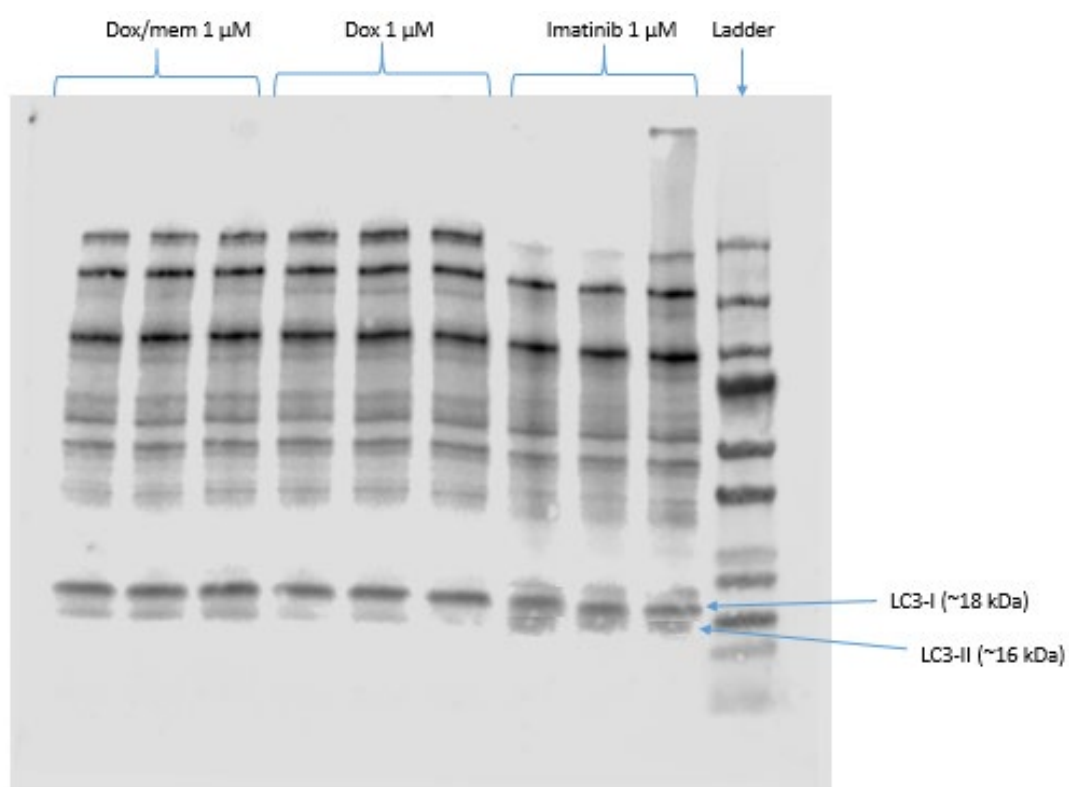




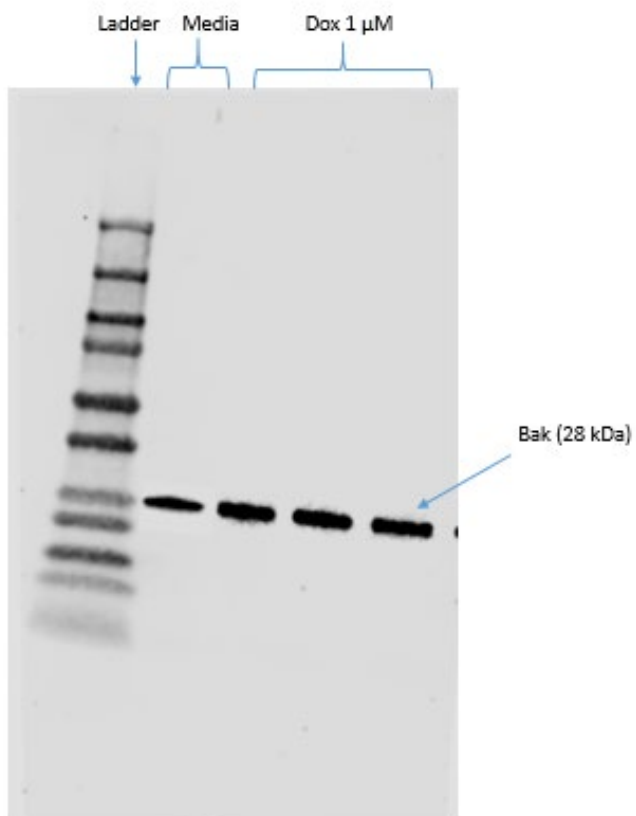
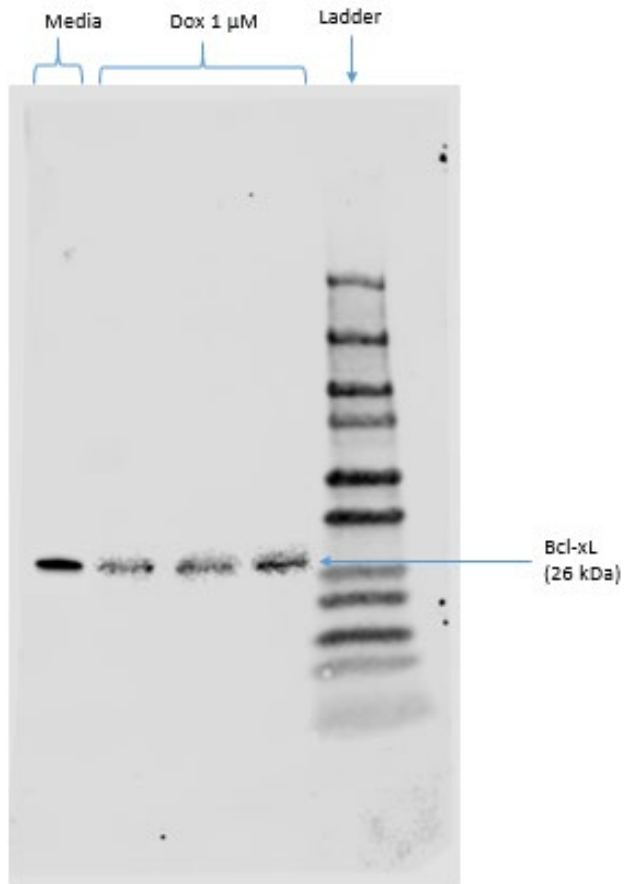


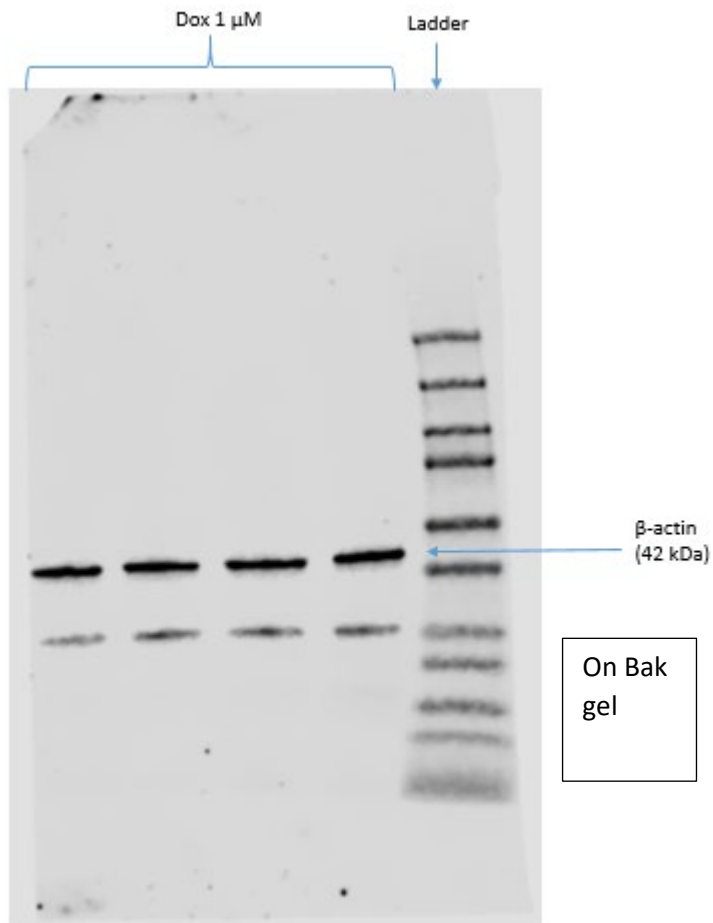
5b) Imatinib 1 μ M, Dox 1 μ M, Dox/Mem 1 μ M (HEK293T cells)



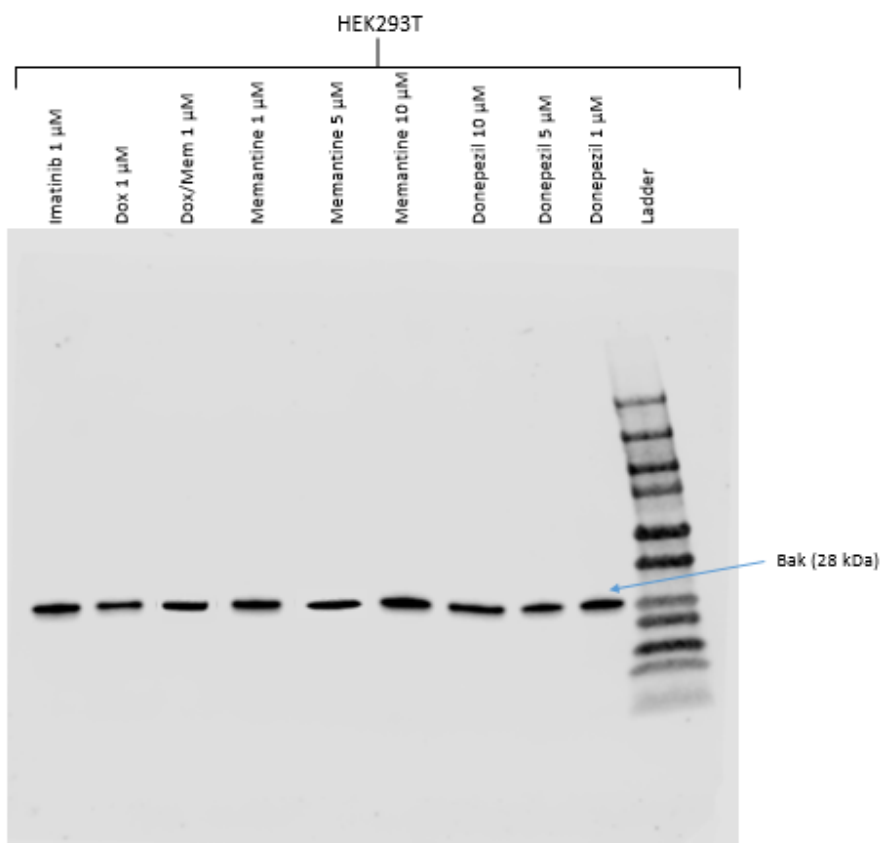
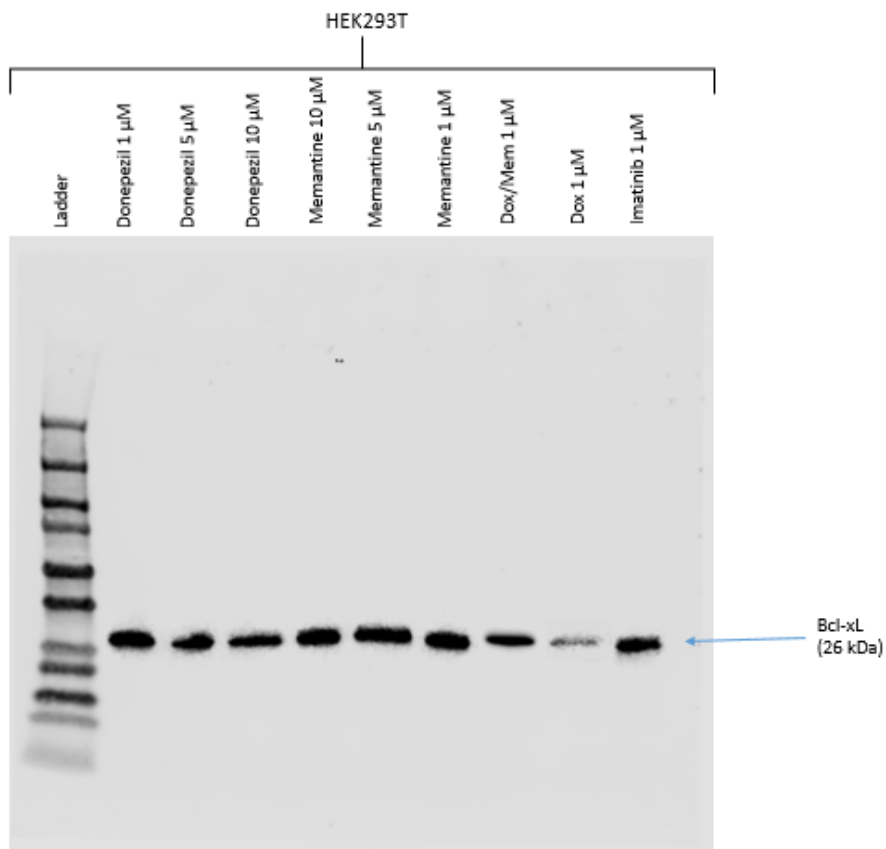


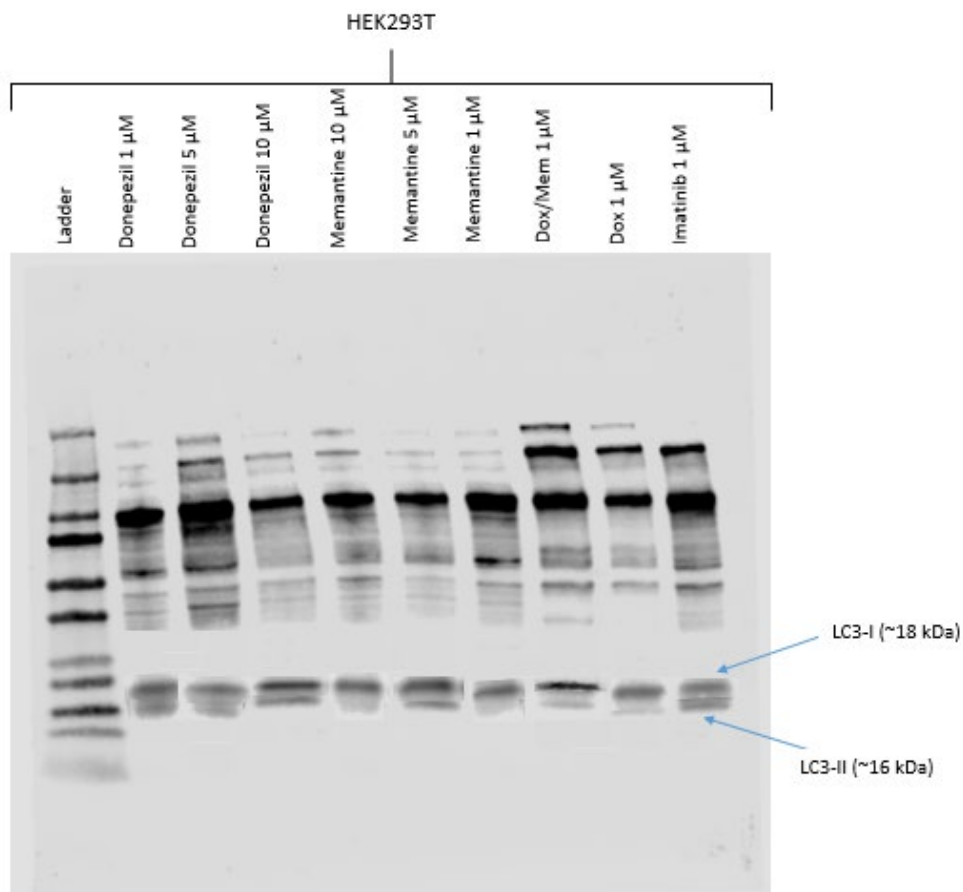
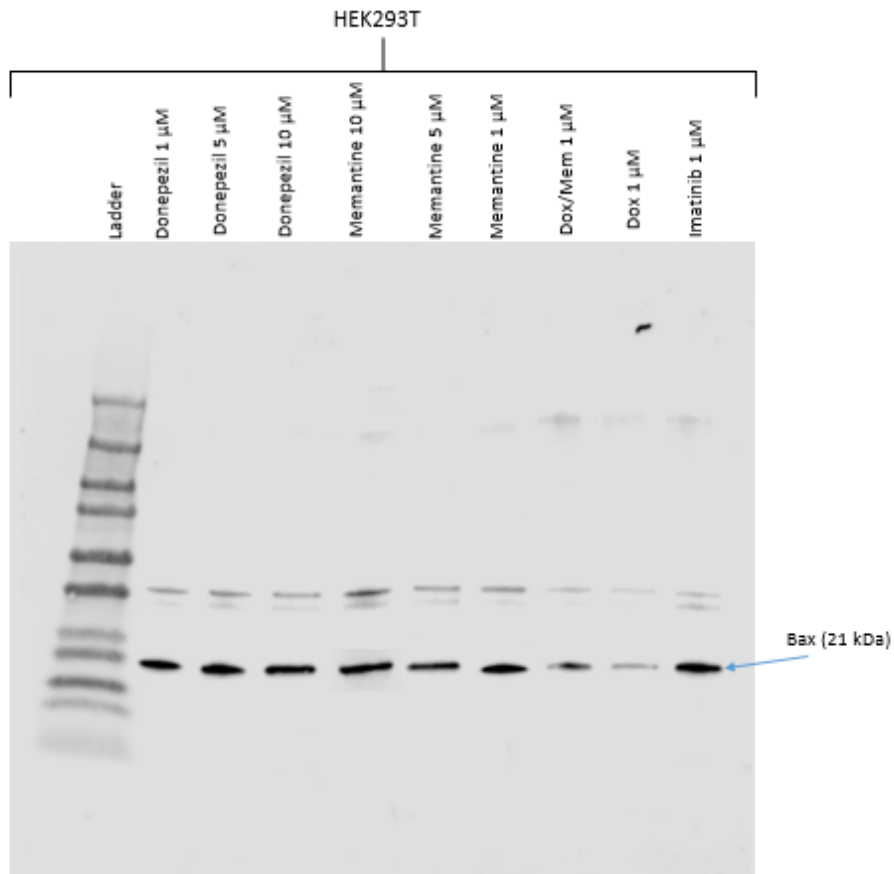
5b) Dox 1 μ M (HEK293T cells)

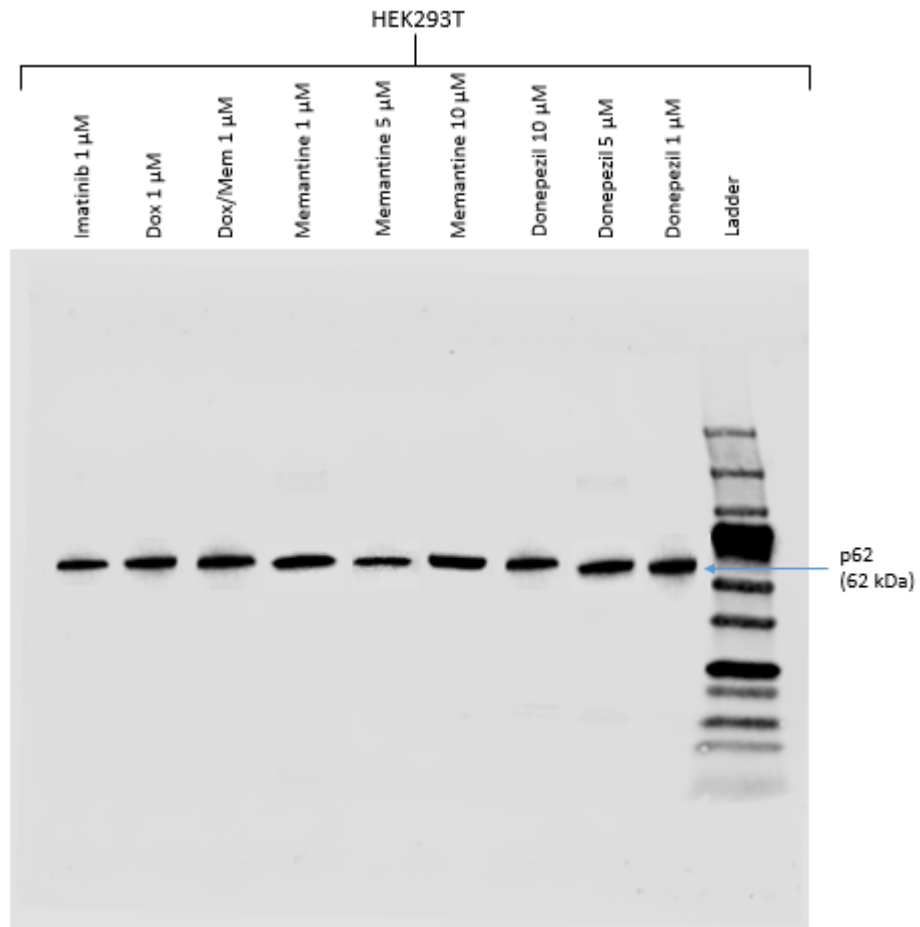




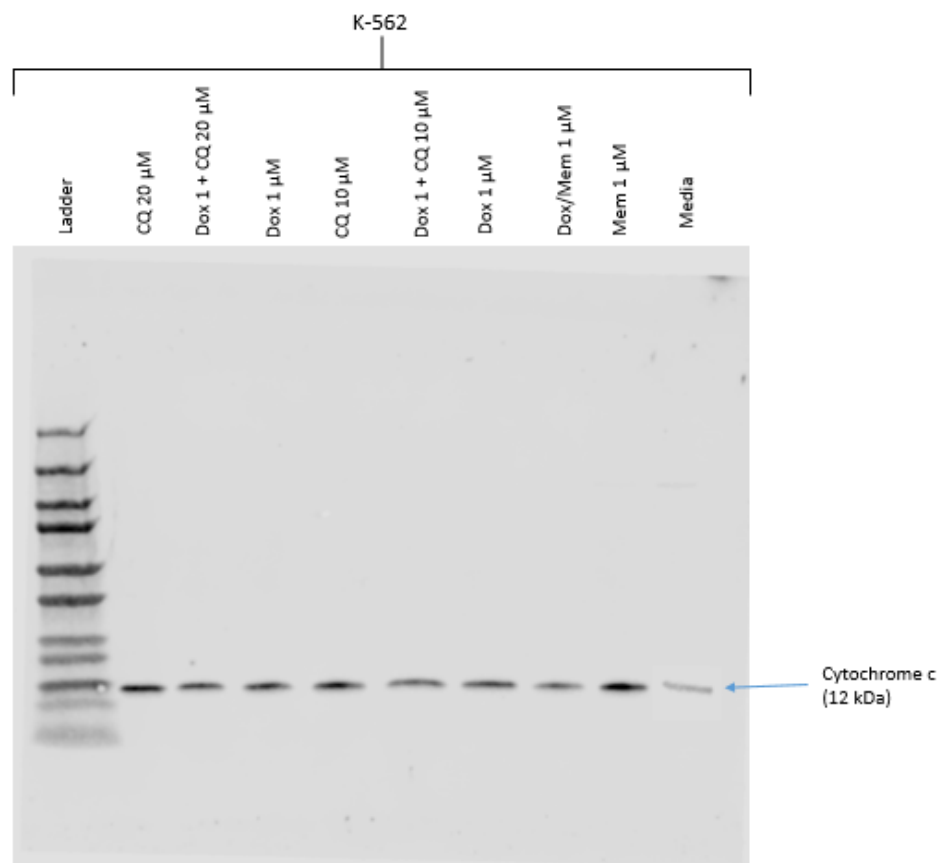
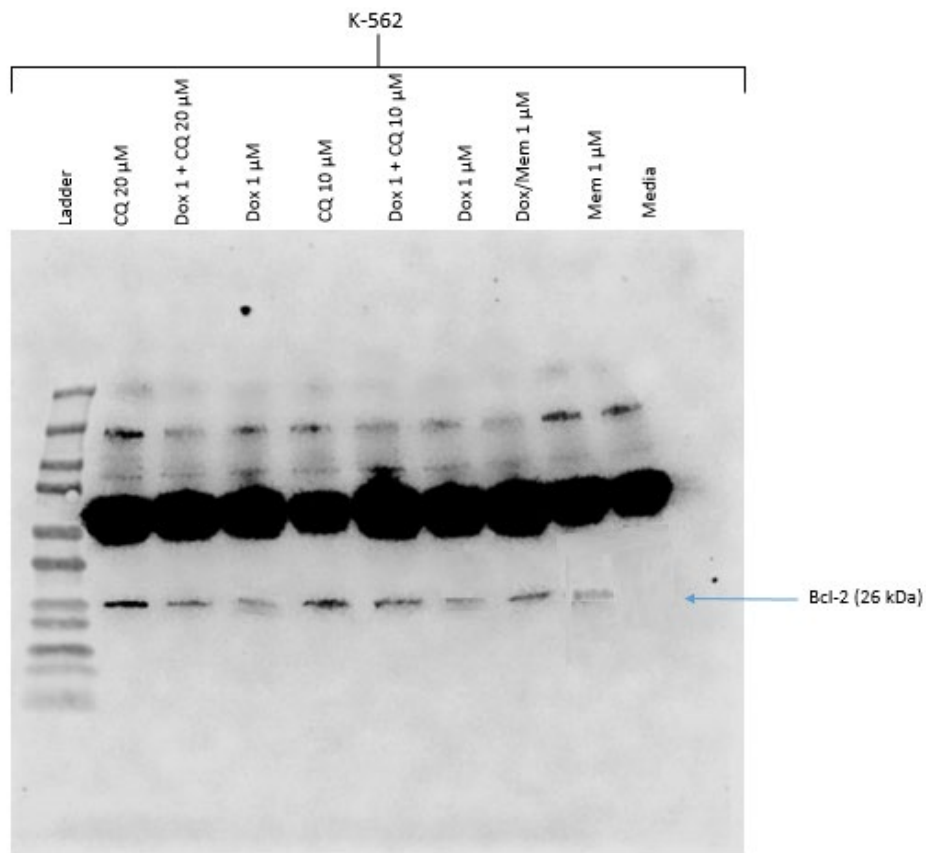
6a) HEK293T – Donepezil 1, 5, 10 μ M; Memantine 1, 5, 10 μ M; Imatinib, Dox and Dox/Mem 1 μ M

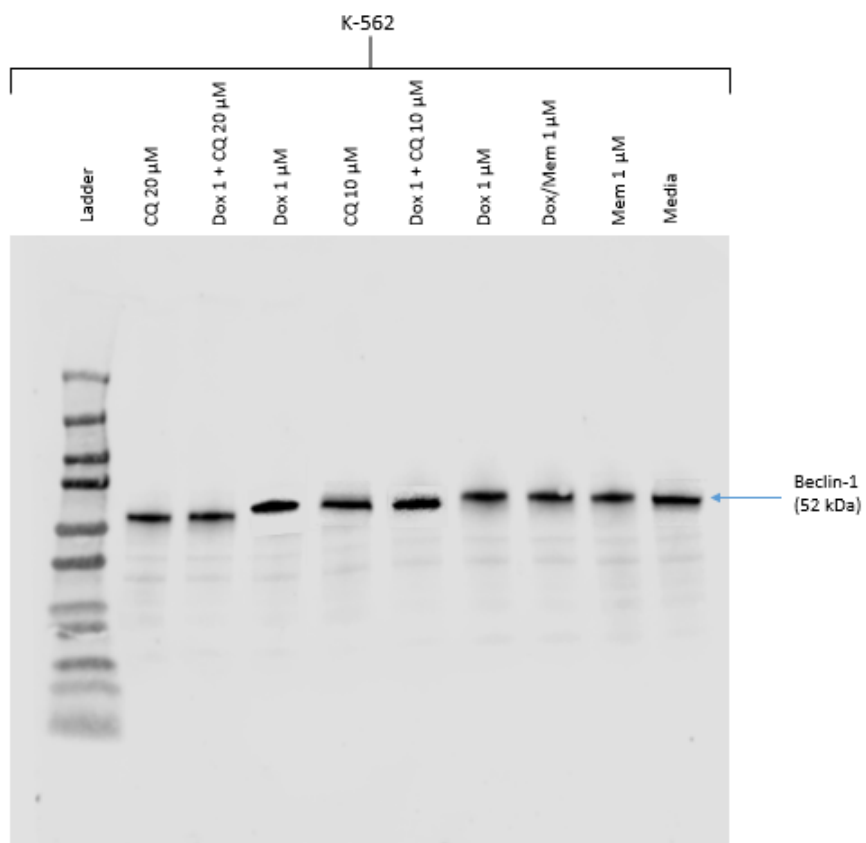
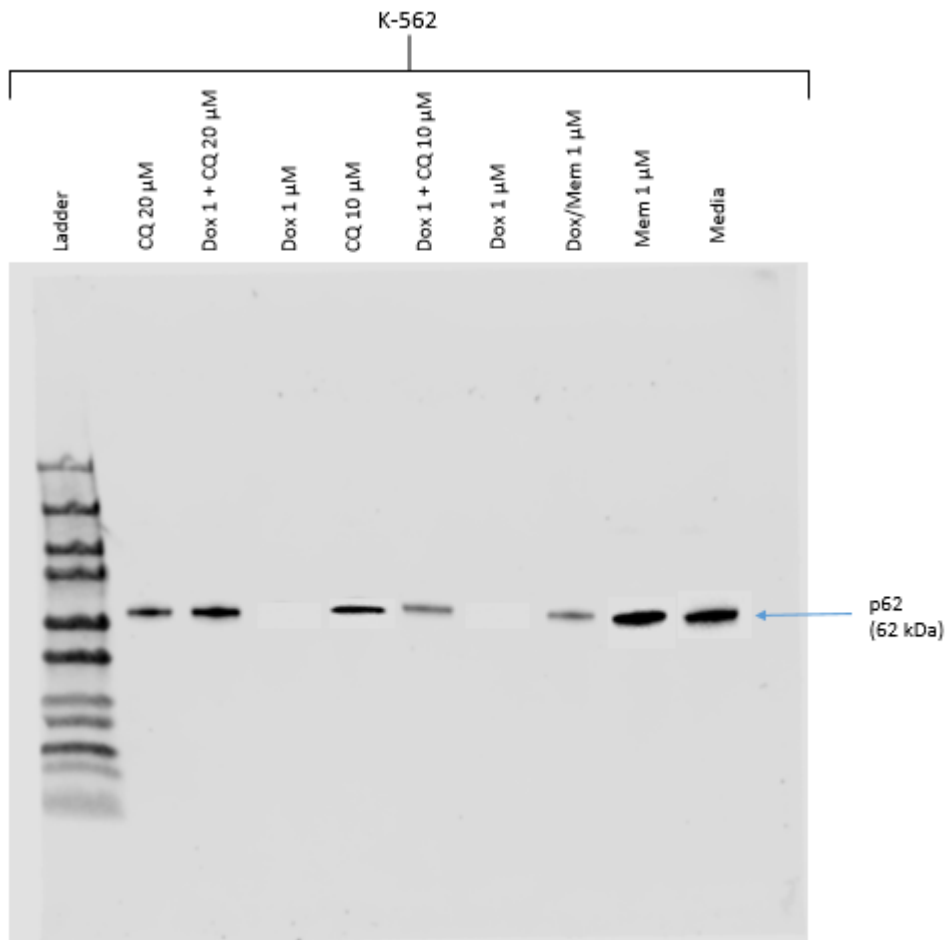






6b) K-562 – Memantine 1 μ M, Dox/Mem 1 μ M, Dox 1 μ M, Dox 1 + CQ 10 μ M, CQ 10 μ M, Dox 1 + CQ 20 μ M, CQ 20 μ M





Appendix XII: Summarised description of the intended experimental procedures for the proposed plasmid construction

To induce an upregulated expression of amyloids, one of the major pathological characteristics observed in AD, HEK293T cell lines will be transfected with a vector containing a mutant form of APP gene.

Commercially available pCAX APP-Swe/Ind (Addgene) would have been a suitable plasmid to transfect the cells for the intended protein expression, unfortunately, the plasmid does not have a selectable marker in mammalian cells. The selection marker cassette is important because not all cells will take up the plasmid of interest after transfection. Hence, this marker (e.g antibiotics resistance) will help identify and keep cells which have taken up the plasmid alive and kill others. The surviving cells carry the APP mutated gene with the ability to express high levels of amyloid proteins. This genetically modified cells will then be sub-cultured for further analysis.

In order to create a construct (Appendix XIII) with the selection element needed, sub-cloning will be carried out using the restriction digest technique. The human APP 695 Swedish/Indiana mutation gene will be cut out from pCAX APP-Swe/Ind vector and inserted into a target vector, pcDNA3-EGFP (Addgene), which possesses neomycin, a mammalian selection marker. The target vector also has a CMV promoter which is functional in mammalian host cell. The digestion of both vectors will be done using NotI and XbaI restriction enzymes (methylation blockage will be considered). These enzymes were selected as they cut within the multiple cloning site. Finally, a ligation reaction will be carried out with DNA ligase to help connect the insert DNA into the compatible digested backbone and form a new construct.

The newly constructed vector will then be transformed into suitable bacterial cells such as DH5alpha for propagation. This cells should be competent enough to produce a good copy number of colonies as the propagated plasmid is <10kb. During transformation, the bacteria cells will be grown in the appropriate antibiotics to aid selection for the cells which have the gene of interest. For the new construct, ampicillin is suitable. The bacteria will form colonies which need to be picked individually and isolated to form a single bacterial colony containing the plasmid. This will be grown overnight and DNA purification will then be performed. The midi prep kit will be used to recover the plasmid DNA from the bacteria culture following manufacturer's instructions.

Plasmid verification will then be carried out using restriction enzymes and Sanger sequencing. Diagnostics restriction digest will be carried out to verify that the vector construct contains the backbone and insert. To carry out this procedure, restriction enzymes will be used to digest the plasmids and then ran on a gel. If the resulting fragment(s) sizes matches the expected size of the plasmid, then the construct was successfully carried out. Also, the plasmid DNA may also be sent to out to a reputable genetic company for validation by sequencing. The use of the Sanger sequencing technique is preferred as it determines the precise order of nucleotides within the DNA molecule. This will help confirm the presence of the APP gene and give assurance that all downstream processes is carried out using the correct plasmid that will express the protein of interest (amyloid beta).

Once the constructed plasmid has been validated, it will be ready for transfection into the mammalian cells and further analytic procedures.

Appendix XIV: Effects of cancer drugs in cancer and non-cancer cells

Imatinib					
Experimental models	Drug(s) used (Conc.)	Incubation time	Experimental assay used for evaluations	Molecular effects	References
Chronic myeloid leukaemia K-562 cells	Imatinib (1 μ M)	48 h	<p>Cell viability was by trypan blue exclusion</p> <p>Protein detection-Western blot analysis</p> <p>Annexin V/propidium iodide staining was used before flow cytometry conducted to determine the response of Imatinib-treated cells to death</p> <p>Senescence was detected by Sa-β-galactosidase labelling, followed by observation using an inverted Nikon Microscope (Eclipse Ti).Results were analysed with the Nikon software.</p> <p>HIV-1 lentivirus based vectors were used to introduce shRNAs against Bim or the complementary DNA of Bcl2 into cells, for apoptosis inhibition, and against ATG7 or Beclin-1, for autophagy inhibition</p>	<p>35% of the cells died via apoptosis</p> <p>\uparrow LC3B-II was detected, when Imatinib treated K-562 cells were treated with autophagay inhibitor, bafilomycin (inhibits autophagolysosome fusion)</p> <p>Inhibition of autophagy by silencing the expression of the proteins ATG7 or Beclin-1 prevents the increase of SA-β-Gal staining in response to imatinib plus Z-Vad</p> <p>\uparrow senescence, as 38% of SA-β-Gal-positive cells was observed compared to the 14% detected in untreated cells</p> <p>\downarrow in p21(3-fold) and \uparrow in p27(4.6-fold) cell cycle inhibitors were observed in imatinib-treated cells compared to the untreated cells</p> <p>Inhibition of apoptosis caused an increase in senescent cells with an increase in p21 (12-fold) and p27 (21-fold) expressions, suggesting that apoptosis limiting the senescent response K-562 cells may be through p21 and p27 downregulation</p> <p>Bim inhibition and Bcl2 overexpression inhibit imatinib-induced apoptosis</p>	Drullion <i>et al.</i> , 2012

Human gastric cancer cell lines: AGS, MKN45, and SNU638 Mouse Embryonic Fibroblasts (MEF)	Imatinib (30, 50, 100 μ M)	48 h	Cell viability was determined by MTT assay Annexin V/propidium iodide staining was used before flow cytometry was employed in conducting cell cycle analysis Protein detection was by Western blot analysis ROS levels were determined by using 2',7'-dichlorodihydrofluorescein diacetate (DCFH-DA)	↓ cell viability in all three gastric cancer cell lines ↓ cell proliferation in a time- and dose-dependent manner Caused cell cycle arrest at the G2/M phase Induced apoptosis in gastric cancer AGS cells by inhibiting platelet-derived growth factor receptor (PDGFR) signalling Induced a mitochondria-mediated apoptosis through the expression of ER stress associated proteins (GRP94, p-eIF2 α , p-IRE1 α and CHOP) in a concentration- and time-dependent manner in both AGS and SNU638 cells Induced ROS production in the AGS cells in a time-dependent manner ↑ phosphorylated JNK in AGS cells	Kim <i>et al.</i> , 2019
BCR/ABL+ leukaemia cells: K562, BV173, KCL22, KU812, MC3, LAMA84 BCR/ABL negative neoplastic cell lines: KG1, SU-DHL-1, U937, Daudi, NB4, NB4.306 Non-neoplastic cells: PHA blasts, LAK, fibroblasts, LCL, renal epithelial	CGP57148B (Imatinib 0.1, 0.3, 1, 3, 10 μ M and 1,2,4,16 μ M)	1 h – 4 days	RT-PCR technique was used to determine the BCR-ABL fusion type Protein detection, phosphorylation of the BCR/ABL protein was evaluated using Western blot analysis Annexin V/propidium binding technique was used to determine apoptosis and cell cycle distribution Cell growth and proliferation was evaluated	All six BCR/ABL+ lines showed a dose dependent inhibition of their spontaneous proliferative rate, which was not accompanied by differentiation. Within minutes, dephosphorylation of the BCR/ABL protein, followed in 16-24 hours by a decrease in cycling cells and induction of apoptosis Inhibition of DNA synthesis in fibroblasts and CD34 cells Proliferation inhibition was observed also when using fresh samples obtained from two Ph+ ALL and 12 consecutive CML patients. And induction of apoptosis his molecule possibly exerts its effects through the inhibition of the kinase activity of BCR/ABL and the	Gambacorti-Passerini <i>et al.</i> , 1997

<p>cells, endothelial cells, CD34(+) cells</p> <p>Leukemic cells obtained from 12 CML patients (10 patients in chronic phase and 2 patients in blast crisis phase) and 2 ALL patients</p>			<p>using thymidine (TdR) uptake assay</p> <p>Induction of differentiation was assayed by immunofluorescence using multiple antibodies</p>	<p>subsequent initiation of apoptosis, without inducing cell differentiation.</p> <p>Dose-dependent inhibition of proliferation in the BCR/ABL+ leukaemia cells; the IC50 was reached in all lines between 0.05 and 0.3 μM</p> <p>No significant (50%) inhibition of proliferation was reached in all BCR/ABL negative at concentrations \leq 3 μM. But at 10 μM fibroblasts and CD34 cells were inhibited 53% and 79%, respectively.</p> <p>In the two ALL samples and in 5 out of six untreated CML patients, IC50 values 0.1-0.6 μM was obtained</p> <p>Tyrosine phosphorylation was inhibited in K562 and LAMA84 cells</p> <p>Induced apoptosis in LAMA84 cells and in fresh CP-CML samples</p> <p>After 97-110 hours of treatment apoptosis was induced in two chronic phase CML cells</p>	
<p>Mouse neuroblastoma cell line N2a</p> <p>Murine neuronal septum SN56 cells</p> <p>Murine fibroblast cell line NIH3T3</p> <p>Mouse hypothalamic cell line GT1</p>	<p>Imatinib (0.25 - 20 μM)</p>	<p>24 h</p>	<p>Transfection: GFP-LC3 N2a stably expressing GFP-LC3 were generated by transfecting N2a cells with the plasmid pGFP-LC3 using Fugene 6 (Roche Diagnostics GmbH, Mannheim, Germany)</p> <p>Confocal laser scanning microscopy and electron microscopy were used for the examination of cells</p>	<p>\uparrow in size and amount of lysosomes</p> <p>Dose-dependently induces the formation of LC3-II</p> <p>Induction of autophagosome formation in mammalian cells (N2a, COS-7, A549, GTI and SN56)</p> <p>Dose dependently activates the cellular autophagy machinery in immortalized as well as in primary mammalian cell</p> <p>c-Abl is the molecular target of Imatinib and that its inhibition leads to the induction of autophagy</p>	<p>Ertmer <i>et al.</i>, 2007</p>

<p>Mouse muscle cells C2C12</p> <p>Monkey kidney cell lines COS-7 and Vero</p> <p>Chinese hamster ovary cells CHO</p> <p>Human lung carcinoma cell line A549</p> <p>Semi-permanent human foreskin fibroblasts (HFF)</p> <p>Human peripheral blood mononuclear cells</p>					
<p>Human leukaemia cell lines: K-562 and TK6 cells</p>	<p>Imatinib (0.01 - 10 μM)</p> <p>Dox (0.001 - 1 μM)</p> <p>Fucoxanthin (0.1 - 10 μM)</p>	<p>24, 48, 72 h</p>	<p>Assessment of cells was done using phase contrast microscopy</p> <p>Cytotoxicity was assessed by cell count after staining cells with trypan blue</p> <p>To assess proliferation: total suspension growth (TSG) and relative suspension growth (RSG) were calculated. *TSG = ratio between the number of cells seeded and</p>	<p>Imatinib (5, 10 μM) \uparrow cytotoxicity in TK6 cells Imatinib \downarrow proliferation in K-562 cells</p> <p>Dox decreased cell viability and proliferation in both K-562 and TK6 cell lines.</p> <p>Fucoxanthin (10 μM) \uparrow cytotoxicity in K-562 cells Fucoxanthin \downarrow cell proliferation 56% and 51% in K-562 and TK6 cells, respectively.</p> <p>In K-562 cells, the IC₃₀ for Imatinib was 0.05 μM the IC₃₀ for Dox was 0.001 μM</p> <p>In TK6 cells,</p>	<p>Almeida <i>et al.</i>, 2018</p>

			<p>the number of cells present at the end of the assay *RSG = ratio of the TSG of each condition and the TSG of the mean of the negative control (expressed as a percentage)</p> <p>IC₃₀ (concentration that reduces the number of viable cells by 30%) was estimated by dose-response curves.</p> <p>Comet assay or alkaline version of the single-cell gel electrophoresis (SCGE) was used to determine DNA damage</p> <p>Cell death assay was by nuclear condensation, annexin V staining coupled with propidium iodide uptake</p> <p>Protein (Bax, caspase-3, and Bcl-2) detection was by Western blot analysis.</p>	<p>the IC₃₀ for Imatinib was 10 μM the IC₃₀ for Dox was 0.0004 μM</p> <p>In co-incubation (Fucoxanthin (0.1 - 10 μM) + Imatinib or Dox (at IC₃₀ of either cell line): Fucoxanthin did not potentiate the cytotoxic activity of both drugs in either cell line. However, at the highest concentration tested (10 μM), the combination of Fucoxanthin + 0.05 μM Imatinib in K562 cells significantly increased cytotoxicity, when compared with Imatinib alone, but no differences compared with Fucoxanthin alone Fucoxanthin (10 μM) increased the anti-proliferative effects of both drugs in both cell lines tested, however no difference was observed relative to Fucoxanthin alone.</p> <p>Combination of Fucoxanthin (1 μM) and Imatinib (10 μM) also increased the anti-proliferative effects in TK6 treated cells compared to Fucoxanthin alone.</p> <p>Combination of Fucoxanthin (10 μM) and Dox (0.001 μM) at 48 h, increased the percentage of condensed nuclei in K-562 cells, compared to Dox alone treated K562 cells.</p> <p>After 72 h of incubation, Fx alone or in co-incubation decreased the percentage of cells with condensed nuclei relative to respective controls</p> <p>Fucoxanthin decreased the expression of the anti-apoptotic protein bcl-2 and caspase-3</p>	
--	--	--	--	--	--

Dox					
Experimental models	Drug(s) used (Conc.)	Incubation time	Experimental assay used for evaluations	Molecular effects	References
Hela tumour cells	Dox (0.1, 1 and 2 μM) Simvastatin (0.25, 0.5, 1, 2, 5 and 10 μM)	72 h	Cytotoxicity/cell survival/ Cell viability- MTT assay and trypan blue exclusion assay	Dox (0.1, 1 and 2 μM): \downarrow cell survival Simvastatin (0.25 μM): \uparrow cell viability (112%, $p < 0.05$) Simvastatin (2, 5 and 10 μM): \downarrow cell survival	Sadeghi-Aliabadi <i>et al.</i> , 2010
Breast cancer cells MCF-10F (non-tumorigenic, not expressing estrogen receptor, progesterone receptor (PR) or human epidermal growth factor receptor 2 (HER2)) MCF-7 (tumorigenic triple-positive expressing ER, PR and HER2) MDA-MB-231 (tumorigenic triple-negative breast cancer cell line)	Dox (1, 2, 4 and 8 μM)	24 and 48 h	Cell viability/ Cytotoxicity- MTT assay and an automated cell counter Protein detection-Western blot analysis using the following primary antibodies: Bax (1:4000) Bcl-2 (1:5000) caspase-8 (1:200) caspase-3 (1:200) NF- κB (1:200) SOD2 (1:200) β -actin (1:5000) Gene expression- Differential display reverse transcriptase-PCR (DDRT-PCR) H_2O_2 production measurement- Amplex Red Hydrogen	Increased concentration of Dox decreased the viability of all three cell lines in a time- and dose-dependent manner for 48 h The IC_{50} for Dox was observed and employed for each cell line: 1 μM for both MCF-10F and MDA-MB-231 cell lines, 4 μM for MCF-7 cells Dox activated apoptosis by inducing the proteolytic processing of the Bcl-2 family of proteins, caspases and by simultaneously decreasing oxidative stress by influencing ROS damage: In MCF-10F (Dox 1 μM treated cells; 48 h): \uparrow Bax gene ($p < 0.05$) and protein expressions of Bax ($p < 0.01$) \downarrow Bcl-xL gene expression ($p < 0.05$) \downarrow Bcl-2 protein expression ($p < 0.001$) \uparrow caspase-8 gene ($p < 0.01$) and protein expression ($p < 0.001$) NSD in caspase-3 gene expression vs control. The amount of caspase-3 expressed in MCF-10F control cells was much lower compared to the amount expression in the other 2 cell line controls.	Pilco-Ferreto and Calaf, 2016

			<p>Peroxide/Peroxidase assay kit, then plate reader</p>	<p>↑ caspase-3 protein expression ($p < 0.05$) ↑ SOD2 gene expression ($p < 0.01$) and ↓ SOD2 protein expression ($p < 0.05$) NSD H_2O_2 production vs control ↑ NF-κB gene expression ($p < 0.01$) and ↓ NF-κB protein expression ($p < 0.001$) MCF-10F control cells expressed a higher level of NF-κB proteins compared to the other 2 cell lines.</p> <p>In MCF-7 cells (in Dox 4 μM treated cells; 48 h): ↓ Bax gene with no significant increase of Bax protein No significant decrease in Bcl-xL gene expression ↓ Bcl-2 protein expression ↓ anti-apoptotic Bcl-2 protein expression ($p < 0.001$) => apoptosis induction ↓ caspase-8 gene expression ($p < 0.01$) and non-detectable levels of caspase-8 proteins ↓ caspase-9 gene expression ($p < 0.05$), which was much lower compared to the other 2 cell lines. The other two cell lines were not different from their control cells. ↓ caspase-3 gene expression ($p < 0.001$) and NSD in caspase-3 protein expression vs control. ↓ SOD2 gene expression ($p < 0.01$), NSD in SOD2 protein expression ↑ H_2O_2 production ($p < 0.01$) => ↑ oxidative stress Also, MCF-7 control cells showed a higher H_2O_2 production compared to MCF-10F control ($p < 0.05$) ↓ NF-κB gene ($p < 0.01$) and ↓ NF-κB protein expression ($p < 0.01$)</p> <p>In MDA-MB-231 cells (in Dox 1 μM treated cells; 48 h): ↑ Bax gene ($p < 0.05$) and Bax protein expression ($p < 0.01$) ↓ Bcl-xL gene ($p < 0.001$) ↓ anti-apoptotic Bcl-2 protein expression ($p < 0.001$) => apoptosis induction ↓ caspase-3 gene expression ($p < 0.001$) ↑ caspase-3 protein expression ($p < 0.01$) ↓ caspase-8 gene expression ($p < 0.01$) and ↑ caspase-8 protein expression ($p < 0.001$)</p>	
--	--	--	---	--	--

				<p>Caspase-9 gene expression was highest in MDA-MB-231 control cells compared to the other 2 cell line controls. However, the expression in the Dox treated MDA-MB-231 cells was not different from the untreated control cells.</p> <p>On the contrary, \uparrow SOD2 gene ($p < 0.01$) and \uparrowSOD2 protein expression ($p < 0.001$) \Rightarrow \downarrow ROS damage \uparrow H₂O₂ production ($p < 0.01$) \Rightarrow \uparrow NF-κB gene expression ($p < 0.05$) and \downarrow NF-κB protein expression ($p < 0.01$)</p>	
Male rats (Sprague Dawley; 500-520g; fed ad libitum)	DOX (12 mg/kg) (i.p administration)	Sacrificed 7 days later	<p>Nephrotoxicity was determined through histopathologic examination of the kidney tissues using Hematoxylin and eosin (H & E) staining</p> <p>Levels of serum urea nitrogen (reflects the metabolism of proteins and rate of excretion of urea nitrogen in the body) were determined using Raichem kit</p> <p>Levels of serum creatinine were quantified using Quantichrom™ Creatinine Assay kit (DICT-500)</p> <p>Lipid peroxidation was measured by determining both the increase in the tissue</p>	<p>\uparrow serum urea nitrogen (5.6-fold) vs control \uparrow serum creatinine (2.65 fold) \uparrow serum urea nitrogen/creatinine ratio \uparrow lipid peroxidation (quantified by increased MDA levels) (1.7-fold) \downarrow in total SOD activities \Rightarrow which could be an indirect reflection of overutilization of SOD or lack of induction of sufficient enzymes to inactivate superoxide. \uparrow genomic DNA fragmentation (2.8 fold) \Rightarrow \uparrowof cells committed to the apoptotic cascade \uparrow APAF-1 proteins (175%) vs control \uparrow Caspase-3 proteins (158%) vs control \uparrow Bax proteins (130%) vs control \uparrow Bad proteins (173%) vs control \downarrow anti-apoptotic Bcl-2genes (45%) vs control \downarrow Bcl-xL genes (22%) vs control 89% \uparrow of p53 vs control and 30% \downarrow of its regulator, Mdm2 vs control As evaluated by H & E staining, features of both apoptosis and necrosis was observed in the kidney cells</p>	Lahoti <i>et al.</i> , 2012

			<p>levels of malodialdehyde (MDA) and decreased superoxide dismutase (SOD) activity</p> <p>Protein detection-Western blot analysis</p>		
MCF-7 breast cancer cells	Adriamycin (Dox) (1-5 μ M)	0 - 48 h	Quantitation of Bcl-2 and Bax mRNA levels- Rt-PCR	<p>↓ in Bcl-2 mRNA levels in a time- and concentration-dependent manner</p> <p>↓ in Bcl-2, in a time- and concentration-dependent manner</p> <p>The EC₅₀ for Adriamycin on Bcl-2 mRNA levels was at 0.4 μM, and inhibition can be observed at a concentration as low as 0.1 μM</p> <p>↑ Bax mRNA levels in a time- and concentration-dependent manner</p> <p>↑ Bax protein levels</p> <p>The EC₅₀ for Adriamycin on Bcl-2 mRNA levels was at 0.1 μM</p> <p>↑ apoptotic death index</p>	Leung and Wang, 1999
Human hepatoblastoma cell line HepG2	Taxol (50 nM) Dox (5 μ M)	0 - 72 h	<p>Construction of antisense Bcl-xL gene expression vectors and isolation of Bcl-2 gene from HL-60 cells was done by PCR</p> <p>The insertion orientation of the genes into a new vector was confirmed by restriction enzyme digestion analysis</p> <p>Stable transfection was carried out using Lipofectamine</p> <p>Protein detection-Western blot analysis</p>	<p>The chemosensitivity in elevated Bcl-2 transfected HepG2 treated Dox and Taxol cells, remained unaffected</p> <p>↑ chemosensitivity of Dox and Taxol treated HepG2 transfected cells with lowered Bcl-xL protein levels after 24 h of treatment, with a significant difference in IC₅₀ values.</p> <p>In the absence of Bax protein, HepG2 cells with elevated Bcl-2 protein levels did not exhibit any significant increase in chemosensitivity towards the drugs.</p> <p>This results suggest that the Bcl-2 protein alone could not protect HepG2 cells from drug-induced apoptosis, and that the Bcl-xL protein may be a target for gene therapy in hepatoblastoma treatment.</p>	Luo <i>et al.</i> , 2000

			<p>Cell viability was measured using trypan blue exclusion method</p> <p>Chemotherapy-induced cytotoxicity was determined by XTT [sodium 3'-1-(phenylaminocarbonyl)-3,4-[tetrazolium]-bis(4-methoxy6-nitro) benzene sulfonic acid hydrate] (Sigma) dye reduction assay</p>		
<p>Acute myeloid leukaemia cells: MOLM-13 cells OCI-AML2</p> <p>U-937 histiocytic lymphoma monocytic cells</p> <p>Chronic myeloid leukaemia K-562 cells</p>	Dox (0.5, 1, 5 μ M)	48 h	<p>Cell viability was measured using trypan blue exclusion method</p> <p>Annexin V/propidium iodide staining was used before flow cytometry was conducted to determine the effects of Dox on cell death</p> <p>5(6)-carboxyfluorescein diacetate succinimidyl ester (CFSE) flow cytometric analyses was used to determine the effects of Dox on cell proliferation</p> <p>Protein detection-Western blot analysis Using the following primary rabbit</p>	<p>Dox reduced the viability of MOLM-13 cells partly by inhibiting cell division and inducing cell apoptosis, mainly early apoptotic death with minimal necrosis</p> <p>Dox demonstrated a level of selectivity in its cytotoxicity against MOLM-13 compared to U-937 cells ($P<0.05$)</p> <p>Dox reduced MOLM-13 cells proliferation in a time- and concentration- dependent manner</p> <p>Different concentrations of Dox induced death of U-937 cells by different mechanisms. Dox 5 μM induced death mainly by necrosis. A lower concentration of Dox, 0.5 μM, induced greater late apoptotic cell death and was more potent than treatment with 1 μM Dox; the reason for this is currently uncertain.</p> <p>The basal expression levels of Beclin-1 protein were not statistically significant ($P>0.05$) between the MOLM-13, OCI-AML2, CML K562 and U-937 cells. However, Dox induced a significant decrease of Beclin-1 in MOLM-13 cells</p>	Vu <i>et al.</i> , 2020

			<p>monoclonal antibodies in PBS-T with 5% BSA: Anti-Bcl-2 (1:1,000; cat. no. ab32124), anti-Bax (1:1,000; cat. no. ab32503), or anti-Becclin 1 (1:2,000; cat. no. ab207612) (all from Abcam).</p>	<p>without significantly affecting the protein levels in U-937 monocytes.</p> <p>A novel Bcl-2 15-20 kDa (p15-20-Bcl-2) isoform was found to be selectively s</p> <p>MOLM-13 cells contained lower levels of p15-20-Bcl-2 protein, compared to the p26-Bcl-2-α protein (P<0.01)</p> <p>Dox induced a highly significant inhibition of p15-20-Bcl-2 at concentrations of 0.5, 0.75 and 1 μM (P<0.01)</p> <p>Dox did not affect the 26 kDa Bcl-2 (p26-Bcl-2-α) isoform protein expression in either the MOLM-13 or U-937 cells</p>	
--	--	--	---	---	--